Design and Synthesis of High Affinity Ligands for Cyclophilin A

Elizabeth Margaret Moir

The University of Edinburgh

A thesis submitted for the degree of Doctor of Philosophy November 2001

Acknowledgements

Initially I would like to thank my supervisor Professor Nick Turner for advice and encouragement in the past three years. I am especially indebted to Yuan De Yang, Sally Shirran and Professor Malcolm Walkinshaw for their contributions, without which this thesis would not have been possible. Likewise I would like to thank the Technical Staff in the Chemistry Department, in particular John Millar and Wesley Kerr for their NMR work. Additional thanks are to due to the Carnegie Trust for funding. I am very grateful to my contemporaries in labs 34 and 120 for friendship and some great nights out. A special thankyou to my parents for the timely loan of their computer, and to Dr Kenneth Macnamara for his perseverance.

Abstract

Cyclophilin A (CypA), an 18 kDa cystolic immunophilin protein, is the receptor for the immunosuppressant drug cyclosporin A (CsA), as well as a potential target for anti-parasitic and anti-HIV drugs. Although the CypA binding and immunosuppressant action of many natural and synthetic CsA derivatives have been studied, there are relatively few examples of the binding of low molecular weight organic molecules to CypA.

A number of dimedone-based ligands have been synthesised and the binding affinities for CypA investigated using one or more of the following methods: crystal preparation and determination of the crystal structure of the ligand:CypA complex; fluorescence assay; PPIase assay; and observation of the ligand:CypA complex by mass spectrometry.

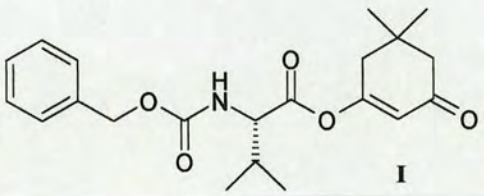

I

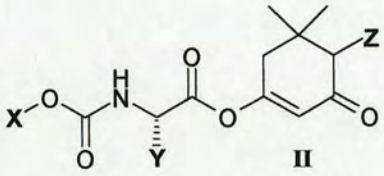

II

X = alkyl, aryl group
Y = amino acid side chain, or dialkyl substituent
Z = alkyl, aryl group

Based on the highest affinity ligand **I** (K_d=22 μM), discovered during preliminary screening, a parallel array of ligands have been generated around the library template **II** using automated methods.

Progress towards the development of a resin-bound cyclohexane-1,3-dione species, with potential scavenger resin and backbone amide linker applications, has been reported.

Contents

Abbreviations

Abu	L-α-aminobutyric acid
Ac	acetyl
ADCC	4-acetyl-3,5-dioxo-1-methylcyclohexane carboxylic acid
Ala	alanine
Alloc	allyloxycarbonyl
Amc	7-amino-4-methylcoumarin
Ar	aryl
Arg	arginine
Asn	asparagine
BAL	backbone amide linker
Bmt	(4*R*)-4[(*E*)-2-butenyl]-4,*N*-dimethyl-L-threonine
Bn	benzyl
Boc	*tert*-butoxycarbonyl
CA	capsid
Cbz	benzyloxycarbonyl
CsA	cyclosporin A
CaM	calmodulin
CLA	cyclolinopeptide A
CN	calcineurin
CV	cone voltage
Cyp	cyclophilin
Dav	deaminovaline
DBU	1,8-diazabicyclo[5.4.0]undec-7-ene
DCC	1,3-dicyclohexylcarbodiimide
DCM	dichloromethane
DCU	1,3-dicyclohexylurea
Dde	1-(4,4-dimethyl-2,6-dioxocyclohex-1-ylidene)ethyl
DDQ	2,3-dichloro-5,6-dicyano-1,4-benzoquinone
DEAD	diethyl azodicarboxylate
DIBALH	diisobutylaluminium hydride

DIC	1,3-diisopropylcarbodiimide
DIPEA	*N,N*-diisopropylethylamine
DMAP	4-dimethylaminopyridine
DMF	*N,N*-dimethylformamide
DMSO	dimethylsulphoxide
DSC	*N,N'*-disuccinimidylcarbonate
ELISA	enzyme-linked immunosorbent assay
ESI	electrospray ionisation
Et	ethyl
FAB	fast atom bombardment
FKBP	FK 506 binding protein
Fm	fluorenylmethyl
Fmoc	9-fluorenylmethoxycarbonyl
Gln	glutamine
Gly	glycine
HATU	*O*-(7-azabenzotriazol-1-yl)-*N,N,N',N'*-tetramethyluronium hexafluorophosphate
HBTU	*O*-benzotriazol-1-yl-*N,N,N',N'*-tetramethyluronium hexafluorophosphate
His	histidine
HIV-1	human immunodefficiency virus
HMPT	hexamethylphosphoric triamide
HOBt	1-hydroxybenzotriazole
HPLC	high performance liquid chromatography
HRMS	high resolution mass spectrometry
h	hour
Hz	Hertz
IL-2	interleukin-2
Ile	isoleucine
IR	infra red
LCMS	liquid chromatography mass spectrometry
LDA	lithium diisopropylamine
Leu	leucine

LIDAEUS	Ligand Design At Edinburgh UniverSity
Lys	lysine
MA	matrix
Me	methyl
MeLeu	*N*-methylleucine
MDR	multidrug resistance
Met	methionine
MeVal	*N*-methylvaline
min(s)	minute(s)
MLR	mouse lymphocyte reaction
mp	melting point
MS	mass spectrometry
NC	nucleocapsid
ND	not determined
NF-AT	nuclear factor of activated T cells
NMM	*N*-methyl morpholine
NMR	nuclear magnetic resonance
PEG	poly(ethyleneglycol)
Ph	phenyl
Phe	phenylalanine
pNa	*p*-nitroaniline
PPIase	peptidyl-prolyl isomerase
ppm	parts per million
Pro	proline
p-TSA	*p*-toluenesulfonic acid
pyr	pyridine
Rf	retention factor
Rt	retention time
Sar	sarcosine
SAR	structure-activity relationships
Ser	serine
Suc	succinyl
T_1	spin-lattice relaxation time

TBAF	*tert*-butylammonium fluoride
TBDMS	*tert*-butyldimethylsilyl
TBTU	*O*-(benzotriazol-1-yl)-*N,N,N',N'*-tetramethyluronium tetrafluoroborate
TFA	trifluoroacetic acid
TFE	2,2,2-trifluoroethanol
TG	Tentagel
THF	tetrahydrofuran
TIPS	triisopropylsilyl
TLC	thin layer chromatography
TMSCl	trimethylsilyl chloride
TPTU	*O*-(1,2-dihydro-2-oxo-1-pyridyl) *N,N,N',N'*-tetramethyluronium tetrafluoroborate
Trp	tryptophan
Trt	trityl
Ts	tosyl
UV	ultra violet
Val	valine

1 Introduction

This thesis concerns the design and synthesis of high affinity ligands for cyclophilin A (CypA). By way of introduction, certain aspects of ligand design within the drug discovery process have been discussed. The functions of CypA have been described, along with a review of the literature on CypA substrates/inhibitors, culminating in an account of the discovery of the lead compound for this project, dimedone.

1.1 Drug Discovery

1.1.1 Classical Lead Discovery

Historically, natural products were the most important source of new drug leads. Active compounds were isolated from plants and their derivatives; from animal toxins; or from secondary metabolites of microorganisms: a relevant example being the discovery of the immunosuppressants cyclosporin A, FK 506 and rapamycin[1] by the screening of microbial broths.

In traditional drug research, these natural product leads were systematically modified using standard medicinal chemistry methods based on cycles of synthesis and screening to obtain analogues with improved activity, selectivity, bioavailability, biological half life and/or reduced toxicity and fewer side effects.

The face of drug discovery has changed dramatically in recent years due to the development of technologies in several fields. Currently, the complementary approaches of chemical synthesis, protein engineering and computational technologies form a design cycle of drug discovery, in which rational structure based design is becoming increasingly important.[2]

1.1.2 Chemical Synthesis

In recent years the high throughput screening of combinatorial libraries has become an important tool in the discovery of drug candidates. Combinatorial chemistry, most simply defined as "the synthesis of all possible combinations of a set of building blocks",[3] began with the concept of huge libraries of compound mixtures and deconvolution of biologically active mixtures to detect new leads. Modern research concentrates more on automated parallel synthesis of focused small libraries of single compounds, in both the lead discovery and lead optimisation stages.

1.1.3 Protein Engineering

In recent years there has been a substantial increase in the number of known 3D protein structures[4] due to improvements in gene technology,[5] protein biochemistry and structure elucidation techniques.[6] Advances in protein isolation and purification by cloning and expression in bacterial or cell culture have meant that key proteins are now available in sufficient quantities for biological assays, NMR studies and structure determination by X-ray crystallography. Recombinant DNA methods allow isolation of stable domains for crystallisation, while site directed mutagenesis allows specific changes in target enzymes or other receptors to make them more useful for clinical applications.[7] The sequence and primary structure of a protein can be derived from the sequence of the corresponding gene. Gene manipulation (modulation by amplifying or destroying a gene) produces transgenic animals, which can be used to investigate the relevance of a gene in certain diseases.[8]

With the full characterisation of the human genome[9] will come many new potential targets for disease therapy and an increase in demand for new structures. Advances in combinatorial chemistry and protein engineering have an important role in this revolution in drug discovery, in combination with new computational technologies for lead structure searching and optimisation.

1.1.4 Structure Based Design[10]

It is in the area of rational drug design that molecular graphics and computer aided drug design come in to play. In biological systems, physiological processes depend on specific molecular interactions, which are in turn governed by the specific features that enable molecules to recognise and bind to each other. Structure based design aims to identify compounds that bind to key regions of biologically active molecules, such as enzymes or receptors, for which the 3D structures are known. The compound leads should inhibit or stimulate the biological action of the target. Using the wide base of structural information on known biologically active compounds, it has been possible to correlate aspects of biological activity with models of specific intermolecular interaction. Proteins bind ligands in specific conformations. The topographies of the complementary surfaces of protein and ligand determine both affinity and specificity. For binding to occur, the drug and receptor molecules must have a complementary shape and charge distribution to achieve the required negative interaction energy. Equation 1, relating the binding energy (ΔG) to the binding constant, K, shows that a small increase in binding energy can lead to an almost tenfold increase in potency. The factors influencing these energy differences include molecular shape, hydrogen bonding, electrostatic interactions, van der Waals interactions, and solvent (hydrophobic interactions).[11]

$$\Delta G = -RT\ln K \qquad \textbf{(Equation 1)}$$

A combination of these factors is considered in the rational design of a ligand for a particular receptor site. Use of a molecular modelling programme to model the binding site involves consideration of many points in space and calculation of the energetics of binding at these points. Values for van der Waals bonding, hydrogen bonding, and electrostatic effects must be taken into account. This information may be used to build up a picture showing areas where particular atoms will bind most strongly. Computer graphics allow us to visualise the placing of a molecule in the binding site in order to determine the strongest interactions.

Thus, structure based design is an iterative process of computational design, synthesis, screening, testing, structure elucidation and data analysis. 3D structures can be used as a basis for drug design in several ways:

1.1.4.1 Design of novel leads

Using known structures of protein receptors, ligands and/or protein-ligand complexes, computational graphics can be used to design novel ligand molecules (*de novo* design). This may involve the screening of 3D databases of small molecules for predicted binding to a known protein target (computational virtual screening).

1.1.4.2 Modification of existing leads

Structure based and computer aided design methods can also be applied to optimise leads, discovered by X-ray crystallography or NMR methods, for affinity and selectivity. This approach is based on the principle that small structural modifications or extensions will result in ligands with similar conformation that should bind to the target in a similar manner.

1.1.5 Protein-Ligand Interactions

Quantitative prediction of binding affinity based on non-bonded protein-ligand interactions is very difficult, but several structure-activity relationship studies indicate that the following criteria are important for strong interactions:[12]

- Enhanced binding affinity is frequently observed by enlargement of the lipophilic contact surface of the ligand by addition of a lipophilic substituent, capable of forming hydrophobic interactions with the protein surface.
- Although not always leading to improved binding affinities, additional hydrogen bonds between polar groups may improve the selectivity and make the ligand more water soluble.

- The displacement of water molecules always occurs upon ligand binding to a protein. Strong binding can be achieved if the ligand forms more hydrogen bonds than the water molecules that are released.
- When binding occurs, there is a corresponding entropy loss due to freezing of internal degrees of freedom. Thus, conformationally constrained ligands often bind more strongly than flexible ligands.

A number of programs have become available which enable *de novo* design of ligands for specific protein active sites. These methods are generally classified as three types:

i. Automated docking of the whole molecule in the active site.
ii. Fitting molecules to precalculated potentials at grid points within the active site.
iii. Docking fragments or atoms and either joining or growing them into molecules.

According to Kubinyi,[13] a computer-assisted approach to *de novo* design should include the following functionalities:

- Ability to search large 3D databases for potential ligands.
- Consideration of conformational flexibility, at least of the ligand.
- The option to create new ligands or to modify existing leads by fusion of groups, fragments or rings.
- A scoring function which is appropriate to evaluate and sort the hits.

1.1.6 Modification of Existing Leads

Many methods are employed to improve the therapeutic profile of a lead compound. Some classical concepts for the rational optimisation of lead structures include:[14]

- Bioisosteric replacement (the exchange of atoms and groups by isoelectronic groups).
- Optimisation of lipophilicity, electronic properties and hydrogen bond donor/acceptor properties.
- Variation of substituents at aromatic or heteroaromatic rings, or at heteroatoms.

- Introduction or elimination of heteroatoms
- Variation of chain lengths or ring sizes.
- Conformational stabilisation by ring formation, intramolecular association of hydrophobic groups, branching, or addition of bulky substituents in order to form more rigid molecules.
- Increasing flexibility by ring opening.
- Introduction or elimination of chiral centres.

1.1.7 Peptidomimetics[15,16] in Structure Based Design

Most peptides have poor bioavailability and are easily degraded by enzymatic proteolysis, making them unsuitable candidates for pharmaceutical development. Peptidomimetics are compounds with peptide characteristics but non-peptide structures, which maintain the ability to bind to peptide receptors. Peptide leads are, therefore, good starting points for the design of peptidomimetics, which may display more favourable pharmacological properties than the natural ligand.[17] The advantage of this approach is that a peptide with known biological activity is used as the starting point for design. A peptide lead is identified by screening libraries of synthetic peptides, by phage display, or from the primary structure of a binding partner. Peptidomimetics can then be designed to mimic the conformation of the key amino acids in the parent peptide, often by incorporation of unnatural or pseudo amino acids, in order to imitate or block the biological action. Ideal peptidomimetics should show increased potency, selectivity and metabolic stability over the parent peptide. Often peptidomimetic ligands are much smaller than the original peptide lead as often only a small set of the peptide residues make energetically significant contact in the complex. The other interactions may be primarily associated with specificity or conformation.[18]

Many methods are used to modify peptide structures to generate efficient drug candidates.[19] Peptidomimetic libraries can be constructed by introduction of amino acid analogues; peptide backbone modifications, such as isosteric replacements of the amide bond; conformational restrictions, such as cyclic or bridging dipeptides; and other structural additions which maintain the overall peptide scaffold but increase affinity and stability.

1.1.8 SAR by NMR (structure-activity relationships by nuclear magnetic resonance spectroscopy).

This new experimental technique for structure based design, pioneered by Stephen Fesik,[20] involves the combination of fragments which bind to proximal subsites of a certain protein. Libraries of small molecules are screened for binding to the subsite of a specific protein. The ligand binding is observed by shifts in the corresponding amide proton signals of the ^{15}N-labelled protein. The protein is then saturated with the highest affinity ligand for this site, and the screening process repeated for another proximal site using a different library. When two ligands have been successfully identified they can be combined with an appropriate linker which connects them in a relaxed conformation. In this manner, construction of a high affinity ligand for FK-506 binding protein (FKBP) was achieved by combining two low affinity small molecules with a linker. Although SAR by NMR can be a relatively fast method for drug design, it does depend on the time taken for assignment of the protein NH signals. Large amounts of pure ^{15}N-labelled protein with sufficient aqueous solubility are required, and the technique is limited to proteins of molecular weight < 53-40 kD. Some constraints on the distance between the two subsites must be employed to avoid linkers which are too large, and the design of the linker is also important to ensure that it does not interfere with binding affinity.

Fesik has reported a related method which does not require ^{15}N-labelled protein. By monitoring the T_1 relaxation times, binding of small molecules in a library to a protein can be observed.[21]

1.1.9 Conclusion

Perhaps the greatest limitation in designing molecules based on protein-ligand interactions is that because the molecular features determining affinity and selectivity are so little understood, it becomes apparent that ligand design does not equate to drug design. Different binding effects observed by small changes in a lead ligand are often non-additive, and very similar members of a series may bind in an entirely different manner due to different hydrophobic, electrostatic, H-bonding and charge

distributions, resulting in a varying and unpredictable biological action. Structure based design gives no information on pharmacological profile or toxicity. This limitation has been further complicated by the switch from using animal models to in *vitro* models for pharmacological screening, which means that some complicated disease pathways or side effects cannot be properly investigated. It therefore becomes important that other properties of the drug candidate affecting transport, bioavailability, metabolic stability, toxicity and synthetic accessibility be expressly addressed from the very beginning by consideration of the properties of the fragments in the early stages.

Traditional drug discovery by natural product screening and systematic modification is therefore likely to remain important as the leads identified may show closer resemblance to the natural ligand or substrate, possibly corresponding to greater selectivity. An additional advantage is the enormous structural diversity found in nature. However, the effort required to isolate active compounds and elucidate structures from these sources, does constitute a major limitation.

Cycles of structure based design and lead optimisation will probably become increasingly important in the future as the amount of structural information on proteins rises and more of the factors controlling affinity and specificity are understood. The powerful combination of emerging new techniques and traditional methods employed within an increasingly interdisciplinary environment promises an exciting future for drug design.

1.2 PPIases (immunophilins)

Peptidyl-prolyl *cis-trans* isomerases (PPIases) catalyse the interconversion of the *cis* and *trans* isomers of the peptidyl-prolyl (Xaa-Pro) bonds in peptide and protein substrates (Scheme 1.1). These enzymes are present in all cell types examined and in most subcellular compartments. PPIases can constitute up to 1-2 % of the total cellular protein and occur in abundance in mammals, plants, bacteria and fungi.

Scheme 1.1

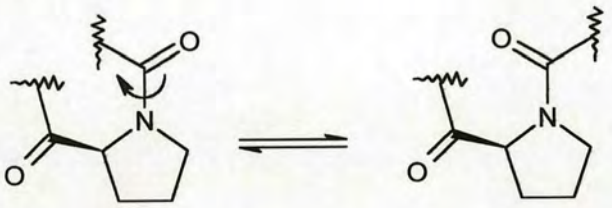

cis *trans*

PPIase activity was first reported for an 18 kDa protein isolated from a porcine kidney cortex by Fischer *et al.*[22] At this time another 18 kDa protein from mammalian thymocytes[23] was found to be the major intracellular receptor for the immunosuppressant drug cyclosporin A (Figure 1.1), and this receptor protein was named cyclophilin A (CypA). Several further cyclophilins were characterised and by 1989, it had been demonstrated that cyclophilins and PPIases were species variants of the same protein.[24] At the same time another prolyl isomerase was discovered[25,26] during the search for the receptor of the immunosuppressive drug FK506 (Figure 1.1). This receptor protein was named FK506-binding protein (FKBP). FK506 is a polyketide produced by *Streptomyces tsukubaesis*,[27] a species discovered in a soil sample. FK506 is structurally related to rapamycin (Figure 1.1), an antifungal agent first described in 1975, and isolated from *S. hygroscopicus*.[28] Rapamycin also binds to FKBP.

Figure 1.1

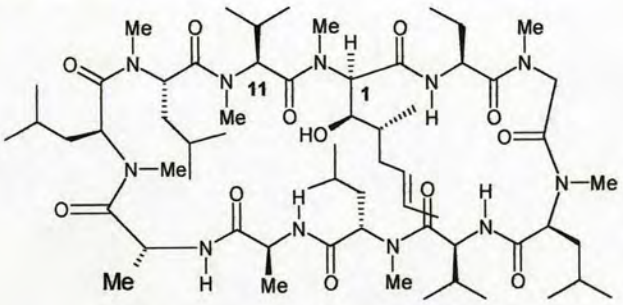

Cyclosporin A

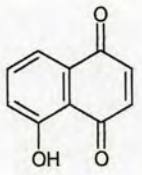

Juglone

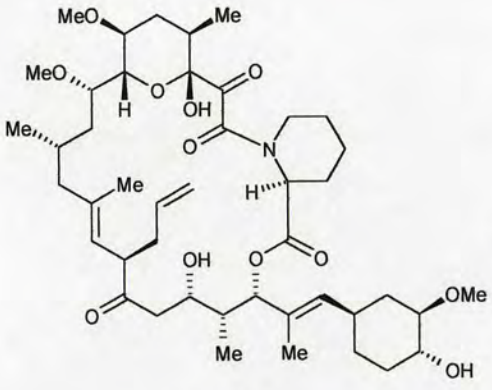

FK506

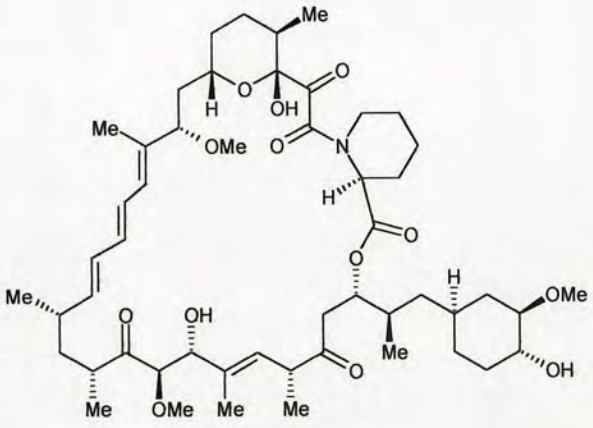

Rapamycin

It became obvious that PPIases could be divided into different classes according to their binding affinity. Three structurally unrelated families have thus far been classified: the cyclophilins, which selectively bind CsA; the FKBP's which bind FK506 and rapamycin with selective high affinity; and a third group known as the parvulins, whose first member was isolated from *Escherichia coli*.[29] It was recently discovered that juglone (Figure 1.1), 5-hydroxy-1,4-naphthoquinone, irreversibly inhibits the enzymatic activity of several parvulins.[30] The three structurally unrelated families differ in subsite specificity, inhibitor sensitivity, molecular mass and amino acid sequence. Within each family however, there is a highly conserved core region, and additional *C*-and *N*-terminal extensions bear sequence motifs. CypA and FKBP are known as immunophilins because they bind the immunosuppressive drugs CsA, FK506 and rapamycin. CypA binds CsA with a reported dissociation constant K_d = 30 nM.[31] FKBP binds FK506 and rapamycin with K_d's of 0.4 nM and 0.2 nM

respectively.[32] Both FKBP and CypA have been shown to bind a number of proline-containing peptides, including the PPIase assay substrate Suc-Ala-Ala-Pro-Phe-pNa (succinyl-Ala-Ala-Pro-Phe-*p*-nitroaniline).

1.2.1 Cyclosporin

Cyclosporin A (Figure 1.1) is a lipophilic 11 amino acid cyclic peptide originally isolated from the fungus *Tolypocladium inflatum*. Its immunosuppressive properties were first described in 1978,[33] and it is currently the drug of choice in transplantation surgery to prevent graft rejection, and in the treatment of autoimmune diseases. CsA (Sandimmun ®) also has anti-fungal, anti-parasitic and anti-inflammatory properties. The free and CypA-bound structures of CsA are very different. In solution, free CsA exhibits a *cis* MeLeu9-MeLeu10 amide bond, whereas the CypA-bound form has a *trans* bond in this position. Free CsA in the crystal state or non-polar solvents has a tightly folded structure with hydrophobic surface, mediated by four intramolecular hydrogen bonds between non-methylated amide-NH groups. The CypA-bound CsA has an open ring structure with one intramolecular hydrogen bond between MeBmt1-MeLeu4.

1.2.2 The Cyclophilin A-Cyclosporin A Complex

NMR spectroscopy and X-ray diffraction data indicate that CypA is an approximately spherical molecule composed of an 8-stranded anti-parallel β-barrel with ends closed off by two α-helices. The core is filled with hydrophobic side chains preventing ligand binding in the centre of the barrel. At the active site of CypA, two loops protrude from the globular protein core and form the sides of the binding groove on top of two β-strands.[34] The CsA binding site has been confirmed as the PPIase active site.[35]

CypA-bound CsA has a flat disc-shaped structure which docks into the binding pocket of CypA. Only residues 9,10,11,1,2 and 3 of the CsA ligand are in contract with CypA. The remaining residues protrude out from the CypA surface and are

implicated in specific interactions with calcineurin. The X-ray crystal structure reveals that the side chain of MeVal11 is completely buried in the hydrophobic pocket of CypA, and this residue dominates the non-bonded contacts to CypA. There are five direct hydrogen bonds between CypA and CsA, and five well-defined water molecules mediating intermolecular interactions.

Other Cyp's show features that are fairly conserved overall. CypB (22 kDa) and CypC (23 kDa) are localized in the endoplasmic reticulum, while CypD (18 kDa) is found in the mitochondria.[36]

1.2.3 PPIase Activity

Most amide bonds in peptides adopt the *trans* configuration. In the case of proline-containing peptides, however, about 10 % of the peptidyl-prolyl bonds are in the unusual *cis* conformation, compared to an estimated occurrence of less than 1.5 % *cis*-amides in other amino acids.[37] This anomaly can be explained by the much smaller free energy difference between the *cis* and *trans* conformations of the amide bond preceeding the proline residue, in comparison to non-proline amide bonds. *Cis/trans* isomerisation of amide bonds is necessary for protein folding, and isomerisation of peptidyl-prolyl bonds has been shown to be rate limiting[38] in some cases. PPIases are therefore thought to catalyse this slow rate-determining isomerisation step. The PPIase activity of these enzymes is abolished upon binding the respective immunosuppressants, which are thought to mimic an intermediate state of the *cis-trans* peptidyl-prolyl bond interconversion of peptide and protein substrates.

1.2.3.1 Enzymatic mechanism of CypA

Several mechanisms have been proposed to explain the *cis-trans* interconversion. In general, conjugation of the C-N amide bond with the carbonyl group to form a planar amide bond, results in a C-N bond with considerable double bond character. Consequently, *cis-trans* isomerisation of the prolyl amide bond has to overcome the

barrier to rotation, and any factors which can weaken the C-N double bond character can be expected to accelerate isomerisation.

In the covalent tetrahedral intermediate mechanism,[24] a cysteine or a nucleophilic reside was assumed to form a covalent bond with the carbonyl carbon as the intermediate, however since no candidate nucleophile has been located in the vicinity of the amide bond, this mechanism seems unlikely. A "catalysis by distortion" mechanism[39] has also been proposed in which the N-C=O plane is distorted in binding to CypA and the intermediate is stabilised by bonding to CypA. A further mechanism assumes that the side chains of serine, threonine, or tyrosine protonate or form a hydrogen bond to the amide nitrogen to deconjugate the O=C-N amide bond. This suggestion is backed up by molecular orbital calculations which indicate that protonation of the nitrogen lowers the barrier for *cis-trans* rotation.[40] The "catalysis by desolvation" mechanism[41] is based on the observation that the rate of *cis-trans* isomerisation is significantly accelerated in non-polar solvents, a theory supported by the hydrophobic character of the active site. Lastly, a "solvent-assisted" mechanism has been proposed on the basis of the CypA:Ala-Pro structure.[42] This mechanism assumes two steps of catalysis: desolvation by binding to the hydrophobic pocket and stabilisation of the intermediate by a solvent molecule.

Although there is a wealth of information available on the structures of CypA complexed with proline-containing di-, tri- and tetrapeptides, it is still unclear whether CypA catalyses *cis-trans* isomerisation with equal rates for both directions. Studies on the three dimensional structure of CypA complexed with the tripeptide Suc-Ala-Pro-Ala-pNa[43] indicate that CypA preferentially recognises a *cis*-proline isomer, since the proline ring can more easily fit into the hydrophobic pocket than in the *trans*–isomer. Distortion of the *trans* isomer could lead to better binding, but at an energetic cost of the distortion energy. Zhao *et al.*[44] have revealed that only the *cis* isomer of the substrate Suc-Ala-Ala-Pro-Phe-pNa binds to the active site of CypA in a stoichiometry of 1:1, while model docking implied that the *trans* conformer does not fit into the active site. On the basis of these results they propose that the

isomerisation occurs predominantly in the *trans* to *cis* direction, *via* a hydrogen bonding mechanism.

1.2.4 Mechanism of Immunosuppression

The immunosuppressive mechanism of CsA requires formation of a tightly bound CsA-CypA complex which inhibits Ca^{2+} dependent events, resulting in failure to activate genes encoding interleukin-2 and other lymphokines, and ultimately preventing T-cell activation in response to antigen recognition (Figure 1.2).

Figure 1.2[45]

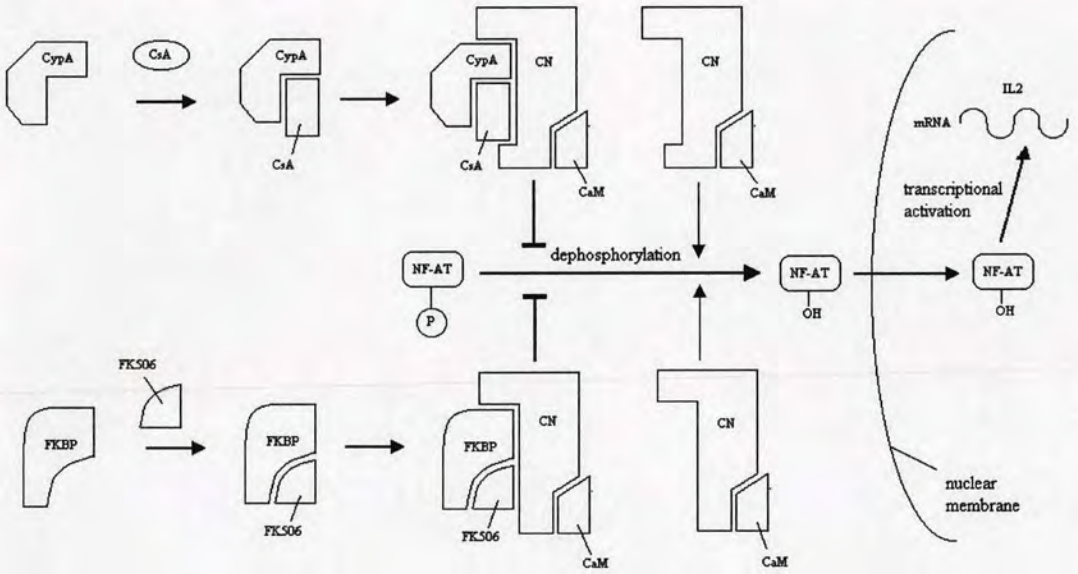

During T-cell activation calmodulin (CaM) binds to the serine/threonine phosphatase calcineurin (CN) as a result of elevated levels of free intracellular calcium. This complex dephosphorylates the nuclear factor of activated T cells (NF-AT), which in the dephosphorylated form is able to cross the nuclear membrane. In the nucleus NF-AT acts as a transcriptional activator for interleukin-2 (IL-2) transcription. The CypA-CsA complex binds to calcineurin and blocks the phosphatase activity of the CN/CaM complex. Neither CsA nor CypA alone affects the calcineurin activity and the complexed CypA-CsA with protruding CsA effector region is required.[46]

Despite exhibiting no structural similarity to the CypA-CsA complex, the FKBP-FK506 complex can similarly interfere with this signal transduction pathway by binding to calcineurin and inhibiting phosphatase activity. The complexes are competitive inhibitors of CN, thought to bind at overlapping but not identical sites near the active site of the enzyme. While the crystal structure of the FK506-FKBP-CN complex has been published,[47] no such structure for a CsA-CypA-CN complex has been reported. The mechanism of immunosuppression is independent of PPIase activity, established by studies on active site mutants of CypA.[48] Despite their structural similarities, rapamycin and FK506 have very different mechanisms of immunosuppression. In fact, the specific target of the FKBP:rapamycin complex is not known, although it is believed to inhibit T-cell protein synthesis by blocking a ribosomal kinase.[49] The immunosuppressant activity of FK506 and rapamycin is approximately 100-fold greater than that of CsA.[50]

1.3 Other Functions of Cyclophilin

The high abundance of cyclophilins and their wide distribution implies that cyclophilins have more general functions than modulating the activation of T cells. Facilitating the folding, assembly and trafficking of polypeptides may constitute some of their major functions, but evidence suggests that cyclophilins are involved in regulation of a variety of other cellular processes, some of which will now be described.

1.3.1 HIV

Cyclophilin A has been reported to bind human immunodeficiency virus type 1 (HIV-1) gag protein, and is required for the infectious activity of HIV-1 virions. In 1994, Luban *et al.*[51] demonstrated that CypA is integrated within the viral core of HIV-1 and is essential for the release of viral RNA and hence for multiplication of the virus. HIV gag is a polyprotein and CypA interacts specifically with the capsid domain of the dimerised gag, to promote assembly of the viral core. In subsequent steps the polyprotein is cleaved into several functional proteins: matrix (MA), capsid

(CA), nucleocapsid (NC) and small peptides.[52] The crystal structure of CypA complexed with a 25 amino acid peptide of HIV-1 gag protein has been determined.[53] The sequence Ala88-Gly89-Pro90-Ile91 of the gag fragment is the major portion to bind within the active site of CypA. Residues Pro90-Ile91 of the 25-mer bind to CypA in a similar manner to two residues (Pro-Phe) of the CypA substrate Suc-Ala-Ala-Pro-Phe-p-Na. However, the peptidyl-prolyl bond between Gly89-Pro90 adopts a *trans* conformation, in contrast to the *cis* conformation usually observed in CypA-peptide complexes. The unfavourable backbone conformation adopted by the Gly89 residue suggests that this Gly-Pro sequence may be a requirement for CypA-gag binding, since a conformation of this sort is usual only for glycine. This finding has been confirmed by several groups,[54] with different peptide substrates. As expected, the pyrrolidine ring of Pro90 binds within the hydrophobic pocket of CypA, and a *trans*-Gly-Pro conformation is adopted due to stereochemical constraints, resulting in full occupancy of this pocket.

The exact function of CypA in the HIV-1 viral cycle remains controversial. It is not yet understood whether the *cis-trans* isomerase activity of CypA plays a role in HIV-1 virion activity, but results thus far indicate that it may be more likely to function as a chaperone or functional component. Genetic and biochemical studies show that CypA is required for HIV-1 replication and infectivity, but not for virion assembly.[55] Some results suggest that it disrupts the viral core and enables virus uncoating, but this theory has been recently questioned.[56] It has been observed that virus which contains less CypA, either as a result of treatment with CsA[57] during virion budding, or because of a mutation in the capsid region of gag, is less infectious.

Nevertheless, it is obvious that CypA plays an important role in HIV-1 viral infection. As a consequence, inhibition of the CypA-HIV-1 interaction is a promising target for the design of anti-AIDS drugs. A further intriguing finding is that CsA, the selective high-affinity ligand of CypA, can inhibit the CypA-gag interaction.[58] The immunosuppressant function of CsA is not however responsible for the antiviral activity, because the non-immunosuppressive analogue

SDZ NIM811 (Table 1.1) inhibits HIV-replication to a similar extent as CsA (Figure 1.3).[59]

Figure 1.3[60] When HIV-1 infected cells are treated with CsA or SDZ NIM811, the resulting virions are depleted of cyclophilins and are therefore only poorly infectious.

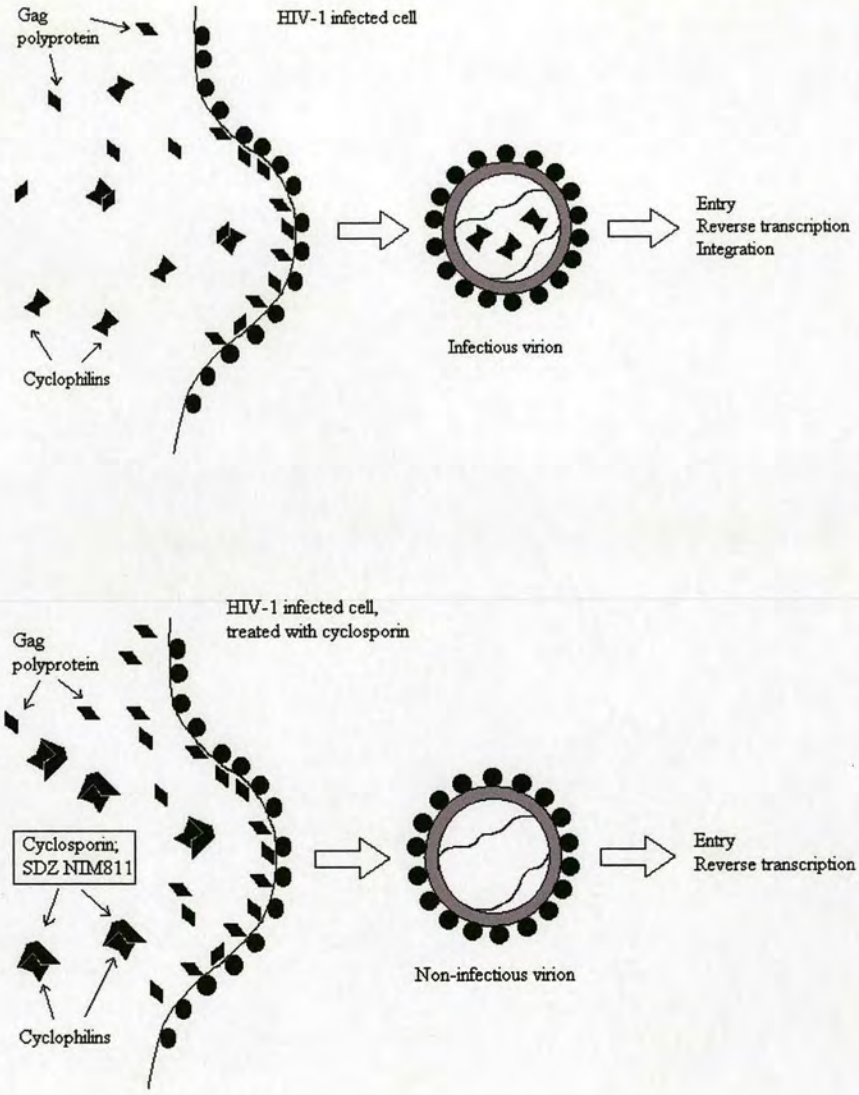

CsA derivatives are interesting as inhibitors because of the selective high affinity of CsA for CypA, although the synthesis of cyclic undecapeptides is generally difficult and time-consuming. Furthermore, the concentrations of CsA analogues required to inhibit HIV-1 replication may be toxic to cellular events *in vivo*, and given the

abundance of cyclophilins, they are probably involved in many cellular processes. However, part of this problem may be overcome by using sub-optimal amounts of CsA derivatives in conjunction with other anti-HIV-1 drugs.

Another possible strategy is the design of small linear peptides or pseudopeptides that mimic a fragment of the HIV-gag protein that interacts with CypA. This course of action has been investigated by several groups.[61] Li *et al.*[62] focused on the linear heptapeptide Ac-Val-His-Ala-Gly-Pro-Ile-Ala-NH_2, which binds to CypA with low affinity (IC_{50} = 850 ± 220 μM) but potentially useful selectivity for CypA relative to the PPIase FKBP-12. On the basis of X-ray structures of gag fragments-CypA complexes, they generated a series of modified peptides in order to select one displaying a higher affinity for CypA than the capsid domain of HIV-gag. They discovered that the histidine residue was important for interaction, and that substitution of the *N*- and *C*-terminal residues with deaminovaline (Dav) and benzylamide respectively, led to a significant improvement in affinity. Combination of both modification gave the most potent inhibitor Dav-His-Ala-Gly-Pro-Ile-NHBn, which has a higher affinity for CypA (K_d = 3 ± 0.5 μM) than the entire capsid protein (K_d = 16 ± 4 μM) and greater selectivity for CypA over FKBP-12. Results also suggest that this gag analogue preferentially binds CypA in a *trans*-Gly-Pro conformation and is not a substrate of CypA. Design of compounds based on the gag protein, like this modified pentapeptide, or non-immunosuppressant derivatives CsA, may represent an attractive starting point for the discovery of peptidomimetic anti-HIV-1 agents.

1.3.2 Multidrug Resistance

Multidrug resistance (MDR) is a major cause of cancer treatment failure. Tumour cells survive by exhibiting intrinsic resistance to multiple drugs on exposure to a single drug.[63] Overexpression of P-glycoprotein (P-gp), a plasma membrane protein that functions as a drug efflux pump for chemotherapeutic agents, is believed to be one of the main mechanisms of MDR.[64] Multidrug-resistant cancer cells have also been shown to display elevated levels of the glycolipid glycosylceramide.[65]

A major challenge in cancer therapy today is to find drugs that inhibit MDR, rendering cancer cells sensitive to chemotherapy. Some MDR reversing agents, such as tamoxifen,[66] are thought to work by direct binding to P-gp, thus interfering with the binding and export of anticancer agents and restoring cytotoxicity. However, these agents may also affect glycolipid metabolism within the cell,[67] by inhibition of ceramide glycosylation, resulting in a lowering of glycosylceramide levels. Ceramide is suggested to be involved in programmed cell death (apoptosis), a mechanism important for cytotoxic response to anticancer agents.

CypA and its derivative SDZ PSC 833, [3′-keto-Bmt-1]-[Val-2]-cyclosporin (Table 1.1), have been shown to be MDR reversing agents,[68] with PSC 833 proving to be the more potent of the two. The action of PSC 833 is believed to involve inhibition of drug efflux by P-gp, and direct interaction between PSC 833 and P-gp has been demonstrated.[69] PSC 833 also has a profound impact on ceramide formation, whereas CypA has little influence. The increase in cell ceramide caused by PSC 833 results in a parallel decrease in cell survival. Although the exact mechanism of action of PSC 833 on MDR resistant cells is not yet known, results imply that its influence on ceramide synthesis may be independent of P-gp. It is hoped that further studies in this area may provide new insights into the mechanisms by which MDR modulators reverse drug resistance.

1.3.3 Antiparasitic Activity

It is now clear that multiple forms of cyclophilin exist in parasites.[70,71] Since cyclophilins are known to catalyse the rate-limiting *cis-trans* isomerisation of proline-containing peptides and accelerate their refolding mechanisms, it has been suggested that they may play an important role in parasitic development. In past years CsA has been shown to exhibit potent antiparasitic activity independent of its immunosuppressant action. Since this discovery, CsA has been shown to adversely affect a large number of protazoa and helminths both *in vivo* and *in vitro*, although not all parasites tested are susceptible.[72] The precise mechanism of action of CsA and reasons for its apparent species/or stage specificity are not yet understood, but

the mode of action may involve inhibition of endogenous cyclophilins, or of an essential signal-transduction pathway. It has been demonstrated that CsA can bind to parasite cyclophilin.[73] Although the biological function of parasite cyclophilins and their role in the host-parasite relationship is unclear, it is possible that these proteins may modulate the host's immune response during infection. There is still much to be learned in this area but recent findings concerning the potent anti-malarial[74] action of non-immunosuppressant CsA analogues, indicate that this may be an important field in the design of novel antiparasitic drugs.

1.4 Review of Cyclophilin A Substrates

The reported substrates/inhibitors for cyclophilin A can be divided into four main categories:

1. modified CsA derivatives
2. substrates isolated from natural sources
3. peptide ligands
4. non-peptide ligands

1.4.1 Modified CsA Derivatives

Table 1.1 summarises some of the information available on the CypA-binding of CsA derivatives and, where possible, their immunosuppressive activity. The K_d, K_i and IC_{50} results have been difficult to correlate as each paper uses a slightly different assay technique (see references for a description of assays used) resulting in discrepancies even in the calculated K_d of CypA-bound CsA. The values have therefore been tabulated as ratios, relative to the value obtained for CsA (*eg.* IC_{50} for CsA derivative / IC_{50} for CsA).

Table 1.1

Residue (R)										
1	2	3	4	5	6	7	8	9	10	11
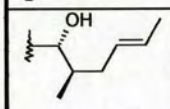			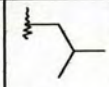		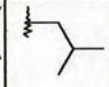			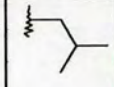	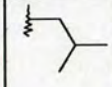	

Deriv-ative	Modifiation(s)	Assay: CypA Binding	Assay: Immuno-suppress-ion	Additional Information	
116450	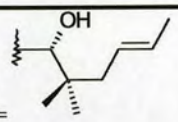 R1=	ELISA (Rel. IC_{50}) 26	IL-2 (Rel. IC_{50}) 4.2	X-ray structure. Decreased immuno. activity over CsA may be due to induced conformational change in MeLeu6.	[75] [76]
33804	 R2=	6	3.1	X-ray structure.	
27402	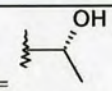 R2=	1.4	1.0	X-ray structure.	
224698	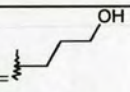 R2=	7.2	7	X-ray structure.	
209313 CsC	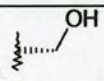 R3=	0.33	2.4	X-ray structure.	
209650	 R2= 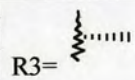 R3=	0.69	2.4	X-ray structure.	
209217	 R2= 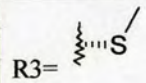 R3=	0.24	1	X-ray structure.	
209825	R1= 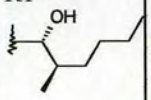 R2=  R3= 	0.53	1.8	X-ray structure.	
211810	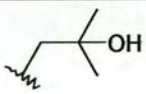 R4=	1	110	X-ray structure.	

211811 SDZ NIM 811	R4= 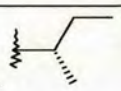	0.6	>1700	X-ray structure. Active against HIV-1 by inhibition of CypA:HIV-1 interaction.	[77]
SDZ PSC 833	R1= 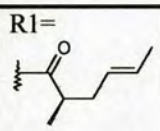 R2= 			MDR Shown to bind Pgp directly, and have independent effect on ceramide metabolism	[78]
214103	R2= 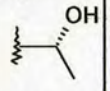 Leu10 non-methyl-ated R5= 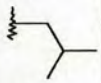 Residue 8= 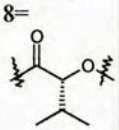	K_d similar to that of CypA/ CsA	Activity similar to CsA	X-ray structure. Free ligand: *cis* amide between residues 3 & 4. CypA complex : similar to CypA/CsA complex.	[79]
	Residue 5, NR= 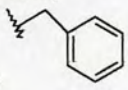	Compet. ELISA (IC_{50}) 1.47	MLR No immuno. activity	^{1}H NMR : ligands exist in a single, all *trans* conformation (cf. multiple soln. CsA conformations). Comparison of solution data with X-ray data of a CypA-bound derivative indicates that solution structure does not correspond to the bioactive conformation. Conformational stabilisation of soln. structure is possible by removal of NH Val5 H-bond. NH-5 plays crucial role in CsA's calcineurin binding.	[80]
	Residue 5, NR= 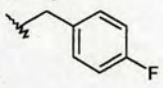	2.21			
	Residue 5, NR= 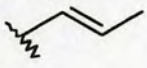	2.37			
	Residue 5, NR= 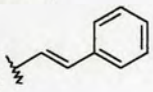	1.84			
	R7= 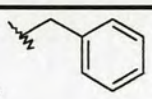	PPIase (Rel. K_i) 5.5	IL-2 (Rel. IC_{50}) 8.92	Individual modifications resulted in decreased activity.	[81]
	R3=  R7= 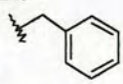	1	5.17		

	R7= 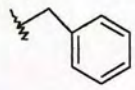 R8= 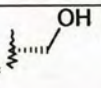	1	1.75	Modifications combined led to tighter CypA binding than CsA, with full immuno. effect retained.	
	R3=  R7= 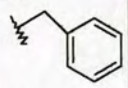 R8= 	0.5	1.69	Substituent effects on PPIase inhibition and immuno. activity are non-additive.	
NBDL-CsA	R8= 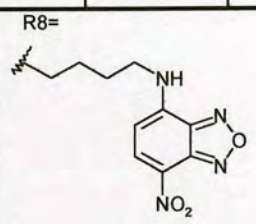			MDR Used to measure Pgp secretion of CsA.	82
	R8= 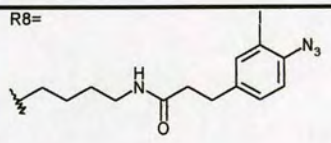		Retains partial biologi-cal activity of CsA	Radiolabelled and photoreactive immunosuppressive CsA analogue.	83
	R8= 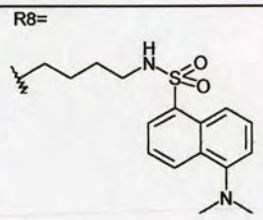	Fluo. Assay (Rel. K_d) 0.17		Identification of actin and HSP 70 as CsA binding proteins using photoaffinity labelling. Fluorescent CsA used in displacement assay to measure binding constants to bovine actin and yeast homologue of HSC 70.	
	R8= 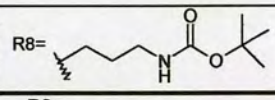	0.07			
	R8= 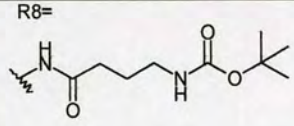	PPIase (Rel. K_i) 0.8	MLR (Rel. IC_{50}) 3.33	Binding constants also determined by competition experiment with fluorescent CsA.	84
	R8= 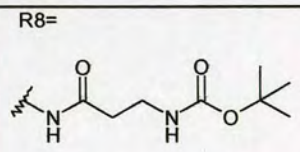	0.8	10	Significant lowering of calcineurin affinity for CypA-complex.	
	R1= 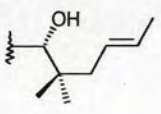	108	2	Poor CypA binding but minimal change in calcineurin binding affinity	

Ψ Pro CsC Deriv-atives	Residues 1&2 cyclised to oxazolidine or thiazolidine. 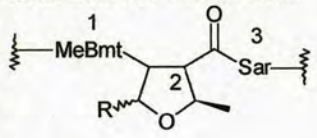 R Ph p-Ph-C_6H_4 CH_2=CH p-MeO_2C-C_6H_4 p-$MeOC_6H_4$ p-AllOOC-C_6H_4 p-HOOC-C_6H_4 PEG	PPIase (Rel. IC_{50}) Values indicate moderate to weak binding to CypA	No results reported	Formation: acetylation of 2-threonine hydroxyl group and the preceeding amide nitrogen by dimethyl acetals. HPLC/NMR suggest enhanced backbone rigidity of Ψ Pro CsC derivatives.	[85]
R2 deriv-atives	R2= 1. $CH_2CH_2CH_3$ (CsG) 2. $CH_2CH(OH)CH_3$ 3. $CH(OH)CH_2CH_3$ 4. CH_2CHCl_2 5. 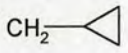 	ELISA (Rel. IC_{50}) 1. 4 2. 207 3. 5.2 4. 250 5. 250	IL-2/ MLR 1. 2.6 / 1.6 2. 57 / 45 3. 3 / 2.3 4. 200 /135 5. 225 /120	Formation: coupling of *N*-protected aa2, with decapeptide, followed by deprotection and ring closure. Disubstitution at γ-C of Abu-2 in CsA is detrimental for binding CypA. Reduced binding in this case correlates with reduced immuno. activity.	[86]
R2 deriv-atives	R2= 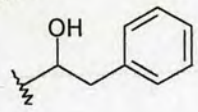 	ELISA (Rel. IC_{50}) 80	IL-2 (Rel. IC_{50}) 200	Abu2 pocket appears large enough to accommodate bulky groups, however	[87]
	R2= 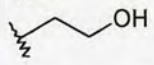 	3	5	only unbranched chains bearing polar substituents are acceptable.	
	R2= 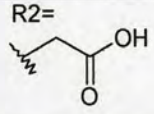 	5	86	Thought to be due to steric and physicochemical influence of water mols.	
	R6= 	PPIase (Rel. K_i) 2.3	IL-2 (Rel. IC_{50}) >1250	Designed as non-immuno. analogues with anti-HIV-1 activity. Promising lead compounds for anti-HIV-1treatment.	[88]
	R1= 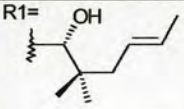 	95.7	57.5		
	R1= 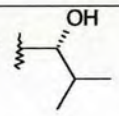 	1.6	77.5		

	R1= 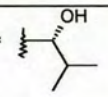 R4=  R6= 	5	>1250		
	R1= 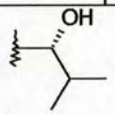 R11= D-MeVal	No binding	>1250		
R4 deriv-atives	R4= NEtLeu	Spectro. Assay (Rel. IC_{50}) 1.2	IL-2 (Rel. IC_{50}) 1.6	Designed as non-immuno. analogues with anti-HIV-1 activity.	89
	R4= NEtVal	0.67	>2500	Comparable binding affinities to CsA for CypA.	
	R4= NEtIle	0.83	300		
	R4= NEtThr	not det.	Not det.		
	R1= 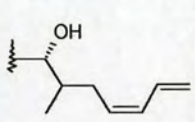 R2= 	Fluo. Assay (Rel. K_d) 2.73		Comparative binding studies of Cyp's and derivatives by fluorescence measurements.	90
	R6= dihydro R7= dihydro R8= methylated	2.88			
	R6= dihydro R7= dihydro	3.61			
	R2= 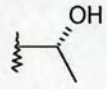	0.70			
Nva-CsA	R2= 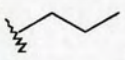	4.29			
	R2=  R3=  R6= dihydro R7= dihydro	2.27			
	R4= 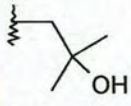	3.07			

	R9= 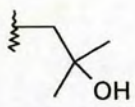	0.40			
R4 deriv-atives	R4= 	ELISA (Rel. IC_{50}) 0.5	IL-2 (Rel. IC_{50}) 2500	Lipophilic & hydrophilic substituents detrimental for immunosuppression.	[91]
	R4= 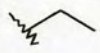	1.2	163	Indicates CN tight-binding pocket for this region.	
	R4= 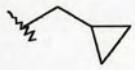	2.8	5.3		
	R4= 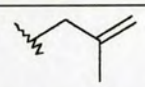	1.8	4.0		
	R4= 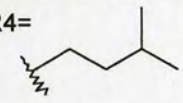	1.9	9.0		
	R4= 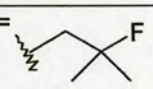	2.1	7.0		
	R4= 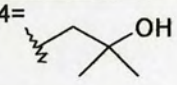	0.9	110		
Lactam	R3,R4= 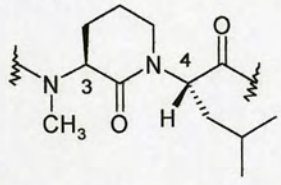		(Rel. IC_{50}) 20	Stabilised II′ β-turn analogue. Weak biological activity probably due to steric hindrance.	[92]
	R7,R8= 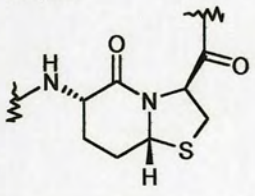	PPIase assay (Rel. K_i) 0.3	T cell assay (Rel. IC_{50}) 0.5	Tricyclic immuno. variant of CsA, designed with conformational constraint. Enhanced binding and immuno. activity.	[93]

1.4.1.1 Discussion

It should be noted that over two hundred CsA derivatives, both natural[94] and synthetic,[95,96] have been reported. Table 1.1 is therefore by no means an exhaustive review of CsA analogues. Nonetheless, several trends can be discerned from the data available for the derivatives in Table 1.1. Analysis of the binding constants and corresponding immunosuppressant activity of selected modified CsA derivatives support the belief that residues 9, 10, 11, 1, 2, and 3 are required for CypA binding, while residues 4, 5, and 6 form the effector loop to CN. Consequently, modification of residues 4-8 has, in general, little effect on CypA binding, but may radically alter the observed immunosuppressant activity. It is also widely observed that residue modifications leading to a drastic change in conformation of the derivative compared to CsA are not tolerated without significant loss of binding and/or biological activity.

1.4.2 Substrates Isolated from Natural Sources

1.4.2.1 Sanglifherins[97, 98]

The sanglifherins (Table 1.2) were discovered by screening of actinomycete strains with a cyclophilin-binding assay, and are produced by *Streptomyces* sp. A92-308110. The chemical structures and absolute stereochemistries of sanglifherins A,B,C and D have been determined by NMR and X-ray crystallography of the complex with CypA. Sanglifherins A and B are genuine metabolites whereas C and D are artefacts formed during the isolation process.

Interestingly, the sanglifherins did not inhibit the phosphatase activity of calcineurin, showing no activity in the reporter gene assay for IL-2 gene expression. There results indicate that this compound class has a different mode of immunosuppressive action than CsA.

Table 1.2

Sanglifherin	**Binding** ELISA. (Rel. IC_{50})	**Immuno Activity** MLR (Rel. C_{50})
A 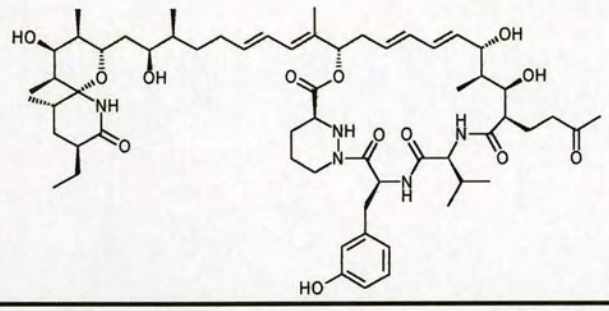	0.05 (20-fold increase)	16
B 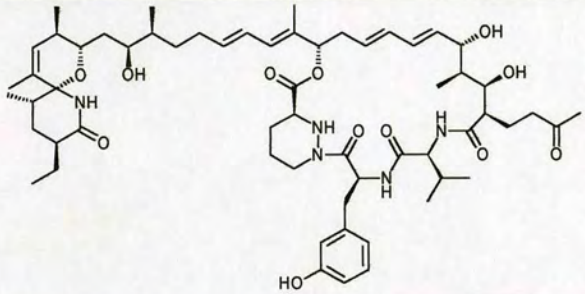	0.05	10 (10-fold decrease)
C 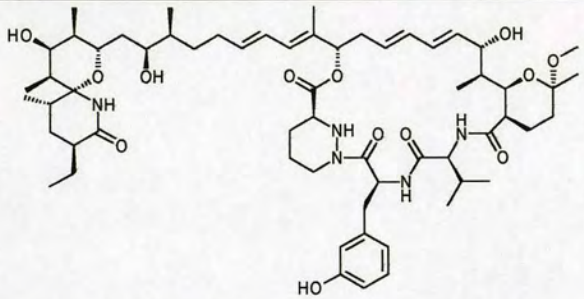	0.61	113
D 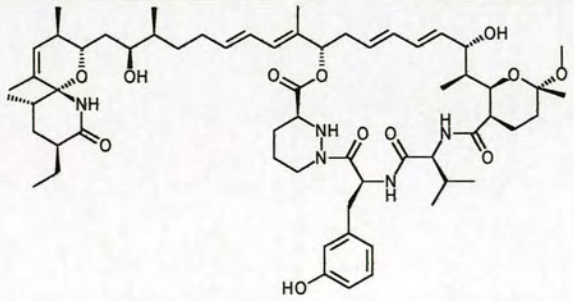	0.71	60

1.4.2.2 Cymbimicins[99]

Cymbimicins A and B were isolated from a strain of *Micromonospora* sp. by screening actinomycete strains for Cyp binding metabolites. The binding affinity of cymbimicin A to CypA is about six times lower than that of CsA, whereas the affinity of cymbimicin B is about 100 fold lower (Table 1.3).

Table 1.3

Cymbimicin	**Binding** ELISA. (Rel. IC_{50})
A 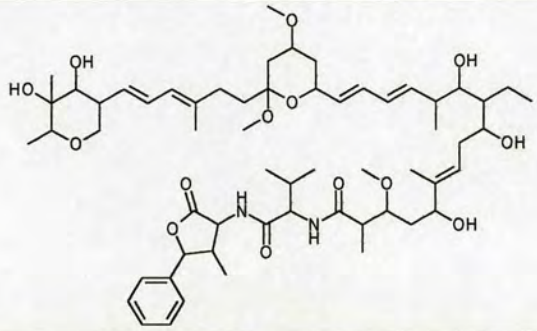	5.5
B 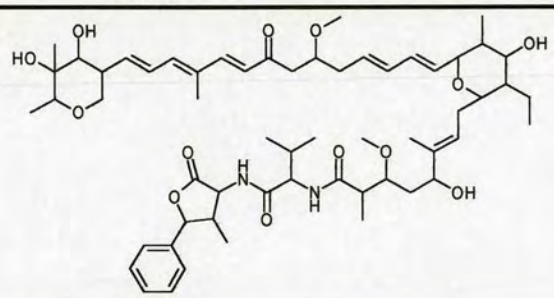	>450

Neither cymbimicin A or B complexed to CypA affected calcineurin activity, measured by the calmodulin dependent dephosphorylation of a 19 amino acid phosphopeptide substrate in a cell-free enzymatic assay. However, cymbimicin A did inhibit calcineurin activity when complexed with CypB (IC_{50} 4 μM). Neither cymbimicin A or B were active in cellular immunoassays measuring T-lymphocyte activation (although this may be due to an inability to enter the cell), or in the IL-2 reporter gene assay.

1.4.2.3 Cyclolinopeptides

The natural occurring cyclic peptide cyclolinopeptide A, cyclo(-Pro-Pro-Phe-Phe-Leu-Ile-Ile-Leu-Val-) (CLA), isolated form linseed oil, and its synthetic analogue cyclo(-Pro-Pro-Phe-Phe-Aib-Aib-Ile-D-Ala-Val-) (CLAIB), were found to bind CypA, inhibiting its peptidyl-prolyl *cis-trans* isomerase activity. Direct binding of CLA was confirmed using tryptophan fluorescence studies and PPIase assays, as no crystal structure is available. Phosphatase assays reveal that CLA is able to bind CypA and inhibit calcineurin phosphatase activity, although higher concentrations are required that with CsA:CypA.[100] CLA is thus the third natural product that can target calcineurin *via* a PPIase. Interestingly, it would appear that the CLA/CypA interface shares no obvious similarity with the CsA/CypA and FK506/FKBP12 interfaces, which interact with calcineurin at slightly different sites. Gallo *et al.*[101] have synthesised a number of synthetic CLA analogues, but fluorescence experiments indicate dissociation constants about 20-fold lower than for CsA binding CypA. A further cyclic peptide, isolated from linseed mill cake, is cyclo(-Pro-Pro-Phe-Phe-Ile-Leu-Leu-X-) (CLX), which contains the non-proteinaceous amino acid, *N*-methyl-4-aminoproline (X). This amino acid substitutes for two amino acid residues of CLA, mimicking a dipeptide moiety with a non-planar *cis* amide bond. This peptide also shows immunosuppressive activity.[102]

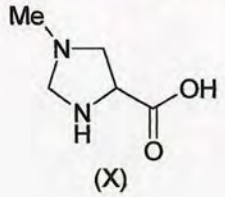

(X)

1.4.3 Peptide Ligands

Crystal structures have been determined for complexes of CypA-dipeptides: His-Pro, Ser-Pro, Ala-Pro, Gly-Pro.[103] The following larger peptides have also been characterised in complex with CypA:

- Ac-Ala-Ala-Pro-Ala-amc[104]
- Succ-Ala-Pro-Ala-*p*-Na[105]
- Succ-Ala-Xaa-Pro-Phe-*p*-Na[44] (where Xaa = Ala, Leu etc.) - used in chymotrypsin coupled PPIase assay

All peptides discussed form the CypA complex with a *cis* peptidyl-prolyl Xaa-Pro amide bond, and it has been observed that the main interactions are widely conserved:

- Proline binds in hydrophobic binding pocket
- CypA residues His126, Phe113, Phe60, (Met61, Leu122) are involved in hydrophobic interactions
- H-bonds to Asn102 from prolyl amide C=O and NH of the next *N*-terminal amino acid.
- Two H-bonds to Arg55 from proline C=O
- Larger peptides also show H-bonding to Trp121 and Gln 63, from amide C=O's

Comparison of the CypA binding of CsA with that of proline-containing peptide ligands reveals that many of the interactions are conserved:

- MeVal11 binds in hydrophobic pocket
- H-bond to Asn102 from Abu2 NH
- Two H-bonds to Arg55 from C=O of MeLeu10
- H-bonding to Trp121 and Gln63 from amide C=O's (E.coli Cyp does not have a Trp residue and is 1000 fold less sensitive toCsA).

It is interesting to note that CsA and the proline-peptides studied were found to bind with the respective peptide chains running in opposite directions. In general, proline-peptides bind CypA with a *cis* peptidyl-prolyl amide bond, whereas CsA and its derivatives bind CypA with a widely conserved *trans* 9-10 amide bond. It has also been reported that the peptides studied have lower affinity for CypA than CsA.[34]

1.4.4 Non-Peptide Ligands

Relatively few examples of rationally designed CypA ligands are available. Several are based on structures that mimic the Xaa-Pro *cis* amide bond. It has been suggested that CypA binds the Xaa-Pro substrate and distorts the amide bond by pyramidilising the prolyl nitrogen through hydrogen bonding,[106] with the active site Arg55 acting as the hydrogen donor. As discussed previously, structural studies

indicate that Cyp is highly selective for *cis* substrates, binding several Xaa-Pro peptide substrates in the *cis* conformation.

Hart and Etzkorn[107] have reported cyclophilin inhibition by a (Z)-alkene *cis*-proline isostere of the Ala-Pro dipeptide. This structure was found to overlay the dipeptide with a RMS deviation of 0.17 Å, indicating that it is an ideal conformationally locked mimic of the bound substrate. The inhibitor **2** was designed based on the succ-AAPF-pNa peptide substrate by replacing the central Ala-Pro core with (Z)-alkene *cis*-Pro mimic **1**. The PPIase assay indicated that the substrate mimic inhibits the enzymatic activity of CypA with an IC_{50} of 6.5 ± 0.5 μM. The peptide mimic was incorporated as shown in Scheme 1.2. Alanine and phenylalanine were coupled in solution using HBTU in the first two steps, and the succinyl *N*-terminus was installed with succinic anhydride.

Scheme 1.2

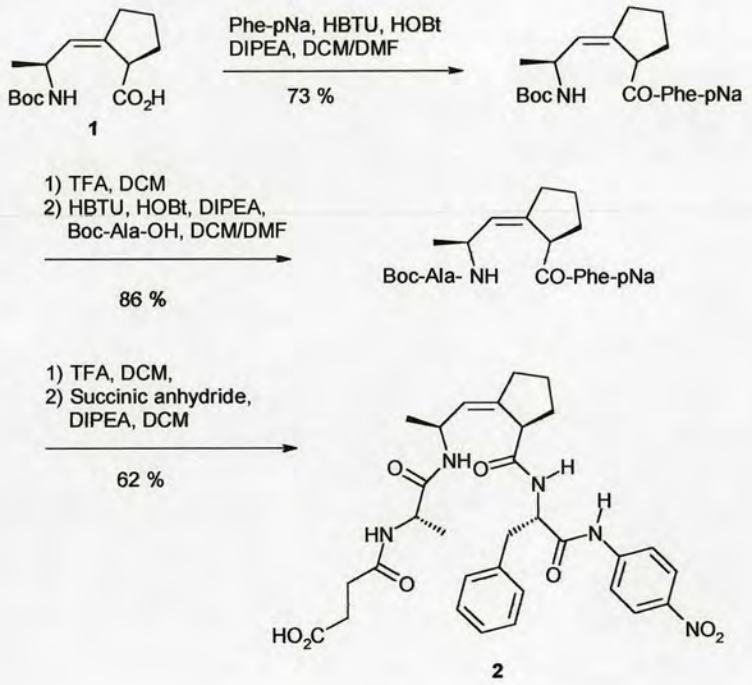

Conformationally constrained analogues (1-(*R*), 1-(*S*) and 2-(*R*), 2-(*S*)) of the Suc-Ala-Gly-Pro-Phe-pNa tetrapeptide have been synthesised by incorporation of fluoroolefin peptide isosteres to control the peptide conformation.[108] Fluoroolefins, suggested to be good steric and electronic mimics for peptide bonds, were used to fix

the conformation of the Gly-Pro amide bond in the *cis* and *trans* conformations. The fluoroolefin was synthesised according to the procedure shown in Scheme 1.3.

Scheme 1.3

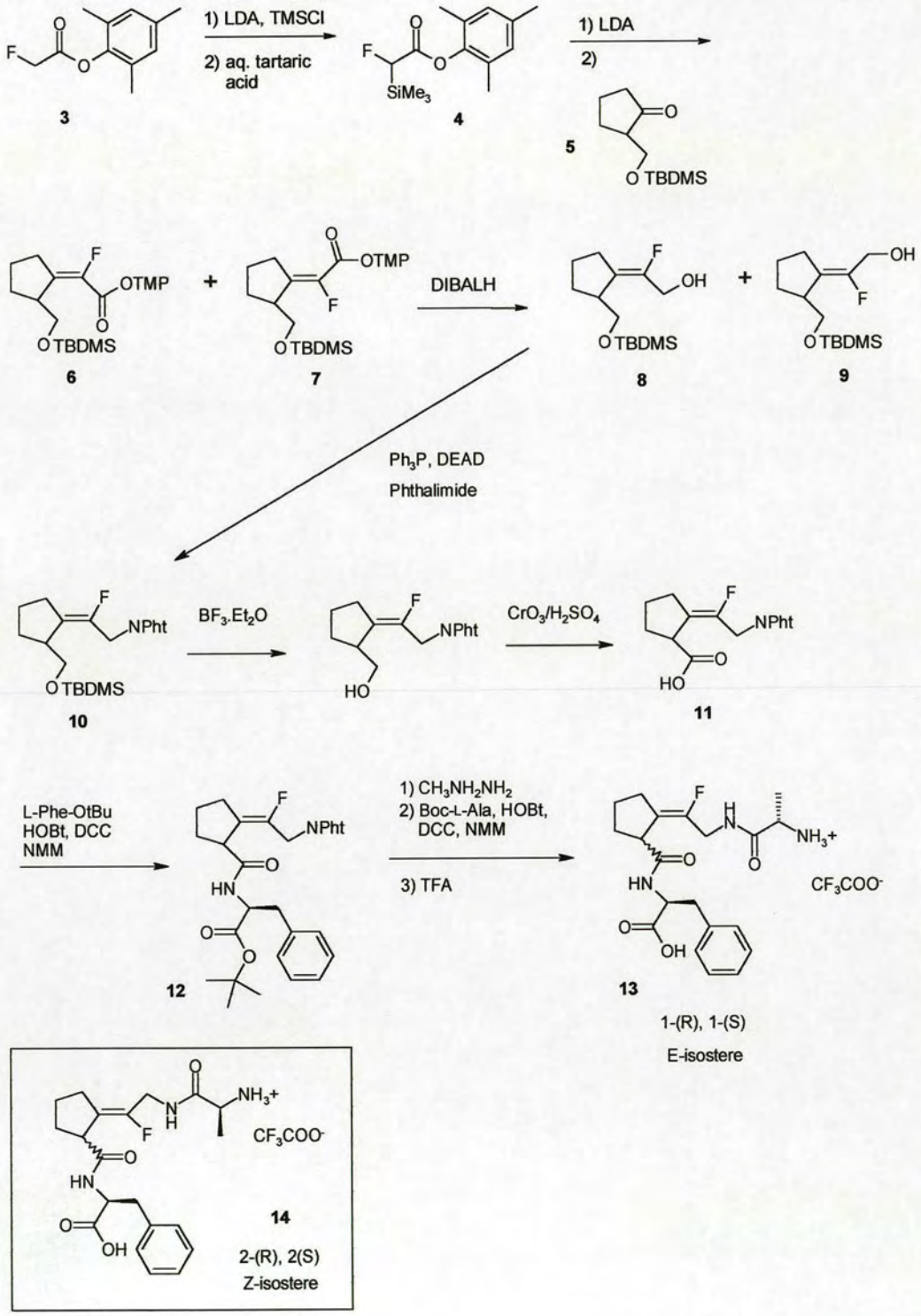

Bissilylation of the α-fluoroacetate **3** by excess lithium diisopropylamide and chlorotrimethylsilane, followed by hydrolysis of the O-silyl group with aqueous tartaric acid solution provided the α-fluoro-α-silylacetic acid ester **4**. Peterson olefination of the 2-hydroxymethylcyclopentanone derivative **5** with the acid ester **4** yielded a 6:1 mixture of the E-and Z-isomers, **6** and **7**. These isomeric esters were reduced with diisobutylaluminium hydride to the corresponding alcohols **8** and **9**, before separation by chromatography on silica gel. Mitsunobu transformation yielded the protected amine **10**, followed by removal of the TBDMS group with boron trifluoride etherate and oxidation with Jones reagent to form the *N*-protected dipeptide isostere **11**. The acid **11** was coupled to L-phenylalanine-*tert*-butyl ester using DCC in the presence of HOBt and NMM to form **12**. The phthaloyl group was removed and the free amine coupled with Boc-L-alanine to form a diastereomeric mixture of isosteres, which were separated by column chromatography and deprotected to give the 1-(*R*) and 1-(*S*) tetrapeptide isosteres **13**. A similar method provided the 2-(*R*) and 2-(*S*) isosteres **14**.

The Z-isomers mimic the *trans* conformation of the natural peptide, while the E-isomers correspond to the *cis* conformation. In a preliminary PPIase assay, the two E-isomers and one of the two Z-isomers were found to inhibit cyclophilin.

Wang *et al.*[109] have described the synthesis of ground- **15** and transition-state **16** analogue inhibitors of CypA, based on the structures of proline containing peptides. Design of the inhibitors was based on the "twisted amide" transition-state mechanism for CypA-catalysed peptide isomerisation, proposed by Stein[39] and others. In this catalysis by distortion, the substrate is thought to adopt a transition-state conformation in which the carbonyl group and the nitrogen lone pair of the Ala-Pro amide bond are orthogonal to each other as shown in Scheme 1.4. After binding to the enzyme in the *trans* conformation, the substrate is distorted by the active site and the amide bond is twisted out of planarity, with simultaneous formation of a hydrogen bond between the active site and the pyramidal Pro nitrogen. Again, the Arg55 residue of CypA is the proposed hydrogen bond donor.

Scheme 1.4

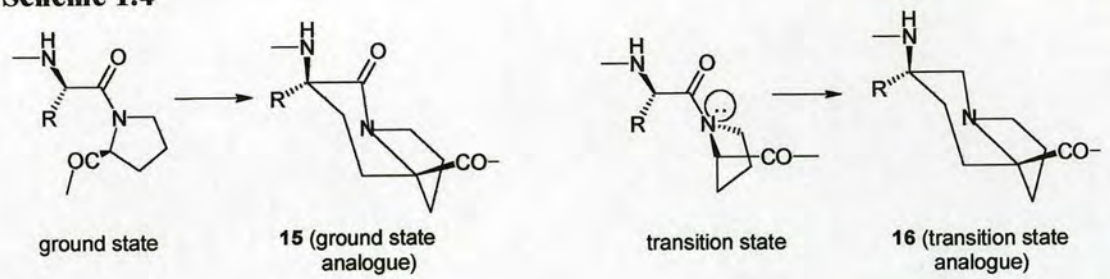

The ground-state inhibitors were based on a bicyclic lactam structure since it was previously found to display structural similarity to *cis*-Gly-Pro in the cyclophilin-bound conformation, and bind to the active site of CypA with $K_d = 200$ μM.[110] The transition-state analogues incorporated an amine functionality in place of the lactam, in order to provide a tertiary amine nitrogen capable of interacting with the Arg55 residue. Synthesis commenced with the bicyclic lactam **17** synthesised previously by this group from L-proline.[111] The benzaldehyde imine **18** was prepared and stereoselective alkylation of the lithium enolate with benzyl bromide or 2-bromomethylnaphthyl furnished the α-aryl lactams **19 (a,b)** (Scheme 1.5). Hydrolysis of the imine, followed by reaction of the resulting free amine with a set of acylating agents yielded the ground-state inhibitors **20 (a-f)**.

Scheme 1.5 (a) TFA; (b) PhCHO, Et_3N; (c) LDA, R^1X, -78 °C; (d) MeOH, HCl; (e) R^2COX.

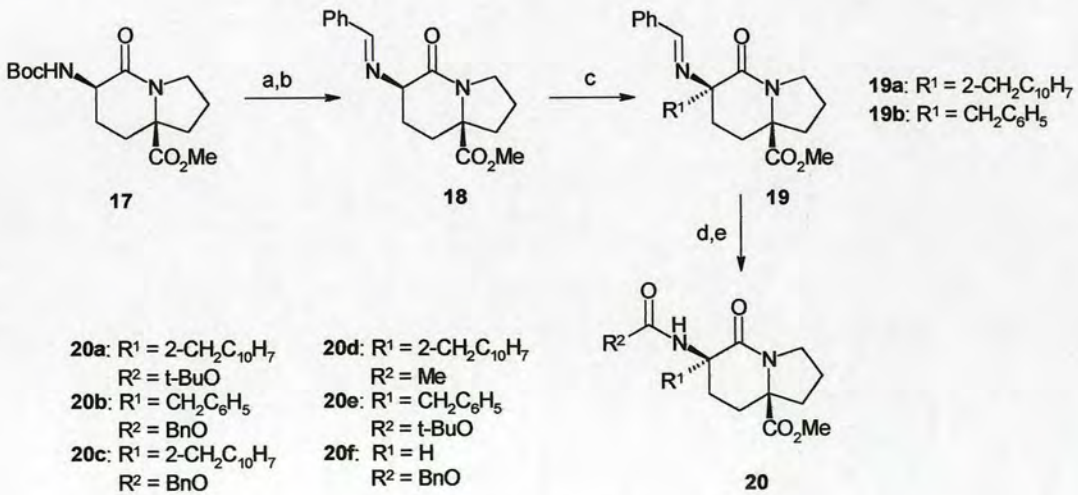

The transition-state inhibitors **22 (a,b)** and **26** were prepared by selective reduction of the thioamide derivative of the amide (Scheme 1.6). Thioamides **23 (a,b)** and **25** were formed from the corresponding lactams **21 (a,b)** and **24** by treatment with Lawesson's reagent.

Scheme 1.6 (a) Lawesson's reagent, $PhCH_3$, 80 °C; (b) Raney nickel, H_2.

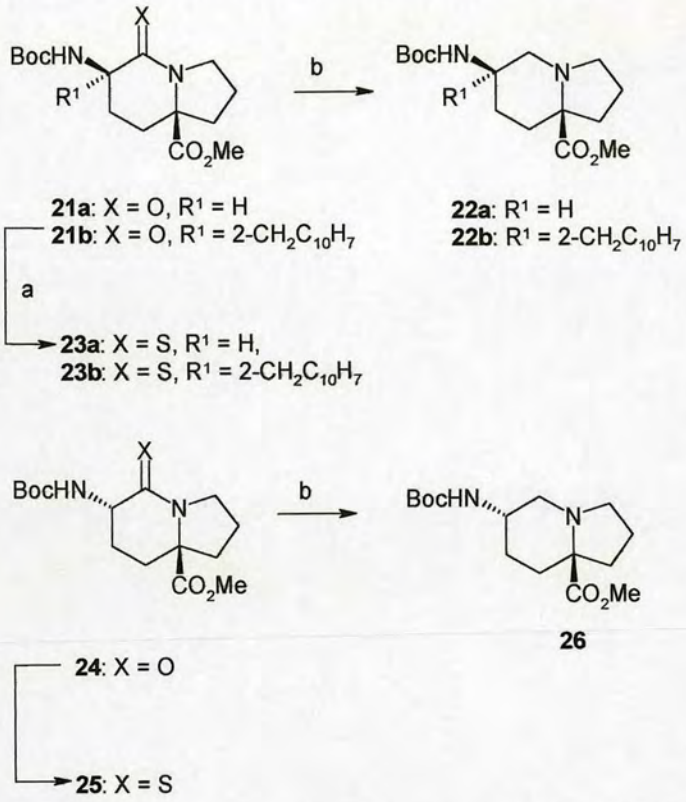

With the rational design of the first transition-state analogue PPIase inhibitors, the authors hoped to observe greater affinity for CypA. Binding of the inhibitors was measured by fluorescence assay and results are shown in Table 1.4.

Table 1.4

Compound	K_d (μM)
21	> 200
20a	17 ± 8
20b	124 ± 30
20c	4.7 ± 2
20d	1.5 ± 0.05
20e	140 ± 32
20f	> 200

Compound	K_d (μM)
22a	> 200
22b	77 ± 18
24	> 200
26	> 200

Several ground-state analogues bound to the enzyme with low micromolar affinity (K_d = 1.5 μM for **20d**), but unexpectedly the transition-state analogues did not display any significant affinity for the active site (K_d = 77 μM for **22b**). Analysis of the binding of bicyclic amides **21**, and amines **22** and **26** to CypA did reveal several distinct structure-activity trends. Little information on the effect of stereochemistry at the position alpha to the lactam carbonyl could be discerned due to the low affinity for analogues **21a** and **24**, and **22a** and **26** for the enzyme. However, with the same α-alkyl group, the affinity of the bicyclic amide was found to increase as the size of the amino substituent, R^2, decreased. With the same alkylamide group, increasing the size of the alkyl substituent, R^1, resulted in a corresponding increase in binding affinity. These findings were consistent with the proposed binding model based on the structure of dipeptide:CypA complexes. In this model there is a relatively narrow groove for incorporation of the amino substituent, R^2, in the region of the active site where the *N*-terminus of a peptide substrate would be located. The alkyl group, R^1, would project into the hydrophobic pocket of the active site, where larger and more hydrophobic groups form favourable interactions. Hence, the highest affinity ligand, **20d**, combined the smallest amide substituent (*N*-acetyl) with the most hydrophobic α-alkyl group (2-methylnaphthyl). Postulated explanations for the lower affinity of transistion-state analogues include the possibility that a conformational change in the enzyme on binding of bicyclic ligands may disfavour formation of the stabilising hydrogen bond to Arg55, or the lone pair of the analogue **22b** may not be appropriately geometrically aligned to form interactions with the active site residues. A second possibility is that the carbonyl oxygen of the lactam is important for binding, perhaps forming a hydrogen bond. Alternatively, it may be that CypA has a different catalytic mechanism to the proposed twisted amide model.

This work represents another example of small molecular weight compounds with the ability to form tight complexes with CypA. The affinity of analogue **20d** is however, still 5000 times lower than that of the undecapeptide CsA.

Choi *et al.*[112] have reported the synthesis of non-peptidic cyclophilin binding compounds for use in neuronal cell regeneration and neurodegenerative conditions. Structures of the form **27-29** of Scheme 1.7 were found to bind to cyclophilin (and in some cases FKBP) inhibiting their PIase activity with an IC_{50} of 1 μM or less.

Scheme 1.7

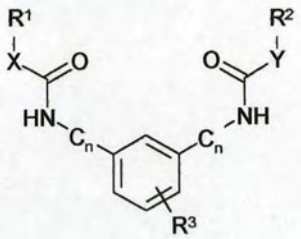

27

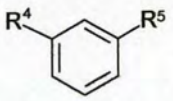

28

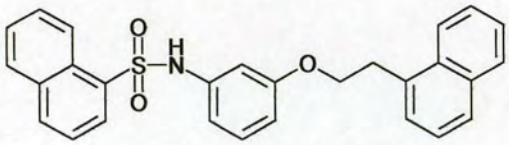

29

C_n = 0,1
X = N, NH, O, S etc.
Y = N, NH, O, S, etc.
R^1 = C1-C6 (branched)alk(en)yl groups with optional cyclic substituents.
R^2 = as R^1
R^3 = halo, OH, NO_2, CF_3, NH_2 C1-C6 (branched) alkyl, C1-C4 alk(enyl)oxy, phenoxy

R^4 = NSO_2R, SO_2NR_2, OR, CONR, COR where R is H, substituted cyclic, or as R^1
R^5 = as R^4

The cyclic urea **30** has been designed to be a potential competitive inhibitor of CypA-Gag binding, thus interfering with HIV virus replication.[113]

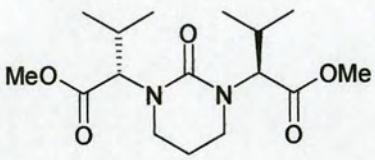

30

1.5 Lead Discovery

In the discovery of the lead ligand for the current work, two methods were used for ligand design: *de novo* construction of novel ligands from atoms using the docking programme LIDAEUS; and modification of lead structures obtained from database searching using the principles of structural similarity. An overview of the entire process is included in Figure 1.4.

Figure 1.4: Ligand Design and Synthesis

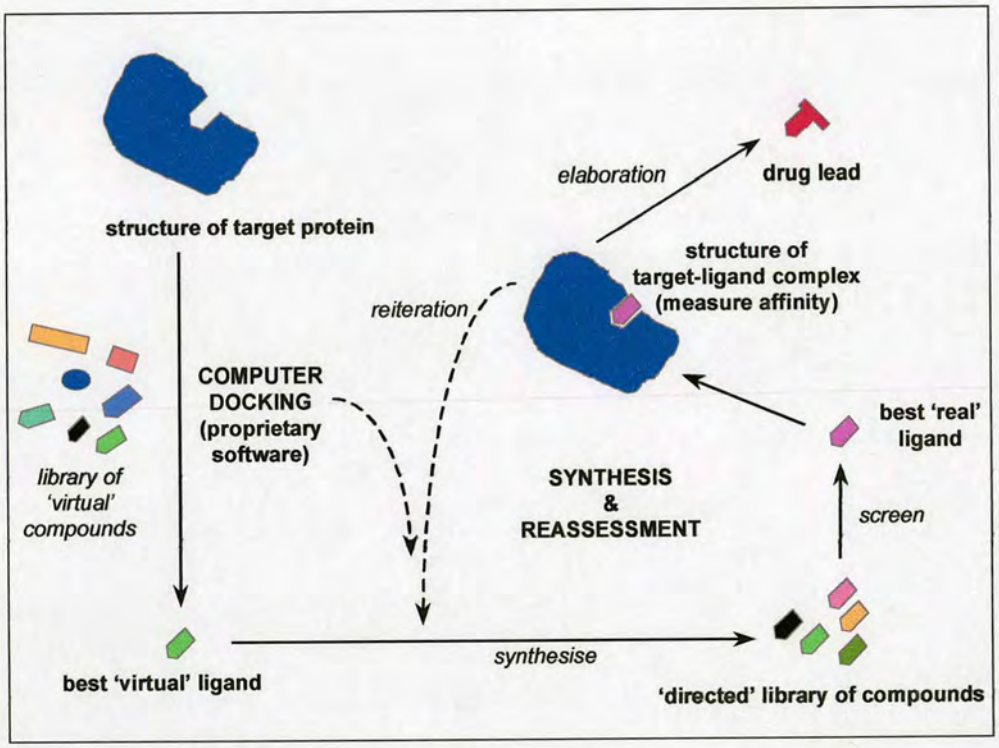

The LIDAEUS programme, developed by Dr Paul Taylor at Edinburgh University, calculates the interaction energy between a "probe atom" and the protein on a 3D grid of site points around the protein active site. In the calculation carbon and oxygen atoms are used as probe atoms, with favoured hydrophilic interactions mapped out by the carbon atoms, to generate areas of low energy in the protein active site. A negative template of the active site of the target protein can then be generated, by

turning the areas of low energy into site points. The template obtained contains information on the geometrical and chemical properties of putative ligands. The data can then be then used to search the Maybridge Fine Chemicals database to select the best-fitting ligand for the site points. The list of commercially available compounds obtained is subjected to a second selection process on the basis of molecular weight and hydrophobicity. The most hydrophobic ligands with molecular weight less than 300 are chosen, since smaller, hydrophobic ligands can more easily penetrate the crystal to reach the binding site.

Using the LIDAEUS programme, the first non-peptide ligands of CypA were discovered and their X-ray structures determined. [114] The novel ligands, which all bind in the same site, belong to three families: the piperidine family (3-acetyl-1-methyl piperidine **31** and ethyl piperidine glyoxylate **32**); the DMSO family (dimethyl sulfoxide **33**, tetramethylene sulfoxide **34** and cyclopentanone **35**); and the dimedone family (5,5-dimethyl-1,3-cyclohexanedione **36**), as indicated in Table 1.5. This thesis will focus on the dimedone family.

Table 1.5

Piperidine family	DMSO family	Dimedone family
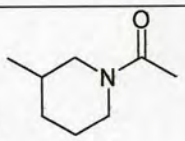 **31**	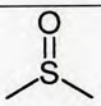 **33**	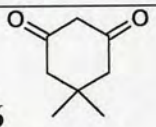 **36** K_d= 22 mM
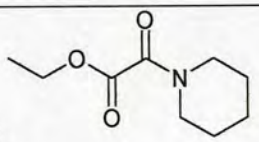 **32**	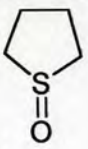 **34**	
	 **35**	

1.5.1 The Discovery of Dimedone

The LIDAEUS programme indicated that 2,2,5-trimethyl-1,3-dioxane-4,6-dione **37** (Scheme 1.8) could potentially bind to the protein active site. However, crystal soaking experiments proved unsuccessful and no evidence of the ligand could be observed in binding site by X-ray crystallography. The lead **37** was then partially modified (Scheme 1.8), based on knowledge of the binding of other families of ligands and on modelling studies, which indicated that the side of the molecule facing the binding site should be hydrophobic. The two ether oxygens of the lead **37** were therefore replaced by carbon atoms, in order to increase the hydrophobicity in that domain. The new molecule **38** was then used to search for structurally similar molecules in the ISIS database and dimedone **36** was found to be the most structurally similar and commercially available compound.

Scheme 1.8

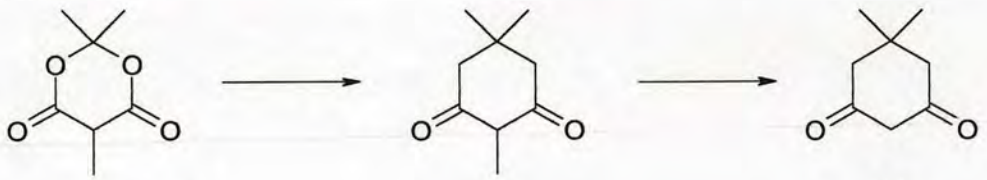

37 **38** **36**

The computationally designed lead structure, dimedone, was then tested experimentally for binding to the CypA protein. A K_d of 22 mM was determined for the inhibition of CypA by dimedone using the PPIase assay. For comparison, the K_d of CsA has been measured as 36.8 nM[115] using the same assay. The crystal structure of dimedone bound to the active site of CypA was obtained after soaking CypA crystals in a solution of the dimedone ligand, according to the method described in Chapter 2. Figure 1.5 shows the crystal structure of the dimedone(green):CypA complex, with the CsA(white):CypA complex superimposed. The dimedone geminal dimethyl groups bind within the hydrophobic pocket of the CypA active site, mimicking the hydrophobic interaction of the MeVal11 residue of CsA with CypA. The MeLeu10 residue of CsA is known to form a hydrogen bond to Arg55 of CypA.

One of the carbonyl groups of dimedone is within range of Arg55 to mimic this hydrogen bonding interaction.

Figure 1.5

1.6 References

[1] Armistead, D. M.; Harding, M. W., *Ann. Rep. Med. Chem.*, 1993, **28**, 207.

[2] Klebe, G., *J. Mol. Med.*, 2000, **78**, 269-281.

[3] Wieland, T., *J. Math. Chem.*, 1997, **21**, 141-157.

[4] Laskowski, R. A.; Hutchinson, E. G.; Michie, A. D.; Wallace, A. C.; Jones, M. L.; Thornton, J. M., *Trends Biochem. Sci.*, 1997, **22**, 488-490.

[5] Venuti, M. C., *Ann. Rep. Med. Chem.*, 1990, **25**, 289.

[6] Clore, G. M.; Gronenborn, A. M., *Science*, 1991, **252**, 1390.

[7] Whittle, P.; Blundell, T., *Ann. Rev. Biophys. Biomol. Struct.*, 1994, **23**, 349-375.

[8] Swanson, M. E.; Grass, D. S., *Ann. Rep. Med. Chem.*, 1994, **29**, 265.

[9] Trainor, G. L., *Anal. Chem.*, 1990, **62**, 418-426.

[10] Babine, R. E.; Bender, S. L., *Chem. Rev.*, 1997, **97**, 1359-1472.

[11] Walkinshaw, M.D.; Weber, H. P.; Widmer, A., *Triangle*, 1986, **25**, 131-142.

[12] Gubernator, K.; Boehm, M., *Methods Princ. Med. Chem.*, 1998, **6**, 1-13.

[13] Kubinyi, H., *Curr. Opin. Drug Disc. Dev.*, 1998, **1**, 1, 16-27.

[14] Kubinyi, H., *Chimica Oggi*, 1998, **16**, 17-22.

[15] Ripka, A. S.; Rich, D. H., *Curr. Opin. Chem. Biol.*, 1998, **2**, 441-452.

[16] Beeley, N. R., *Drug Disc. Today*, 2000, **5**, 354-363.

[17] Hirschmann, R., *Angew. Chem. Int. Ed. Engl.*, 1991, **30**, 1278.

[18] Kessler, H., *Angew. Chem. Int. Ed. Engl.*, 1982, **21**, 512.

[19] Grøn, H.; Hyde-DeRuyscher, R., *Curr. Opin. Drug Disc. Dev.*, 2000, **3**, 5, 636-645.

[20] Shuker, S. B.; Hajduk, P. J.; Meadows, R. P.; Fesik, S. W., *Science*, 1996, **274**, 1531-1534.

[21] Hajduk, P. J.; Olejniczak, E. T.; Fesik, S. W., *J. Am. Chem. Soc.*, 1997, **119**, 12257-12261.

[22] Fischer, G.; Bang, H.; Mech, H., *Biomed. Biochim. Acta*, 1984, **43**, 1101-1111.

[23] Handschumacher, R. E.; Harding, M. W.; Rice, J.; Drugge, R. J.; Speicher, D. W., *Science*, 1984, **226**, 544-546.

[24] Fischer, G.; Wittmann-Liebold, B.; Land, K.; Kiefhaber, T.; Schmid, F. X., *Nature*, 1989, **337**, 476-478.

[25] Harding, M. W.; Galat, A.; Ueling, S. L.; Schreiber, S.; *Nature*, 1989, **341**, 761-763.

[26] Sikierka, J. J.; Hung, S. H. Y.; Poe, M.; Lin, S. C.; Singal, N. H., *Nature*, 1989, **341**, 755-757.

[27] Kino, T.; Hatanaka, H.; Hashimoto, M.; Nishiyama, M.; Goto, T.; Okuhara, M., *J. Antibiotics*, 1987, **40**, 1249-1255.

[28] Sehgal, S. N.; Baker, H.; Vezina, C., *J. Antibiotics*, 1975, **28**, 727-732.

[29] Rahfeld, J. U.; Schierhorn, A.; Mann, K.; Fischer, G., *FEBS Lett.*, 1994, **343**, 64-69.

[30] Henning, L.; Chistner, C.; Kipping, M.; Schelbert, B.; Rücknagel, K.; Grabley, S., *Biochemistry*, 1998, **37**, 5953-5960.

[31] Liu, J.; Albers, M. W.; Chen, C. M.; Schreiber, S. L.; Walsh, C. T., *Proc. Natl. Acad. Sci. U.S.A.*, 1990, **87**, 2304-2308.

[32] Bierer, B. E.; Mattila, P. S.; Standaert, R. F.; Herzenberg, L. A.; Burakoff, S. J.; Crabtree, G.; Schreiber, S. L., *Proc. Natl. Acad. Sci. U.S.A.*, 1990, **87**, 9231-9235.

[33] Borel, J. F., *Pharmacol. Rev.*, 1989, **41**, 259-371.

[34] Taylor, P.; Husi, H.; Kontopodis, G.; Walkinshaw, M. D., *Prog. Biophys. Molec. Biol.*, 1997, **67**, 151-181.

[35] Kallen, J.; Mikol, V.; Taylor, P.; Walkinshaw, M. D., *J. Mol. Biol.*, 1998, **283**, 435-449.

[36] Göthel, S. F.; Marahiel, M. A., *Cell Mol. Life Sci.*, 1999, **55**, 423-436.

[37] Stewart, D. E.; Sarkar, A.; Wampler, J. E., *J. Mol. Biol.*, 1990, **214**, 253-260.

[38] Kiefhaber, T.; Quaas, R.; Hahn, U.; Schmid, F. X., *Biochemistry*, 1990, **29**, 3061-3070.

[39] Harrison, R. K.; Stein, R. L., *Biochemistry*, 1990, **29**, 1684-1689.

[40] Kofron, J. L.; Kuzmic, P.; Kichore, V.; Colon-Bonilla, E.; Rich, D. H., *Biochemistry*, 1991, **30**, 6127-6134.

[41] Radzacki, A.; Acheson, S. A.; Wolfenden, R.; *Bioorg. Chem.*, 1992, **20**, 382-386.

[42] Ke, H. M.; Mayrose, D.; Cao, W., *Proc. Natl. Acad. Sci. U.S.A.*, 1993, **90**, 3324-3328.

[43] Konno, M.; Ito, M.; Hayano, T.; Takahashi, N., *J. Mol. Biol.*, 1996, **256**, 897-908.

[44] Zhao, Y.; Ke, H., *Biochemistry*, 1996, **35**, 7356-7361.

[45] Göthel, S. F.; Marahiel, M. A., *Cell Mol. Life Sci.*, 1999, **55**, 423-436.

[46] Kallen, J.; Mikol, V.; Taylor, P.; Walkinshaw, M. D., *J. Mol. Biol.*, 1998, **283**, 435-449.

[47] Griffith, J. P.; Kim, J. L.; Kim, E. E.; Sintchak, M. D.; Thompson, J. A.; Fitzgibbon, M. J.; Fleming, M. A.; Caron, P. R.; Hsiao, K.; Navia, M. A., *Cell*, 1995, **82**, 507.

[48] Zydowsky, L. D.; Etzkorn, F. A.; Chang, H. Y.; Ferguson, S. B.; Stolz, L. A.; Ho, S. I.; Walsh, C. T., *Protein Sci.*, 1992, **1**, 1092-1099.

[49] Morris, R.E., *Ther. Drug Monit.*, 1995, **17**, 564-569.

[50] Starzl, T.; fung, J.; Venkataramman, R.; Todo, S.; demetris, A. J.; Jain, A., *The Lancet*, 1989, 1000.

[51] Franke, E. K.; Yuan, H. E.; Luban, J., *Nature*, 1994, **372**, 359-362.

[52] Gelderblom, H. R., *AIDS*, 1991, **5**, 617-638.

[53] Zhao, Y.; Chen, Y.; Schutkowski, M.; Fischer, G.; Ke, H., *Structure*, 1997, **5**, 139-146.

[54] Vajdos, F. F.; Yoo, S.; Houseweart, M.; Sundquist, W. I.; Hill, C. P., *Protein Sci.*, 1997, **6**, 2297-2307.

[55] Braaten, D,; Franke, E. K.; Luban, J., *J. Virol.*, 1996, **70**, 3551-3560.

[56] Wiegers, K.; Rutter, G.; Schubert, U.; Grattinger, M.; Krausslich, H.-G., *Virology*, 1999, **257**, 261-274.

[57] Luban, J.; Bossolt, K. L.; Franke, E. K.; Kalpana, G. V.; Goff, S. P., *Cell*, 1993, **73**, 1067-1078.

[58] Franke, E. K.; Luban, J., *Virology*, 1996, **229**, 279-282.

[59] Mlynar, E.; Bevec, D.; Billich, A,; Rosenwirth, B.; Steinkasserer, A., *J. General Virology*, 1997, **78**, 825-835.

[60] Thali, M., *Mol. Med. Today*, 1995, 287-291.

[61] Schutkowski, M.; Drewello, M.; Wöllner, S.; Jakob, M.; Reimer, U.; Scherer, G.; Schierhorn, A.; Fischer, G., *FEBS Lett.*, 1996, **394**, 289-294.

[62] Li, Q.; Moutiez, M.; Charbonnier, J.-B.; Vaudry, K.; Ménez, A.; Quéméneur, E.; Dugave, C., *J. Med. Chem.*, 2000, **43**, 1770-1779.

[63] Bradley, G.; Juranka, P. F.; Ling, V., *Biochim. Biophys. Acta*, 1988, **948**, 87-128.

[64] Gottesman, M. M.; Pasta, I., *Biochim. Biophys. Acta*, 1993, **948**, 385-427.

[65] Lavie, Y.; Cao, H.; Burnsen, S. L.; Giuliano, A. E.; Cabot, M. C., *J. Biol. Chem.*, 1996, **271**, 19530-19536.

[66] Nayfield, S. G., *J. Cell Biochem.*, 1995, **22**, 42-50.

[67] Lavie, Y.; Cao, H.; Volner, A.; Lucci, A.; Han, T.; Geffen, V.; Giuliano, A. E.; Cabot, M. C., *J. Biol. Chem.*, 1997, **272**, 1682-1687.

[68] Slater, L. M.; Sweet, P.; Stupecky, M.; Gupta, S., *J. Clin. Invest.*, 1986, **77**, 1405-1408.

[69] Archinal-Mattheis, A.; Rzepka, R. W.; Watanabe, T.; Kokubu, N.; Itoh, Y.; Combates, N. J.; Blair, K. W.; Cohen, D., *Oncol. Res.*, 1998, **7**, 603-610.

[70] Page, A. P.; Kumar, S.; Carlow, C. K. S., *Parasitology Today*, 1995, **11**, 385-388.

[71] Taylor, P.; Page, A. P.; Kontopidis, G.; Husi, H.; Walkinshaw, M. D., *FEBS Lett.*, 1998, **425**, 361-366.

[72] Chappell, L. H.; Wastling, J. L., *Parasitology*, 1992, **105**, S25-S40.

[73] Leech, J. H., *J. Exp. Med.*, 1984, **159**, 1567-1575.

[74] Hsiao, L. L., *Biochem. J.*, 1991, **274**, 121-132.

[75] Ke, H.; Mayrose, D.; Belshaw, P. J.; Alberg, D. G.; Schreiber, S. L.; Chang, Z. Y.; Etzkorn, F. A.; Ho, S.; Walsh, C. T., *Structure*, 1994, **2**, 33-44.

[76] Kallen, J.; Mikol, V.; Taylor, P.; Walkinshaw, M. D., *J. Mol. Biol.*, 1998, **283**, 435-449.

[77] Billich, A.; Hammerschmid, F.; Peichl, P.; Wenger, R.; Zenke, G.; Quesniaux, V.; Rosenwirth, B., *J. Virology*, 1995, **69**, 2451-2461.

[78] Cabot, M. C.; Han, T.; Giuliano, A. E., *FEBS Lett.*, 1998, **431**, 185-188.

[79] Mikol, V.; Taylor, P.; Kallen, J.; Walkinshaw, M. D., *J. Mol. Biol.*, 1998, **283**, 451-461.

[80] Papageorgiou, C.; Kallen, J.; France, J.; French, R., *Bioorg. Med. Chem.*, 1997, **5**, 187-192.

[81] Hu, M.-K.; Badger, A.; Rich, D. H., *J. Med. Chem.*, 1995, **38**, 4164-4170.

[82] Schramm, U.; fricker, G.; Wenger, R.; Miller, D. S., *American J. Physiology*, 1995, **37**, F46-F52.

[83] Moss, M. L.; Palmer, R. E.; Kuzmič, P.; Dunlap, B. E.; Henzel, W.; Kofron, J. L.; Mellon, W. S.; Royer, C. A.; Rich, D. H., *J. Biol.Chem.*, 1992, **267**, 22054-22059.

[84] Nelson, P. A.; Akselband, Y.; Kawamura, A.; Su, M.; Tung, R. D.; Rich, D. H.; Kishore, V.; Rosborough, S. L.; DeCenzo, M. T.; Livingston, D. J.; Harding, M. W., *J. Immunology*, 1993, **150**, 2139-2147.

[85] Keller, M.; Wöhr, T.; Dumy, P.; Patiny, L.; Mutter, M., *Chem. Eur. J.*, 2000, **6**, 4358-4363.

[86] Papageorgiou, C.; Florineth, A.; French, R.; Haltiner, R.; Borer, X., *Bioorg, & Med. Chem. Lett.*, 1993, **3**, 2559-2564.

[87] Papageorgiou, C.; Weber, H.P.; French, R.; Borer, X., *Bioorg. & Med. Chem. Lett.*, 1995, **5**, 213-218.

[88] Bartz, S. R.; Hohenwalter, E.; Hu, M.-K.; Rich, D. H.; Malkovsky, M., *Proc. Natl. Acad. Sci.* U.S.A., 1995, **92**, 5381-5385.

[89] Hubler, F.; Rückle, T.; Patiny, L.; Muamba, T.; Guichou, J.-F.; Mutter, M.; Wenger, R., *Tet. Lett.*, 2000, **41**, 7193-7196.

[90] Husi, R.; Zurini, M. G. M., *Anal. Biochem.*, 1994, **222**, 251-255.

[91] Papageorgiou, C.; Borer, X.; French, R.R., *Bioorg. & Med. Chem. Lett.*, 1994, **4**, 267-272.

[92] Aebi, J.D.; Guillaume, D.; Dunlap, B.E.; Rich, D.H., *J. Med. Chem.*, 1988, **31**, 1805-1815.

[93] Alberg, D. G.; Schreiber, S. L., *Science*, 1993, **262**, 248-250.

[94] Traber, R.; Hofmann, H.; Loosli, H-R.; Ponelle, M.; von wartburg, A., *Helvetica Chimica Acta*, 1987, **70**, 13-34.

[95] Ko, S.Y.; Wenger, R.M., *Helvetica Chimica Acta*, 1997, **80**, 695-705.

[96] Lawen, A.; traber, R.; Geyl, D.; Zocher, R.; Kleinkauf, H., *J. Antibiotics*, 1989, **42**, 1283-1289.

[97] Sanglier, J.-J.; Quesniaux, V.; Fehr, T.; Hofmann, H.; Mahnke, M.; Memmert, K.; Schuler, W.; Zenke, G.; Gschwind, L.; Maurer, C.; Schilling, W., *J. Antibiotics*, 1999, **52**, 466-473.

[98] Fehr, T.; Kallen, J.; Oberer, L.; Sanglier, J.-J.; Schilling, W., *J. Antibiotics*, 1999, **52**, 474-479.

[99] Fehr, T.; Quesniaux, V.F. J.; Sanglier, J.-J.; Oberer, L.; Gschwind, L.; Ponelle, M.; Schilling, W.; Wehrli, S.; Enz, A.; Zenke, G.; Schuler, W., *J. Antibiotics*, 1997, **50**, 893-899.

[100] Gaymes, T. J.; Cebrat, M.; Siemion, I. Z.; Kay, J. E., *FEBS Lett.*, 1997, **418**, 224-227.

[101] Gallo, P.; Rossi, F.; Saviano, M.; Pedone, C.; Colonna, G.; Ragone, R., *J. Biochem.*, 1998, **124**, 880-885.

[102] Picur, B.; Lisowski, M.; Siemion, I. Z., *Lett. Pept. Sci.*, 1998, **5**, 183-187.

[103] Zhao, Y.; Ke, H., *Biochem.* 1996, **35**, 7362-7368.

[104] Zurini, M.; Kallen, J.; Mikol, V.; Pfluegl, G.; Jansonius, J. N.; Walkinshaw, M. D., *FEBS Lett.*, 1990, 276, **1**, 63-66.

[105] Konno, M.; Ito, M.; Hayano, T.; Takahashi, N., *J. Mol. Biol.*, 1996, **256**, 897-908.

[106] Fischer, S.; Dunbrack, R. L., Jr.; Karplus, M., *J. Am. Chem. Soc.*, 1994, **116**, 11931-11937.

[107] Hart, S. A.; Etzkorn, F. A., *J. Org. Chem.*, 1999, **64**, 2998-2999.

[108] Boros, L. G.; De Corte, B.; Gimi, R. H.; Welch, J. T.; Wu, Y.; Handschumacher, R. E., *Tett. Lett.*, 1994, **35**, 6033-6036.

[109] Wang, H. C.; Kim, K.; Bakhtiar, R.; Germanas, J. P., *J. Med. Chem.*, 2001, **44**, 2593-2600.

[110] Germanas, J. P.; Kyonghee, K.; Dumas, J.-P., *Adv. Amino Acids Peptidomimetics*, 1997, **1**, 233-250.

[111] Wang, H.; Germanas, J. P., *Synlett*, 1999, 33-35.

[112] Choi, C.; Hamilton, G.; Steiner, J.; Vaa,. M.; Ling, W., *PCT Int. Appl.*, 2001, 57.

[113] Hoye, T.; Van Veldhuizen, J., *Abstracts of Papers Amer. Chem. Soc.*, 1999, **217**, 278.

[114] Thesis: Kontopidis, G.A., *Immunophilin Ligand Design*, Edinburgh University, 1999, 7.13.

[115] Husi, H.; Zurini, M., *Anal. Bioch.*, 1994, **222**, 251-255.

2 Results and Discussion I

2.1 Aim

The overall aim of this project was to use combinatorial methods to generate a library of potential CsA mimics based on the lead compound dimedone. The compounds generated would have potential application as probes for the biological mechanisms of action of cyclophilins and CsA. Initial studies concentrated on the development of robust dimedone chemistry, which could then be adapted for automated library generation.

There are several advantages to using dimedone as a lead structure for library synthesis. Firstly, dimedone is commercially available and inexpensive, and secondly, the symmetrical molecule makes a good scaffold for further reaction. Additionally, there are several positions at which dimedone can be derivatised in order to prepare a diverse range of combinatorial building blocks. Investigation of the literature on reactions concerning dimedone, revealed that a wealth of different derivatives had been prepared. With such a choice available it was necessary to begin with a more simplified approach for creation of a few structures that would potentially give us some preliminary information on the interaction of dimedone with the CypA binding site. Rather than attempting to generate many different analogues, our initial strategy was to design ways to build out from the dimedone core in several directions, in order to gain a better understanding of the available space within the CypA binding site. The 1,3-dicarbonyl group is compatible with a range of synthetic chemistry both at the carbonyl group and methylene group, while still preserving the two points of interaction with the protein active site (Figure 2.1).

Figure 2.1

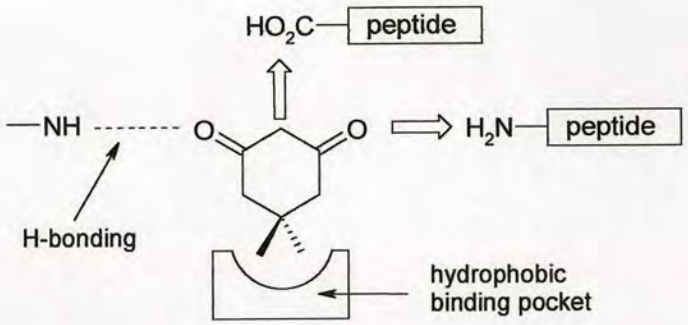

The first design decision was to prepare peptide analogues of dimedone. Since the natural ligand CsA is an undecapeptide, it seemed reasonable that we could locate our core dimedone scaffold within the hydrophobic binding pocket of the CypA binding site and then expect to mimic some of the hydrogen bond contacts between the peptide backbone of CsA and the protein, by attachment of amino acids to this fixed core. The initial task was therefore to design a method of incorporation of the dimedone structure into the peptide chain. With library generation in mind, the reaction conditions established at this stage should then be applicable to a range of dimedone derivatives. It should be noted that the idea was not to try to mimic the whole structure of CsA, since only one half of CsA (residues 9-11, 1-3) is involved in binding to CypA, while the remaining residues form the effector loop and bind to calcineurin phosphatase. Consequently the aim was not to mimic the biological immunosuppressant action of CsA, as this involves the entire CsA ring. It should also be noticed that the proposed ligands are not "drug-like" molecules, since the limitations of peptides as drug candidates are widely known and were discussed in the introduction. However, the potential to substitute unnatural or constrained amino acids, or replacements, in order to form dimedone-based peptidomimetics remains a possibility. The advantages and disadvantages of using the peptidomimetic strategy in drug design were also covered in the introduction.

From these first ligands, we hoped to fulfil the following objectives: firstly, development of some reproducible dimedone chemistry suitable for library generation; secondly, preparation of a number of dimedone-based ligands; thirdly,

development of a means for investigating the binding of these ligands to the CypA protein, and perhaps quantifying this in the form of a measured dissociation constant, K_d; and generally, an idea of the available space and important interactions within the binding site.

2.2 Amino Acid Derivatives of Dimedone

2.2.1 Analogues Based on the Dde Protecting Group

As stated previously, the initial objective was to establish reaction conditions for the incorporation of dimedone into the peptide chain. The *N*-1-(4,4-dimethyl-2,6-dioxocyclohexylidene)ethyl (Dde) primary amine protecting group (**39**, R=CH_3), and its derivatives, developed by Chhabra *et al.*[1], are used in the protection of amino acids in solid phase peptide synthesis. These dimedone-based protecting groups are readily synthesised by acylation of dimedone with the appropriate DCC/DMAP activated carboxylic acid as shown in Scheme 2.1. The amine, in this case the side chain ε-amino group of Fmoc-Lys-OH, is then protected by condensation with the Dde group.

Scheme 2.1

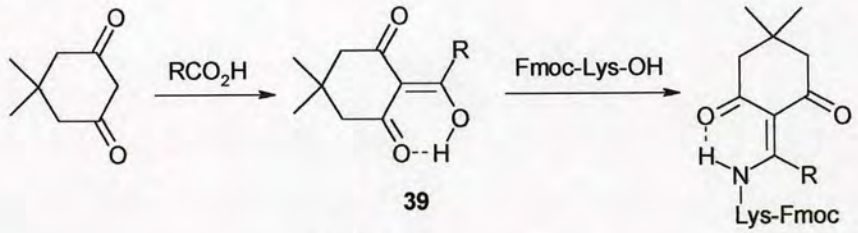

39

R=CH_2CH_3
R=$CH_2CH_2CH_3$
R=$CH_2CH(CH_3)_2$
R=CH_2Ph
R=CH_3 [Dde]

The success of this synthetic strategy suggested that it may be possible to incorporate dimedone into peptides using the route shown in Scheme 2.2. Initial studies used the commercially available *N*-Cbz-protected amino acids.

Scheme 2.2

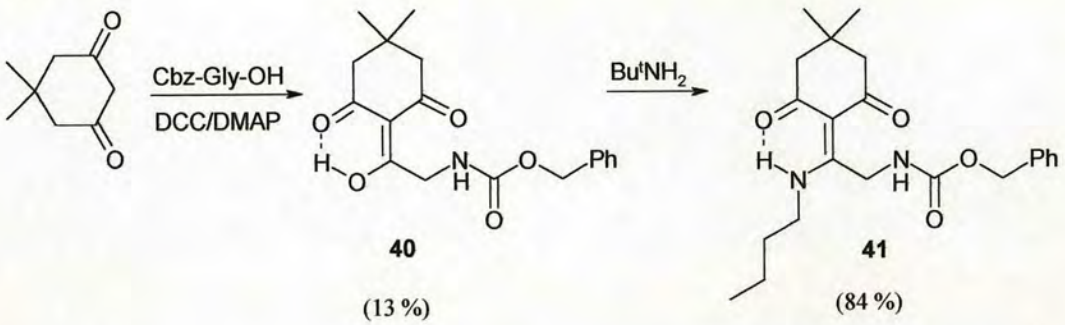

The dimedone adduct **41** was synthesised by acylation of dimedone with *N*-Cbz-glycine, activated using DCC/DMAP, to form the alcohol **40**, followed by condensation with butylamine. The yield for the initial *C*-acylation step was only 13% and attempts to perform this reaction with protected amino acids other than glycine resulted in recovery of starting material, or low (<10 %) yields of *O*-acylated product such as the valine derivative **42** (Scheme 2.3).

Scheme 2.3

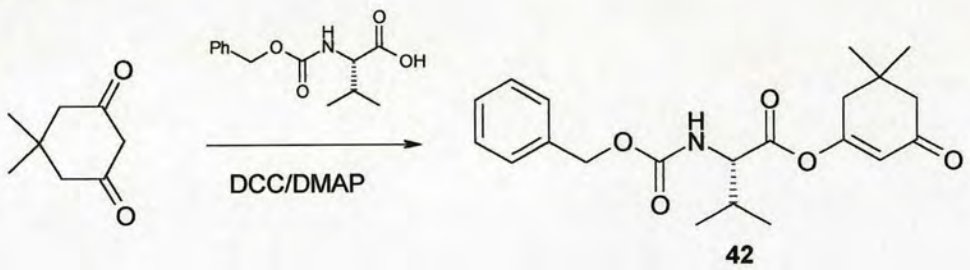

No previous examples of the *C*-acylation of dimedone with an α-substituted carboxylic acid using this method were found in the literature. It was thought at this stage that the α-substituted amino acids might have a steric barrier to reaction.

The *O*-acylated enol ester derivatives **42** constituted a novel class of ligands which could be tested for binding to CypA. This part of the project was taken on by Yuan De Yang at Edinburgh University, who at this point started to investigate potential screening methods for the new compounds. Screening methods will be discussed in Chapter 3.

While the assay methods were being developed, work continued towards optimisation of enol ester formation by the *O*-acylation mechanism, and also towards direct *C*-acylation of the dimedone C-2 position to produce activated alcohols such as **40**. This second class of *C*-acyl derivatives were considered important as this strategy involved incorporation of the dimedone scaffold within the amino acid chain, thus affording greater scope for building out from the dimedone core than was possible with the *O*-acylated analogues. Studies were therefore performed in order to establish conditions for both *O*- and *C*-acylated species, by investigation of differing modes of activation of the amino acid *C*-terminus.

2.2.2 Amino Acid Activation Methods – Attempts to Effect *C*- versus *O*-acylation of Dimedone

2.2.2.1 Azide formation

The method for the preparation of acyl azides reported by Chorev *et al.*[2] was employed in the activation of amino acids for attempted coupling to dimedone as shown in Scheme 2.4. The mixed anhydride **44** was formed by treatment of Cbz-L-valine **43** with ethyl chloroformate in the presence of triethylamine. *In situ* addition of sodium azide and aqueous work-up resulted in a colourless oil which exhibited a strong azide peak at 2140 cm^{-1} in the IR spectrum, although an additional peak at 2252 cm^{-1} suggested that some rearrangement of azide **45** to the isocyanate **46** may be occurring. However, ^1H NMR of the oil gave inconclusive data as a solid precipitated out after sample preparation resulting in broad spectral peaks. It was postulated that the acyl azide species **45** may be prone to hydrolysis to regenerate valine in the presence of any water remaining from the work-up. Reaction of the colourless oil with dimedone was therefore attempted immediately without further analysis. The oil was treated with dimedone in the presence of DMAP, with the aim of forming either or both of the dimedone derivatives **42**,**47** shown in Scheme 2.4. Unfortunately the yellow solid obtained was found to be a mixture of Cbz-L-valine and dimedone starting materials by ^1H NMR.

Scheme 2.4

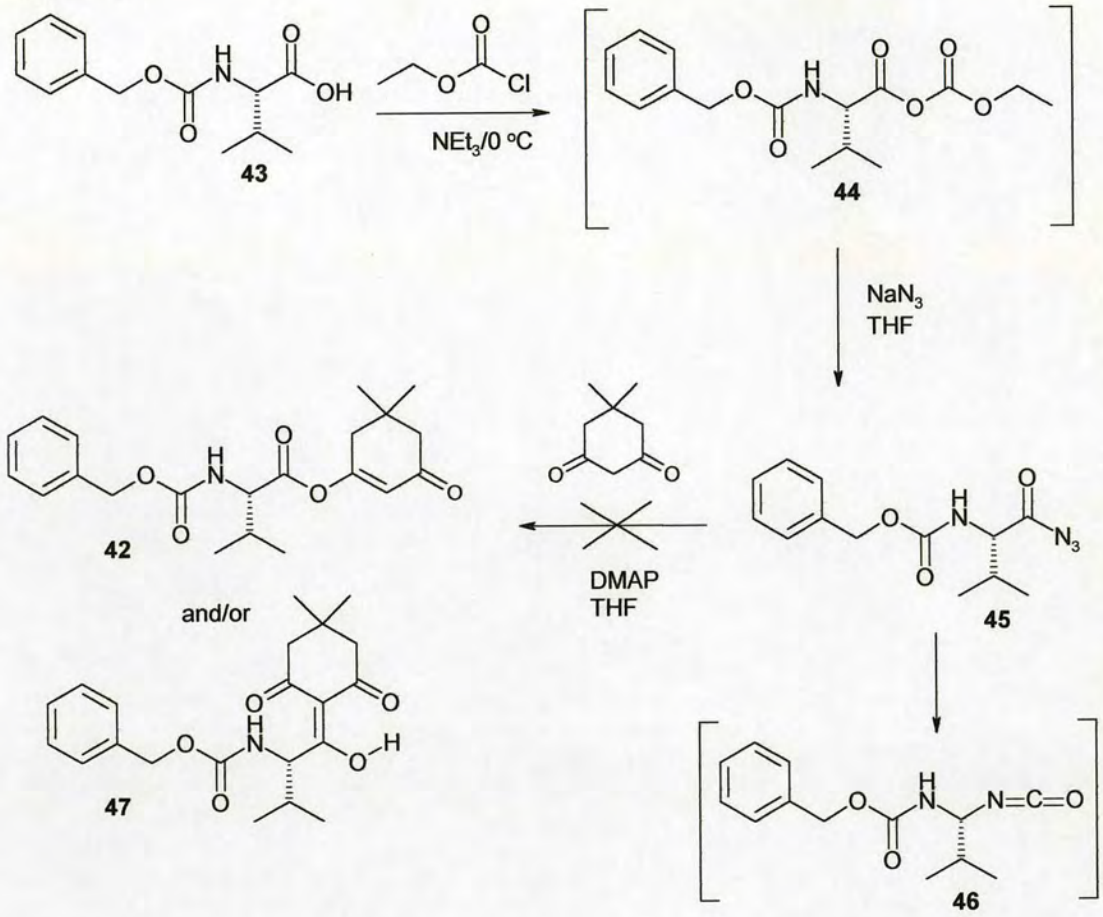

2.2.2.2 Mixed anhydride formation

It was proposed that direct coupling of dimedone to the amino acid mixed anhydride might be possible without formation of the azide. Reaction of dimedone with the anhydride of leucine **49**, generated by reaction of Cbz-L-leucine **48** with ethyl chloroformate in the presence of triethylamine (Scheme 2.5), resulted in the *O*-acylated product **50**. Solvent effects are known to be important in determining the ratio of keto to enol forms of dimedone,[3] but changing the solvent did not alter the outcome of this reaction.

Scheme 2.5

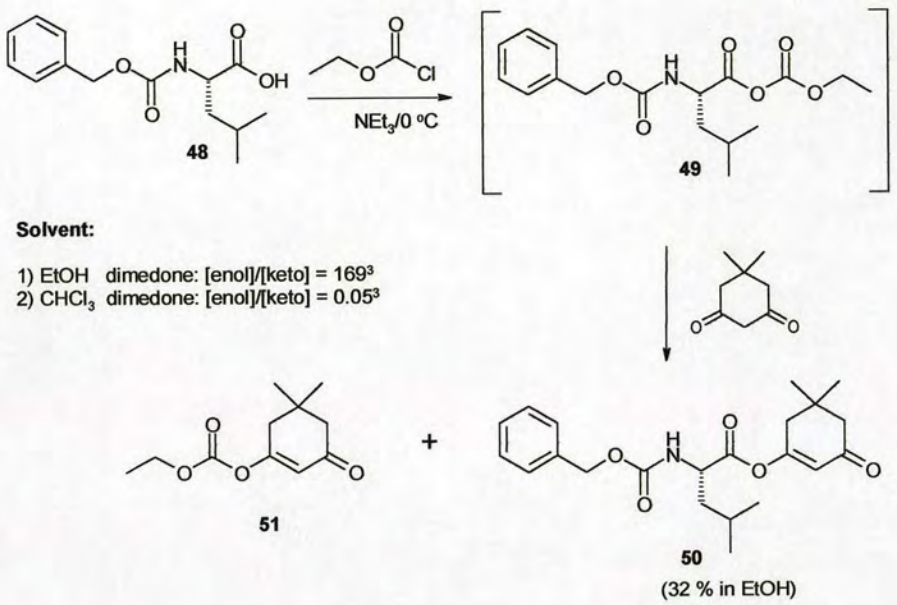

It was also noted that the both carbonyl groups of the anhydride were attacked by dimedone resulting in both the amino acid derivative **50** and the carbonate by-product **51**. Carbonate by-product was observed even when isobutyl chloroformate was substituted for the ethyl chloroformate.

Enol ester **52** was prepared by reaction of dimedone with the mixed anhydride of L-phenylalanine (Scheme 2.6).

Scheme 2.6

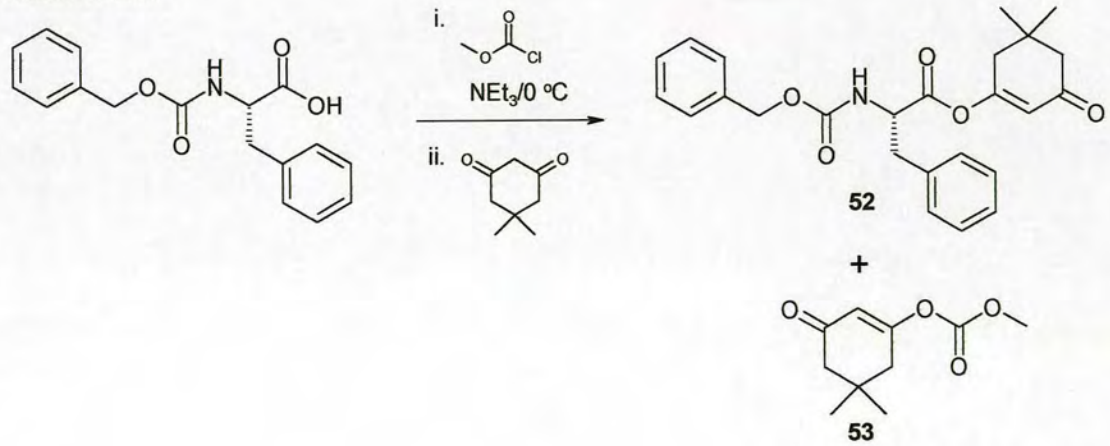

Problems were encountered in the purification step as a small amount of the impurity **53** was formed by attack of dimedone on the mixed anhydride as described previously, and this proved to be difficult to separate by column chromatography.

2.2.2.3 Acyl fluoride formation

The acylation was then attempted *via* the *N*-Cbz-amino acid fluorides using conditions described by Carpino *et al.*[4], as shown in Scheme 2.7. *N*-Benzyloxycarbonyl-L-leucine **48** was treated with cyanuric fluoride and pyridine to form the acid fluoride **54**, which then reacted with dimedone under basic conditions to form the enol ester **50**.

Scheme 2.7

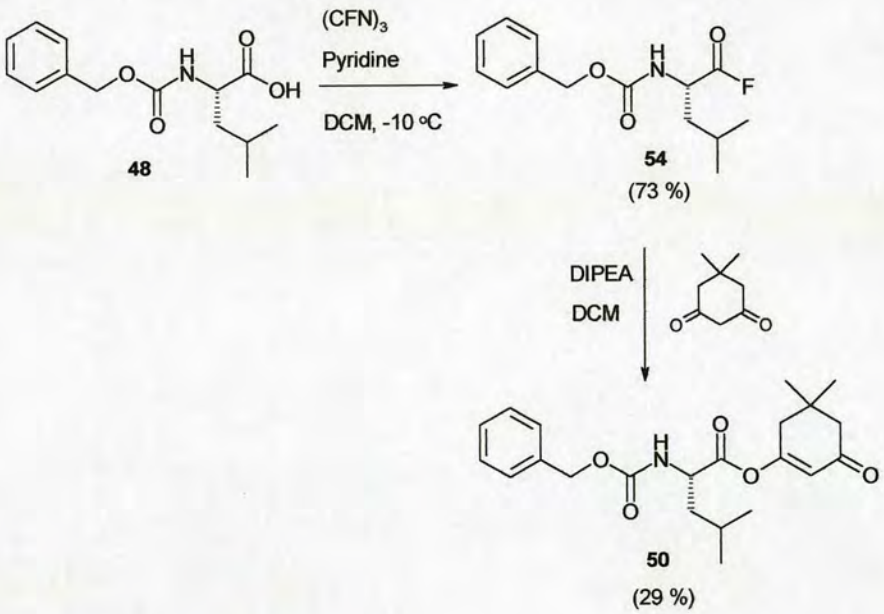

The overall yields were much improved by proceeding directly to the dimedone addition step after aqueous wash of the acyl fluoride reaction mixture, rather than isolation and characterisation of the acyl fluoride itself.

Despite investigation of different conditions, all attempts to form the *C*-acylated product directly at this stage were unsuccessful. The next alternative appeared to be attempted rearrangement of the *O*- to *C*-acyl species.

2.2.3 Rearrangements

2.2.3.1 Lewis Acid catalysis

An alternative route to 2-acylcyclohexane-1,3-diones **56**, reported by Akhrem *et al.*[5], involves *O*→*C* isomerisation of the enol ester **55** in the presence of aluminium chloride (Scheme 2.8). The enol esters were synthesised by reaction of an equimolar mixture of dimedone and pyridine with a 10 % excess of acyl chloride.

Scheme 2.8

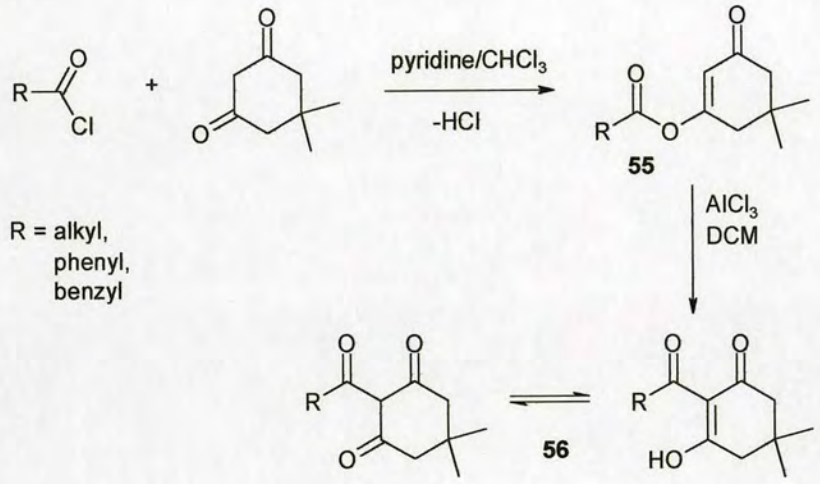

Attempted rearrangement of the enol ester **42** using aluminium chloride was unsuccessful, resulting in recovery of starting material (Scheme 2.9).

Scheme 2.9

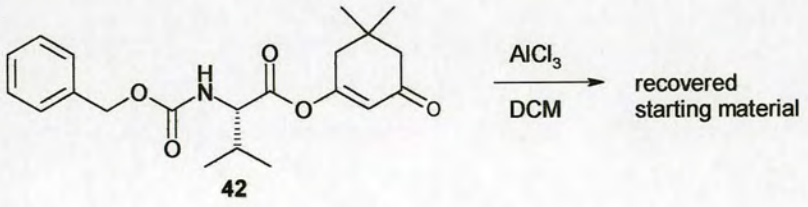

2.2.3.2 Cyanide catalysis

Eventually, however, cyanide catalysed rearrangement[6] of enol ester **42** using acetone cyanohydrin and triethylamine resulted in the *C*-acylated product **58** in good yield (Scheme 2.10). Treatment of the 2-acyl-1,3-cyclohexanedione **58** with L-phenylalanine methyl ester at 50 °C afforded the desired dimedone containing dipeptide **59**.

Scheme 2.10

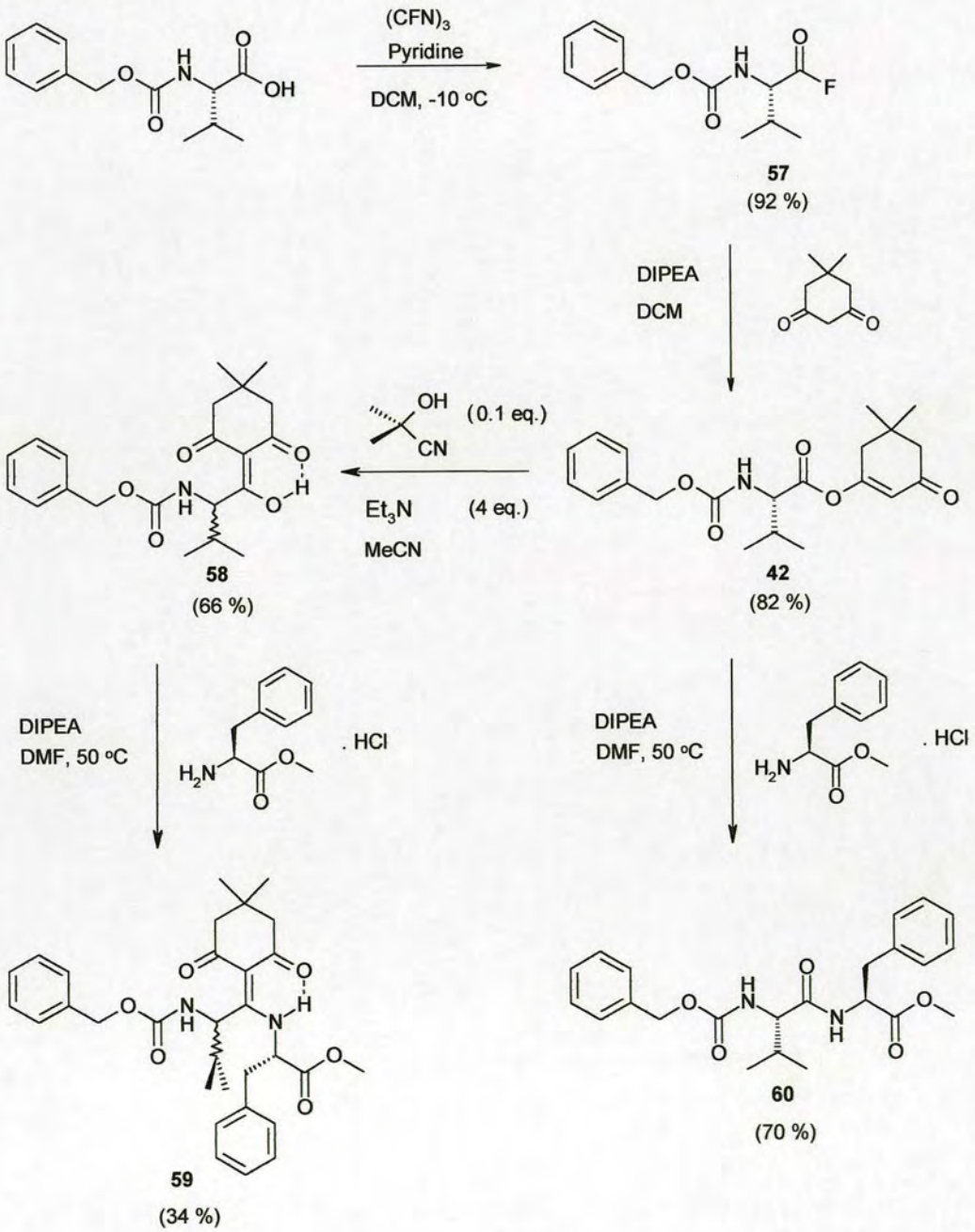

The dipeptide **59** was found to be a 60:40 mixture of diastereomers by ^{1}H NMR. When the synthesis was repeated using racemic *N*-Cbz-valine, the same ratio of diastereomers was obtained indicating that epimerisation occurs at the initial amino acid (in this case valine). Formation of the amide **60** by reaction of the enol ester **42** with a second amino acid resulted in a single diastereomer, which confirmed that the stereochemistry was conserved in forming the enol ester, but suggested that epimerisation may occur during the cyanide catalysed rearrangement step. This reaction proceeds via the acyl cyanide **61**, which may enolize[7] resulting in the loss of chirality at this centre (Scheme 2.11). The alternative explanation is that the acidic nature of the α-proton (*) may result in spontaneous epimerisation on formation of the final product **62**.

Scheme 2.11

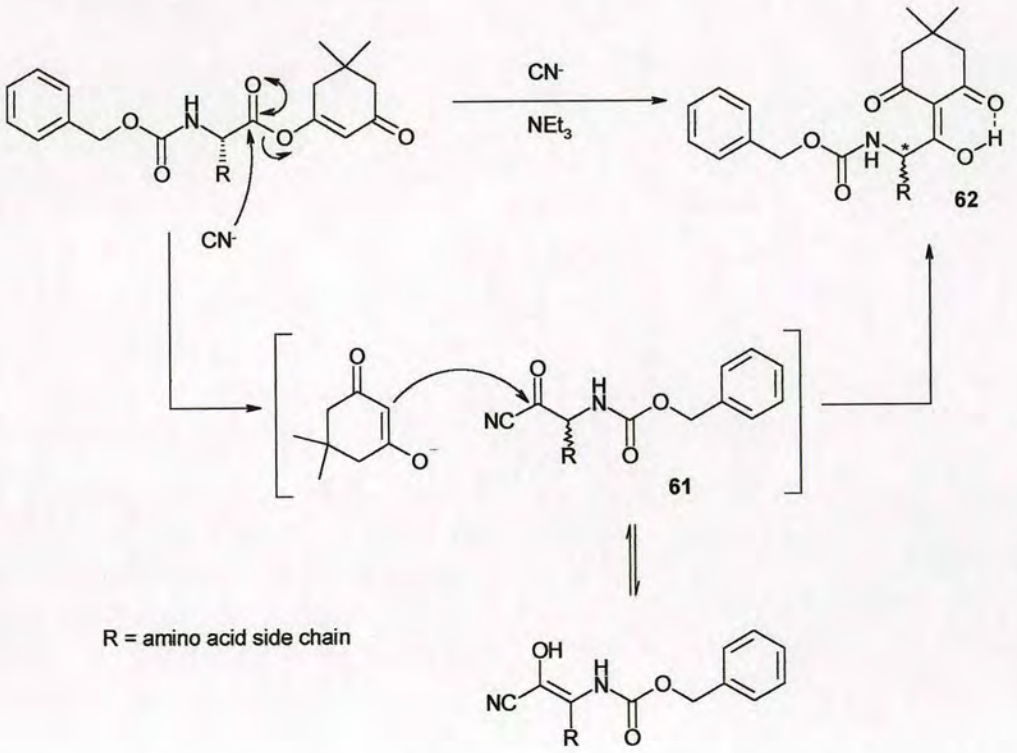

At this stage it was important to establish whether preservation of the stereochemistry at this position would be possible. Additionally, we wanted to investigate the possibility of preparing solid supported dimedone derivatives using

this route, in combination with some solid phase chemistry previously developed by Dr Anita Long at Edinburgh University, for the synthesis of *C*-terminally modified peptides.

2.2.4 Solid Phase Chemistry

Solid phase combinatorial chemistry has found wide application in the field of protein-ligand interactions for the generation of large numbers of peptidomimetics used as probes in the investigation of structure-activity relationships. The advantages offered by solid phase chemistry over the solution phase equivalent are widely reported.[8] With regard to library generation, the main advantage is in the ease of purification of resin bound libraries in comparison to purification of the last step of a library synthesis in solution. When compounds are synthesised on solid support, excess reagents can be used to drive the reaction to completion and then washed out in a simple filtration step. The use of excess reagents has obvious advantages when preparing a combinatorial library where one reaction will be performed on all combinations of a set of building blocks, but may only be optimised for a small trial set of these components. The disadvantages of solid phase are often discovered in the transferral of established solution reactions to a solid phase system, because reagents can often behave very differently in the solid phase environment. With regard to the proposed library of dimedone-based ligands, a method for the attachment of amino acids to solid support had already been established, so it seemed sensible to investigate the possibility of using this strategy in combination with the solution phase synthesis detailed in section.

Scheme 2.12 shows the method, adapted by Dr Anita Long from the published methods of Roussel *et al.*[9] and Henkel *et al.*,[10] for immobilisation of an amino acid on polystyrene resin, by attachment via the *N*-terminus. This strategy uses the Wang linker.

Scheme 2.12

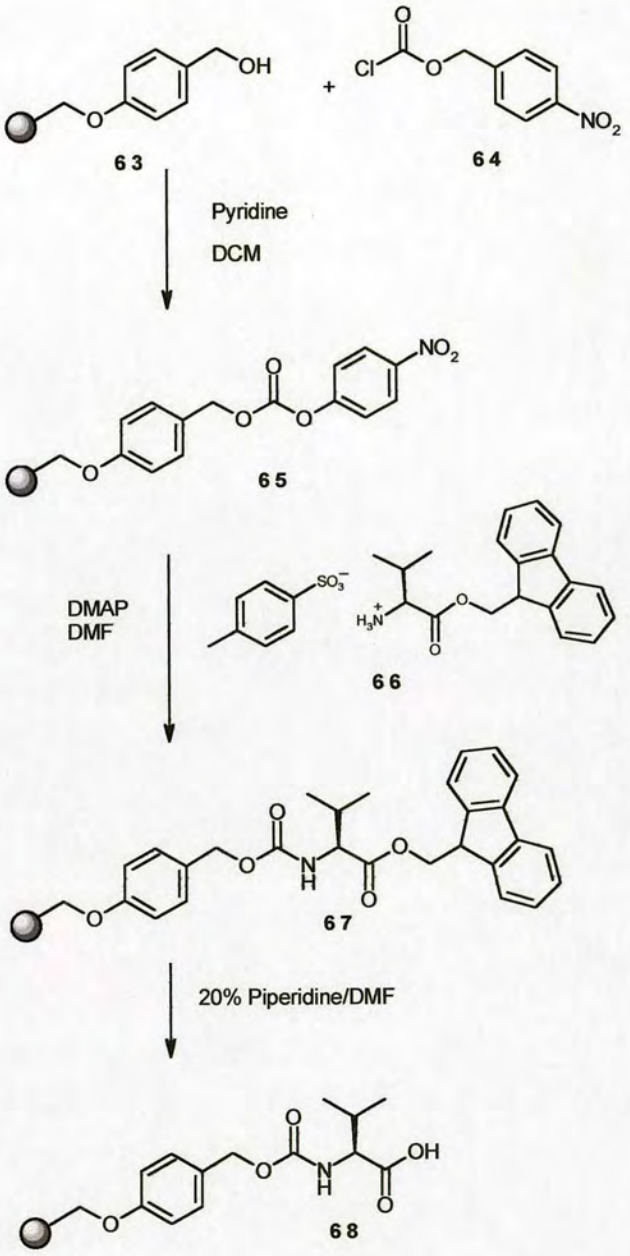

Wang resin **63** was activated by reaction with *p*-nitrophenol chloroformate **64** to form the resin-bound carbonate **65**. Formation of the carbonate was indicated by the distinctive IR (C=O) stretch at 1765 cm^{-1}. Resin loading could also be established at this stage by cleavage of the *p*-nitrophenol group using 20 % piperidine/DMF, and photometric analysis. The activated resin **65** was then reacted with the *p*-toluene sulfonic acid salt of L-valine fluorenyl methyl ester **66** to yield the resin-bound amino acid **67**. The resin-bound Fm-ester was deprotected using 20 % piperidine/DMF to

give the free acid **68**. Resin loading was established at this stage by UV analysis of the dibenzofulvene piperidine adduct. The synthesis of dimedone-based ligands was then attempted using the strategy shown in Scheme 2.13. The resin-bound acyl fluoride **69** was formed from the acid **68** by reaction with cyanuric fluoride and pyridine in DCM at room temperature. A strong acyl fluoride peak was observed in the IR spectrum at 1843 cm^{-1}.

Scheme 2.13

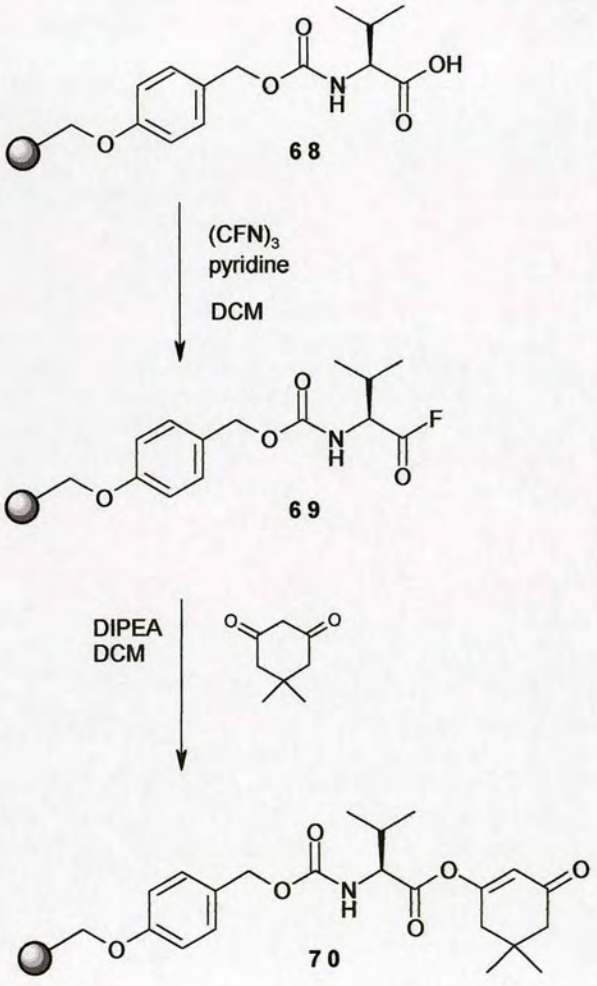

The enol ester **70** was formed by treatment of the acyl fluoride **69** with dimedone in the presence of DIPEA. This step was accompanied by disappearance of the acyl fluoride stretch in the IR.

Attempts to perform the proposed cyanide catalysed rearrangement step on resin (Scheme 2.14) resulted in incomplete conversion, with a mixture of unreacted enol ester **70** and rearranged product **71**, observed by Gel ^{13}C NMR (identified by comparison with solution ^{13}C NMR spectra of the previously characterised compounds **42** and **58** (Scheme 2.10)).

Scheme 2.14

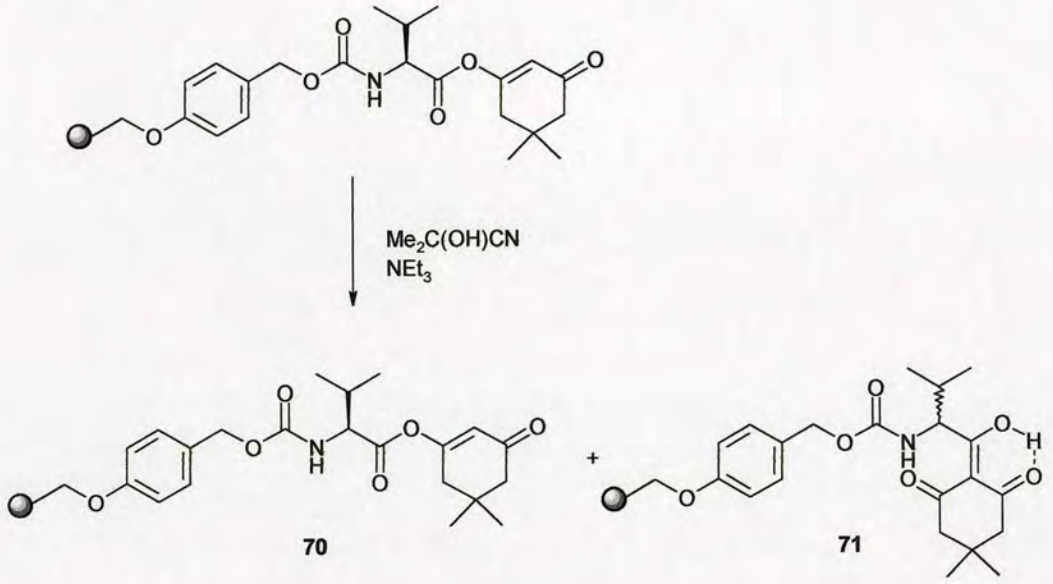

It should be noted that during the rearrangement step, the mechanism of which is outlined in Scheme 2.11, dimedone is cleaved from the resin on formation of the tethered acyl cyanide, and then re-attaches *via* the C-2 position. Due to the comparatively lower concentrations of reagents when working with solid support as opposed to solution chemistry, it was anticipated that incomplete rearrangement may have been attributable to a dilution effect where a low concentration of free dimedone is available for re-reaction with the supported acyl cyanide species. In order to compensate for this, the reaction was repeated with a 20-fold excess of dimedone added during the rearrangement step, however the same mixture of products was observed by Gel ^{13}C NMR.

In order to attempt complete rearrangement of the resin-bound enol ester **42**, further studies were performed on the established chemistry in solution. Firstly, this step was optimised in a 'one-pot' reaction which proceeded in 94 % yield to the *C*-acylated product **58**, as shown in Scheme 2.15.

Scheme 2.15

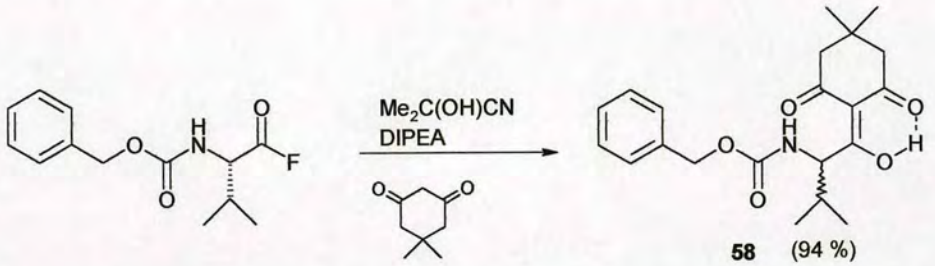

58 (94 %)

However, the solid phase yields of *C*-acylated product could not be improved upon and it became obvious that an alternative route for direct *C*-acylation of dimedone with the acyl fluoride was required, in order to dispense with the cyanide catalysed rearrangement step. Formation of derivatives such as **59** using a strategy of this sort also had the potential to clarify the step at which epimerisation of the chiral centre (*) of **59** occurs.

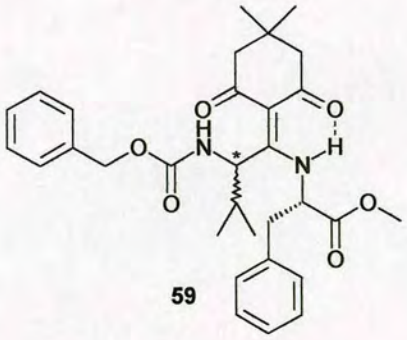

59

A search of the literature suggested that employment of alkyl ammonium fluoride salts could offer a promising alternative.

2.2.5 TBAF Salt

The tetrabutylammonium fluoride (TBAF) salt of dimedone, **72** (Scheme 2.16) was formed using the method described by Clark *et al.*[11], by simply stirring a stoichiometric mixture of TBAF and dimedone in DMF in the presence of molecular sieves. Interestingly, the ^{1}H NMR spectrum of the salt **72** in deuterated chloroform reveals that the TBAF-complexed dimedone is present exclusively in the enol form. The opposite situation occurs with uncomplexed dimedone in chloroform, where dimedone exists predominantly in its keto form.[12] The authors findings indicate that formation of the salt predisposes dimedone to *C*-acylation, by formation of a tightly hydrogen bonded complex anion with fluoride. The enhanced reactivity presumably arises by transfer of the electron density from the fluoride anion *via* the hydrogen bond. The overall result is, therefore, to shield the oxygen atom of dimedone, hence inhibiting *O*-alkylation while at the same time increasing the effectiveness of the compound as a nucleophile.

Reaction of the salt **72** with the acyl fluoride of benzyloxycarbonyl-L-valine **57**, resulted in a 3:2 ratio of *C*- to *O*-acylated products (**58**,**42**) by ^{1}H NMR, the first time that direct *C*-alkylation of dimedone had been observed. Chromatographic purification of this mixture proved difficult so the mixture was reacted directly with L-phenylalanine methyl ester (Scheme 2.16). Four compounds were isolated from the resulting mixture: unreacted *C*-acylated compound **58**; the dipeptide **60** (as a single diastereomer) from reaction of *O*-acylated compound **42**; and dimedone dipeptide **59**, from reaction of the *C*-acylated compound **58**.

Scheme 2.16

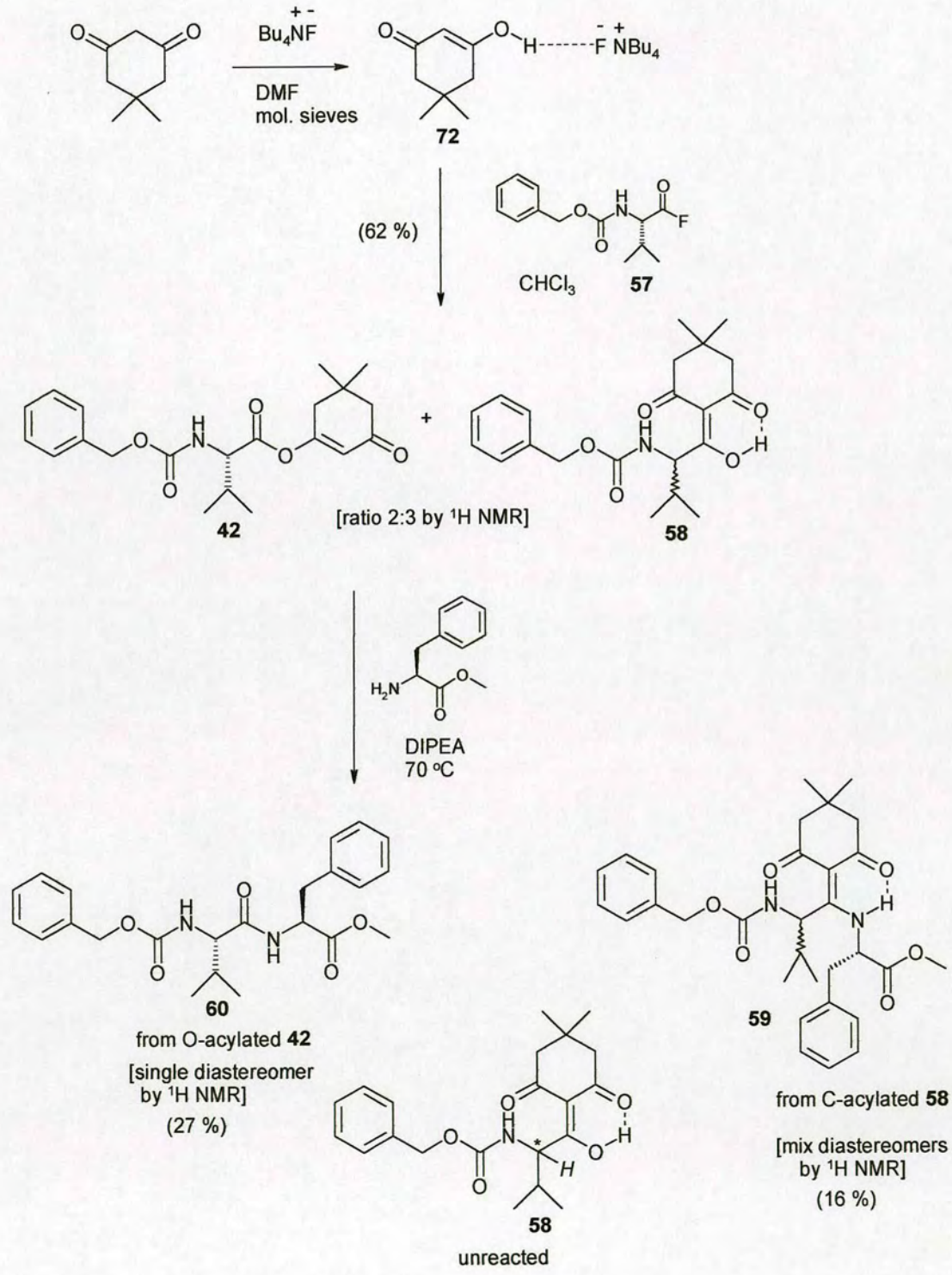
Bu4NF
DMF
mol. sieves
72
(62 %)
CHCl3
57
42
[ratio 2:3 by 1H NMR]
58
DIPEA
70 °C
60
from O-acylated 42
[single diastereomer by 1H NMR]
(27 %)
59
from C-acylated 58
[mix diastereomers by 1H NMR]
(16 %)
58
unreacted

The dipeptide **59** was observed to be a mixture of diastereomers by ^{1}H NMR. This result suggests that epimerisation of the chiral centre (*) occurs spontaneously on formation of *C*-acylated dimedone **58**, due to the acidic nature of proton *H*.

It is interesting to note that dimedone required to be "fixed" in the enol form by complexation with TBAF for *C*-acylation to occur. Contrast this finding with the *O*-acylation that occurred when dimedone was reacted in ethanol, where the enol form almost exclusively predominates. These results further confirm that there is an additional, probably electronic, effect operating in the TBAF-dimedone reaction.

At this point, several assay results became available indicating the possible binding of the preliminary ligands tested to CypA. These results, reported in Chapter 3, suggested that the *O*-acylated derivatives were a more promising template for further adaptation than the *C*-acylated species. Additionally, it was obvious that additional investigation would be required in order to achieve 100 % *C*-acylation on solid support, in order to build a library. For this reason, it was decided that work towards a solid supported library would be suspended at this stage. Nevertheless, this investigation was valuable in solving the question of when the epimerisation was occurring, and an additional application of this chemistry, which will be discussed in Chapter 5, was also suggested.

2.2.6 Further Solid Phase Investigation

Further work in this area could concentrate on optimising the reaction of TBAF-dimedone with the acyl fluoride of benzyloxycarbonyl valine in order to maximise *C*-acylation. If *O*-acylation occurs due to the presence of uncomplexed dimedone (perhaps formed as a result of water in the reaction), then more efficient elimination of moisture from the reaction should increase the yield of desired product.

If a reasonable yield of the resin-bound *C*-acylated species **71** could be generated, it should then be possible to couple in a second fluorenyl methyl ester-protected amino

acid as its *p*-TSA salt, in order to form the dipeptide **73** on resin (Scheme 2.17). The final compound could potentially be cleaved from the Wang linker using TFA.

Scheme 2.17

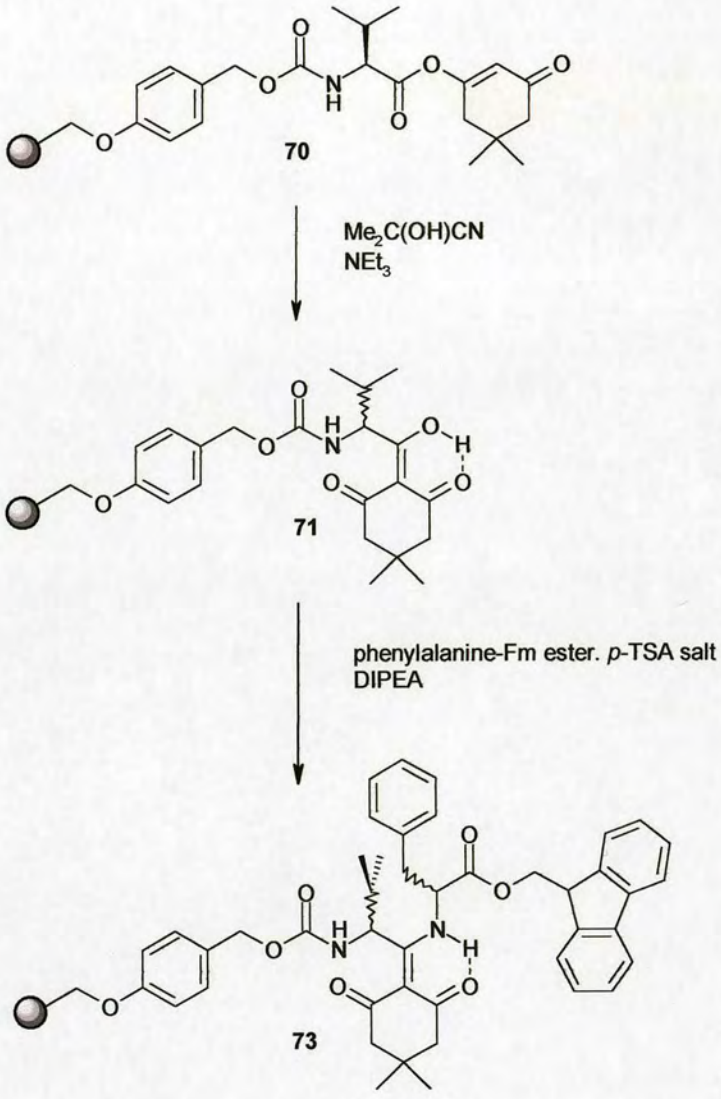

The *p*-toluene sulfonic acid salt of L-valine fluorenyl methyl ester **66** can be synthesised by the method shown in Scheme 2.18. The protected ester **76** is formed by reaction of Boc-L-valine **74** with 9-fluorenemethanol **75** using DIC/DMAP. The Boc protecting group can then be removed using TFA, and the fluorenyl methyl ester-protected amino acid triturated out as the *p*-toluene sulfonic acid salt. Protected

amino acids are suggested because previous work carried out by Dr Anita Long[13] has shown that this step is necessary to prevent additional unwanted couplings.

Scheme 2.18

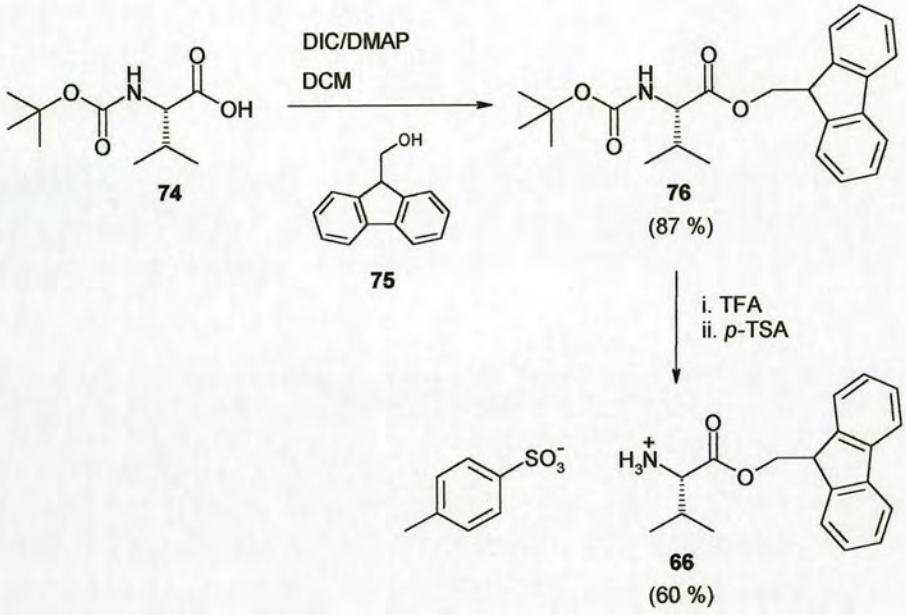

2.2.7 Formation of Additional Dimedone Ligands

2.2.7.1 Vinylogous amide

Two other ligands were prepared at this stage, the first of which was the vinylogous amide **77**, formed by the route shown in Scheme 2.19, by simply treating dimedone with the hydrochloride salt of L-valine methyl ester in the presence of triethylamine, as reported by Halpern et al.[14]

Scheme 2.19

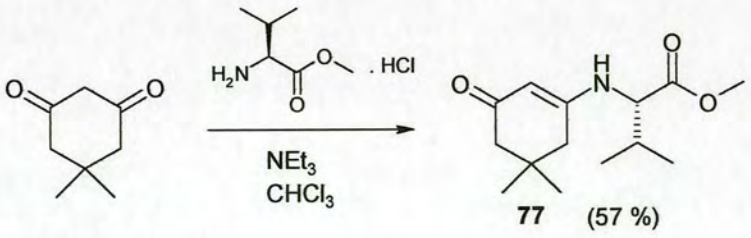

This reaction was chosen from the literature because it is a simple way of generating dimedone-amino acid conjugates and the mild conditions are suitable for library generation. The attachment of the amino acid via the amino as opposed to the acid terminus obviously alters the backbone arrangement of the hydrogen donor and acceptor atoms with respect to their distance from the dimedone core. Preparation of a range of these derivatives would constitute a complimentary family of ligands to the *O*-acyl ligands previously described. This was therefore an interesting molecule for testing in the initial CypA binding assay.

2.2.7.2 Di-protected amino acids

In order to establish whether it is indeed the dimedone core that is important for binding, the diprotected amino acid **79** was prepared, by the method shown in Scheme 2.20. *N*-(Benzyloxycarbonyloxy)succinimide **78** was reacted with the hydrochloride salt of L-valine methyl ester in the presence of diisopropylethylamine.

Scheme 2.20

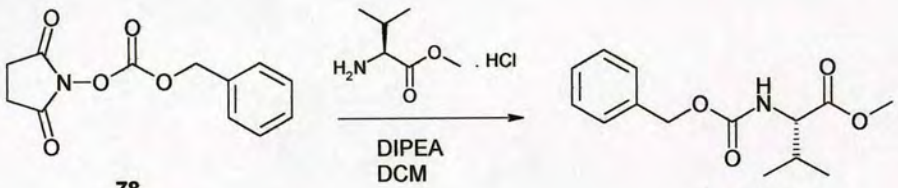

78 **79** (88 %)

2.2.8 Summary

Several ligands had so far been prepared using the routes summarised in Scheme 2.21 below.

Scheme 2.21

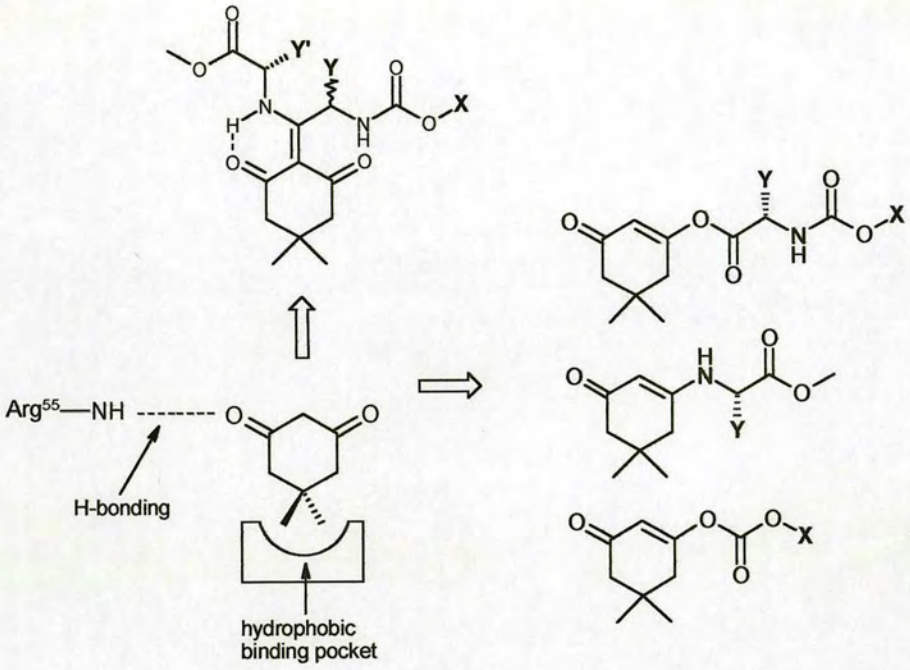

It now became possible for these to be tested for binding affinity to CypA using a fluorescence assay set up by Yuan De Yang. The preliminary screening results are discussed in Chapter 3.

2.3 References

[1] Chhabra, S. R.; Hothi, B.; Evans, D. J.; White, P. D.; Bycroft, B. W.; Chan, W. C., *Tetrahedron Lett.*, 1998, **39**, 1603-1606.

[2] Chorev, M.; Macdonald, S. A.; Goodman, M., *J. Org. Chem.*, 1984, **49**, 5, 821.

[3] Mills, S. G.; Beak, P., *J. Org. Chem.*, 1985, **50**, 8, 1217.

[4] Carpino, L. A.; Mansour, E. M. E.; Sadat-Aalace, D., *J. Org. Chem.*, 1991, **56**, 8, 2611-2614.

[5] Akhrem, A. A.; Lakhvich, F. A.; Budai, S. I.; Khlebnicova, T. S.; Petrusevich, I. I., *Synthesis*, 1978, 925-927.

[6] Montes, I. F.; Burger, U., *Tetrahedron Lett.*, 1996, **37**, 7, 1007-1010.

[7] Hünig, S.; Schaller, R., *Angew. Chem. Int. Ed. Engl.*, 1982, 36-49.

[8] Gallop, M.A.; Barrett, R.W.; Dower, W.J.; Fodor, S.P.A.; Gordon, E.M., *J. Med. Chem.*, 1994, **37**, 1233-1251.

[9] Roussel, P.; Bradley, M.; Kane, P.; Bailey, C.; Arnold, R.; Cross, A., *Tetrahedron*, 1999, **55**, 6219-6230.

[10] Henkel, B.; Zhang, L. S.; Bayer, E., *Liebigs Annalen-Recueil*, 1997, 2167-2168.

[11] Clark, J.M.; Miller, J.M., *J. Chem. Soc. Perkin Trans. I*, 1977, 1743-1745.

[12] Mills, S.G.; Beak, P., *J. Org. Chem.*, 1985, **50**, 1216-1224.

[13] Thesis: Long, A.M., *Progress Towards the Solid Phase Generation of New Peptidomimetic-Based Libraries via 5(4H)-Oxazolone Intermediates*, Edinburgh University, 1999.

[14] Halpern, B.; James, L.B., *Aust. J. Chem.*, 1964, **17**, 1282-1287.

3 Results and Discussion II

3.1 Analysis of Ligand Binding

Having prepared a number of dimedone-based ligands, the next stage of the process was to establish whether any of these molecules could penetrate the binding site of CypA and form interactions with the protein. Several methods for determining protein-ligand binding were investigated and will now be described. All assay and crystallography work was carried out by Yuan De Yang.

3.1.1 Crystal Structure

3.1.1.1 Crystal soaking

CypA protein was produced from *E.coli* bacteria and purified in house by Yuan De Yang. The hanging drop vapour diffusion method was used to grow crystals of CypA. The principle of vapour diffusion crystallisation is that a droplet containing protein, buffer, crystallising agent and additives, is equilibrated against a reservoir containing a solution of crystallising agent at higher concentration than the droplet. Equilibration occurs by diffusion of the water until vapour pressure in the droplet reaches that of the reservoir. A crystal soaking procedure was employed to introduce ligands into the CypA active site. This method involved placing a well-diffracting CypA crystal into a solution containing an appropriate ligand concentration. A number of CypA:ligand complexes were obtained by this method and the crystal structures analysed by X-ray diffraction. The limitations of this technique with regard to screening of ligands for binding to CypA are firstly, that several time and labour intensive steps are involved in isolation and purification of the protein, preparation of the CypA crystals, soaking in the ligand solutions, and collection and manipulation of X-ray data. Additionally, crystals must be able to withstand the soaking conditions, for reasonable periods of time, without cracking or dissolving. A further consideration is that the ligand must be small and flexible enough to pass through solvent channels in the crystal lattice in order to access the active site. The great advantage of obtaining crystallographic data on CypA:ligand complexes is that

very detailed information on the binding of the ligand within the CypA active site, including ligand orientation and potential protein:ligand interactions can be acquired. However, crystals of CypA:ligand complexes can only be obtained under certain conditions, and the failure to produce a crystal of a particular protein:ligand complex by soaking experiments, does not necessarily mean that the ligand is unable to bind to the protein active site. For example, a large ligand might not be suitable for soaking into the CypA crystal if its bulk restricts passage through solvent channels in the crystal lattice. However, a large ligand might be able to enter the CypA active site in the solution form of the protein, and in this situation co-crystallisation might prove more useful. Alternatively, a ligand that is only sparingly soluble under the chosen soaking conditions can also cause problems since only a comparatively low concentration of ligand can be achieved.

3.1.1.2 Co-crystallisation

Co-crystallisation is another method of obtaining CypA:ligand crystals, especially useful where a complex with a large ligand is required. In co-crystallisation the conditions for crystal growth of the protein:ligand complex may be different from that of the native molecule, so that screening of many conditions may be required. For this reason, the co-crystallisation method was used less than the crystal soaking technique.

3.1.2 Fluorescence Assay

Fluorescence spectroscopy can be used to detect interactions between proteins and other molecules, provided that the optical properties of the protein-ligand complex differ from those of free ligand and free protein.[1] Aromatic residues such as phenylalanine, tyrosine and tryptophan are responsible for fluorescence of proteins in the near ultraviolet region, with tryptophan fluorescence dominating at λ_{emit}= 340 nm in most proteins.

CypA has a single tryptophan residue located about 8 Å from the centre of the active site, which makes a hydrogen bond to CsA when bound. The fluorescence spectrum can therefore be used to detect changes in the environment of this tryptophan. If the

binding of a ligand within the active site causes sufficient perturbation of the microenvironment in the region of the tryptophan, then a corresponding change in the fluorescence emission will be observed.

The fluorescence titration was performed using a Perkin Elmer LS50B fluorescence spectrophotometer, by fluorescence measurement on a solution of protein with successive additions of ligand dissolved in 100 % ethanol. Measurements were taken at a single wavelength and recorded when the reading became stable. The excitation wavelength was 280 nm. Using the method reported by Handschumacher *et al.*[2] numerical evaluation of the emission readings allowed calculation of the dissociation constant K_d for some ligands.

After each addition of ligand, the portion of protein bound is proportional to the fractional fluorescence change. When 50 % of the binding sites are filled, the fractional fluorescence change is 50 %, when the protein:ligand stoichiometry is 1:1. The K_d is estimated by assuming a 50 % occupancy of the protein at a fractional fluorescence change of 50 %. At this point the concentration of the bound ligand equals that of the free protein.[3] The most meaningful values in a titration curve are those near to 50 % of fractional fluorescence change because they allow more accurate determination of ligand concentration at that point.

The mathematical formula is as follows:

$P + L = PL$

$[P]$ = free protein concentration

$[P]_b$ = bound protein concentration

$[L]$ = free ligand concentration

$[PL]$ = protein ligand complex concentration

$[P]_o$ = total protein concentration

$[L]_o$ = total ligand concentration

$[L]_b$ = bound ligand concentration

$K_d = [P][L]/[PL]$

When 50 % fluorescence change occurred: $[P] = [PL] = ½[P]_o$

$[L]_o = [L]_b + [L]$

$[L]_b = [P]_b = ½[P]_o$

$K_d = [P].[L]/[PL]$

$= ½[P]_o.([L]_o-[L]_b)/(1/2[P]_o)$

$= [L]_o - [L]_b$

$\mathbf{K_d = [L]_o - ½[P]_o}$ **Equation 3.1**

A typical plot of ligand concentration against fluorescence quenching is given in Figure 3.1, from measurements taken for Ligand **42**.

Figure 3.1

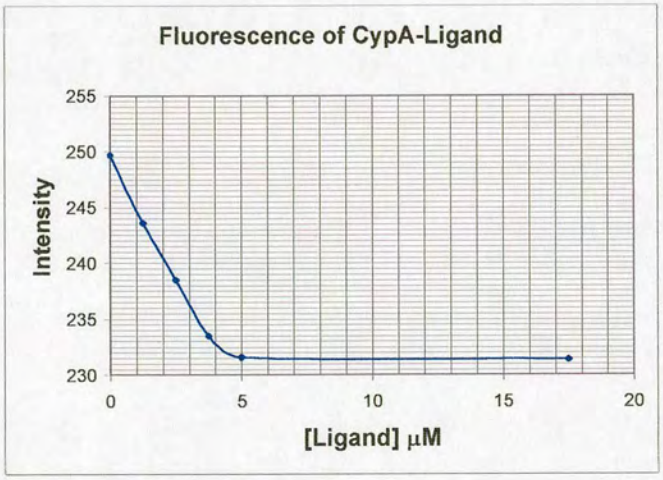

From the graph $[L]_o = 2$ μM. Experimentally $[P]_o = 2$ μM and the K_d was then calculated using Equation 3.1.

3.1.2.1 Limitations of fluorescence assay

Other causes of fluorescence quenching must be taken into account in fluorescence titration when the ligand concentration becomes high:

i. Quenching effect

Apparent quenching of fluorescence can occur if the excitation and/or the emitted light is/are absorbed by the solution containing the fluorophore, resulting in less light reaching the detector. This effect was accounted for by conducting a control experiment using tryptophan instead of protein, and increasing the concentration of ligand under identical experimental conditions. New corrected fluorescence values were obtained by calculation of the difference between protein and control values.

ii. Scattering effect

Insoluble ligands can form precipitates which scatter the emission and the excited light, so less quenching is recorded.

iii. Dilution effect

After each addition of ligand the final volume of protein solution increases, and the protein concentration decreases, resulting in a decrease in fluorescence intensity. The control experiment was also used to correct for this dilution effect due to addition of ligand.

3.1.2.2 Discussion

Different, sometimes contrasting, effects on the fluorescence were observed on binding of the ligands. In some cases fluorescence quenching was observed, which can be accounted for by fluorescence transfer from the excited tryptophan residue to a group or groups on the ligand (eg. an aromatic ring). With other ligands (including CsA) an increase in emission from the tryptophan was observed. This may be explained if we postulate that a water molecule is displaced from the vicinity of the tryptophan on binding of the ligand. If the water molecule was close enough to enable fluorescence transfer from the tryptophan, then its removal means that a

reduced quenching effect is observed, especially in the case where the bound ligand itself is too far removed from the tryptophan for quenching to occur.

The main limitation of this technique when used for determination of ligand binding, is that the ligand must either bind close enough to the tryptophan to cause a direct change in its fluorescence (by quenching or displacement of a water molecule), or the ligand must cause sufficient change in the protein conformation and consequently in the environment of the tryptophan, in order to show a corresponding fluorescence change. The assay results shown in Table 3.1 (Section 3.2) are therefore useful for indicating those ligands which do bind to the protein (and for calculation of K_d in some cases), but ligands which show no change in fluorescence are not necessarily uncomplexed. For this reason the fluorescence assay results were used as a guide, rather than irrefutable proof of ligand binding, when designing later ligands. However, this set of information was very useful as it was the first data available to indicate ligand binding. The results were especially informative when used in conjunction with crystallographic information.

3.1.3 PPIase Assay

Figure 3.2[4]

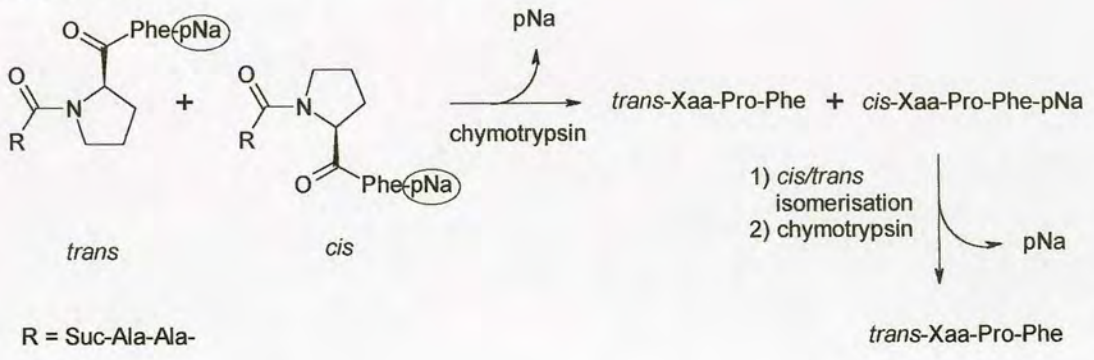

The PPIase activity of CypA in the presence of the novel inhibitors was assessed using an α-chymotrypsin-coupled enzymatic assay (Figure 3.2).[5] The substrate used was Suc-Ala-Ala-Pro-Phe-pNa, which exists in an equilibrium between the *cis* and *trans* forms. The *C*-terminal 4-nitroaniline group is cleaved instantaneously by

α-chymotrypsin if the Ala-Pro bond is in the *trans* form. Release of the chromogenic 4-nitroaniline is monitored by measuring the absorbance with time at 390 nm. The assay is carried out at 4 °C in order to limit thermal isomerisation of the substrate. The *trans* peptide present initially is then cleaved within the deadtime, so that this cleavage does not contribute to the measurement of *cis/trans* isomerisation observed in the slower second step of the reaction. In the presence of CypA the rate of isomerisation of the substrate is accelerated, resulting in faster release of 4-nitroaniline. Conversely, addition of a CypA inhibitor will retard the rate of nitroanilide release. Analysis of the reaction kinetics can be used to determine the rate constants for the reaction and ultimately, the dissociation constant for the inhibitor. A plot of the rate of enzymatic isomerisation against ligand concentration was used to determine the total concentration of ligand at which 50 % inhibition occurred. In a similar manner to the fluorescence assay calculations, Equation 3.1 was used to determine the K_d by assuming a 50 % occupancy of the protein when the rate of enzymatic isomerisation changes by 50 %. Limitations of this protease-coupled, irreversible assay include:

i. The calculations assume that the rate of *cis* to *trans* isomerisation is directly comparable to the rate of 4-nitroaniline release.

ii. Only the *cis* to *trans* and not the reverse *trans* to *cis* isomerisation can be investigated.

iii. Due to the fact that only about 10 % of the substrate (the *cis* content) is monitored, the signal-to-noise ratio can cause problems as well as the solubility of the substrate.

iv. The assay is fairly time consuming and several repetitions were required in order to achieve reproducible results.

Different solvents can be used to shift the *cis/trans* equilibrium, and the *cis* content of the substrate is increased to about 70 % by using LiCl/TFE as solvent.[6] This allows for more precise measurement of kinetics and inhibition parameters.

3.1.4 Mass Spectrometry

The technique of electrospray ionisation mass spectrometry (ESI-MS) has the capability to transfer even weakly bound noncovalent complexes intact from solution to the vacuum of the mass spectrometer. Ganem *et al.*[7] have used ESI-MS (performed in water without co-solvent) to detect gas-phase complexes of FK506 and rapamycin with FKBP. A competition experiment between FKBP and equimolar amounts of the two ligands showed both receptor-ligand complexes with relative peak integration 1:2, in agreement with the relative K_d values (FK506 K_d=0.4 nM, rapamycin K_d=0.2 nM). Further evidence of specific FKBP-ligand interactions was obtained by MS studies at varying pH.[8] FKBP is known to undergo reversible denaturation at low pH. Unfolding the protein's binding pocket by acidifying the FKBP-FK506 solution to pH 3.3 caused the complex ion signal to disappear, while restoration of the pH to 7.5 restored the complex ion signal. Although absolute determination of the binding affinities of FK506 and rapamycin for FKBP by MS has not yet been reported, the utility of MS for measuring solution association constants has been demonstrated for complexes between vancomycin group antibiotics and bacterial cell wall peptide analogues. Jørgensen *et al.*[9] report the determination of solution K_A's from the relative ion abundances in the ESI mass spectra. The solution-phase equilibrium concentrations of the various complexes were determined from the ratio of the ion peak intensity of the given complex relative to the summed peak intensities of all the complexes and the free antibiotic. The measured values were found to be in good agreement with previously reported values obtained by standard spectroscopic titration techniques.

The literature precedence for observing protein-ligand interactions by mass spectrometry, coupled with the information obtained on comparative binding of ligands by competition experiments, was very promising with repect to testing the dimedone analogues prepared for binding to CypA. Ligand:CypA complex formation could indeed be observed by MS and the results are described in Section 3.6.

3.2 Results of Binding Assay

Table 3.1

Ligand	Structure	Interaction with hCyp K_d *	Resolution of hCypA-Ligand Complex
58	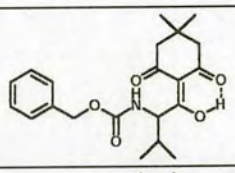	No binding	ND
59	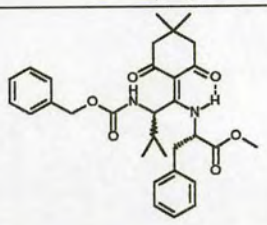	No binding	ND
42	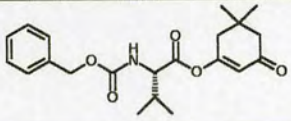	1 μM 22 μM#	1.85 Å R:18.7 % Rfree:23.3 %
80	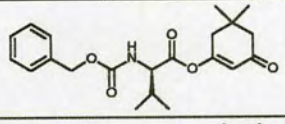	ND	ND
52	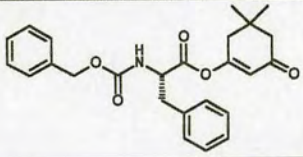	No binding	ND
50	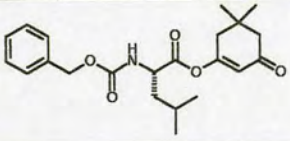	Possible binding	ND
81	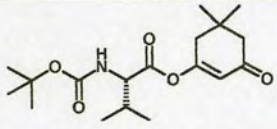	Possible binding	ND
77	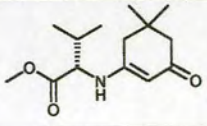	No binding	ND
79	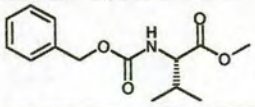	Possible binding	ND

* K_d determined by fluorescence assay
# K_d determined by PPIase assay
ND not determined

As explained previously (3.1.2.2), the fluorescence assay results were used as a guide to indicate possible binding of the ligands tested to CypA. From Table 3.1 it can be deduced that ligands such as **58** and **59**, where the dimedone core has been fuctionalised at C-2, appear less likely to bind within the CypA active site. On the other hand, structures in which dimedone is functionalised at oxygen were shown to be more likely to complex with CypA, although most of these structures have been marked as exhibiting 'possible binding' because the change in fluorescence measured was close to the range of experimental error.

To our delight the first round of screening using the fluorescence assay highlighted a ligand, **42** (Table 3.1), with a dissociation constant (K_d) of 1 μM, a 22,000 fold improvement on the dissociation constant of the lead ligand, dimedone (K_d=22 mM). A slightly higher, but comparable value (K_d=22 μM) was obtained using the PPIase assay. Crystals of the CypA:**42** complex were obtained by the co-crystallisation method. The crystal structure was refined to 1.85 Å and is shown in Figure 3.3.

Figure 3.3: Ligand **42** and **CsA** superimposed

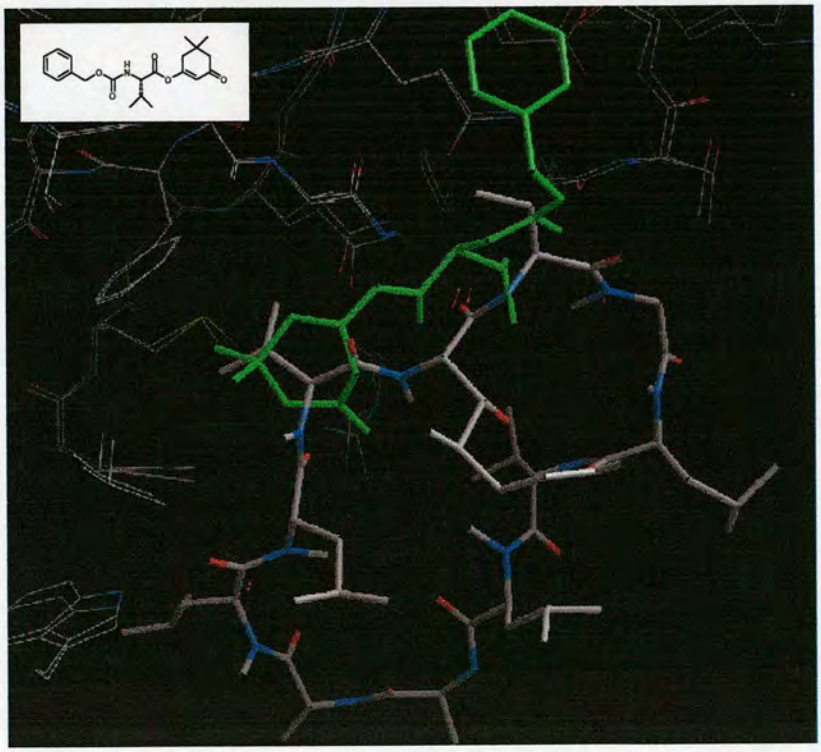

The ligand **42** is shown in green. The X-ray structure of the CsA (white):CypA complex has been superimposed on the crystal structure of CypA:**42**. The main interactions between the dimedone lead and CypA, detailed in Chapter 1, have been preserved. Ligand **42** and CsA have similar positioning within the active site and several other interactions are conserved, as illustrated in Figure 3.4.

Figure 3.4

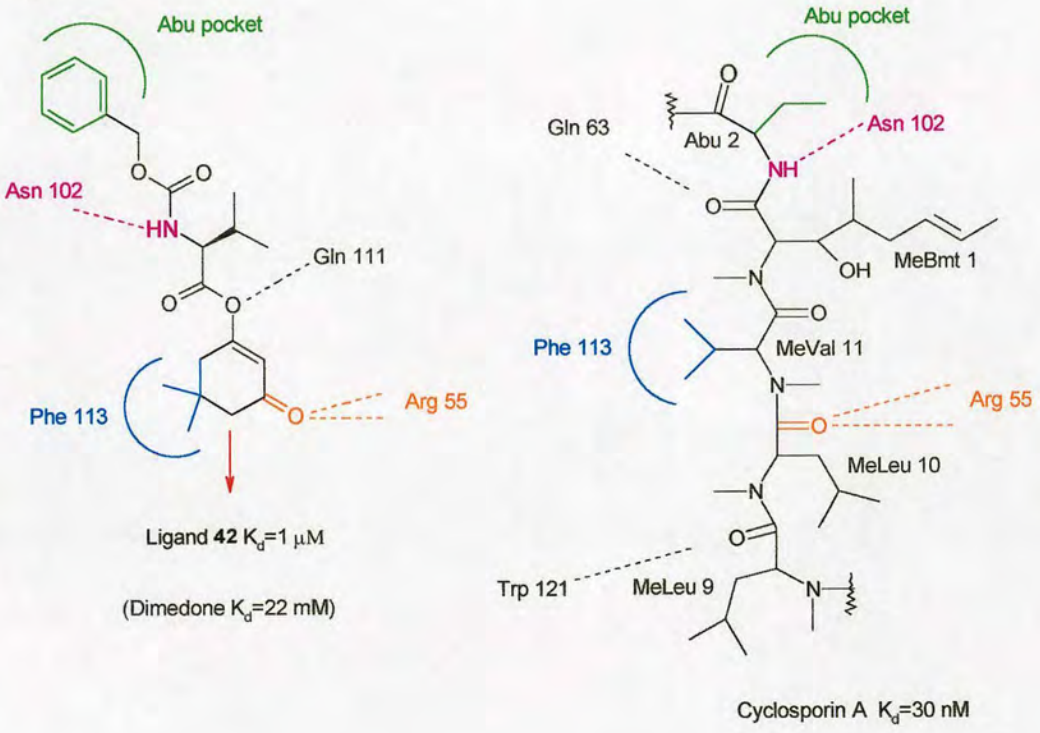

Examination of the X-ray structure indicates space available within the CypA active site for further extension of the dimedone core (represented in Figure 3.4 by the red arrow). With this in mind, a route to 4-alkyldimedone derivatives was developed, in order to enable incorporation of these analogues into future ligands of the type **82** (Scheme 3.1). This further extension of the dimedone core continued to allow for preservation of the main interactions of the ligand with the active site, and introduced the potential for additional binding interactions.

Scheme 3.1

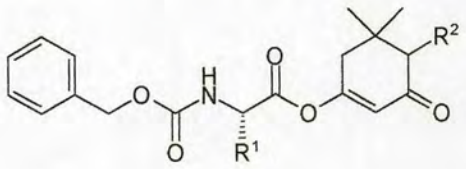

82

3.3 4-alkyldimedones

Berry *et al.*[10] reported the direct 4-alkylation of dimedone by alkyl bromides *via* the dianionic species **83,** generated at -78 °C using lithium diisopropylamide and hexamethylphosphoric triamide (Scheme 3.2).

Scheme 3.2

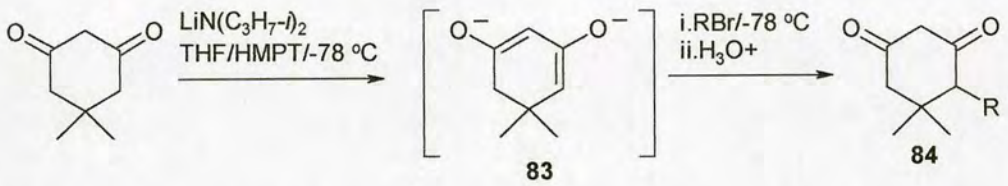

83 **84**

R= $CH_2CH{=}CH_2$, $CH_2CH_2CH_3$, $CH(CH_3)_2$, cyclohexyl, benzyl

Reaction of dimedone with benzyl bromide and allyl bromide under these conditions resulted in a complex mixture (>6 spots by TLC), which on purification by column chromatography, was found to be mainly dimedone starting material. Only a negligible yield of the desired 4-alkyl species could be recovered.

Despite the literature precedence, none of the alkyl bromides studied could be coupled to the active dianionic dimedone with any great success. However, it was later discovered that treatment of dimedone with methyl iodide under the reported conditions resulted in formation of 4-methyldimedone in 55 % yield. The alkyldimedone **85** was then coupled to *N*-benzyloxycarbonyl-L-valine **43** in the usual manner (Scheme 3.3).

Scheme 3.3

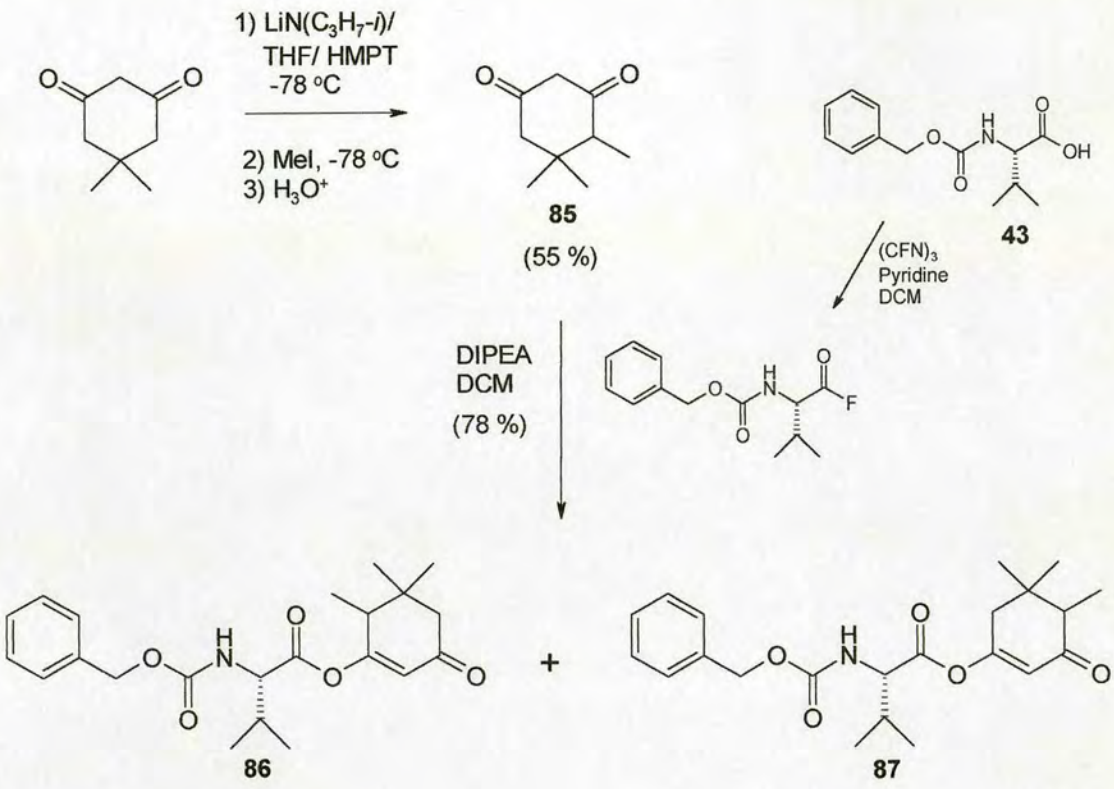

^{1}H and ^{13}C NMR of the crude reaction mixture indicated that a small amount of the diastereomeric mixture **86** might be present in addition to the expected diastereomers **87**. Separation of the two sets of regioisomers by column chromatography, isolated diastereomeric mixture **87**, with recovery of only a trace amount of the more sterically hindered reaction products **86**. The diastereomeric mixture **87** could not be purified further into the component diastereomers by chromatography or by chiral HPLC.

Successful alkylation of dimedone by methyl iodide implied that cleaner reactions might be achieved by adapting the conditions reported by Berry *et. al.* Indeed, the results were much improved by addition of sodium iodide to the reaction in order to affect halogen exchange. Using the new conditions, analogues **88** and **89** were prepared from the corresponding bromides (Scheme 3.4).

Scheme 3.4

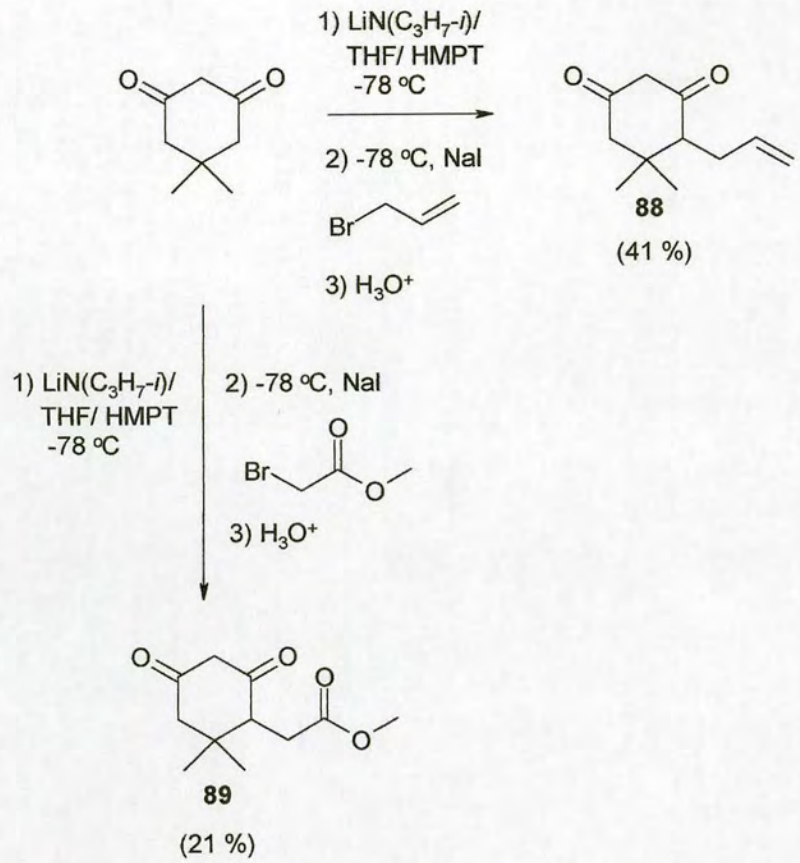

The preparation and successful coupling of 4-alkyldimedones to protected amino acids could now be performed in reasonable yield. However, the alkyldimedone analogues were generated as a mixture of enantiomers, resulting in a diastereomeric mixture of ligands on coupling to the amino acid, as seen with the 4-methyldimedone ligand **85** (Scheme 3.3). The possibility of separating the 4-alkyldimedone enantiomers prior to coupling therefore required to be investigated as the next step towards library generation.

3.3.1 Separation of 4-Alkyldimedone Enantiomers

3.3.1.1 Chiral camphanic acid

The first strategy studied was the resolution of enantiomers by coupling with a chiral camphanic acid species, followed by separation of the resulting diastereomers by column chromatography then cleavage of the chiral agent. (-)-Camphanic acid chloride **90** was coupled to 4-methyl dimedone **85** under basic conditions to produce the enol ester **91** as a 1:1 mixture of diastereomers, as shown in (Scheme 3.5). Attempted separation of the diastereomeric mixture **91** by column chromatography resulted in isolation of one diastereomer **91a** (12 % yield of the most polar component by TLC, one peak by chiral HPLC) as a pure compound, and recovery of a quantity of the diastereomeric mixture. The camphanic acid group was cleaved using sodium methoxide in methanol.

In general, successful separation of the diastereomers using the camphanic acid strategy was found to be very dependent on the alkyl group involved. Additionally, only the first diastereomer eluted from the column was ever recovered pure, with later fractions recovered as a mixture, indicating the difficulty of the separation.

Scheme 3.5

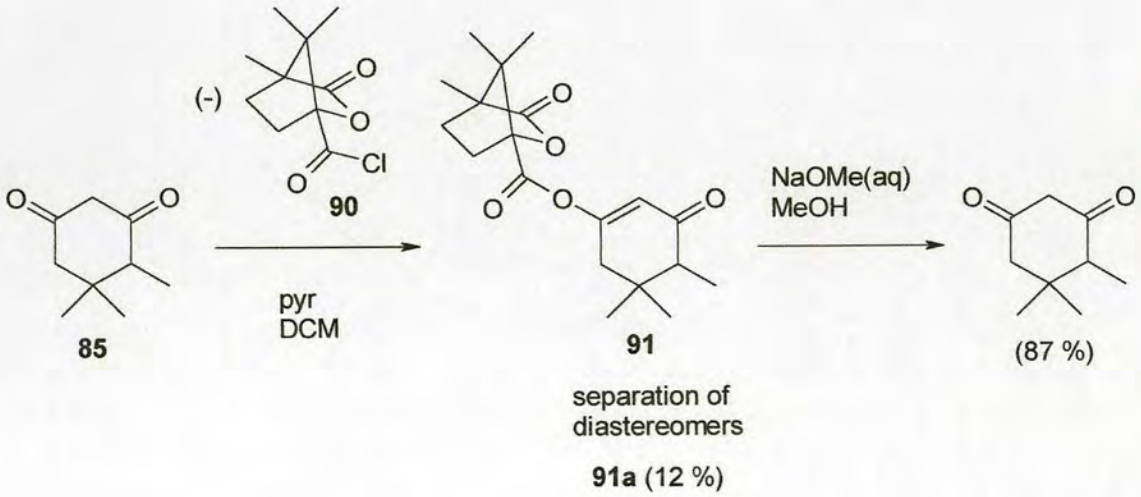

3.3.1.2 Chiral alcohols

Further investigation of the literature revealed that 4-alkylation of the enol ether **92** of dimedone could be achieved using LDA, as reported by Lange *et al.*[11] (Scheme 3.6).

Scheme 3.6

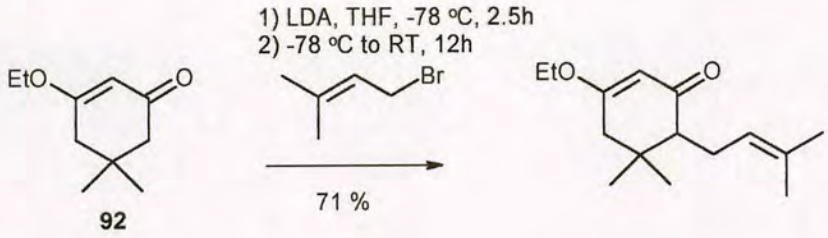

92

It was proposed that this might be a cleaner method of generating the required 4-alkyldimedones compared to the dianion chemistry, with the added advantage that it may be possible to use a chiral enol ether derivative to facilitate separation of the diastereomeric dimedone analogues. It would also be interesting to see if a chiral dimedone ether could direct the course of the reaction to alter the ratio of diastereomers obtained.

Two chiral alcohols were tested using this strategy; [(1*S*)-endo]-(-)-borneol **96** and (1*R*)-endo-(+)-fenchol **93** (illustrated in Scheme 3.7). Although, as expected, cleaner dimedone alkylation reactions were observed in each case, the yields of 4-alkyldimedones isolated were not improved, and separation of the mixtures **95** and **98** into their component diastereomers, was again impossible by chromatography. It was also noted, by analysis of ^{13}C NMR spectra that an almost equal ratio of diastereomers was obtained in mixtures **95** and **98**, indicating that no asymmetric induction of the alkylation by the chiral alcohol auxiliary occurred. This observation was confirmed by chiral HPLC of diastereomeric mixtures **95** and **98**, in which both chromatographs showed two peaks of almost identical percentage area. The chiral alcohol group was successfully cleaved using aqueous acid to regenerate 4-benzyl dimedone **99**. Although the separation of the chiral 4-alkyldimedone enol ether derivatives was possible by chiral HPLC, this was not practical on the preparative

scale required for generation of sufficient quantities for library synthesis. Separation of a racemic mixture of 4-benzyl dimedone **99** was not possible by chiral HPLC using the conditions investigated.

Scheme 3.7

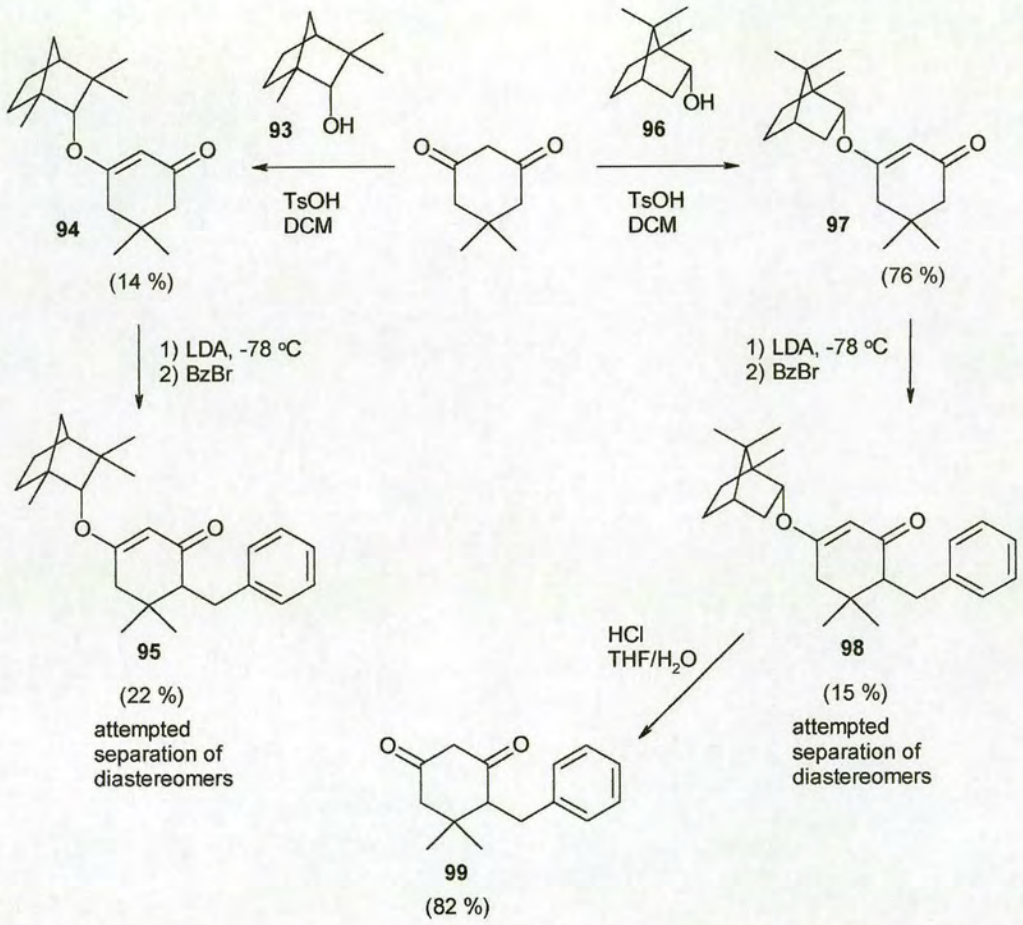

Direct alkylation of the dimedone enol ester **42** (Scheme 3.8) was attempted with no success.

Scheme 3.8

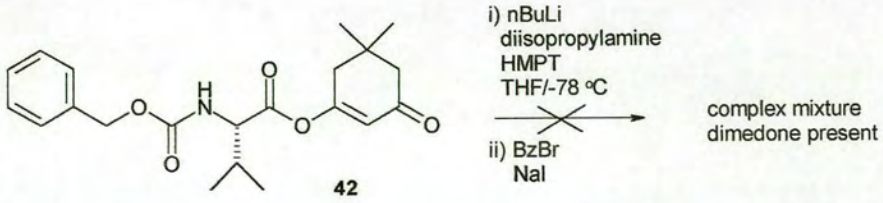

3.3.1.3 Chiral ammonium salts

Chiral resolution of the enantiomeric mixture was attempted by complexation of the dimedone 1,3-diketone system with a chiral ammonium salt. As described in Chapter 2 (2.2.5), the TBAF salt of dimedone **72** can be easily prepared (Scheme 3.9).

Scheme 3.9

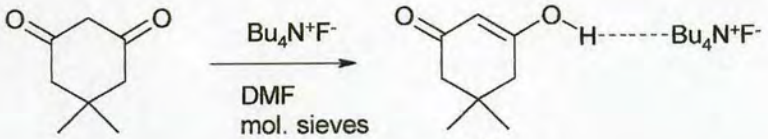

72

The chiral ammonium fluoride salts **100-102** have been reported in the literature[12,13] and appeared to be a reasonable starting point for complex formation. These fluorides can be prepared from the commercially available chloride or bromide salts.

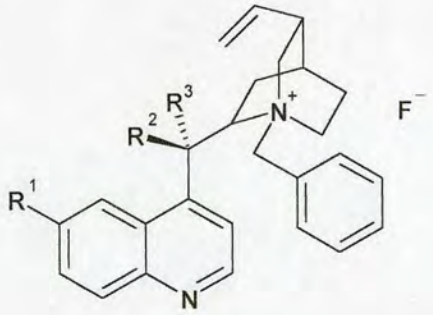

100 R^1 = H, R^2 = H, R^3 = OH
101 R^1 = OMe, R^2 = OH, R^3 = H

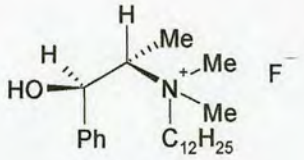

102

Treatment of *N*-benzylcinchonidinium bromide **103** (Scheme 3.10) with CsF in H_2O/MeCN, adapting conditions reported by Hayami *et al.*[14] resulted in only a small percentage conversion to the fluoride. The fluoride salt **104** was instead formed by passing the bromide salt through Amberlite IRA 410 (OH) ion exchange resin, previously treated with aqueous HF, as described by Pless.[15] ^{19}F NMR of the resulting white solid with 4-fluorophenol as internal standard, indicated complete conversion of the quaternary ammonium salt to the fluoride. The peak centred at 125 ppm was in agreement with the reported chemical shifts of quaternary ammonium

fluorides.[16] Comparison of the ^{1}H NMR spectra of the salt **104** and the *N*-benzylcinchonidinium bromide starting material **103** revealed that no decomposition of the *N*-benzylcinchonidinium moiety had taken place during the transformation. The 4-methylcyclohexyldimedone analogue **105**, prepared by reaction of the dimedone dianion with bromomethylcyclohexane in the presence of NaI, was treated with 0.5 molar equivalents of the *t*-alkylammonium fluoride **104**, with the hope of achieving selective complexation of the salt with a single enantiomer of the dimedone analogue. 4-Methylcyclohexyldimedone was chosen as it was the only 4-alkyldimedone adduct isolated in crystalline form. Unfortunately, all signals in the ^{13}C NMR spectra of the reaction mixture were found to correspond to those of the two starting materials **104** and **105** indicating that the desired salt complex **106** had not formed. Additionally, the ^{13}C NMR of the salt complex would be expected to show a peak at *ca.*116 ppm corresponding to the enolic proton (*H*, Scheme 3.10) of the dimedone adduct, and no signals were present in this region of the spectrum.

Scheme 3.10

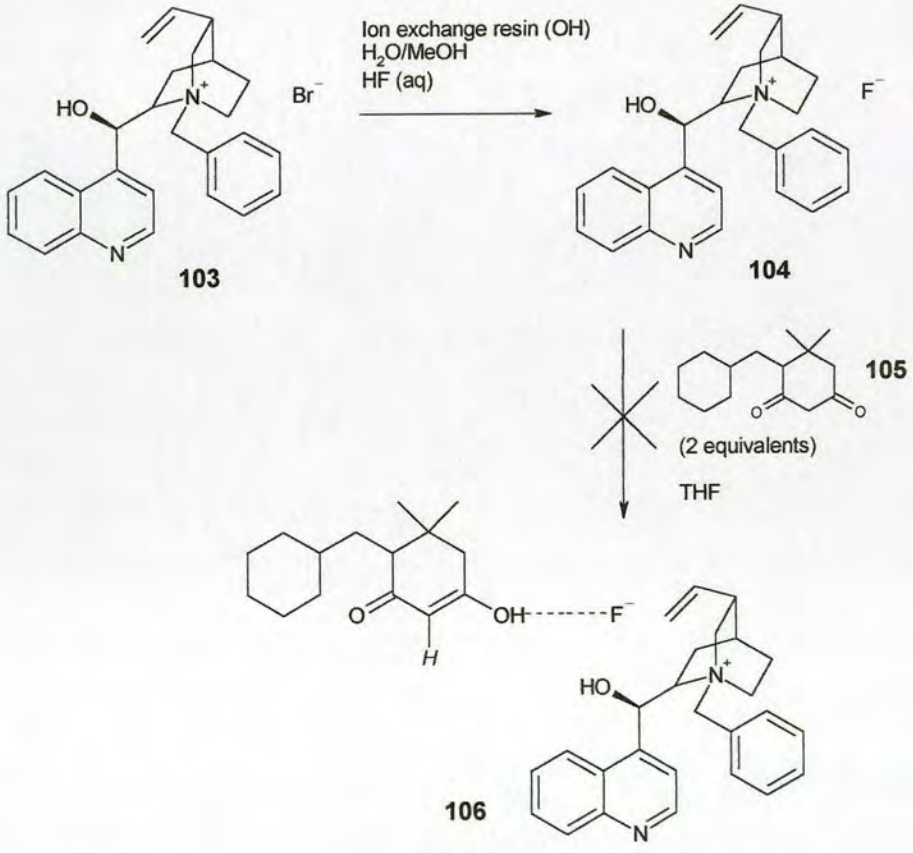

At this point the emphasis of the project changed when the crystal structure of diastereomeric **87** bound to the CypA active site became available. This structure, obtained by crystal soaking and shown in Figure 3.5, indicated that binding of the diastereomeric **87** was very similar to that of the non-methylated ligand **42** described previously (Figure 3.3).

Figure 3.5: Ligand **87** and **CsA** superimposed

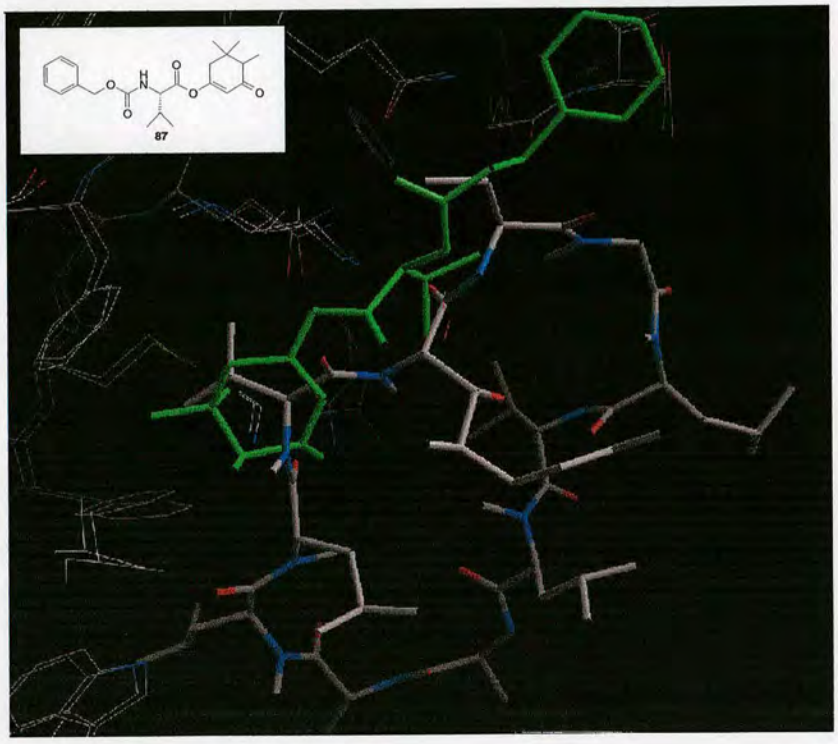

In Figure 3.5 the ligand **87** structure is shown in green and that of CsA is shown in white. The crystal structure of the CsA:CypA complex has been superimposed on that of the ligand **87**:CypA complex. Again, the carboxybenzyloxy group is pointing up towards the Abu pocket, while the dimedone portion remains within the hydrophobic pocket. One slight difference observed is that the orientation of the dimedone dimethyl group is slightly altered so that one methyl group and the adjoining carbon-carbon bond of the dimedone ring form the shortest contacts with the hydrophobic binding pocket residues. It should be noted that although the CypA crystal was soaked in a solution of diastereomers **87**, the crystal structure obtained was not of sufficient resolution to establish whether one or both of the diastereomers

was bound within the active site. However, successful acquisition of a crystal structure using diastereomeric ligands, suggested that it would be possible to screen a library of ligand pairs existing as two diastereomers at the dimedone chiral centre. For this reason and partly due to time constraints, attempts to separate the enantiomeric 4-alkyldimedone building blocks were postponed at this stage in order to concentrate on library generation.

3.4 Introduction of Diversity to the Library Template

In view of the type of structures exhibiting greatest binding affinity to CypA, the proposal was to generate a small diverse library of the form shown in Scheme 3.11. Study of the chemical routes developed thus far indicated three positions (X, Y, Z) where diversity could be introduced into the library template **107**.

Scheme 3.11

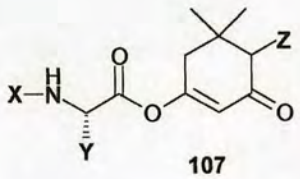

107

X = amino protecting group
Y = amino acid side chain
Z = alkyl, aryl group

3.4.1 Introduction of Diversity at Positions X and Y of Template

3.4.1.1 Coupling/deprotection strategy

The initial idea was to couple dimedone to a set of *N*-protected amino acids, followed by deprotection and acylation with a set of acyl chlorides (Scheme 3.12).

Scheme 3.12

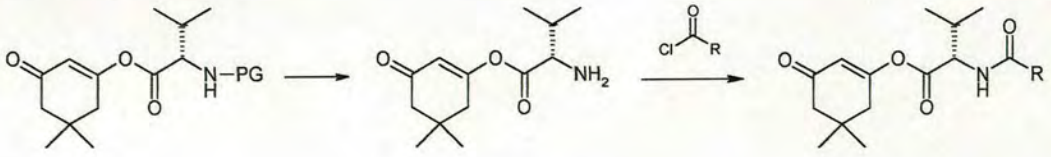

The use of *N-tert*butyloxycarbonyl protected amino acids **81** proved problematic because treatment with trifluoroacetic acid in the deprotection step was found to cleave the enol ester, resulting in recovery of dimedone. TLC and mass spectrometry of the crude reaction mixture indicated the presence of the free amino acid L-valine (Scheme 3.13). Attempted cleavage using 1M H_2SO_4 in EtOAc again resulted in recovery of dimedone.

Scheme 3.13

81 (49 %)

The use of Fmoc protected amino acids was then investigated. In this case the idea was to cleave the Fmoc protecting group using piperidine. However, formation of the dimedone derivative **108** was only possible in low yield (12 %), rendering this route unsuitable for generation of library building blocks.

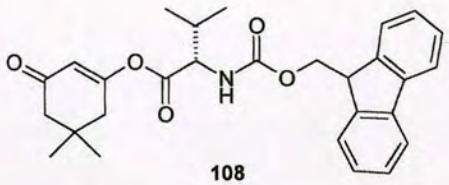

108

In view of the instability of the dimedone enol ether linkage to the conditions investigated for the deprotection of amino acids, a new strategy was sought for the introduction of diversity at position X in the library template **107**. It seemed sensible to change the order of synthetic steps in order to form the less-stable enol ester linkage in the final stage.

3.4.1.2 Protection/coupling strategies

An alternative route for introduction of an amino acid *N*-protecting group has been achieved by reaction of the free amino acid with an acyl chloride using conditions reported by Hartwig *et. al.*[17] (Scheme 3.14). The amino acid **109** was refluxed with chlorotrimethylsilane in DCM for 2h before cooling to -15 °C. Treatment with benzoyl chloride and triethylamine at low temperature, followed by acidic work-up, afforded *N*-benzoyl-L-phenylalanine **110**.

Scheme 3.14

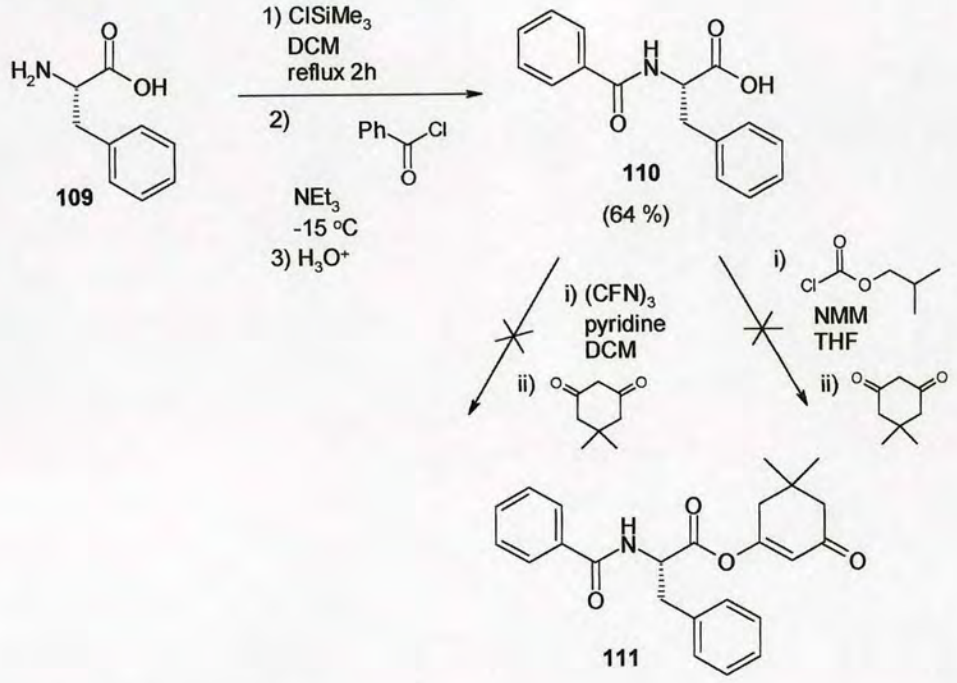

However, attempts to activate the carboxy terminus of the amino acid for further coupling, by acid fluoride formation and *via* the mixed anhydride were unsuccessful. This may be due to cyclisation of the activated *N*-acyl amino acid species **112** resulting in oxazolone **113** formation (Scheme 3.15), evidence of which was observed by ESI MS (+ve) with a peak at 251 (MH^+). Generation of the oxazolone would then prevent formation of the desired dimedone enol ester derivative **111**.

Scheme 3.15

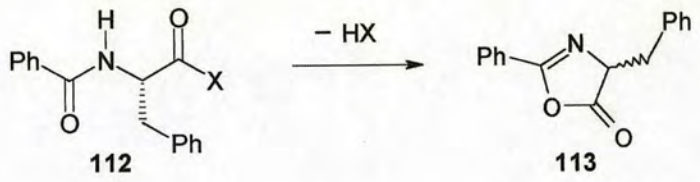

In order to avoid this problem, less reactive carbamates such as **115** (Scheme 3.16) were prepared by reaction of the chosen amino acid with a chloroformate **114** under identical conditions to those described previously. The *N*-methoxycarbonyl-L-valine **115** shown in Scheme 3.16 was successfully coupled to dimedone forming the enol ester **116** by activation *via* the acid fluoride, using cyanuric fluoride and pyridine.

Scheme 3.16

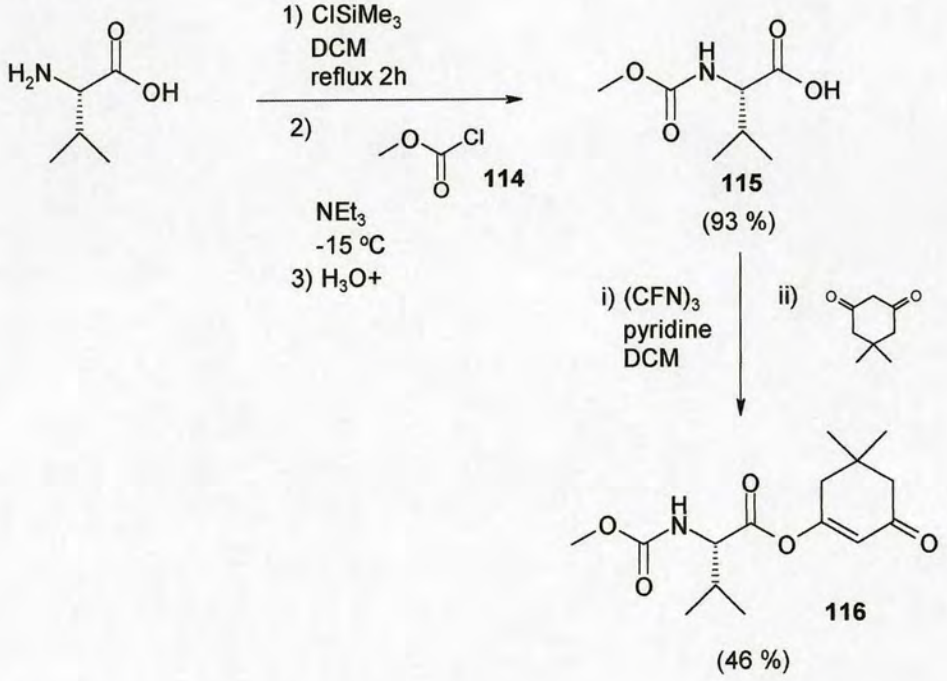

Although the modified Hartwig route worked well for the formation of *N*-carbamoyl amino acids, the conditions were not ideal for library generation because of the heating and cooling steps involved. A search of the ISIS available chemicals database also raised concerns about the number and structural diversity of chloroformates that are commercially available. This would limit the diversity of

library compounds that could potentially be prepared. In view of these drawbacks two new *N*-protection strategies were investigated.

Kobayashi *et al.* [18] have reported that amino acid derivatives of kojic acid **117** can be prepared using DSC **118** and DMAP, as shown in Scheme 3.17.

Scheme 3.17

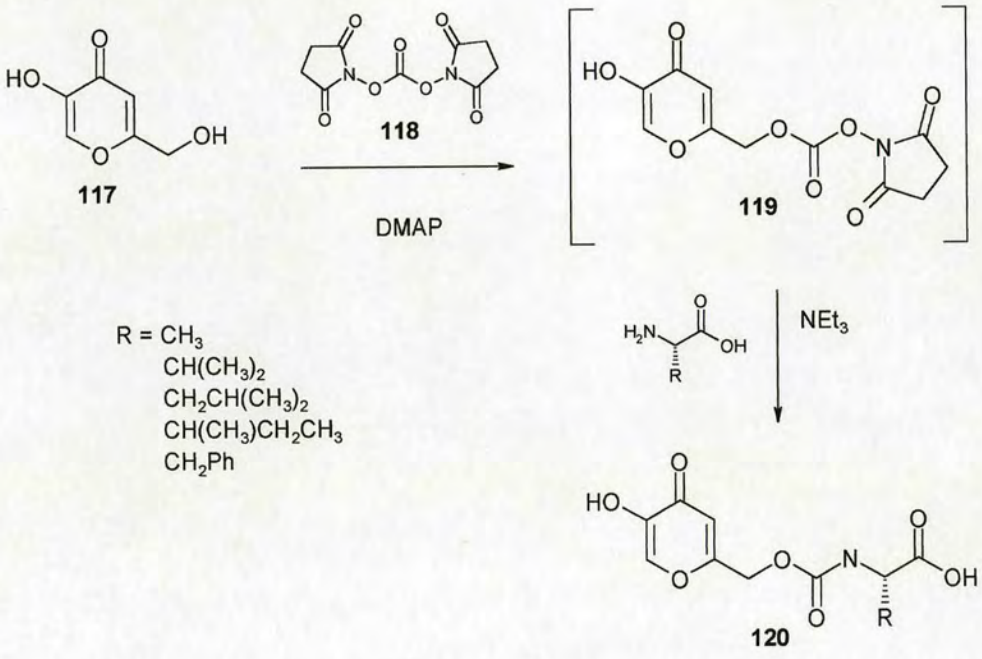

The reaction proceeds by formation of the *N*-succinimidyl carbamate of kojic acid **119**, followed by succinimide displacement by the amino terminus of the amino acid to give the carbamate **120**. The possibility of using different sets of nucleophiles for activation, such as alcohols or amines, forming carbamates **121** or ureas **122** respectively, was investigated (Scheme 3.18).

Scheme 3.18

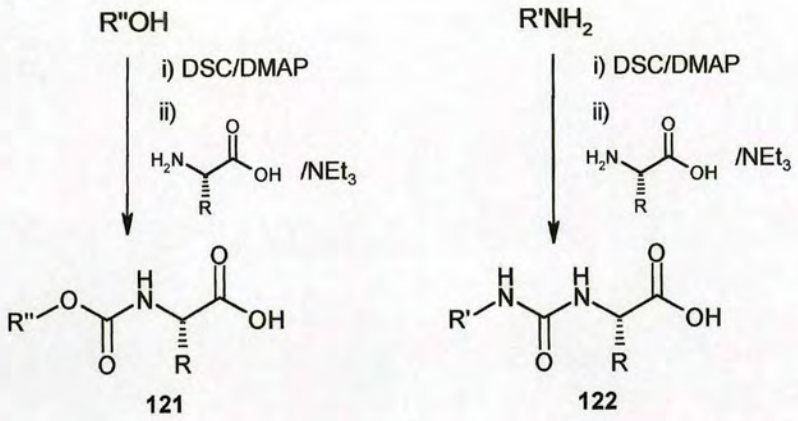

The reaction conditions were tested in the coupling of two alcohols and two amines to L-valine (R=$CH(CH_3)_2$). The results are shown in Table 3.2.

Table 3.2

R"OH	Result	$R'NH_2$	Result
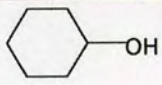	40 % yield of desired carbamate 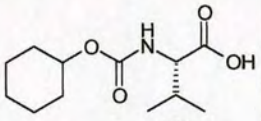 123	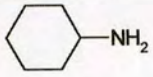	MS evidence of hydantoin formation
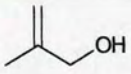	51 % yield of desired carbamate 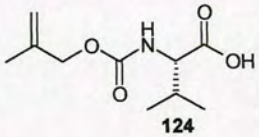 124	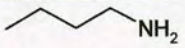	No urea product

The alcohol protection reactions resulted in formation of the desired carbamate in reasonable yield. The advantage of using this strategy for carbamate formation, rather than the chloroformate sequence, is that there are a greater variety of available alcohols and the reaction conditions are milder and more amenable to automation.

In the reactions of amines with L-valine, none of the desired urea product was observed but there was evidence of hydantoin formation in one case. The hydantoin **126** results from cyclisation of the urea **125** as shown in Scheme 3.19. As this reaction would be even more likely on formation of the acyl fluoride **127** for coupling to dimedone, the urea derivatives were not studied further.

Scheme 3.19

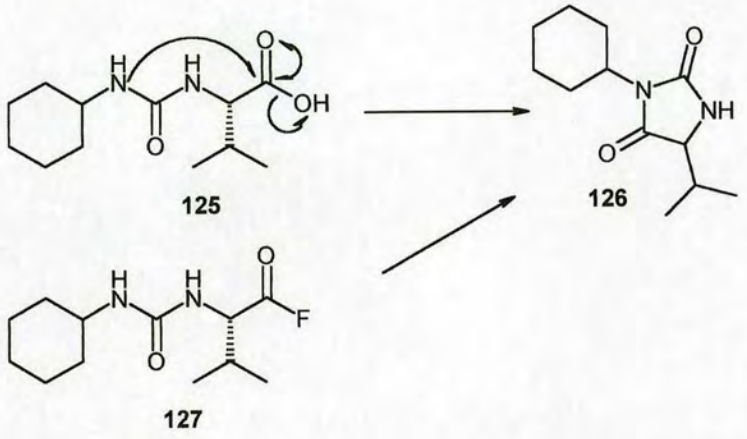

Preparation of carbamate derivatives, such as **123** and **124**, will be discussed further with regard to library preparation in Chapter 4.

3.4.2 Introduction of Diversity at Position Z of Template

A number of 4-alkyldimedone derivatives had now been prepared according to the procedure described in Scheme 3.4. Table 3.3 shows the binding data available on the 4-alkyldimedone ligands along with several other ligands described in this Chapter.

Table 3.3

Ligand	Structure	Interaction with hCyp K_d*	Resolution of hCypA-Ligand Complex
128	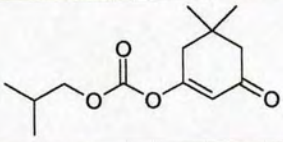	ND	2.70 Å R:20.1 % Rfree:28.4 %
116	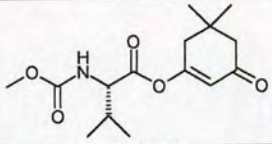	70 μM	1.8 Å R:20.7 % Rfree:26.8 %
85	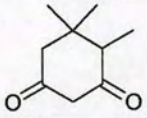	134 μM	2.10 Å R:20.1 % Rfree:26.8 %:
89	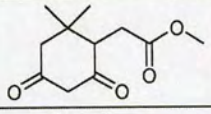	45 μM	1.90 Å R:20.4 % Rfree:26.0 %
88	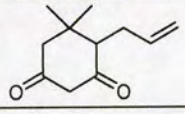	ND	ND
99	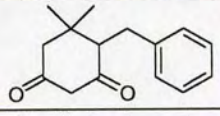	ND	ND
129	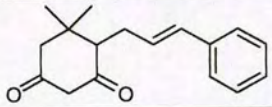	85 μM	2.03 Å R:18.8 % Rfree:24.9 %
105	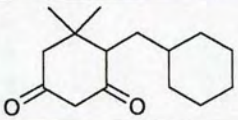	ND	ND
87	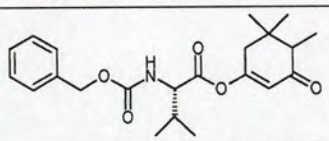	20 μM	2.30 Å R:18.1 % Rfree:33.1 %
130	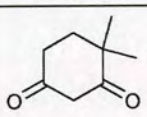	ND	2.2 Å R:19.7 % Rfree:25.3 %
131	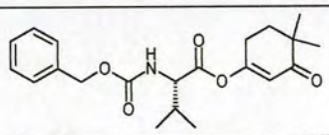	68 μM	2.1 Å R:20.9 % Rfree:28.6 %

* K_d determined by PPIase assay

ND not determined

3.5 Discussion

In the following crystal structures of ligand:CypA complexes, the orientation of the CypA active site is the same in each case, so that some comparisons between different ligand binding conformations can be drawn (oxygen atoms are coloured red and nitrogen atoms blue). The ligand structures can be found in Table 3.3.

3.5.1 Ligands 42, 128 and 116

Figure 3.6: Ligand **128**

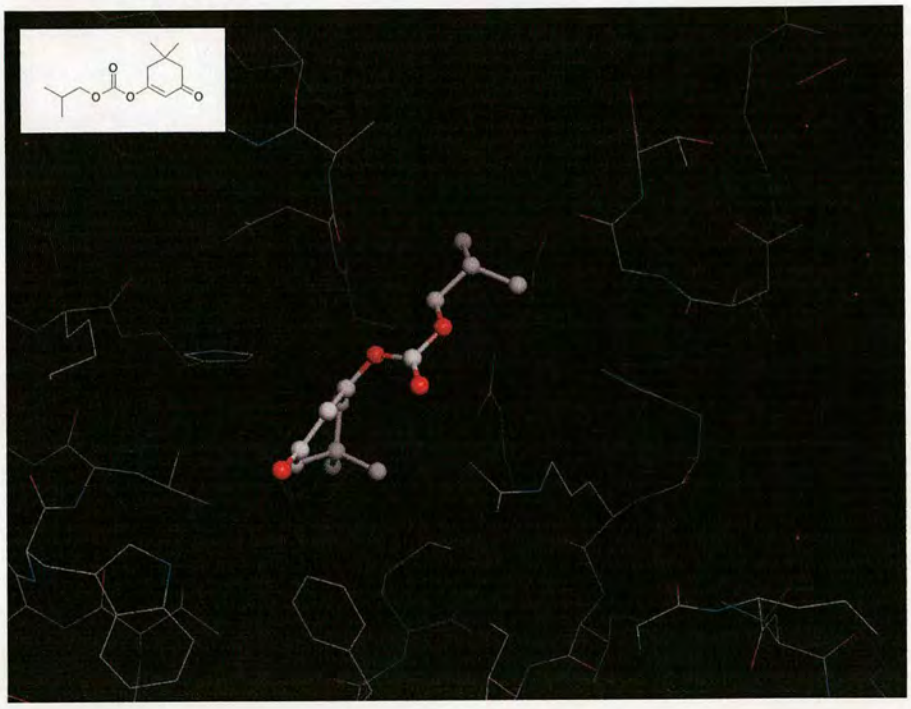

Determination of a dissociation constant of 70 μM for ligand **116**, in the same micromolar range as that obtained for **42**, reinforced the decision to focus on *O*-acyl dimedone derivatives. The crystal structures of ligands **128** and **116** complexed with CypA are shown in Figures 3.6 and 3.7 respectively. For comparison, the X-ray structure of the **42**:CypA complex, viewing the active site in the same orientation as the other two ligand:CypA complexes, is shown in Figure 3.8. The dimedone groups in both ligand **42** and **116** appear to occupy a similar region of space within the binding site of CypA, as do the valine side chains of both ligands. The geminal dimethyl of dimedone in ligand **128** has a slightly different orientation, but

positioning of the *O*-acyl side chain is similar to that of **42** and **116**, as indicated by the superimposed crystal structures of all three complexes (Figure 3.9).

Figure 3.7: Ligand **116**

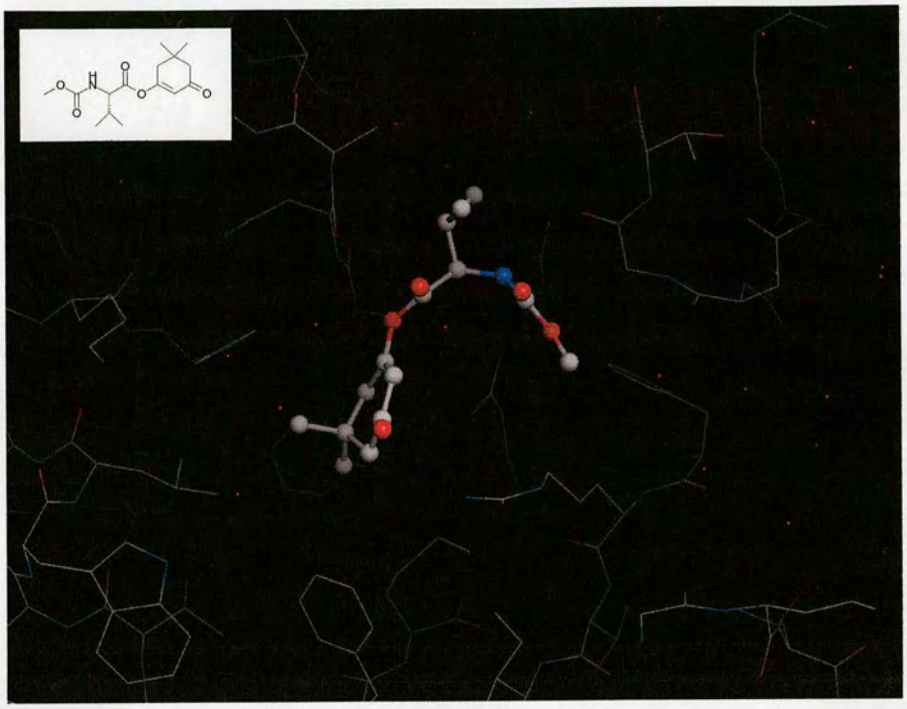

Figure 3.8: Ligand **42**

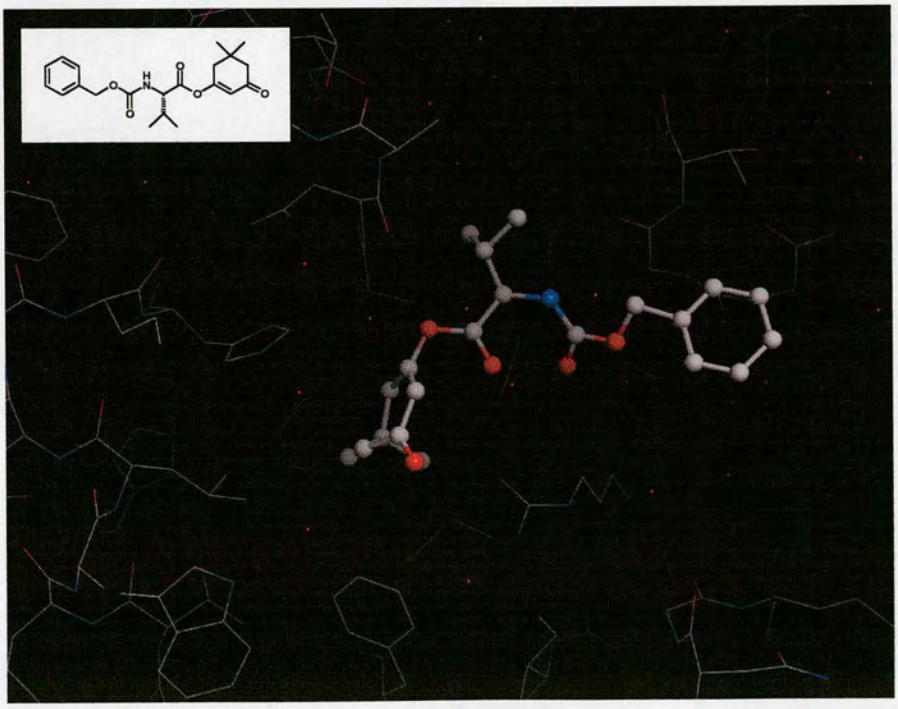

Figure 3.9: Ligands **42, 116** and **128** superimposed

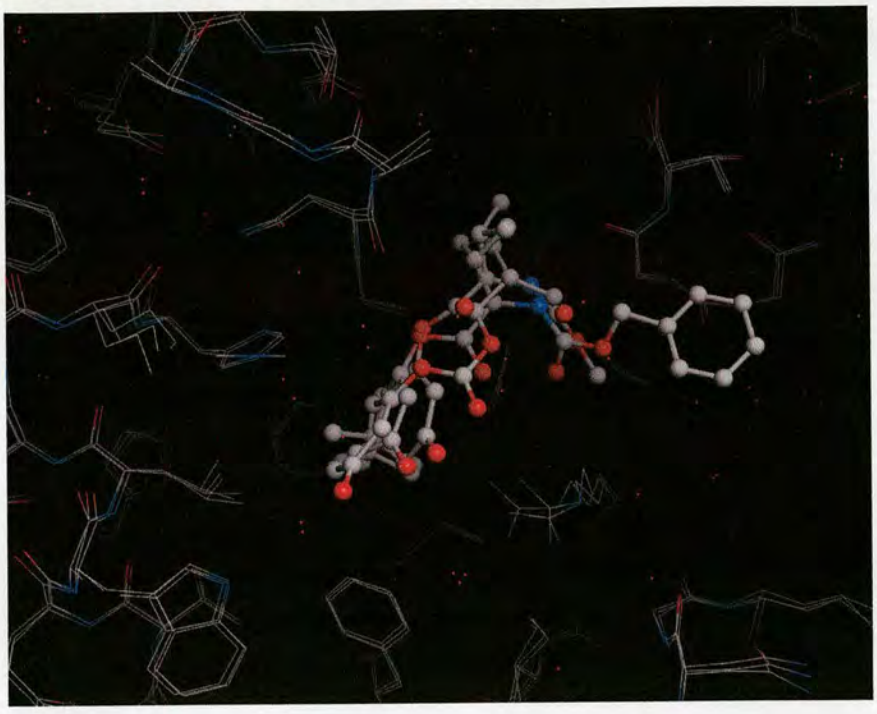

3.5.2 Ligands 89 and 129

Promising results were obtained from PPIase assay of the 4-alkyldimedone ligands **85** (K_d= 134 μM), **89** (K_d= 45 μM), and **129** (K_d= 85 μM). Although the dissociation constants are comparable, the crystal structures of the **89**:CypA and **129**:CypA complexes, Figures 3.10 and 3.11 respectively, reveal that the dimedone groups of these two ligands bind in quite different orientations. Superimposing the **89**:CypA and **129**:CypA complexes (Figure 3.12) does however indicate that the 4-alkyl side chains of both ligands are similarly positioned.

The most surprising result is the K_d= 134 μM measured for ligand **85** (compared with K_d= 22 mM for dimedone). Although the relative orientations of ligand **85** (Figure 3.14) and dimedone within the binding site are different, the addition of a methyl group alone to the dimedone core, would not seem to account for such a large increase in binding affinity. However, observation of micromolar binding for the other 4-alkyldimedone ligands **89** and **129** may go some way towards authenticating this result. Future research should include a more detailed study on the binding of a combination of 4-, 5- and 6- mono-, di- and possibly even tri-methyl substituted

cyclohexane 1,3-diones, along with repeated determination of the original dimedone dissociation constant under controlled conditions.

Figure 3.10: Ligand **89**

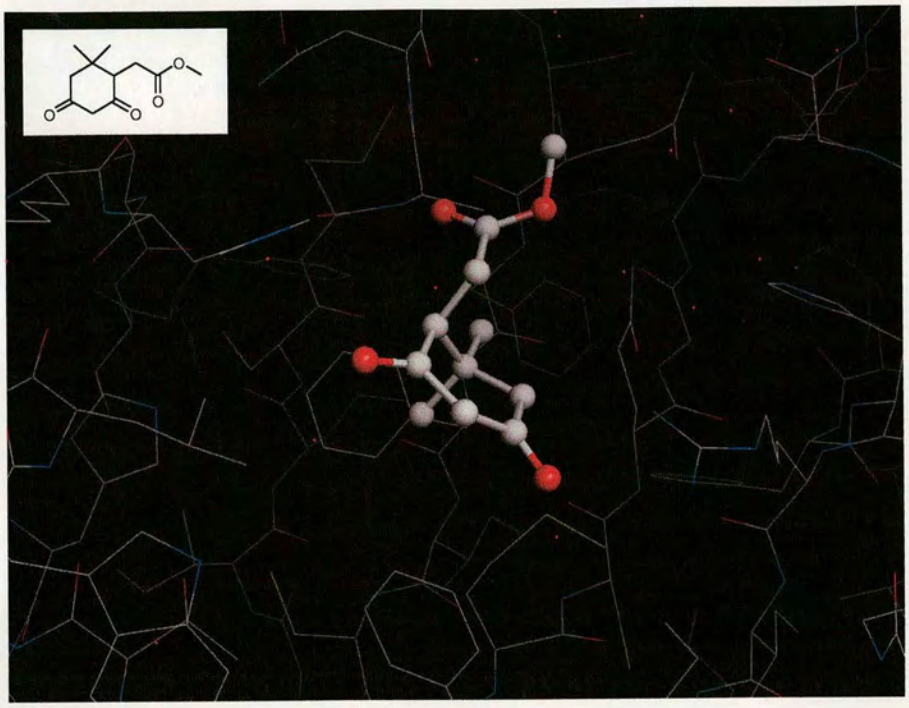

Figure 3.11: Ligand **129**

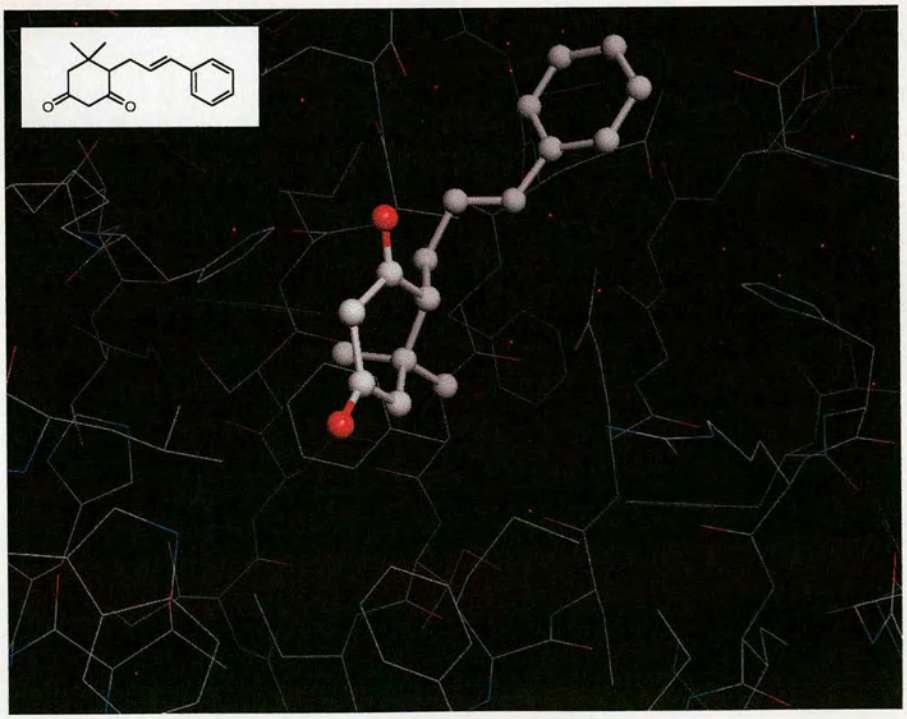

Figure 3.12: Ligands **89** and **129** superimposed

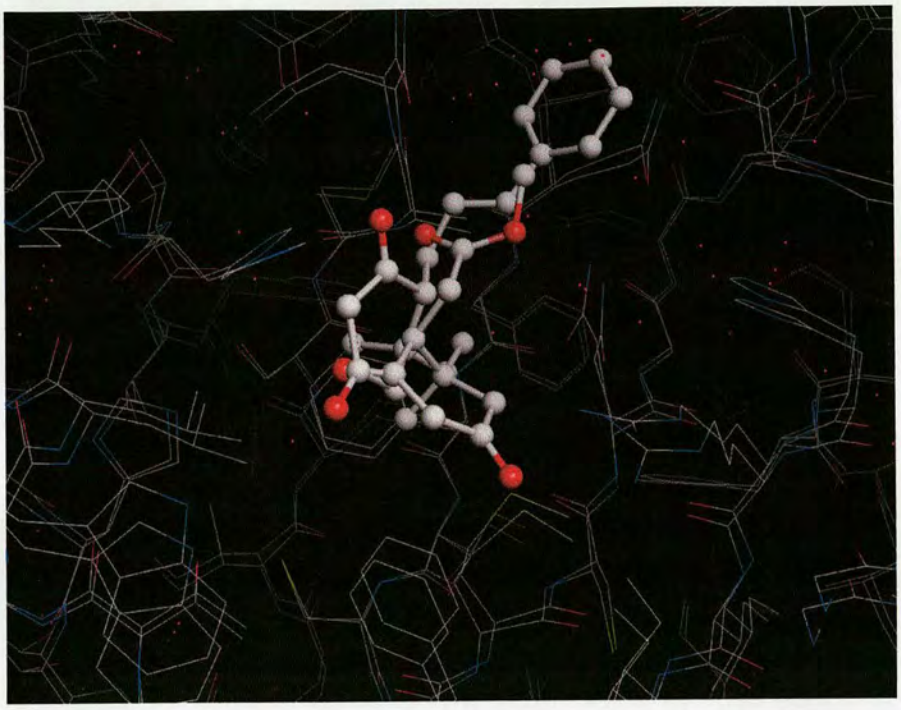

3.5.3 Ligands 85 and 87

By comparison of the crystal structures of **87**:CypA and **85**:CypA complexes shown in Figures 3.13 and 3.14 respectively, it can be seen that 4-methyl dimedone is binding in an entirely different orientation when the *O*-acyl chain is present (ligand **87**). This observation is further clarified by superimposing the two complexes, as in Figure 3.15. This may reflect the relative importance of the interactions of the *O*-acyl chain and dimedone groups respectively, for binding to the protein. It is interesting to note that the *O*-acyl side chain of **87** appears to adopt a rather different orientation to that of **42** (Figure 3.8) and most of the other examples.

Figure 3.13: Ligand **87**

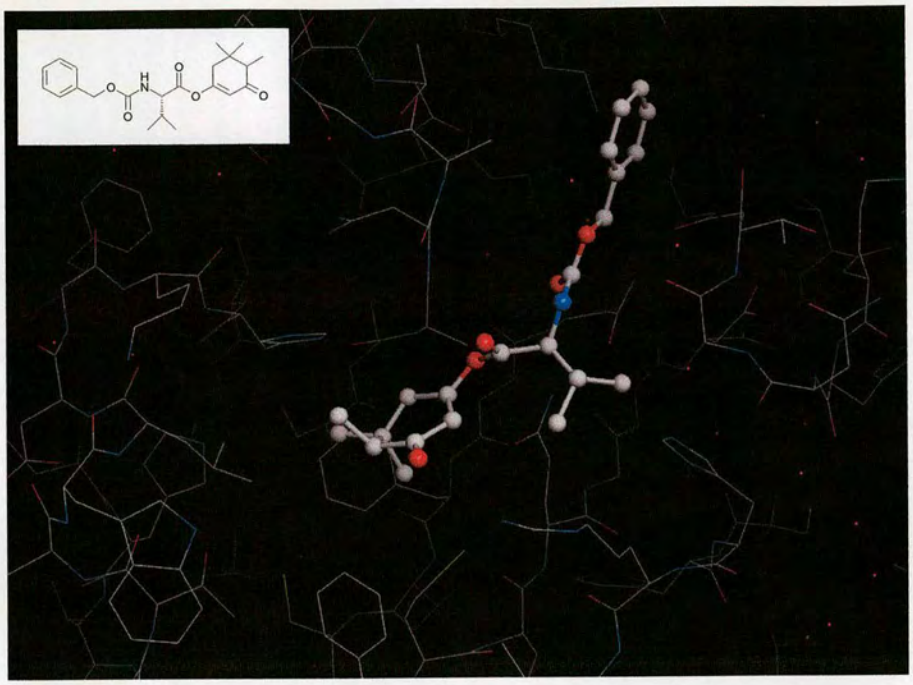

Figure 3.14: Ligand **85**

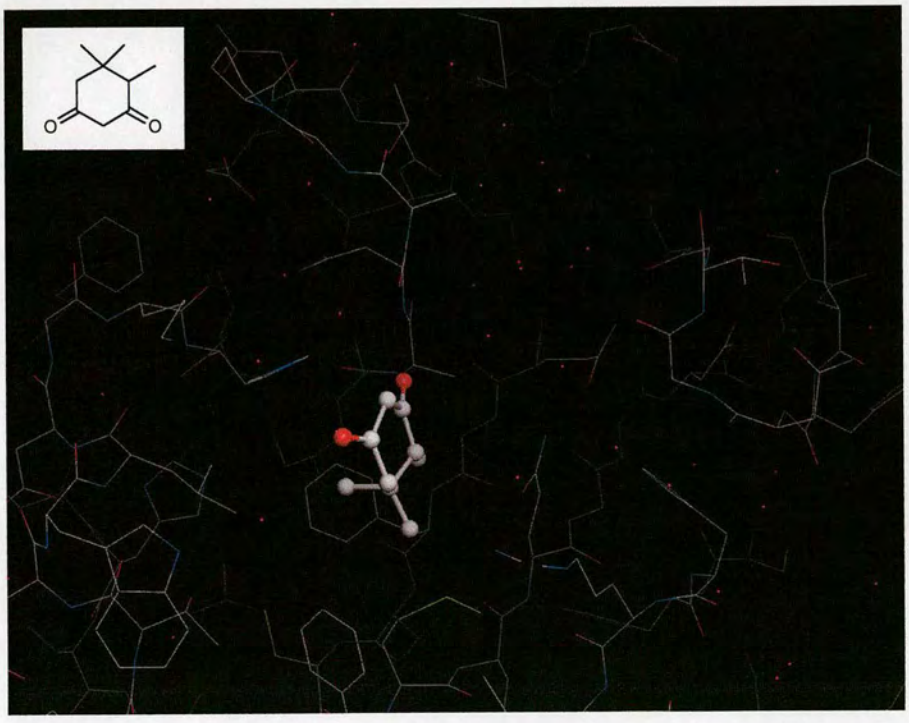

Figure 3.15: Ligands **85** and **87** superimposed

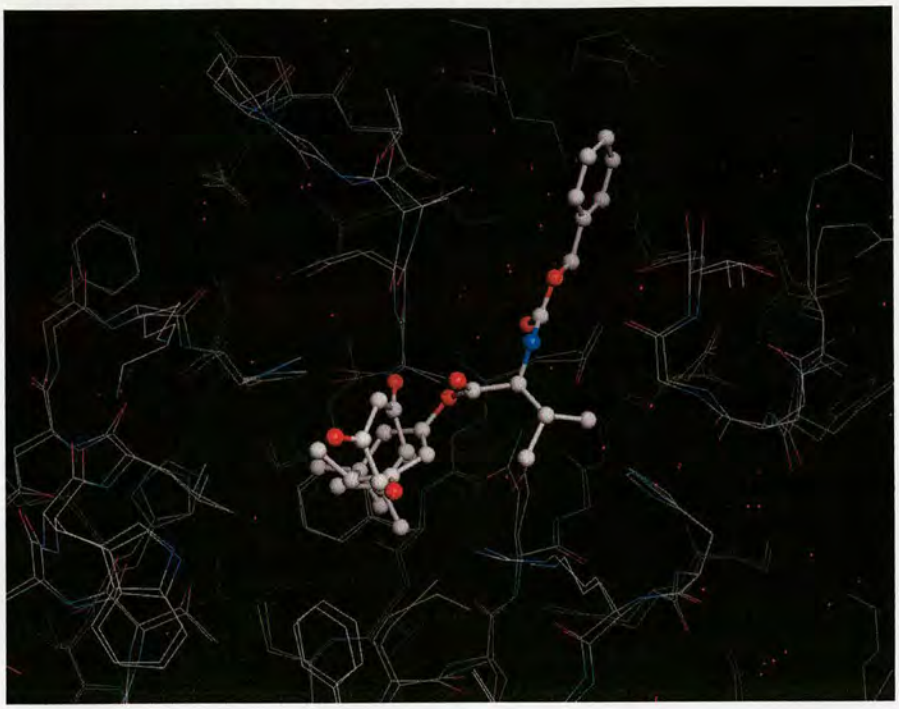

3.5.4 Ligands 130 and 131

The commercially available 4,4-dimethyl cyclohexane-1,3-dione **130** was studied as a means of investigating the effect on CypA-binding of changing the position of the dimethyl group relative to the 1,3-dione in the cyclohexane ring. The isomer **130** was found to complex with CypA in the orientation shown in Figure 3.16, in which the dimethyl group appears to be less closely associated with the hydrophobic binding pocket than in previous examples (Figure 3.8, ligand **42**). Ligand **131** was prepared in the same way as ligand **42** but using 4,4-dimethyl cyclohexane-1,3-dione in place of dimedone, in order to further assess the importance of the *O*-acyl side chain on binding and its influence on cyclohexanedione orientation. Again the orientation of ligand **130** in the binding site is altered when the *O*-acyl chain is present, as in ligand **131**, where the dimethyl group appears to point away from the hydrophobic pocket. The ligand **131**:CypA complex is shown in Figure 3.17, and the two complexes superimposed are illustrated in Figure 3.18. Comparison of Figures 3.8 and 3.17 reveal that the *O*-acyl chains of ligands **42** and **131** adopt similar conformations, despite attachment to different dimethylcyclohexane isomers. These

observations seem to suggest that the hydrophobic interaction of the ligand dimethyl group may not be the major protein-ligand interaction.

Figure 3.16: Ligand **130**

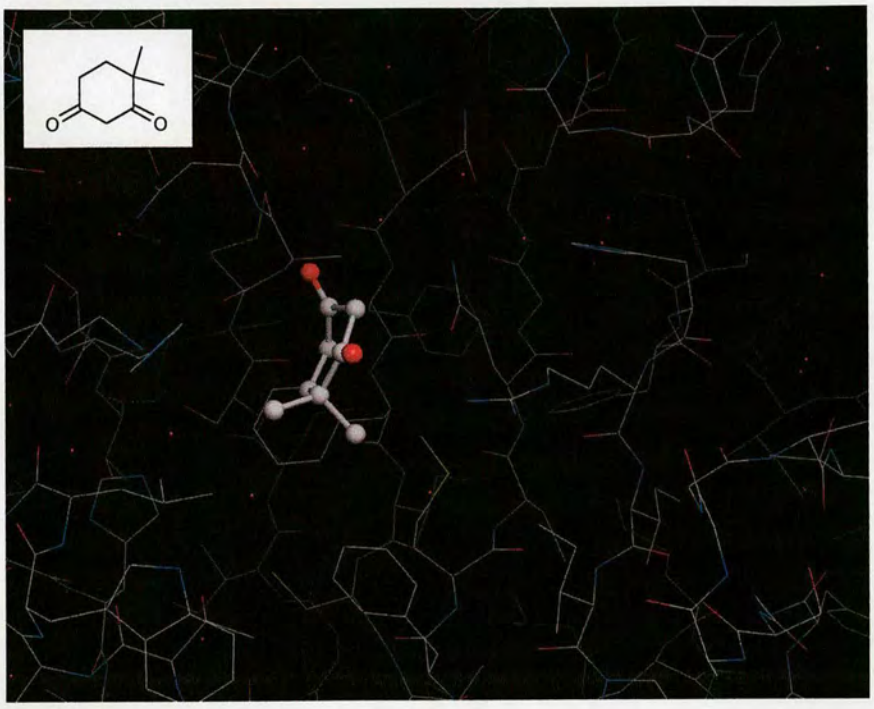

Figure 3.17: Ligand **131**

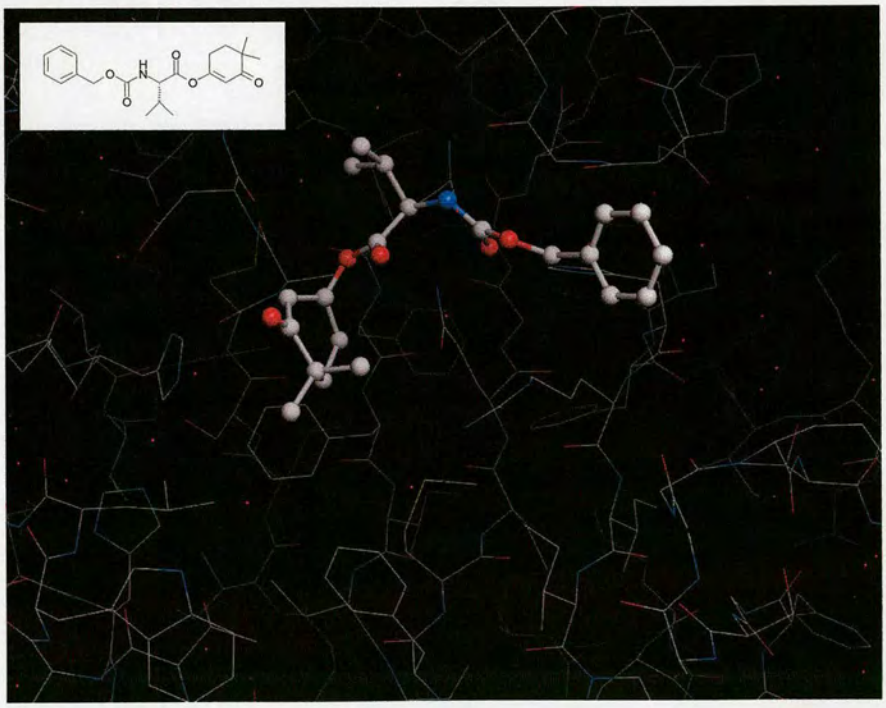

Figure 3.18: Ligands **130** and **131** superimposed

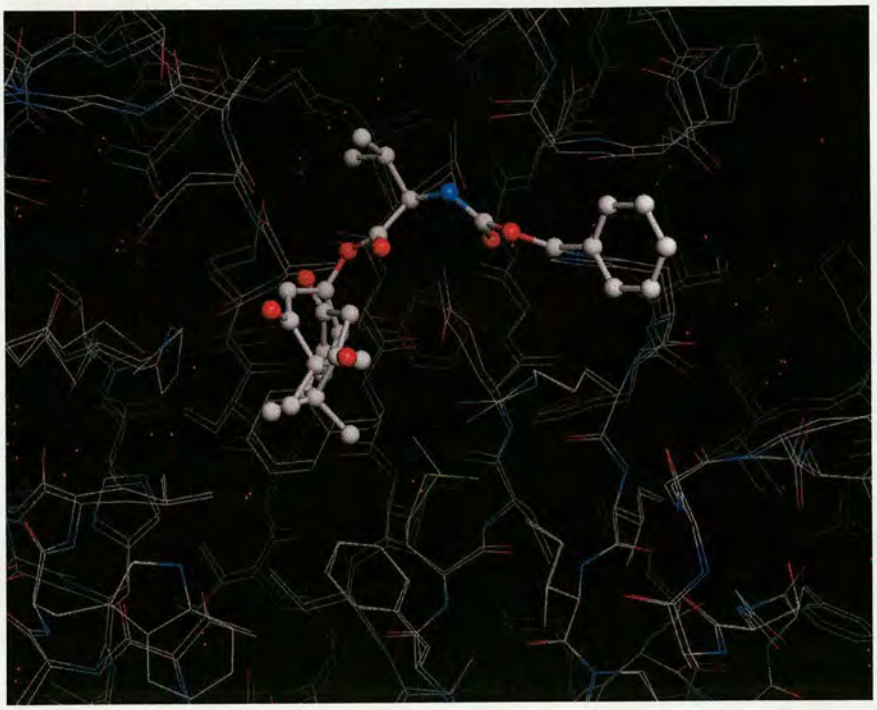

3.6 Initial Mass Spectrometry Results

In experiments carried out by Sally Shirran at Edinburgh University, the binding of CsA to CypA was observed by electrospray mass spectrometry of a 1:1 mixture of CypA and CsA (20 μM concentration of each) in 10 mM aqueous ammonium acetate solution, pH 6.9 (Figure 3.19). The experiment was repeated with the highest affinity dimedone-based ligand **42**, and a mass corresponding to the CypA:**42** complex was observed, as shown in Figure 3.20. In this case, the ratio of CypA:ligand had to be increased to 1:50 in order to observe the complex, which is a reflection of the lower binding affinity of ligand **42** for CypA relative to that of CsA. However, some complications did arise. Firstly, the peak at m/z = 18247.3 in Figure 3.20 corresponds to the mass expected for an acylated enzyme species which may be formed by cleavage of the weak enol ester bond in ligand **42** and acylation of CypA by the *N*-benzyloxycarbonyl-valinyl moiety. Secondly, the spectrum in Figure 3.20 also shows peaks corresponding to complexation of two (m/z = 18763.5) and three (m/z = 19132.5) molecules of ligand **42** to CypA. Both of these observations suggest that a degree of non-specific binding of ligand **42** (and by-products of ligand **42**) to

CypA at positions other than the active site may be occurring. The extent of denaturation of CypA under the ESI conditions has yet to be fully investigated and this study should be included in any future work on this screening method. Nevertheless, initial results indicated that it should be possible to screen a library of dimedone analogues by MS, since under identical experimental conditions to those used to observe the CypA:**42** complex, any library members complexing to CypA with comparable or greater binding affinity to that of ligand **42**, should be visible. For any ligands found to bind to CypA, the issues of specific active site binding, and enzyme acylation would require to be clarified at a later date.

Figure 3.19: Electrospray mass spectrum of a 1:1 mixture of CypA and CsA.

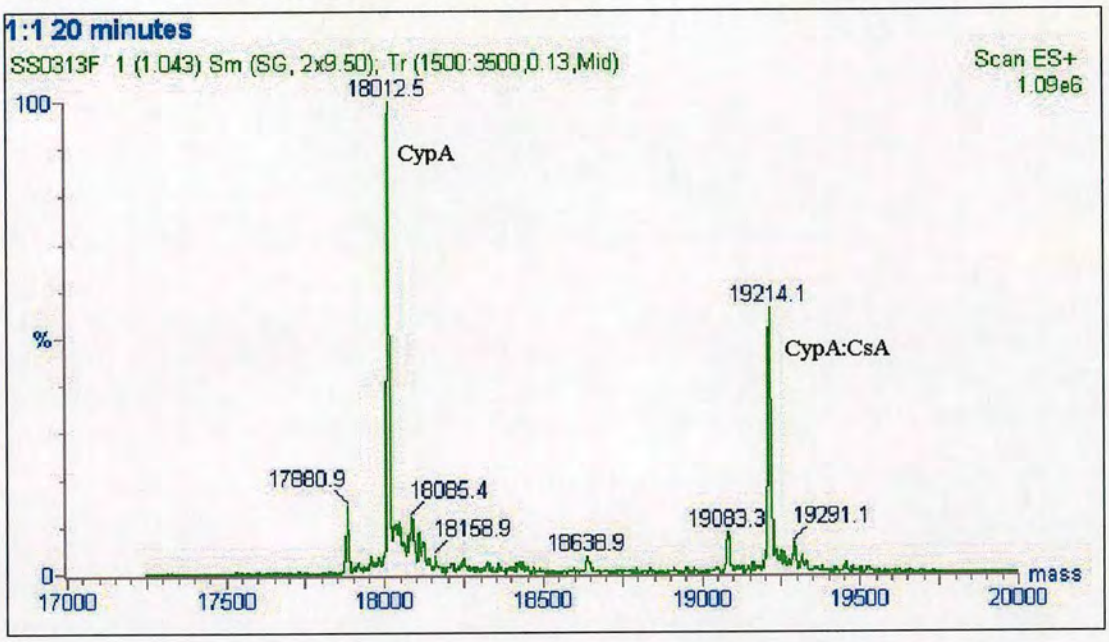

Figure 3.20: Electrospray mass spectrum of a 1:50 mixture of CypA and Ligand **42**.

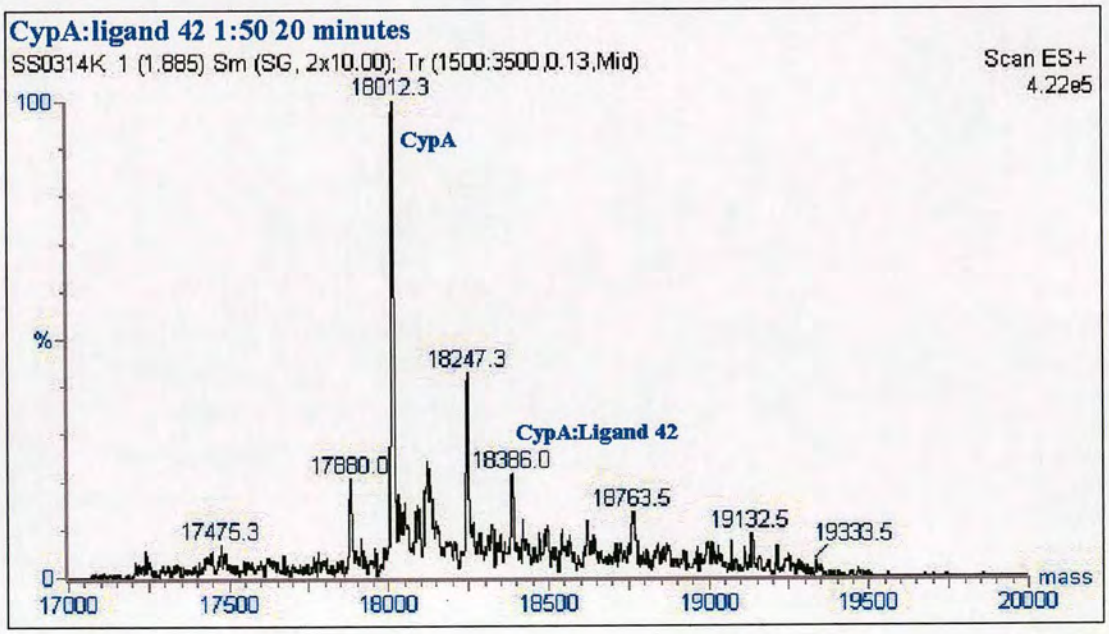

3.7 Conclusion

By examination of the data obtained from the various screening techniques employed, it can be seen that each technique provides rather different information on receptor-ligand binding. While X-ray crystallography is vital for information on the protein-ligand interactions and orientation of the ligand within the active site, quantitative measurement of binding dissociation constants was obtained from the PPIase assay. Although limited information on binding could be taken from the initial fluorescence assay results, the data from the first round of fluorescence screening altered the focus of ligand design towards producing *O*-acyl dimedone derivatives. From early crystallographic data it was initially proposed that the interaction between the geminal dimethyl group of dimedone and the CypA hydrophobic binding pocket was the major binding interaction. However, later crystal structures contradict this theory, since the binding of the geminal dimethyl group of dimedone analogues has been observed in various orientations depending on the 4-alkyl substituent and *O*-acyl side chain, in ligands exhibiting similar K_d's by PPIase assay. In conclusion, the ideal strategy is to employ a combination of all techniques in order to determine as much as possible about the binding of successive groups of ligands within the active site, in order to direct the focus of successive rounds of synthesis. In the meantime the decision was made to use mass spectrometry to screen the proposed dimedone-based library in the first instance, and then to study any promising ligands by PPIase assay and crystallography. The speed and ease of MS screening and the fact that minimal amounts of protein and ligand are required constitute the main advantages of this technique over other screening methods described.

3.8 References

[1] Bagshaw, G.; Harris, D., Measurement of ligand binding to proteins in spectrophotometry and spectrofluorimetry. A practical approach, Ed Bashford, C.; Harris, D., IRL Press, 1987.

[2] Handschumacher, R.; Harding, M.; Rice, J.; Drugge, R., *Science*, 1984, **226**, 544-547.

[3] Thesis: Kontopidis, G.A., *Immunophilin Ligand Design*, The University of Edinburgh, 1999, 4.6.

[4] Göthel, S. F.; Marahiel, M. A., *Cell Mol. Life Sci.*, 1999, **55**, 423-436.

[5] Kofron, J. L.; Kuzmic, P.; Kishore, V.; Bonilla-Kolon, E.; Rich, D. H., *Biochemistry*, 1991, **30**, 6127-6134.

[6] Kofron, J. L.; Kuzmic, P.; Kishore, V.; Gemmecker, G.; Fesik, S. W.; Rich, D. H., *J. Am. Chem. Soc.*, 1992, **114**, 2670-2675.

[7] Ganem, B.; Li, Y-T.; Henion, J.D., *J. Am. Chem. Soc.*, 1991, **113**, 6294-6296.

[8] Li, Y-T.; Hsieh, Y-L.; Henion, J.D.; Ocain, T.D.; Schiehser, G.A.; Ganem, B., *J. Am. Chem. Soc.*, 1994, **116**, 7487-7493.

[9] Jørgensen, T.J.D.; Roepstorff, P., *Anal. Chem.*, 1998, **70**, 4427-4432.

[10] Berry, N.M.; Darey, M.C.P.; Harwood, L.M., *Synth. Comm.*, 1986, 476-480.

[11] Lange, U.; Blechert, S., *Synthesis*, 1995, 1142-1146.

[12] Ando, A.; Miura, T.; Tatematsu, T.; Shioiri, T., *Tetrahedron Lett.*, 1993, **34**, 9, 1507-1510.

[13] Colonna, S.; Hiemstra, H.; Wynberg, H., *J. Chem. Soc., Chem. Commun.*, 1978, 238-239.

[14] Hayami, J-I.; Ono, N.; Kaji, A., *Tetrahedron Lett.*, 1968, **11**, 1385-1386.

[15] Pless, J., *J. Org. Chem.*, 1974, **39**, 2644-2645.

[16] Landini, D.; Molinari, H.; Penso, M.; Rampoldi, A., *Synthesis*, 1988, 953.

[17] Hartwig, W.; Schöllkopf, U., *Liebigs Ann. Chem.*, 1982, 1952-1970.

[18] Kobayashi, Y.; Kayahara, H.; Tadasa, K.; Tanaka, H., *Bioorg. & Med. Chem. Lett.*, 1996, **6**, 12, 1303-1308.

4 Results and Discussion III

4.1 Library Synthesis

4.1.1 Equipment

Figure 4.1 is a representation of the robotic equipment recently purchased at Edinburgh University for parallel array preparation, synthesis, purification and analysis of combinatorial libraries. After the time-consuming installation had been completed, the aim was to prepare a small library of dimedone derivatives in order to become familiar with the operation of each system, and to illustrate the application of the full range of equipment to the synthesis of combinatorial libraries in the ligand design process.

Figure 4.1 Parallel Array Synthesis and Analysis

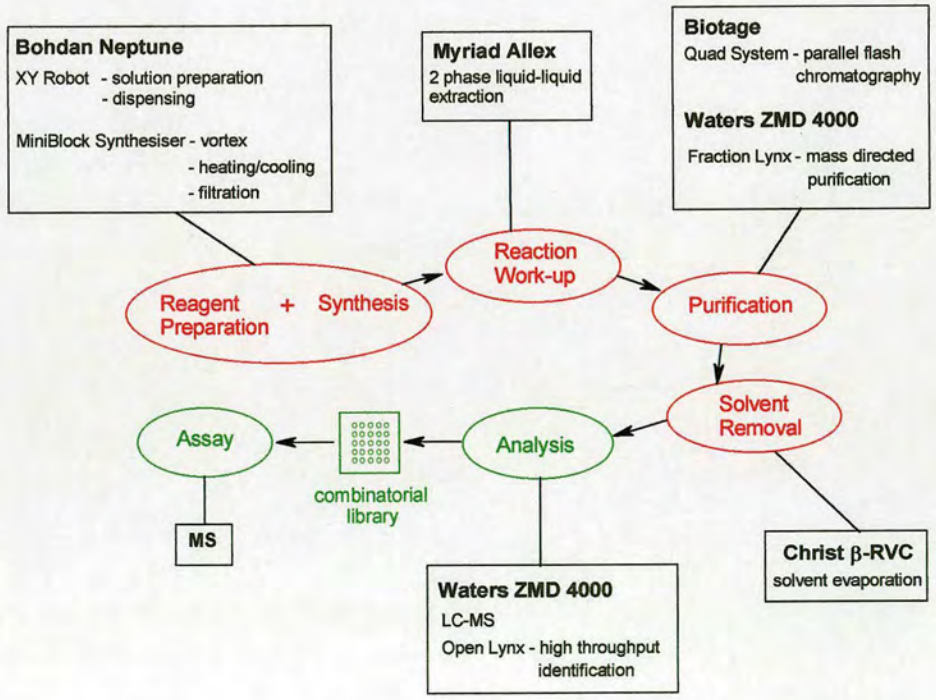

4.1.2 Proposed X-Y-Z Array

The first step in library preparation was development of the synthetic route to the desired dimedone-based compounds of the form shown in Scheme 4.1. The decisions leading to the chosen route have been detailed in previous chapters.

Scheme 4.1

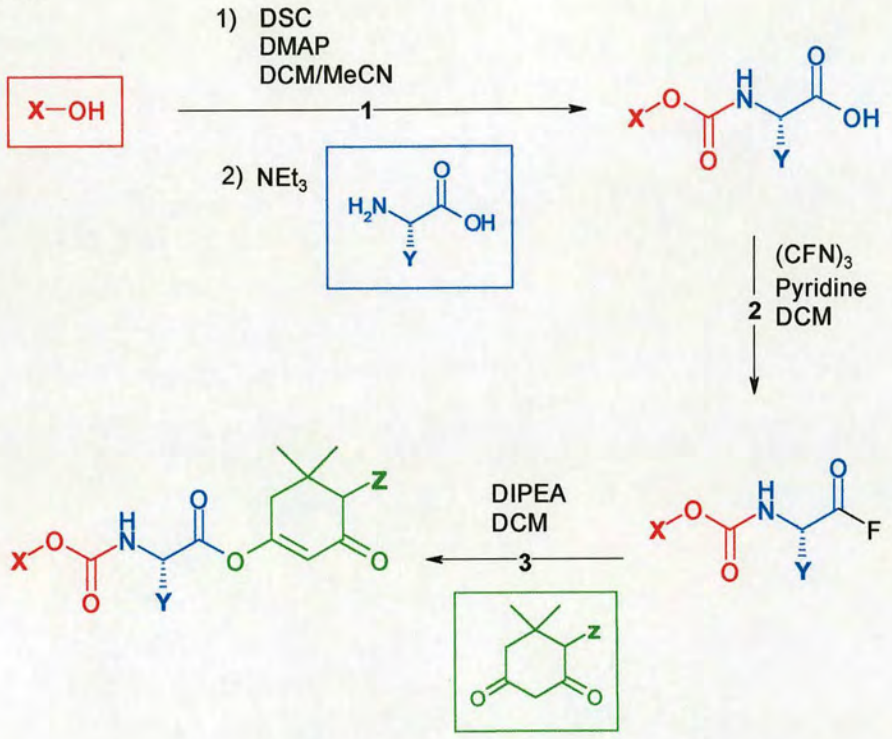

4.2 Automated Synthesis

4.2.1 Step 1

The next major challenge proved to be adaptation of the chosen synthetic route to make it suitable for automation. A test reaction for step 1 (Scheme 4.2) was carried out on the scale required for library synthesis, using various conditions. The reactions were monitored on the ZMD 4000 LCMS system, which was found to give a

reasonable indication of the reaction progress from the mass spectrum, including reagents remaining and product formation.

Scheme 4.2

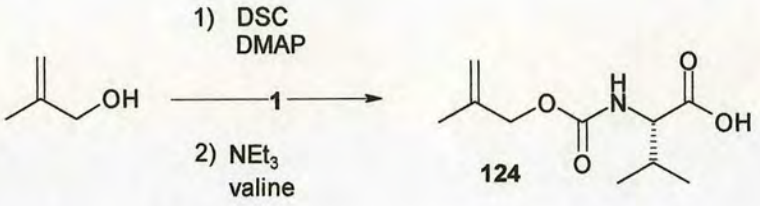

A number of difficulties were encountered at this stage:

4.2.1.1 Dissolution of reagents in step 1

It was anticipated that the Bodhan Neptune™-MB Automated Workstation[1] would be suitable for the preparation and dispensing of reagents in step 1 of the library synthesis. This equipment is capable of tare weighing vials and dispensing solvent to prepare solutions of known concentration, when the compound molecular weights and required solution volumes have been entered. Thus, although the accurate weights and volumes are calculated by the computer, all solid reagents must be weighed out approximately by hand. In the automated synthesis of an array of compounds formed using common building blocks it is therefore important to be able to dispense all of the required reagents as solutions in an appropriate solvent, in order to minimize manual effort and time.

Preparation of the carbamates in step 1 of the original synthetic route (Chapter 3, 3.4.1.2) was initially carried out by dissolution of the appropriate alcohol, DSC and DMAP in DCM:MeCN (1:1) with stirring overnight at room temperature, followed by addition of solid amino acid and neat triethylamine to the reaction mixture. This method was unsuitable for automation because all amino acids would have to be weighed out by hand, which, apart from proving time consuming, would not make full

use of the equipment available. It was therefore necessary to investigate different solvent systems for this reaction.

In test reactions, the DSC and DMAP were weighed out into the reaction vessel and solvent added. Attempted preparation of separate stock solutions of DSC and DMAP in DCM:MeCN revealed that DSC is only soluble in this system when the base, DMAP, is present. DSC did dissolve in DMSO, but the use of this solvent was avoided because of the high temperatures and longer periods required to remove it using the Christ system. A further difficulty was discovered in the selection of an appropriate solvent for amino acid dispensing. Valine was used in the test reaction. Of the numerous solvent systems investigated (MeCN, MeOH, DMF, ether, THF, dioxane, EtOAc, H_2O and $NaHCO_3$), 0.5 M $NaHCO_3$ was found to be the most suitable, but only when triethylamine was added. Although an aqueous component proved necessary for amino acid dissolution, this caused problems on addition to the DCM:MeCN solution of DSC/DMAP, as the DCM and water are immiscible. Altering the solvent ratios did not solve this problem, but it was discovered that the DSC/DMAP could instead be dissolved in MeCN alone, which was compatible with the aqueous amino acid solution. There was some concern over using aqueous solvent with the DSC, as this reagent is easily hydrolysed, however experimental evidence (ZMD 4000 LCMS) indicated that formation of the activated succinimidyl carbonate alcohol species had occurred before addition of the aqueous amino acid solution. Also, sufficient reaction of this activated species with the amino acid took place before it was hydrolysed. All reagents could now be prepared as stock solutions of appropriate concentration, and remain in solution on mixing. Already, it became apparent that transferral of a seemingly facile reaction step for automation was not trivial.

Stock solutions of each reagent were prepared in 20 ml reagent vials, the largest vials available on the Neptune, so several vials were required for some solutions. The reagents were dispensed into MiniBlocks$^{TM\ 2}$ (the MiniBlock consists of 48 fritted tubes, each reversibly sealed at the narrow tube end by a pinching mechanism, and

encased in an insulated block which may be heated or cooled). The reactions were carried out on a 0.4 mmol scale in 1.8 ml total volume of solution.

4.2.1.2 Aqueous work up of step 1

It was anticipated that the Myriad® Allex liquid-liquid extraction system[3] could be used for purification of the crude mixtures from step 1. The Allex is capable of separating a two phase system (aqueous and organic layers) by sensing the change in dielectric constant at the meniscus. It can then be programmed to transfer either the top or bottom layer to a different reaction vessel, with separation just above or just below the meniscus depending on the layer required. Two phase systems can also be mixed before separation.

In the original preparation (Chapter 3 and Chapter 6, 6.2.5.21), the crude reaction mixture from step 1 was evaporated under reduced pressure to leave an oily residue, which was then dissolved in a saturated solution of $NaHCO_3$ and washed with EtOAc. The aqueous layer was then acidified with 2 N HCl, before extracting with EtOAc and concentration under reduced pressure.

The first problem in performing this protocol on the crude mixtures from step 1 was in transferral from the MiniBlock to the test tubes used on the Allex system. The difficulty lay in the limited compatibility of the volume and format of reagent vessels used in the MiniBlock, Allex and Christ systems. MiniBlock tubes can be drained into the commercially available 48 well polypropylene plates, which are compatible with the Christ and Allex. However, these plates have a well volume of 4 ml and the Allex requires at least 2 ml (possibly nearer 3 ml from experience) of solvent in each layer to facilitate accurate separation. This meant that the solutions would have to be transferred from the 48 well plate into larger test tubes on the Allex, following evaporation of the crude mixtures and redissolution in saturated $NaHCO_3$ solution. Although this process can be automated, each transferal step does result in some loss of sample. Additionally, the concentrated crude samples from step 1 were fairly

insoluble in $NaHCO_3$ solution, and would not dissolve without agitation, so it seemed that transferal would have to be done by hand. A further difficulty was that TLC of test reactions indicated some of the required carbamate product remained in the aqueous layer after EtOAc extraction. Repeated extractions and extraction with DCM were attempted, but always with a substantial loss of required product. The DCM also proved to be particularly difficult to work with on the Allex when performing small scale separations, because the high density caused it to drip out of the separation vessel during the settling time. Eventually it seemed more sensible to abandon purification on the Allex altogether. Step 2 of the reaction, involving activation of the amino acid C-terminus as the acyl fluoride, was attempted on the crude mixture. This involved evaporation of the MeCN:$NaHCO_3$ solvent using the Christ, before attempted dissolution of the samples in DCM. Unfortunately, a white precipitate, insoluble in the DCM, resulted indicating that purification would be necessary at this stage.

In the end, purification was achieved using the ZMD 4000 mass-directed LCMS system. This system is quoted to be capable of purifying a maximum of 50 mg/ml of crude sample (found to be less in practice), which meant that for library generation, four 15 minute runs per sample were required to yield enough of each carbamate for the next step. The step 1 samples were therefore prepared in four batches in the MiniBlocks and drained into four polypropylene 96 well plates for direct purification on the ZMD 4000. 96 well plates were used instead of 48 well as less of the sample is lost at the bottom of the smaller well during uptake by the ZMD. In the library synthesis samples were evaporated using the Christ system prior to storage, and then redissolved in MeCN:H_2O (1:1) for purification. This avoided samples sitting around in solution for several days. Although this was a time consuming method of purification, more reasonable yields were obtained than from the Allex system, and all of the steps could be automated, with no need for manual transfer. ^1H NMR of the carbamates synthesized in the rehearsal step (Section 4.5) indicated reasonable purity.

4.2.2 Steps 2 + 3

4.2.2.1 Activation of the amino acid in steps 2 and 3.

Scheme 4.3

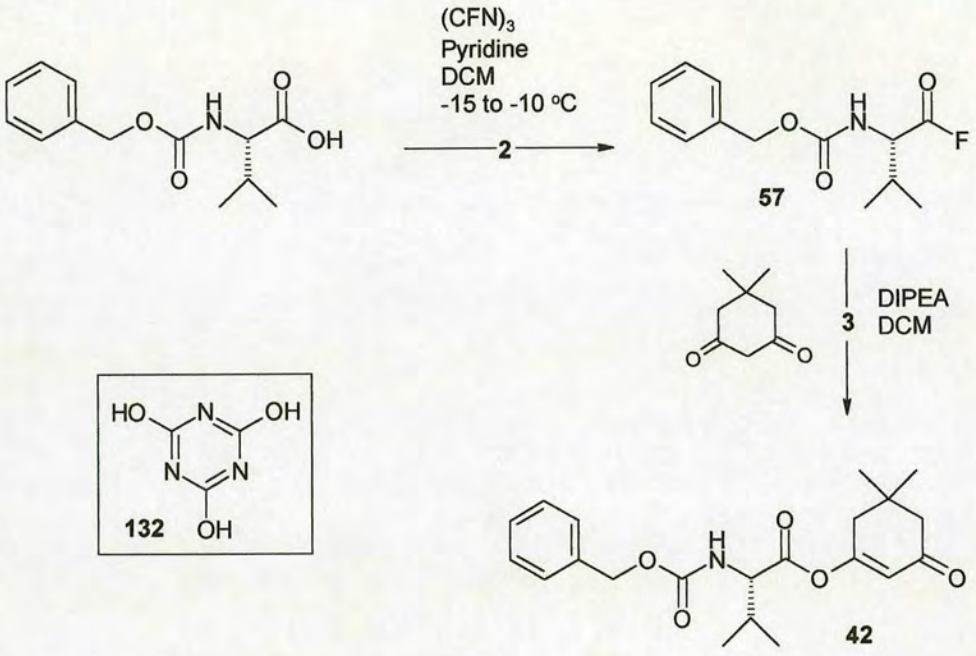

The original route developed for coupling of dimedone to the protected amino acid is shown in Scheme 4.3. The acyl fluoride **57** was prepared by treatment of Cbz-L-valine with cyanuric fluoride in the presence of pyridine, with anhydrous DCM as solvent. The resulting crude mixture containing the required acyl fluoride **57**, excess cyanuric fluoride, pyridine and cyanuric acid **132** by-product, was purified by aqueous work up. The organic layer was washed with ice-water before drying over $MgSO_4$ and evaporation under reduced pressure. The resulting acyl fluoride **57** was then coupled to dimedone in the presence of DIPEA, with DCM as solvent, as shown in step 3.

This route presented several problems for automation:

Firstly, the cyanuric fluoride is very corrosive and consequently unsuitable for robotic dispensing. This reagent would therefore have to be added manually. Cyanuric fluoride is additionally a fairly unstable reagent, and formation of the acyl fluoride is very sensitive to the presence of water, which hinders this reaction. This is particularly problematic when we consider that the protected amino acids formed in step 1 are purified on the ZMD 4000 using an acetonitrile:water gradient. Even after Christ evaporation, it is likely that a small amount of water may remain in the sample. Another point to consider when designing chemistry for library preparation is that the samples will sit around in solution for much longer than when synthesizing an individual compound, because of the time taken to prepare and dispense the reagents to many vials. This is another reason for avoiding sensitive reagents. The aqueous wash presents similar difficulties to those discussed in step 1. Again, using DCM as solvent is not compatible with the Allex system on small volumes.

Test reactions performed using Cbz-L-valine with cyanuric fluoride and pyridine in anhydrous ethyl acetate, indicated that this solvent could be used instead of DCM. However using the Allex to wash out the white cyanuric acid by-product from step 2 was still impractical because of the time taken to transfer and wash larger (>10) numbers of samples: even when ice-water was used, the yields were greatly reduced. Formation of the acyl fluoride in step 2 was done in the MiniBlocks to allow cooling to –15 °C. The MiniBlocks are fritted to enable samples to be filtered. It was thought that this facility could possibly be used to overcome the purification step, since the cyanuric acid by-product is relatively insoluble in the organic solvent used, forming a thick white suspension. Filtration of the MiniBlock samples into a 48 well plate did indeed remove much of this white precipitate, but problems were still encountered at the next stage. The amino acids from step 1 could be further dried by dissolution in ethyl acetate and transferal to MiniBlocks, followed by addition of a small quantity of $MgSO_4$ and filtration, although this did require a couple of extra steps. Experiments were also performed with addition of a basic scavenger resin to the crude acyl fluoride

in order to remove the cyanuric acid. The tetramethylammonium polystyrene resin **133** is available as the bicarbonate salt. Unfortunately, this purification strategy was also unsuccessful.

133

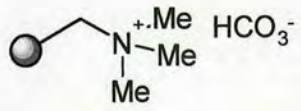

Attempts were made to proceed with the step 3 dimedone coupling without prior purification of the acyl fluoride. Progress of the reaction was again monitored by sampling of the crude reaction mixture and analysis on the ZMD 4000. Although the required dimedone adduct was observed by mass spectrometry, and collected by the fraction collector, after evaporation of the solvent using the Christ, the sample was found to have decomposed. Removal of the solvent at lower temperatures still resulted in decomposition and was a longer procedure. Yields were found to improve by raising the temperature of each step. The cyanuric fluoride was added at 0 °C and the samples shaken at 10 °C for 40 mins before addition of dimedone and warming to room temperature. Alteration of the stoichiometry of reagents amino acid:cyanuric fluoride:pyridine was also investigated with no improvement in results. The use of NEt_3 as an alternative base in steps 2 and 3 did not change the outcome of the reaction. Eventually, it was postulated that the impurities present from the acyl fluoride formation, consisting mainly of cyanuric acid, were somehow causing any dimedone adducts formed to decompose during the concentration step.

In the end an alternative activation of the amino acid was required. In Chapter 2 the various activation methods originally investigated were described. Acyl fluoride formation produced the best yield, followed by formation of the mixed anhydride of the amino acid by treatment with chloroformate. The main disadvantage of the chloroformate reaction was that both carbonyl groups of the anhydride were attacked by dimedone, albeit not to the same extent, resulting in formation of the dimedone by-product **51** (Scheme 4.4). The by-product **51** was impossible to remove fully by standard column chromatography. Fortunately, when this reaction was repeated on a

library scale as shown in Scheme 4.4, and analysed on the ZMD 4000, the required product **42** was separated from by-product **51** under these conditions.

Scheme 4.4

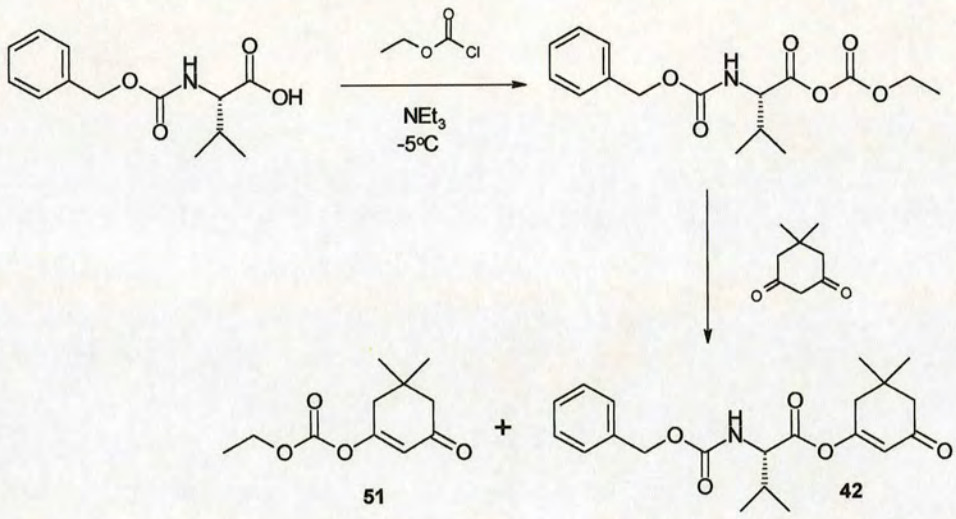

Full experimental details of the final automated synthetic route (Scheme 4.5) are reported in Chapter 6, 6.2.7.

Scheme 4.5

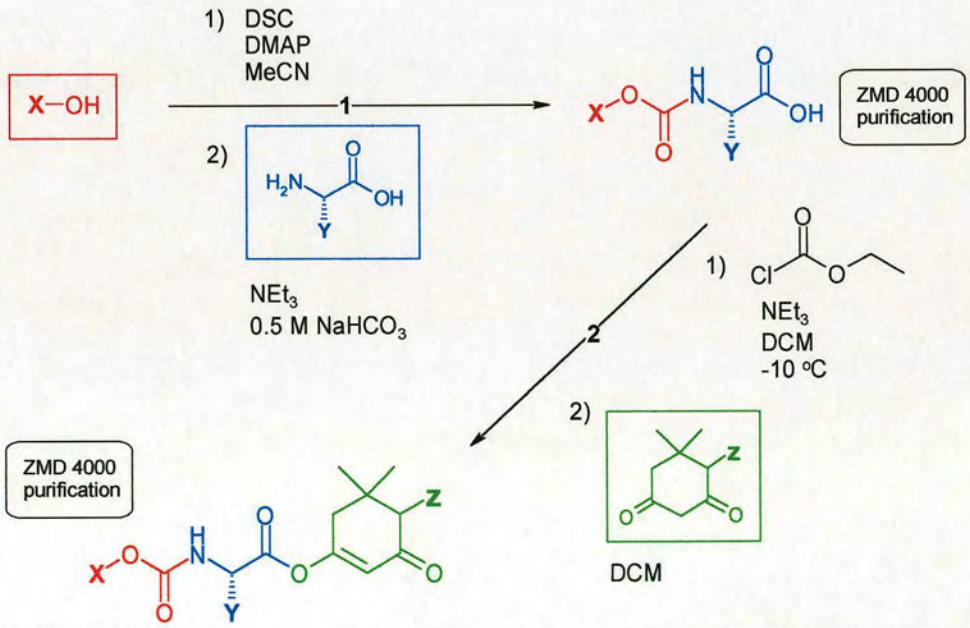

4.3 Selection of Building Blocks

4.3.1 Alcohols

A total of 23 alcohols were tested as potential library components. The reactions were carried out on a 0.4 mmol scale, since a 50 % yield would then result in around 50 mg carbamate product of average molecular weight 250 amu. The ZMD 4000 can purify a maximum of 50 mg/ml of crude sample, with a maximum injection of 2 ml. Alcohols were chosen from those available in the lab. A number of benzyl derivatives were chosen because the highest affinity ligand identified at this stage included an *N*-Cbz-protecting group on the amino acid. The range was also weighted towards relatively hydrophobic alcohols, as crystallographic data thus far indicated a preference for hydrophobic groups in the region of the active site where the alcohol derived portion of the ligand would potentially bind. However, some hydrophilic structures were included as it would be premature to exclude these completely at this stage. The alcohols were reacted with a standard amino acid: L-valine was chosen, as again, this was the amino acid component in the highest affinity ligand. The conditions used were those identified in Scheme 4.6.

Scheme 4.6

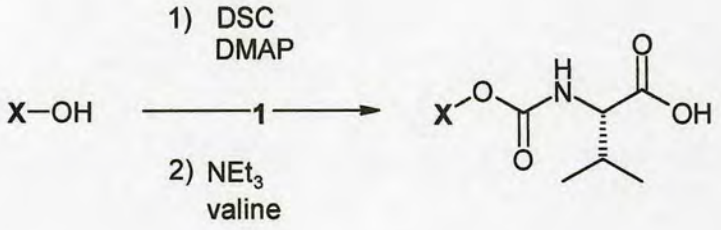

The crude reaction mixture was then analysed using the ZMD 4000. The percentage yield of carbamate product obtained in each reaction was estimated from the total ion count trace of the mass spectrum using the ZMD 4000 software. The list of alcohols tested and yields estimated are shown Table 4.1. In cases where none of the required product was observed by MS, the alcohol has been marked as a fail. A couple of

those tested were found to be insoluble or precipitated out at some stage in the reaction. These are also unsuitable for library generation where all reagents are dispensed in solution. The hydroxybenzyl alcohols displayed solubility problems so these were discounted. 3-Methylbenzyl alcohol was selected as this alcohol gave a higher yield of carbamate than methoxy substituted or benzyl alcohol itself. Reaction with glycerol formyl resulted in the greatest yield of protected valine, but unfortunately this reagent was found to consist of a mixture of 3,5-dioxo and 4,6-dioxocyclohexanol, which made it unsuitable for inclusion in the library. Allyl alcohol and 2-methyl prop-2-enol were selected on the basis of yield, along with cyclohexanol and tryptophol. Ethyl glycolate was selected as a more hydrophilic example. This gave six alcohols of varying size and functionality. The estimated yields were not particularly high (23-57 %), but attempts were made to further optimise the reaction conditions at the rehearsal stage.

Table 4.1

Alcohol	Structure	Y %	Comment	Alcohol	Structure	Y %	Comment
t-butyl		0	fail	4-hydroxy benzyl	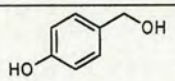	0	fail insoluble
cyclo hexanol		40	selected	2-phenyl ethanol	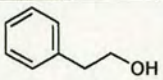	0	fail
2-cyclo hexenol		33		2-phenyl-1-propanol	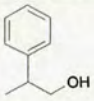	26	
benzyl	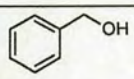	28		allyl	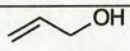	57	selected
2-methyl benzyl	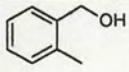	29		2-methyl prop-2-enol	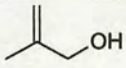	50	selected
3-methyl benzyl	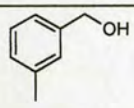	31	selected	glycerol formyl	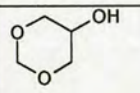	71	mixture of isomers
4-methyl benzyl	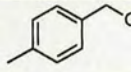	21		ethyl glycolate	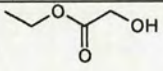	23	selected
2-methoxy benzyl	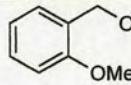	13		tetrahydro-naphthol	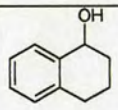	9	
3-methoxy benzyl	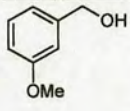	24		2-naph-thalene methanol	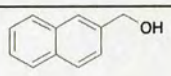	0	fail insoluble
4-methoxy -2-methyl benzyl	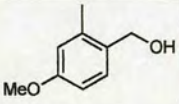	0	fail	tryptophol	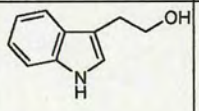	41	selected
2-hydroxy benzyl	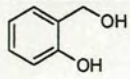	0	fail	borneol	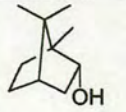	27	
3-hydroxy benzyl	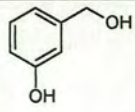	37					

Y = estimated yield

4.3.2 Amino Acids

Selection of the amino acids for the library was a more straightforward process. Only those amino acids which do not require side chain protection were desirable, in order to avoid additional protection and deprotection steps in the synthesis. The acids shown in Table 4.2 were tested by reaction with 2-methyl prop-2-enol, one of the six alcohols selected previously, using the conditions shown in Scheme 4.7. Again, the reactions were monitored using the ZMD 4000. The hydroxy substituted amino acids, tyrosine and serine both exhibited solubility problems so were not selected. Glycine surprisingly did not form any of the carbamate with 2-methyl prop-2-enol. Two amino acid substitutes, 1-amino-1-cyclopentane carboxylic acid and 2-amino-isobutyric acid, were also included and selected, bringing the total to six acids. The substitutes were chosen in order to introduce some conformational constraint into the library.

Scheme 4.7

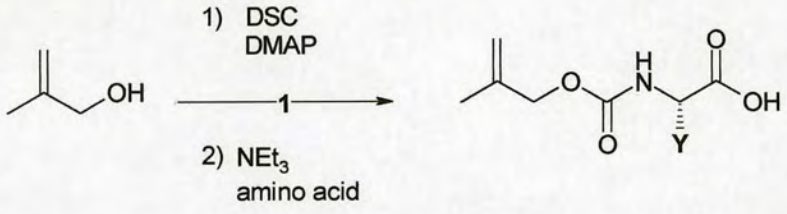

Table 4.2

Acid	Structure	Y %	Comment	Acid	Structure	Y %	Comment
glycine	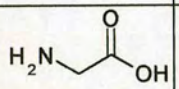	0	fail	serine	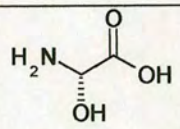	0	fail
alanine	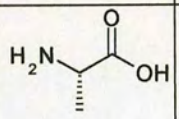	47	selected	tyrosine	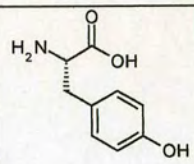	0	fail insoluble-formed white suspension
valine	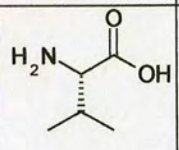	37	selected	1-amino-1-cyclo-pentane carboxylic acid	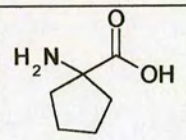	21	selected
leucine	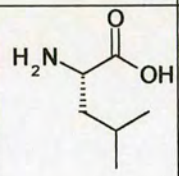	31	selected	2-amino-isobutyric acid	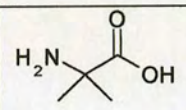	55	selected
phenyl-alanine	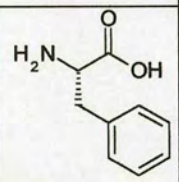	32	selected				

4.3.3 Dimedone Analogues

Dimedone and three of the dimedone analogues that could be prepared in sufficient yield and purity were selected for library generation, as indicated in Table 4.3.

Table 4.3

Dimedone Analogue	Structure	Comments
5,5-dimethyl-cyclohexane-1,3-dione	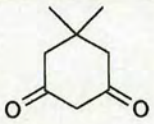	selected (commercially available)
4,5,5-trimethyl-cyclohexane-1,3-dione (**85**)	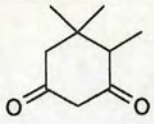	insufficient yield
(2,2-dimethyl-4,6-dioxo-cyclohexyl)-acetic acid methyl ester (**89**)	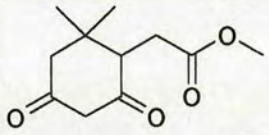	insufficient purity
4-allyl-5,5-dimethyl-cyclohexane-1,3-dione (**88**)	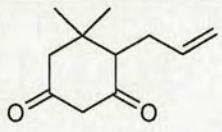	selected
4-benzyl-5,5-dimethyl-cyclohexane-1,3-dione (**99**)	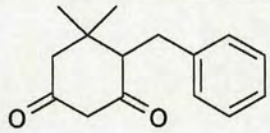	selected
4-cyclohexylmethyl-5,5-dimethyl-cyclohexane-1,3-dione (**105**)	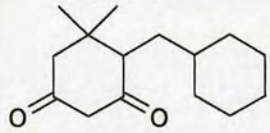	selected
5,5-dimethyl-4-(3-phenyl-allyl)-cyclohexane-1,3-dione (**129**)	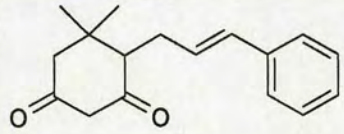	insufficient purity

4.4 Proposed 144 Member Library

A total of 6 alcohols (Table 4.1), 6 acids (Table 4.2) and 4 dimedone analogues (Table 4.3) were selected to generate the proposed 6 x 6 x 4 = 144 member library. Step 1 therefore involved the synthesis of 6 x 6 = 36 carbamates. The carbamate synthesis was done in four batches (as a consequence of the maximum purification capacity of the ZMD 4000 described previously) to produce four plates of 36 carbamates. Each plate was then reacted with one of the four dimedone analogues, in

theory to yield a 144 member library, not accounting for any reaction failures. A rehearsal step was included prior to library synthesis.

The ZMD 4000 system was very useful for investigating all components of the crude mixture in order to determine optimum reaction stoichiometries and times. The amino acid protection step (step 1) was studied using this method. In most cases the activated alcohol was observed by mass spectrometry, indicating that the reaction with DSC was occurring, although some alcohol starting material was seen in certain reactions where the coupling did not go to completion. Observation of the reaction intermediate also suggested that the coupling of the activated alcohol to the amino acid did not go to completion. The reaction stoichiometries, concentrations and times were altered resulting in a small improvement in the yields obtained. However, it became apparent that a lot of the reduction in yield was due to the method of purification on the ZMD 4000. The mass directed fraction collection begins only when detection of the required ion reaches a certain intensity threshold. This threshold can be reduced but not without compromising the purity of the sample obtained.

4.5 Rehearsal of Step 1

In order to obtain a greater indication of the yields and purity of the protected amino acids to be synthesized in step 1 a rehearsal stage was included. This rehearsal involved reacting all 6 selected alcohols with a single amino acid (L-valine), then reacting all 6 selected acids with a single alcohol (2-methyl prop-2-enol), under the conditions established for library synthesis (detailed in Chapter 6, 6.2.7). Table 4.4 shows the proposed set of 36 carbamates with the shaded boxes representing the rehearsal compounds. The percentage yield by mass recovered for each of the rehearsal compounds is shown in Table 4.4.

Table 4.4

Alcohols \ **Acids**	valine	leucine	phenylalanine	1-amino-1-cyclopentane carboxylic acid	2-amino-iosbutyric acid	alanine
allyl alcohol	54					
cyclohexanol	45					
3-methyl benzyl alcohol	40					
2-methyl prop-2-enol	48	45	31	12	17	47
tryptophol	20					
ethyl glycolate	10					

Average yield = 34 %

The yields obtained were moderate to low, which was mainly attributed to the ZMD 4000 purification step, but also to the different reactivities of the various components tested. However, ^{1}H and ^{13}C NMR analysis of the carbamates formed indicated that most were > 80 % pure, with DMAP being the main impurity. The NMR data has been included in Chapter 6, 6.2.6. Due to time constraints, the decision was made to proceed with the library generation, since the recovery of lower yields of each compound than had been hoped should still produce sufficient quantities for CypA binding analysis by MS, especially if the purity was good.

Table 4.5 shows the structures of the 36 carbamates.

Table 4.5: Carbamates

No.	Structure	No.	Structure	No.	Structure
134	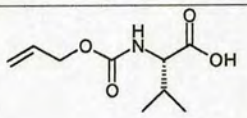	**123**	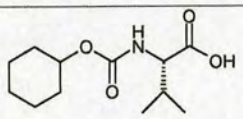	**145**	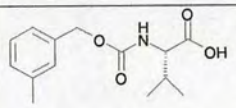
135	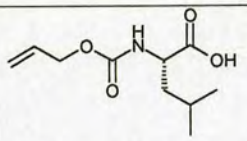	**140**	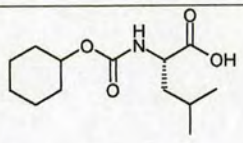	**146**	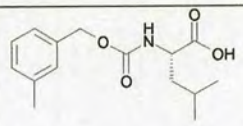
136	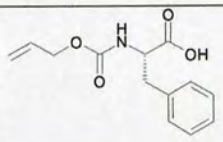	**141**	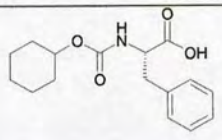	**147**	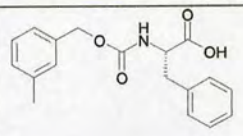
137	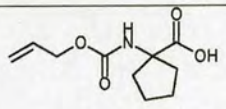	**142**	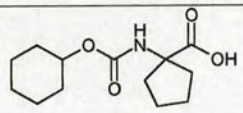	**148**	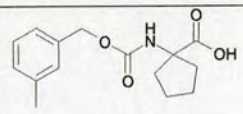
138	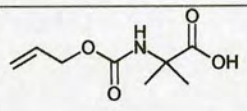	**143**	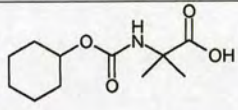	**149**	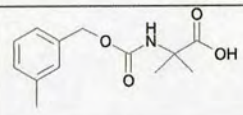
139	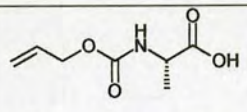	**144**	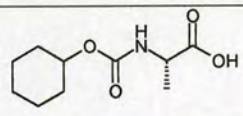	**150**	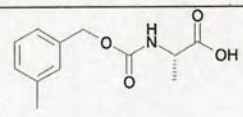
124	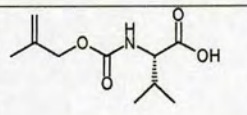	**156**	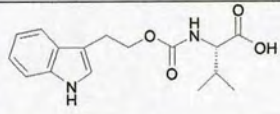	**162**	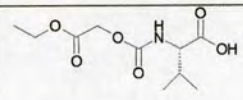
151	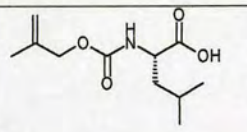	**157**	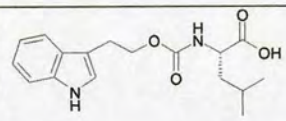	**163**	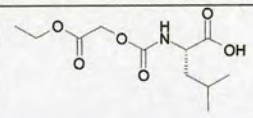
152	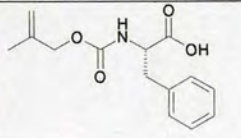	**158**	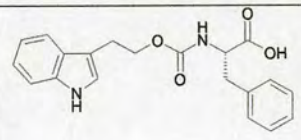	**164**	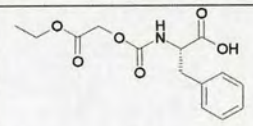
153	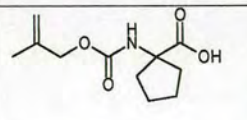	**159**	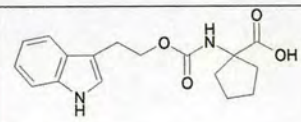	**165**	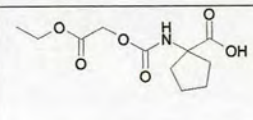

Table 4.5 continued.

No.	Structure	No.	Structure	No.	Structure
154	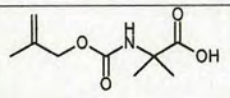	**160**	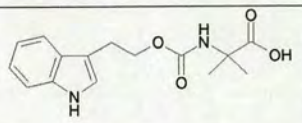	**166**	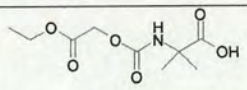
155	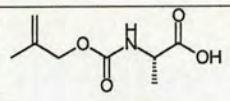	**161**	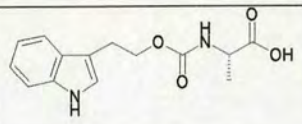	**167**	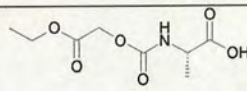

4.6 Results of Library Generation

Of 144 possible compounds from the proposed library, 82 final library members were detected after step 2 of the synthesis and collected using the ZMD 4000. Some of the reactions failed in step 1, generation of the carbamates. In some cases the yields of carbamate were very low, and separate purification of each 36 carbamate plate meant that certain carbamates were not present in all four plates. Overall, only 126 of the possible 144 carbamates were detected by the ZMD 4000 after step 1 of the synthesis.

Graph 4.1

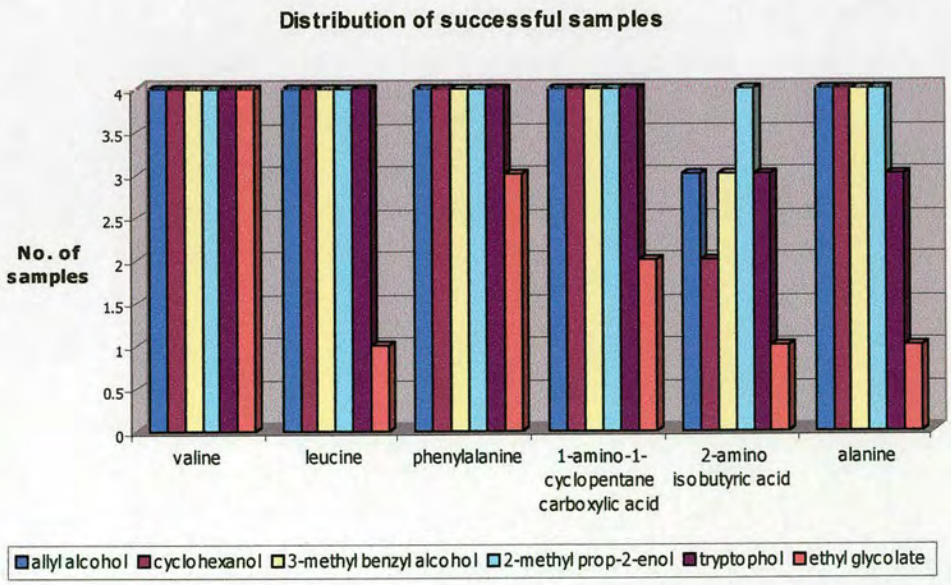

Graph 4.1 shows the distribution of carbamate samples synthesised across the four plates: for example, if a given carbamate is present in each plate then the graph shows a value of 4 samples. From Graph 4.1 it is obvious that carbamates containing ethyl glycolate were much less successful than those generated using the other alcohols. Graph 4.2 gives a more detailed view of carbamate yields from step 1, taken from the mass recovered.

Graph 4.2

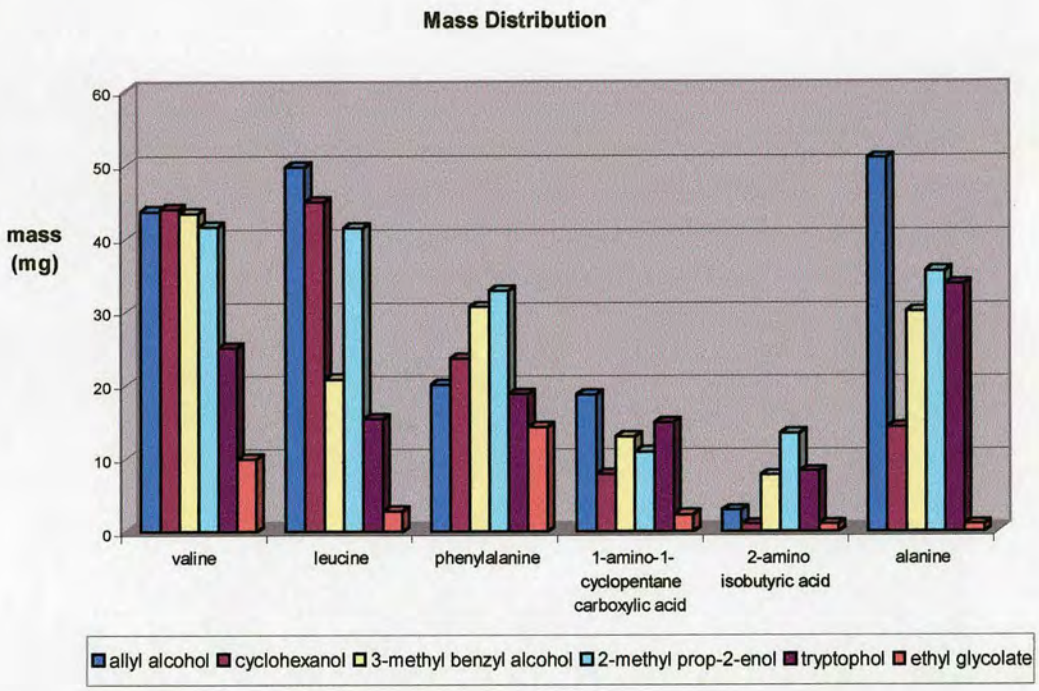

Graph 4.2 indicates the mass distribution of the carbamates synthesised, taken as an average over the four plates. As indicated in Graph 4.1, the carbamates containing ethyl glycolate were shown to be present in very low yield. Additionally, carbamates synthesised from 1-amino-1-cyclopentane carboxylic acid or 2-amino isobutyric acid were generally less successful with lower yields recovered.

For brevity the following sections only report the final library compounds generated in plates 1-4 from reaction steps 1 and 2.

4.6.1 Plate 1 – Reaction of Carbamates with Dimedone

Table 4.6 shows the yields in mg from the reaction of the carbamates in plate 1 with dimedone. 25 final library members were synthesised from this plate. The shaded boxes represent failed reactions. Reaction of carbamates with dimedone on average resulted in the highest yields of library products.

Table 4.6

Alcohols \ **Acids**	valine	leucine	phenylalanine	1-amino-1-cyclopentane carboxylic acid	2-amino-iosbutyric acid	alanine
allyl alcohol		8	9	8		9
cyclohexanol		8	9	6		6
3-methyl benzyl alcohol	7	8	8	12	9	12
2-methyl prop-2-enol		6	8	5		7
tryptophol	7	9	7	7	3	11
ethyl glycolate			6			

4.6.2 Plate 2 – Reaction of Carbamates with 4-Allyl-5,5-dimethyl-cyclohexane-1,3-dione (88)

Table 4.7 shows the yields in mg from the reaction of the carbamates in plate 2 with 4-allyl-5,5-dimethyl-cyclohexane-1,3-dione **88**. 26 final library members were synthesised from this plate.

Table 4.7

Alcohols \ **Acids**	valine	leucine	phenylalanine	1-amino-1-cyclopentane carboxylic acid	2-amino-iosbutyric acid	alanine
allyl alcohol	12	6	6	8	4	
cyclohexanol	7	2	3	3		1
3-methyl benzyl alcohol	7			4		
2-methyl prop-2-enol	3	2	2	6	4	
tryptophol	3	3	6	5		
ethyl glycolate	2	2		2	2	5

4.6.3 Plate 3 – Reaction of Carbamates with 4-Benzyl-5,5-dimethyl-cyclohexane-1,3-dione (99)

Table 4.8 shows the yields in mg from the reaction of the carbamates in plate 3 with 4-benzyl-5,5-dimethyl-cyclohexane-1,3-dione **99**. 20 final library members were synthesised from this plate.

Table 4.8

Alcohols \ **Acids**	valine	leucine	phenylalanine	1-amino-1-cyclopentane carboxylic acid	2-amino-iosbutyric acid	alanine
allyl alcohol			8	6	3	
cyclohexanol		4	3	3	3	
3-methyl benzyl alcohol	5	4	9	4	2	
2-methyl prop-2-enol	2	2	2	6	3	
tryptophol		3	6	5		
ethyl glycolate						

4.6.4 Plate 4 – Reaction of Carbamates with 4-Cyclohexylmethyl-5,5-dimethyl-cyclohexane-1,3-dione (105)

Table 4.9 shows the yields in mg from the reaction of the carbamates in plate 4 with 4-cyclohexylmethyl-5,5-dimethyl-cyclohexane-1,3-dione **105**. 11 final library members were synthesised from this plate, with dimedone analogue **105** proving to be the least successful.

Table 4.9

Alcohols \ Acids	valine	leucine	phenylalanine	1-amino-1-cyclopentane carboxylic acid	2-amino-iosbutyric acid	alanine
allyl alcohol				2	2	
cyclohexanol				8	2	
3-methyl benzyl alcohol		4		34	2	
2-methyl prop-2-enol				3		
tryptophol	1			2	2	
ethyl glycolate						

Graph 4.3 shows the distribution of successful samples from step 2 with regard to the carbamate used. For each carbamate four products are possible from the reaction (step 2) with dimedone and its three derivatives. So, for example, the carbamate prepared from valine and allyl alcohol was found to react with only one of the dimedone analogues (the dimedone analogues have not been specifically identified in Graph 4.3). Interestingly, Graph 4.3 indicates that some of the ethyl glycolate containing carbamates have reacted in step 2 to form the desired library members despite the poor yields obtained in step 1. Additionally, the low yields of carbamates containing 1-amino-1-cyclopentane carboxylic acid and 2-amino isobutyric acid

building blocks, have not prevented these carbamates from reacting with the dimedone analogues in step 2. The alanine containing carbamates were less successful.

Graph 4.3

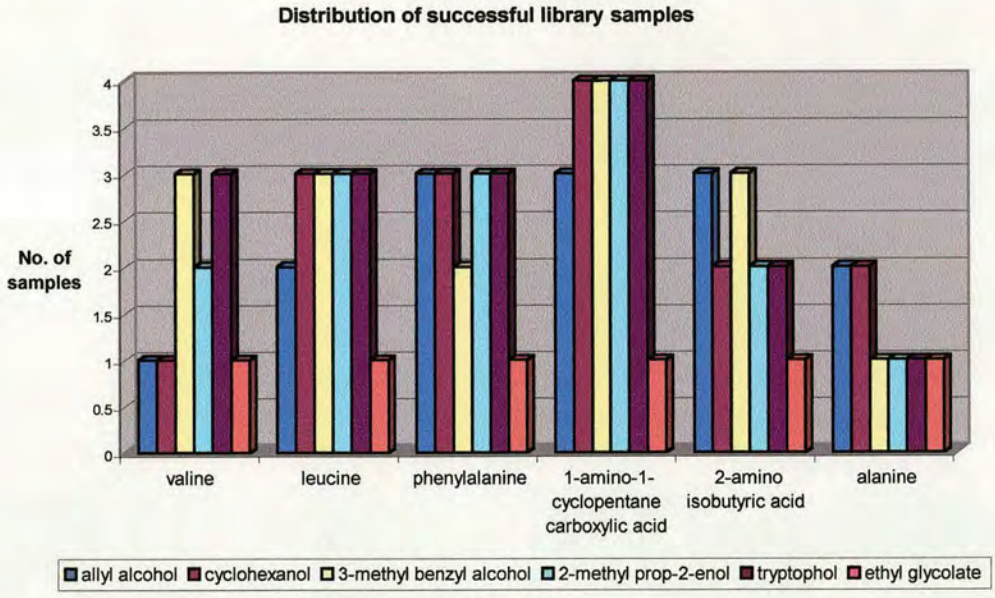

Overall, the final yields of the library were very low. This was partly due to insufficient optimisation of the chemical route with regard to automated synthesis, and also because of the inclusion of two ZMD 4000 purification steps, which were found to result in appreciable loss of material. The purity of the final library also required to be investigated. The initial indication of purity was obtained from the mass spectrum recorded during ZMD 4000 purification. In general the quantities of material recovered were too small to acquire reliable NMR data from the 200 MHz NMR. The mass spectrometry screening of the library for binding to CypA involved dissolution of the samples for dispensing to the assay. A second mass spectrum of each sample was run at this stage. From these spectra and the original ZMD 4000 LCMS data, the purity of each of the library samples was estimated and the results are shown in Table 4.10 along with the chemical structures of the final 82 library compounds synthesised. The key to the purity estimations is included at the end of Table 4.10.

Table 4.10

Structure		Yield (mg)	Purity (%)	Structure		Yield (mg)	Purity (%)
A1	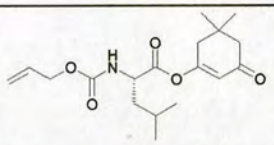	8	C	**A10**	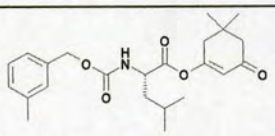	8	D
A2	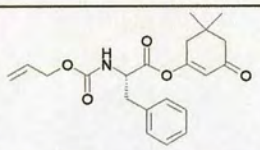	9	C	**A11**	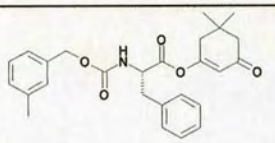	8	C
A3	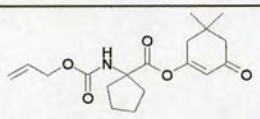	8	A	**A12**	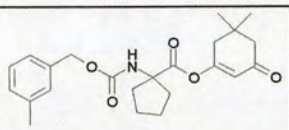	12	B
A4	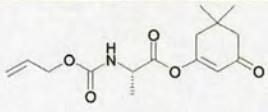	9	C	**B1**	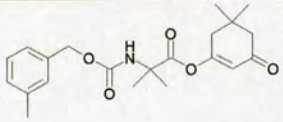	9	A
A5	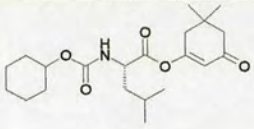	8	C	**B2**	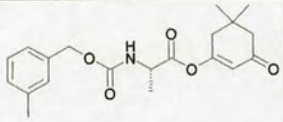	12	B
A6	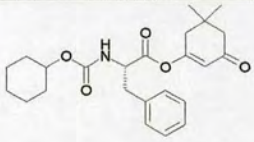	9	D	**B3**	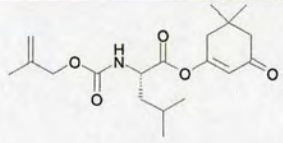	6	B
A7	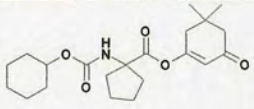	6	A	**B4**	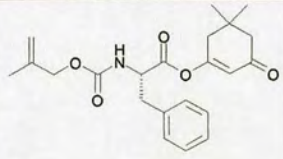	8	D
A8	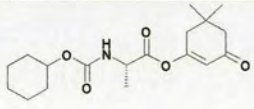	6	D	**B5**	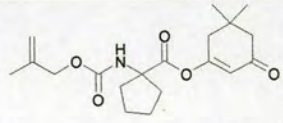	5	D
A9	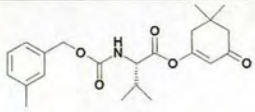	7	D	**B6**	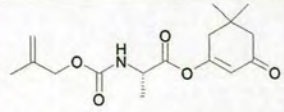	7	B

B7	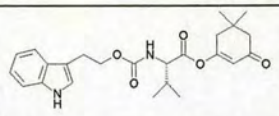	7	D	**C6**	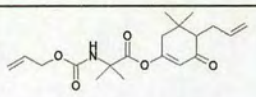	4	A
B8	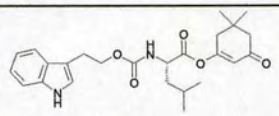	9	C	**C7**	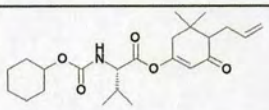	7	B
B9	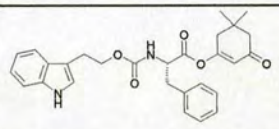	7	C	**C8**	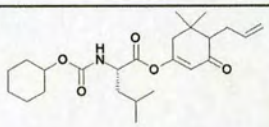	2	C
B10	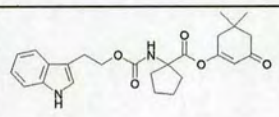	7	B	**C9**	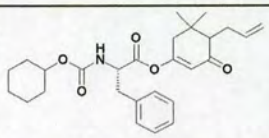	3	D
B11	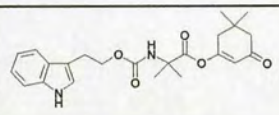	3	D	**C10**	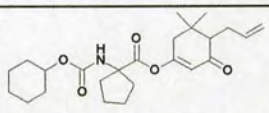	3	C
B12	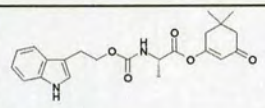	11	D	**C11**	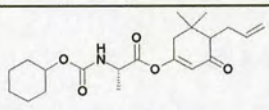	1	D
C1	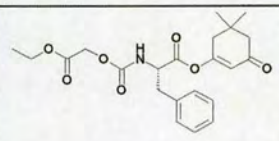	6	A	**C12**	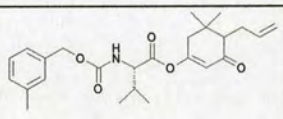	7	B
C2	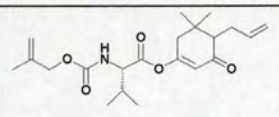	12	C	**D1**	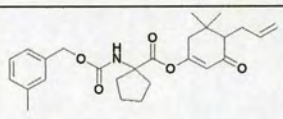	4	B
C3	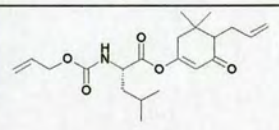	6	D	**D2**	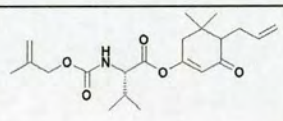	3	B
C4	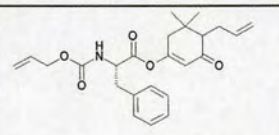	6	D	**D3**	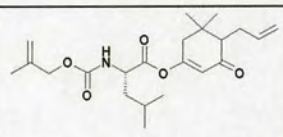	2	D
C5	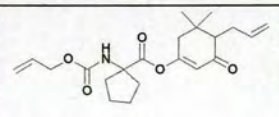	8	A	**D4**	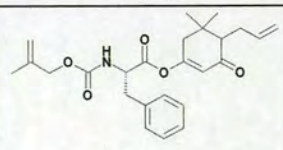	2	C

D5	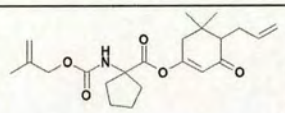	6	A	**E5**	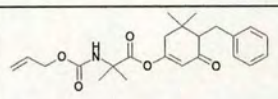	6	C
D6	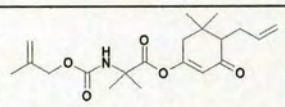	4	A	**E6**	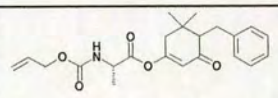	3	D
D7	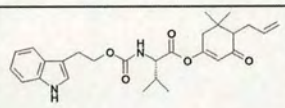	3	D	**E7**	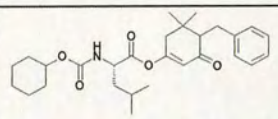	4	D
D8	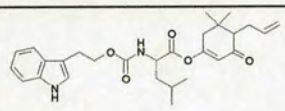	3	D	**E8**	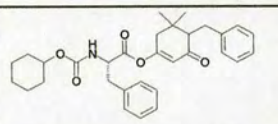	3	D
D9	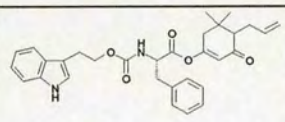	6	D	**E9**	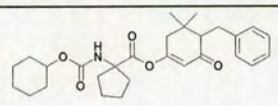	3	D
D10	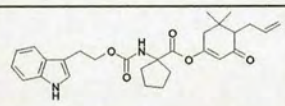	5	C	**E10**	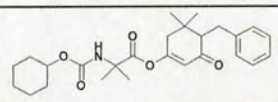	3	B
D11	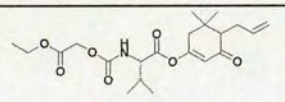	2	D	**E11**	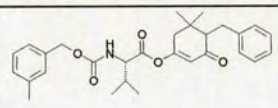	5	A
D12	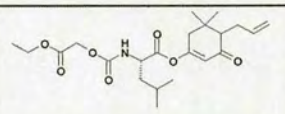	2	D	**E12**	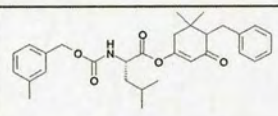	4	D
E1	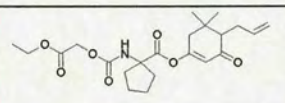	2	D	**F1**	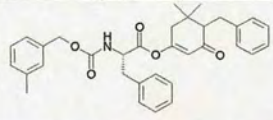	9	B
E2	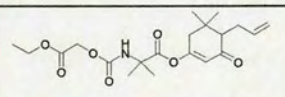	2	D	**F2**	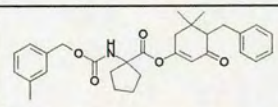	4	B
E3	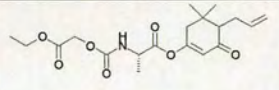	5	D	**F3**	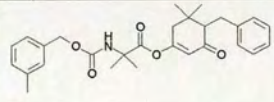	2	D
E4	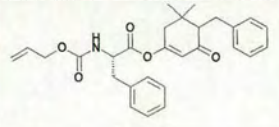	8	D	**F4**	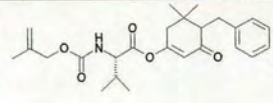	2	C

F5	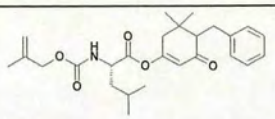	2	C	**G2**	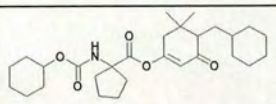	8	C
F6	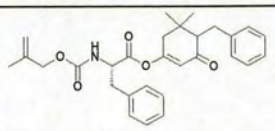	2	B	**G3**	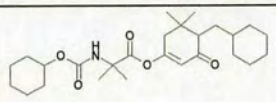	2	A
F7	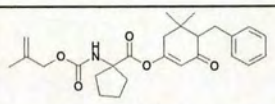	6	A	**G4**	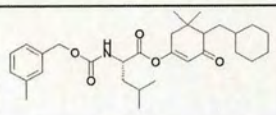	4	C
F8	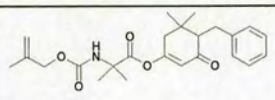	3	C	**G5**	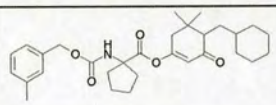	34	C
F9	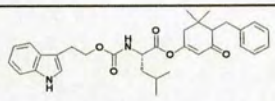	3	C	**G6**	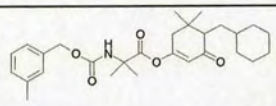	2	C
F10	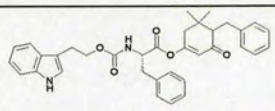	6	D	**G7**	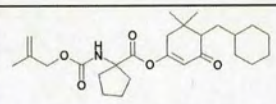	3	A
F11	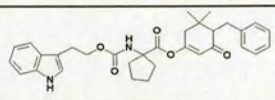	5	D	**G8**	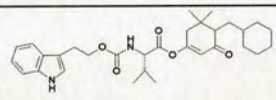	1	D
F12	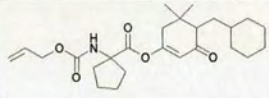	2	D	**G9**	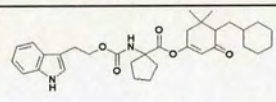	2	A
G1	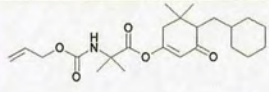	2	D	**G10**	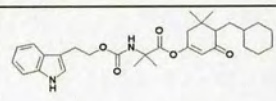	2	D

Key

Estimated Purity	% of library
A = 75-100 %	15.9
B = 50-74 %	15.9
C = 25-49 %	25.6
D = 0-24 %	42.7

4.7 Mass Spectrometry Results

Using identical conditions to those used to obtain the mass spectrum for the CypA:**42** complex described in Section 3.6, the 82 member library was screened for binding to CypA, with the aim of identifying any compounds with equivalent or greater binding affinity for CypA than ligand **42**. The screening experiments were carried out by Sally Shirran. The CypA (20 μM concentration) and ligand (1 mM, assuming 100 % purity) were dissolved in 10 mM ammonium acetate pH 6.9. After standing at room temperature for 30 min the CypA/ligand mixture was infused into the mass spectrometer at 8 μl/min using an infusion pump. The samples were analysed at 50 CV in positive ion electrospray. One compound, ligand **E11** was observed to form a complex with CypA (Figure 4.3). Again, a peak corresponding to the mass expected for an acylated CypA species was observed (m/z = 18250).

Figure 4.2: Electrospray mass spectrum of **E11**

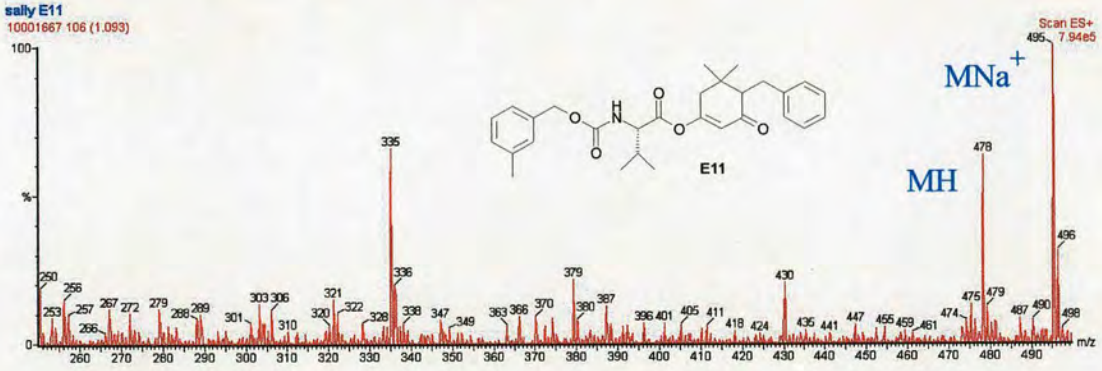

Figure 4.3: Electrospray mass spectrum of a 1:50 mixture of CypA and **E11**

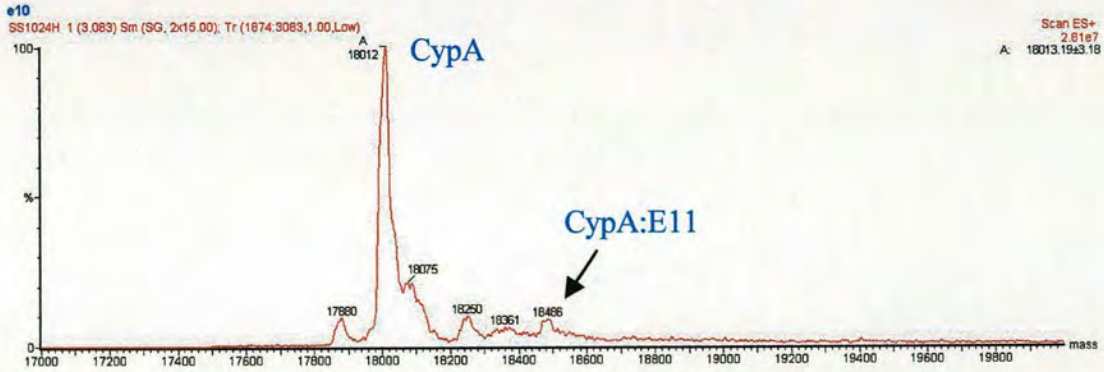

4.8 Discussion

Unfortunately it was difficult to draw many conclusions from the library screening. The assay is still in the development stage and requires further optimisation. Additionally, the purity of the final 82 member library was considerably lower than expected. The amounts of ligand used against the CypA assumed 100 % purity, so in some cases the ligand concentration was a factor of 5 lower than that expected, which obviously affects whether sufficient CypA:ligand complex was formed for detection by mass spectrometry. Future work will include repeating the assay with ligand concentrations taking into account the purity of the samples. Additionally, further work is required to determine the extent of denaturation of CypA under ESI experimental conditions and to investigate the extent to which specific active site binding has occurred. In conclusion, the exercise of preparing a library using the automated equipment and taking the final compounds through to screening was invaluable experience for designing and synthesising future arrays of small molecules. Also, it was promising to observe the CypA:ligand complex in the MS screening, confirming that the principle of using mass spectrometry as an initial screen was still viable, although further investigation would be required both to optimise the chemistry for automation in order to increase the yields and purity of the final library, and to increase the reliability of the MS assay. Further studies should include resynthesis of the ligand **E11** and analysis using the PPIase assay and crystal soaking/crystallography techniques.

4.9 Suggestions for Further Work

Replacement of the enol ester linkage of the high affinity ligand **42** with an enol amide linkage, using the route shown in Scheme 4.8, would be an interesting method of altering the order of hydrogen bond donor/acceptor atoms along the ligand backbone. If binding to CypA could be observed, ligands such as the enol amide **42A** could

provide very useful information on the importance of hydrogen bonding for binding affinity.

Scheme 4.8

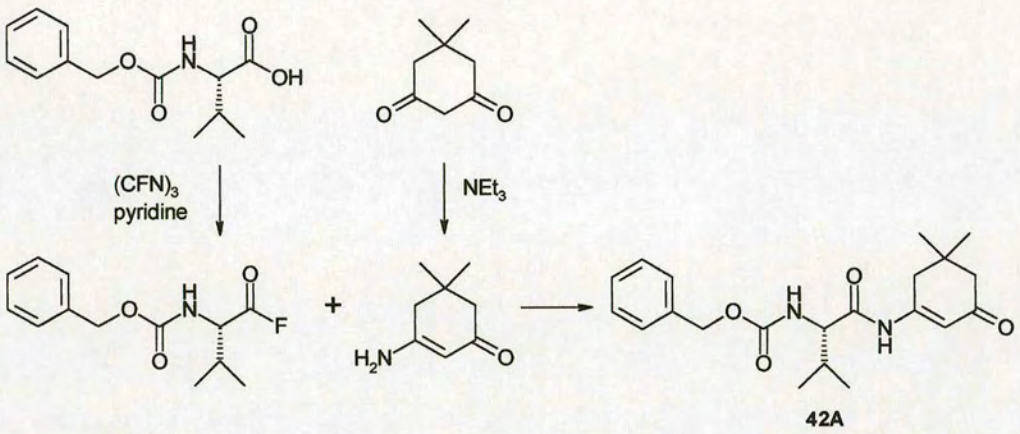

4.10 References

[1] Bräse, S.; Dahmen, S.; Pfefferkorn, M., *J. Comb. Chem.*, 2000, **2**, 710-715.

[2] Moshiri, B.; *Book of Abstracts, 218th ACS National Meeting, New Orleans, Aug. 22-26*, 1999.

[3] Jordan, S.; Moshiri, B.; Durand, R., *JALA*, 2002, **7**, 74-77.

5 Results and Discussion IV

5.1 Backbone Amide Linkers

Since the development of the first resin-bound peptide synthesis strategy by Merrifield in 1963[1], numerous methods have been reported for the generation of peptide libraries on solid support, including conventional *C*-terminal peptide attachment and the less widely used *N*-terminal attachment to resin. A third and more recent strategy concerns attachment of the peptide to the support *via* the amide bond. Linkers of this type, known as backbone amide linkers (BAL), have been relatively unexplored in comparison to *C*- or *N*-terminal linkers. Examples include the strategy reported by Jensen *et al.*[2] where the growing peptide chain is anchored through a backbone nitrogen (Scheme 5.1). The BAL was prepared by coupling 5-(4-formyl-3,5-dimethoxyphenoxy)valeric acid **168** to amino polystyrene or amino PEG polystyrene resin, forming the supported aldehyde species **169**. On-resin reductive amination with an amino acid residue (or an appropriately modified derivative) afforded the resin-bound amino acid **170**. *N*-acylation by an appropriately protected second amino acid residue forms the dipeptidyl unit **171**, linked to the support through the backbone amide nitrogen. The peptide can be cleaved from support by acidolysis using TFA. A number of linear peptides with *C*-terminal modifications, including alcohols, aldehydes, esters and *N,N*-dialkylamides, were prepared using this strategy, with incorporation of different amino acid derivatives. These linkers have the advantage that the peptide chain can be extended in either direction, allowing greater flexibility in modification of the termini, and an alternative route to cyclic peptides.

Scheme 5.1

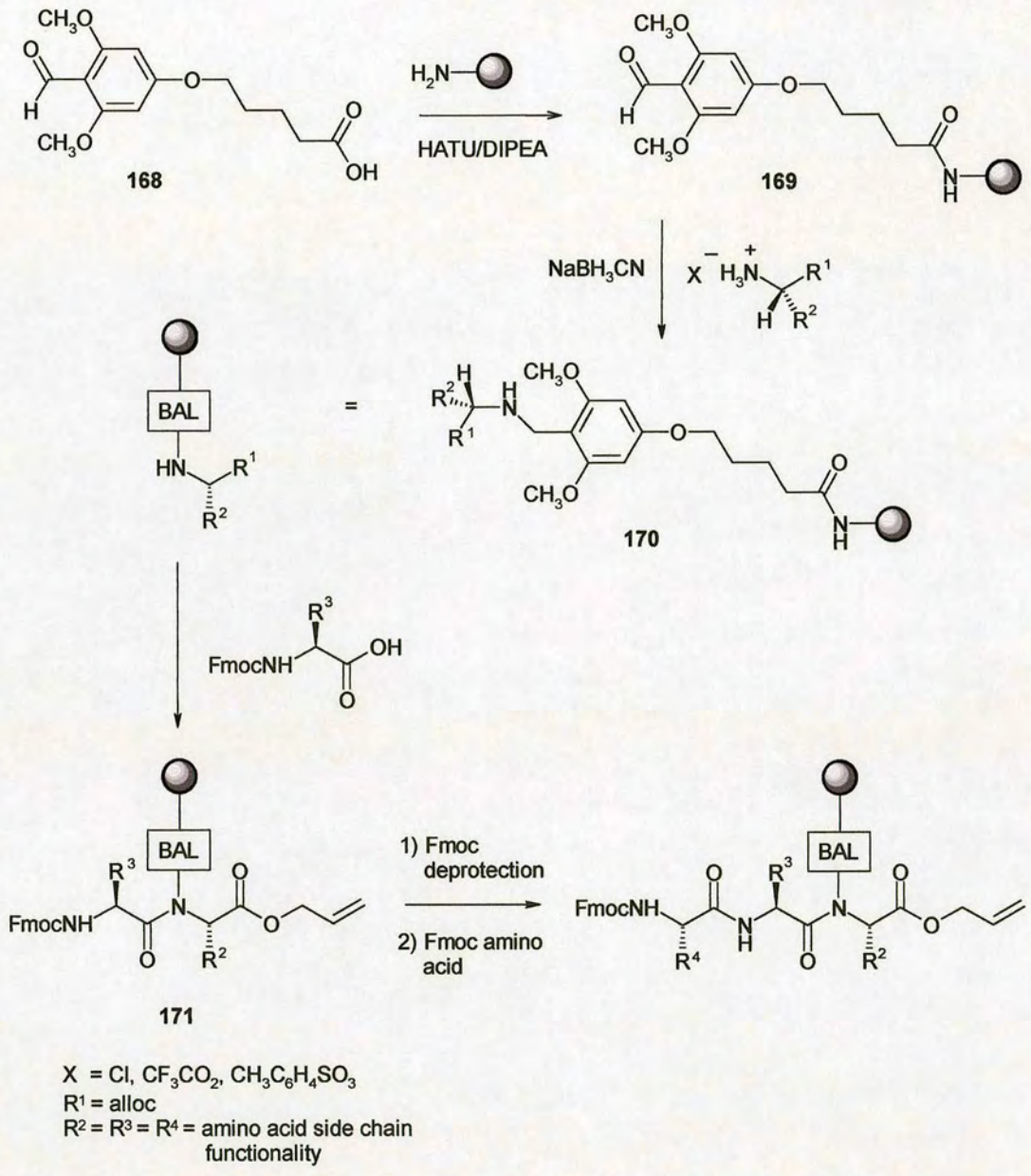

5.2 Applications of Dimedone Chemistry

5.2.1 Amide Linker

Development of routes for the incorporation of dimedone into a peptide chain described in Chapter 2, involved synthesis of ligands of the form **59** (Scheme 5.2).

Although initial screening results indicated that ligands of this type were unable to bind to CypA, study of the BAL strategy described above led to the exploration of other possible applications of this chemistry. More specifically, the idea was to investigate the use of the dimedone system for anchoring a peptide to solid support. Tethering the cyclohexane-1,3-dione system to resin using an additional ring functionality, as shown in **172**, Scheme 5.2, results in a peptide linked to support effectively *via* the carbonyl of a backbone amide. Oxidative cleavage of the double bond connecting the dimedone linker to the peptide would be required to reveal the carbonyl and release the peptide **173** from support. Preliminary solution phase studies on the ligand **59**, indicated that it was possible to oxidatively cleave the methylene double bond using sodium periodate, although yields of recovered dipeptide **174** were very low.

Scheme 5.2

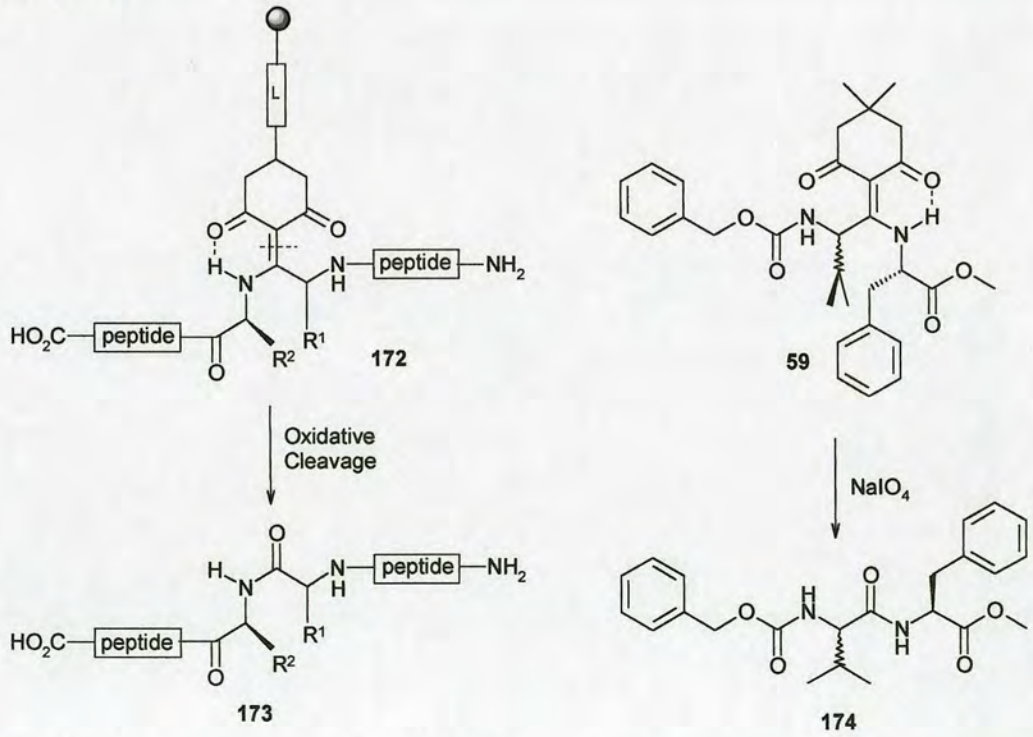

The first requirement for this strategy is generation of a resin-bound cyclohexane-1,3-dione species. Once formed, it seemed acceptable to envisage incorporation of the dione system into a peptide using the chemistry previously developed, and shown

in Scheme 5.3. An additional advantage of this strategy is that the first amino acid attached to support is activated for further coupling by conjugation with the cyclohexanedione system, as in species **175**. In this manner the cyclohexanedione functions as both a coupling agent and linker. It should be noted that racemisation of the amino acid initially coupled to dimedone (L-valine in **59**) would be a limitation in the synthesis of peptides by this method. One solution would be to limit residues at this position to glycine or α,α-disubstituted amino acids. Alternatively, the route may be more applicable to the solid phase synthesis of low molecular weight, amide-containing non-peptidic molecules.

Scheme 5.3

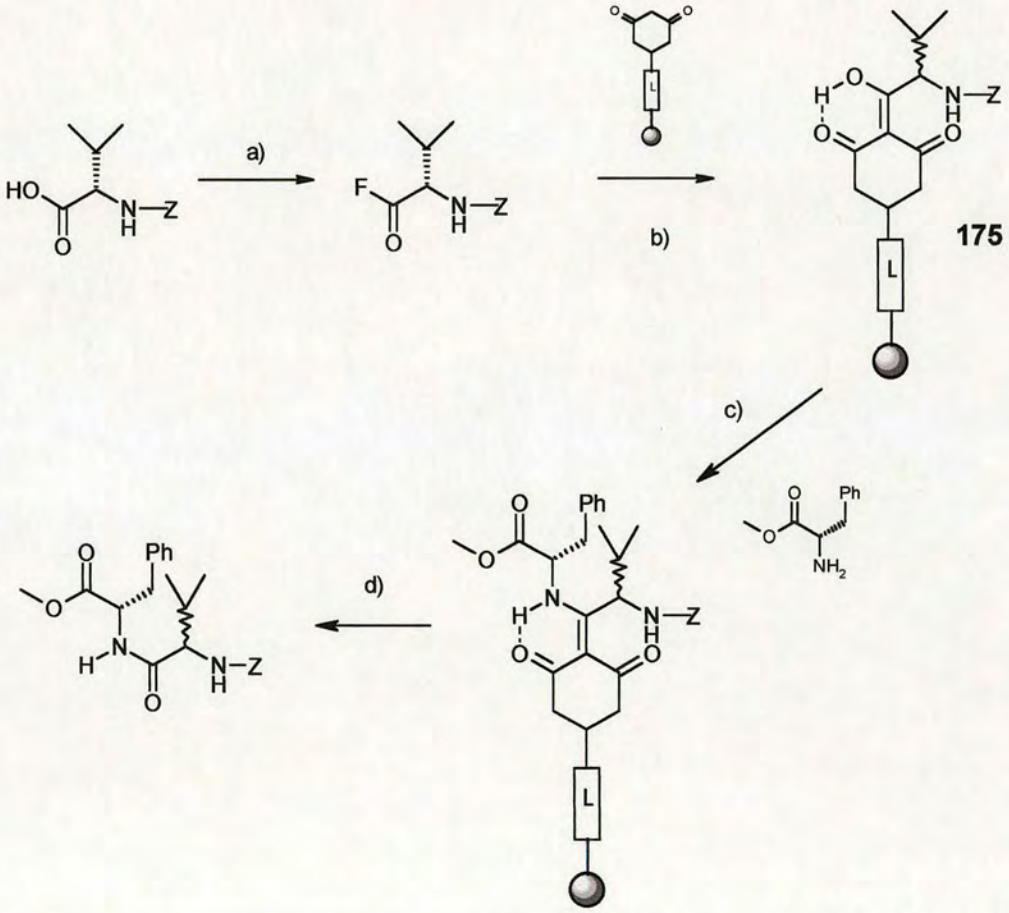

Conditions:

a) $(CFN)_3$, pyridine, DCM, -10 °C; b) i) *N,N*-diisopropylethylamine, DCM, ii) acetone cyanohydrin, triethylamine, dimedone, DCM, c) *N,N*-diisopropylethylamine, DMF, 50 °C; d) $NaIO_4$.

5.2.2 Scavenger Resin

Another useful exploitation of the reactivity of the 1,3-dicarbonyl functionality would be to employ this group as a universal resin-bound scavenger. Cyclohexane-1,3-diones have previously been shown to react with amine nucleophiles at a carbonyl group to form enamines (Chapter 2, 2.2.7.1), and the enolic nature of the 1,3-dione system means that it has potential to react with both hard and soft electrophiles, at the *O*- and *C*- sites respectively. Scheme 5.4 illustrates potential scavenging reactions of an immobilised dione with primary amines, aldehydes and allyl cations (dimedone is commonly employed for the solution capture of allyl cations in palladium catalysed alloc deprotection).[3] If a method could be found for facile synthesis of cyclohexane-1,3-dione on resin, this species will have huge scope as a scavenger of both electrophilic and nucleophilic reactive species from reaction mixtures.

Scheme 5.4

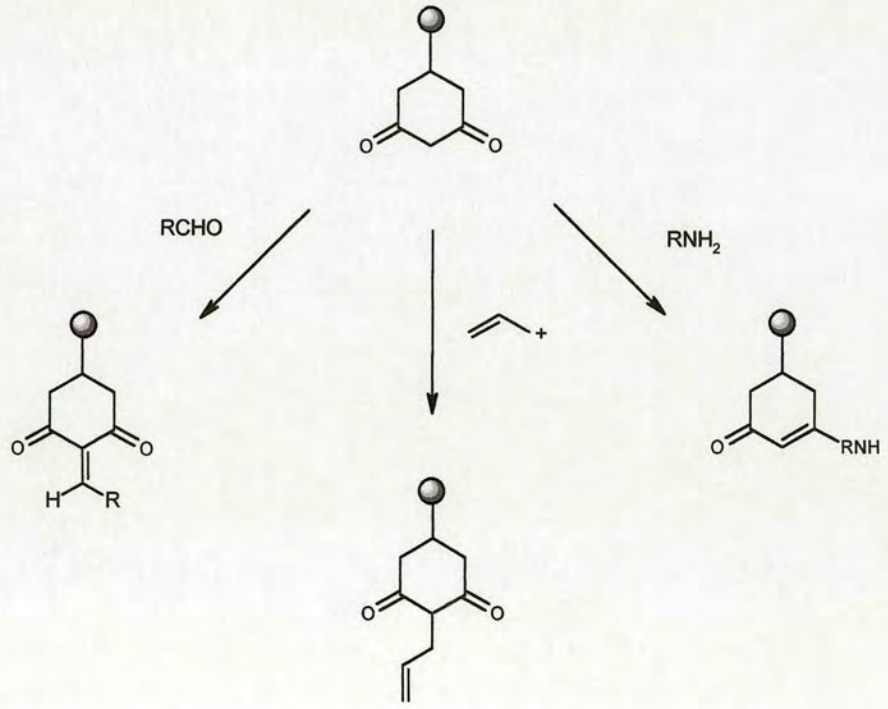

5.2.3 Aim

The objectives of this work were two-fold. Firstly, a route to resin-bound cyclohexane-1,3-diones was required. Secondly, a reliable means of cleavage of the peptide from solid support was sought.

5.3 Route to Resin-Bound Cyclohexane-1,3-diones

5.3.1 Background

A few examples of cyclohexanedione-based linkers have been reported. Graf von Roedern[4] used immobilised cyclohexanedione **176** in the demonstration of an HPLC-based method for characterisation of chemical libraries. A small library of 20 compounds was synthesised on solid support using four different aldehydes (R^1) and five different vinyl ethers (R^2), as shown in Scheme 5.5. A computer algorithm was then used to assign HPLC peaks to their corresponding library compounds by correlation of product retention times with the different substituents in variable positions of the molecule.

Scheme 5.5

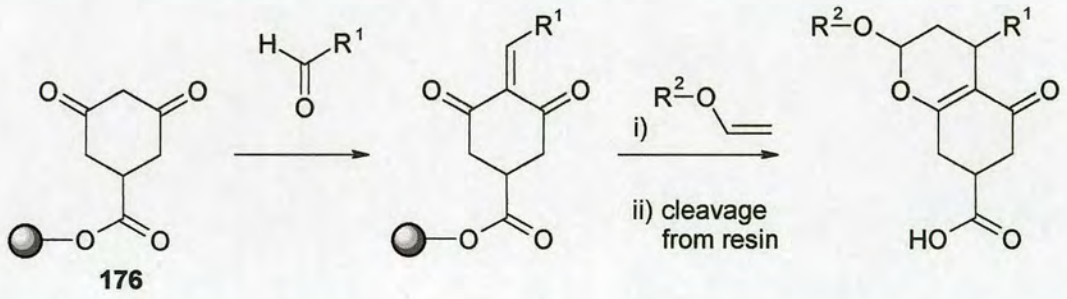

176

R^1 = *n*-octyl, *i*-butyl, 2-thiophenyl, *i*-propyl
R^2 = *O*-ethyl, $O(CH_2)_4OH$, *O*-*t*-butyl, $N(CH_3)Ac$, *O*-cyclohexyl

Bycroft *et al.*[5] have described a primary amine linker based on their 1-(4,4-dimethyl-2,6-dioxo-cyclohexylidene)ethyl (Dde) protecting group strategy (Scheme 5.6).

They first prepared a more base-stable Dde derivative **178**, by acylation of dimedone with the mono-protected dicarboxylic acid **177**. This provided a Dde unit with a terminal carboxylic acid on the side chain for coupling to the support, and an adjustable spacer arm which imparts base stability for the amino attachment. The 2-acyldimedone **178** was then masked with 2-aminopropane and deprotected to yield enamine **179**, which was secured onto TG amino resin. Coupling in 2-aminopropane prevented unwanted amidation of the Dde centre by the support. The utility of the linker **180** was illustrated in the synthesis of pseudoargiopinine III **183**, a pharmacologically active component of spider venom. Transamination of the linker **180** with 1,5-pentanediamine resulted in enamine **181** which was coupled to Fmoc-L-Asn(Trt)-OH using standard peptide chemistry. The Fmoc group was removed using piperidine and the product acylated with indole-3-acetic acid to form **182**. Acidolysis removed the trityl side chain protection and the final product **183** was cleaved from the resin using hydrazine hydrate or propylamine.

Scheme 5.6

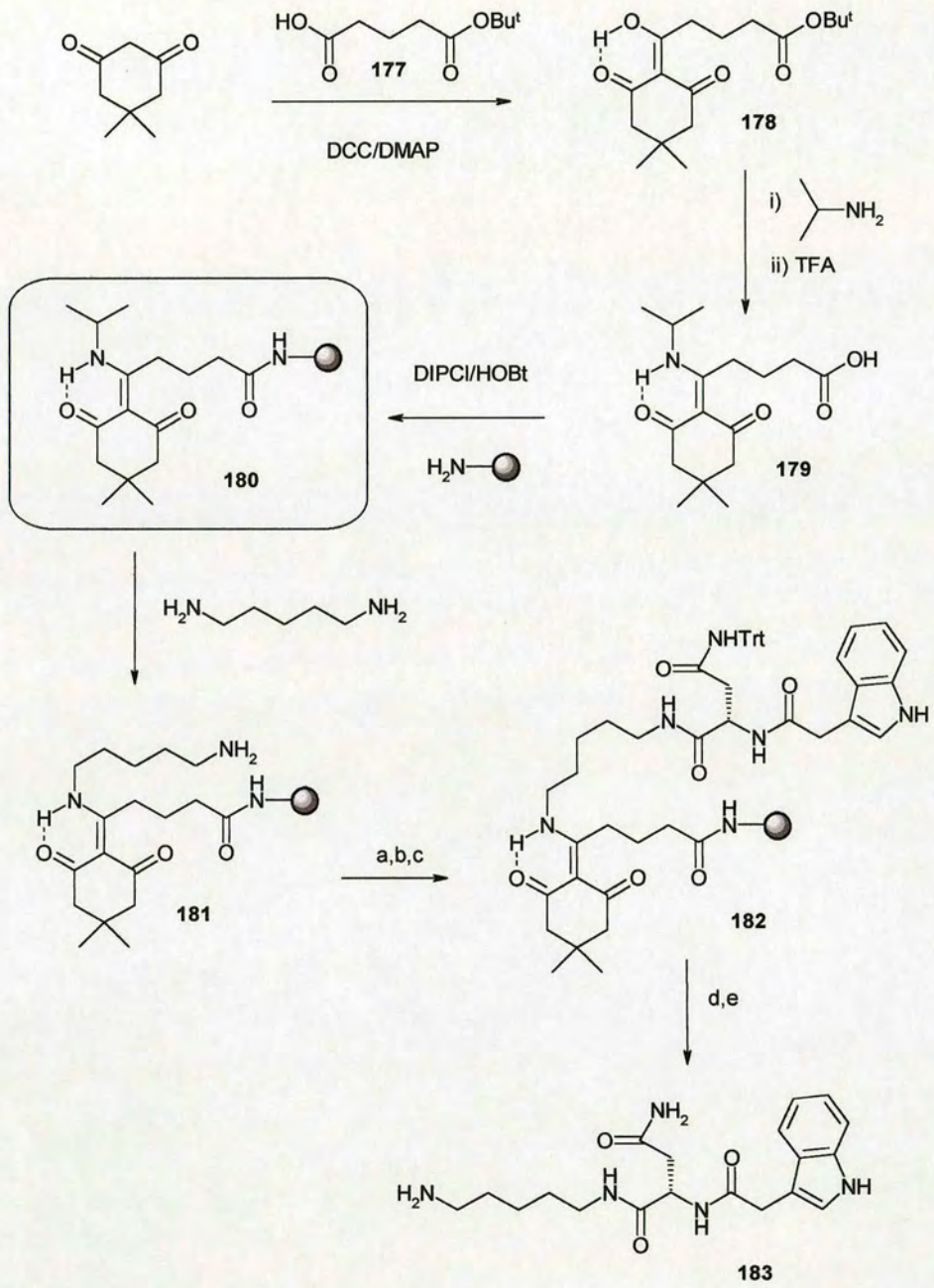

Conditions:

a) Fmoc-Asn(Trt)-OH/TBTU/HOBt/DIPEA; b) 20 % v/v piperidine in DMF; c) indole-3-acetic acid/TBTU/HOBt/DIPEA; d) 50 % v/v TFA in DCM/TIPS/H_2O; e) 5 % v/v NH_2NH_2 or 10 % v/v $C_3H_7NH_2$ in THF/H_2O (1:1).

A variation of the cyclohexanedione linker **184** (Scheme 5.7) has also been applied to the synthesis of oligosaccharides.[6] Aminosugars have been immobilised directly, via the formation of a vinylogous amide bond, as in the resin–bound sugar **185**. Alternatively the linker **184** may be derivatised by reaction with *p*-aminobenzyl alcohol to enable the formation of *O*-linkages to saccharides, as in species **186**. After cleavage from the resin using NH_3, the resulting *p*-aminobenzylglycoside is *N*-acetylated to enable cleavage of the anomeric *p*-aminobenzyl group with DDQ to afford the glycosylated saccharide **187**. The system is stable to a variety of carboydrate reaction conditions and cleavage of the final product is easily performed using ammonia. It is also possible to regenerate the immobilised linker **188** for further use by treatment with hydroxide.

Scheme 5.7

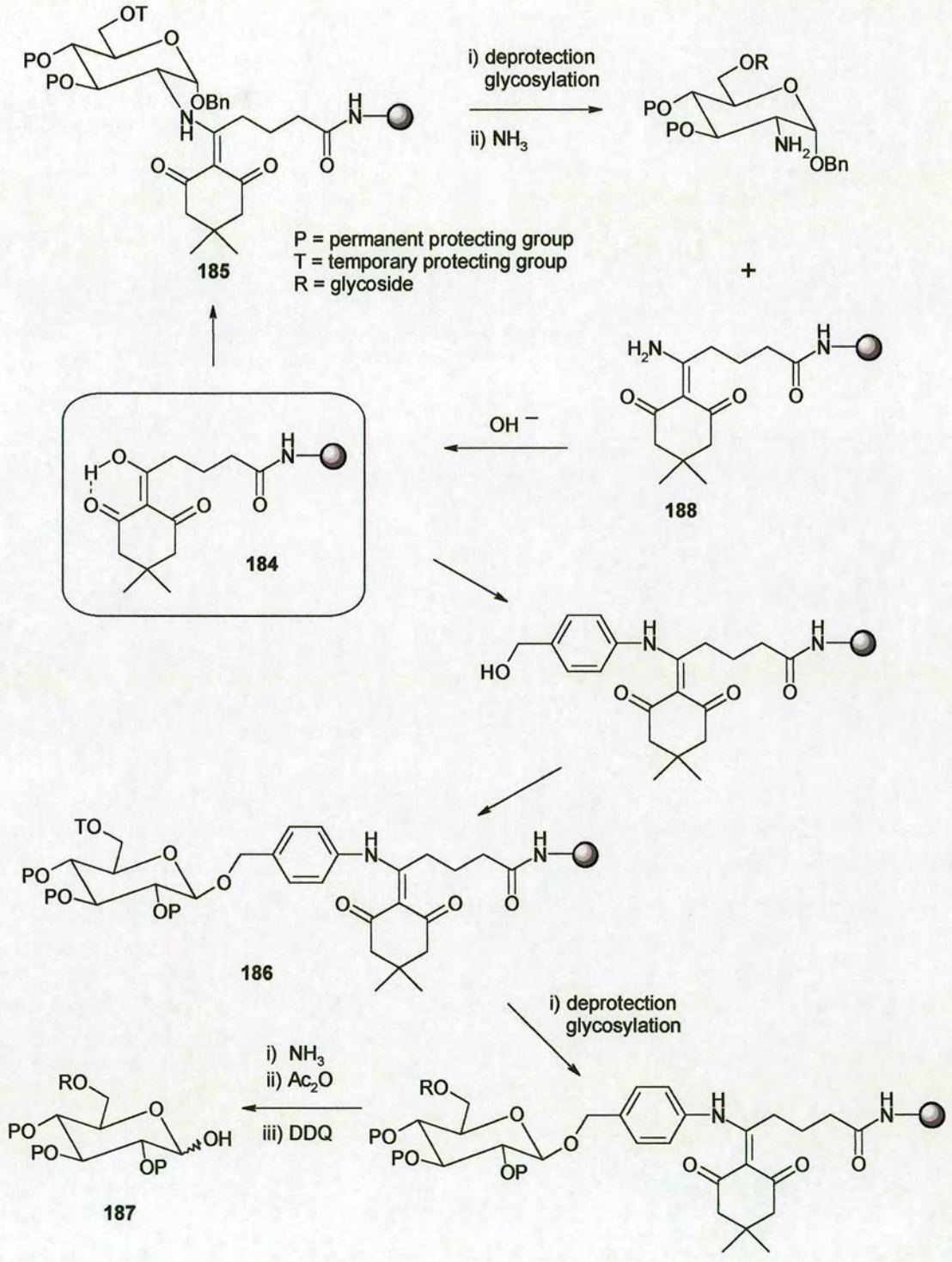
i) deprotection
glycosylation
ii) NH3
P = permanent protecting group
T = temporary protecting group
R = glycoside
185
188
184
OH −
186
i) deprotection
glycosylation
i) NH3
ii) Ac2O
iii) DDQ
187

A further Dde-based linker for the attachment of primary amines to solid support, illustrated in Figure 5.1, has been described by Bannwarth *et al.*[7] The linker is again stable towards acidic conditions (TFA) and basic conditions (piperidine, DBU) as well as uronium type coupling agents.

Figure 5.1

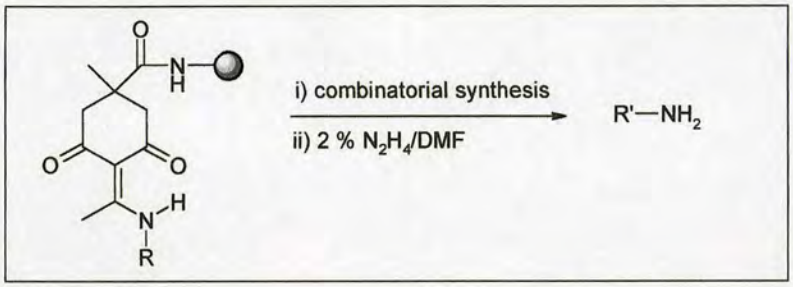

The synthesis of the linker molecule **194** is described in Scheme 5.8. Birch reduction of 3,5-dimethoxybenzoic acid **189**, followed by methylation provided the bis enol ether as the methyl ester **190**. Treatment with HCl resulted in the formation of the 3,5-dioxo-1-methyl-cyclohexane carboxylic methyl ester **191** which was acylated to form the *O*-acyl derivative **192**. DMAP-catalysed rearrangement of the *O*-acyl species **192** afforded the 4-acetyl-3,5-dioxo-1-methyl-cyclohexane carboxylic acid methyl ester **193**. The methyl ester of **193** was converted to the free acid to form the 4-acetyl-3,5-dioxo-1-methylcyclohexane carboxylic acid linker (ADCC linker) **194**. Application of the linker was demonstrated by coupling in phenylalanine methyl ester to form the linker **195**, which was attached to amino polystyrene resin using TPTU to yield the resin-bound amino acid **196**. Successful cleavage of L-phenylalanine methyl ester **198** was performed using 2 % hydrazine hydride solution, with formation of the resin-bound oxotetrahydro-1-H indazole derivative **197**.

Scheme 5.8

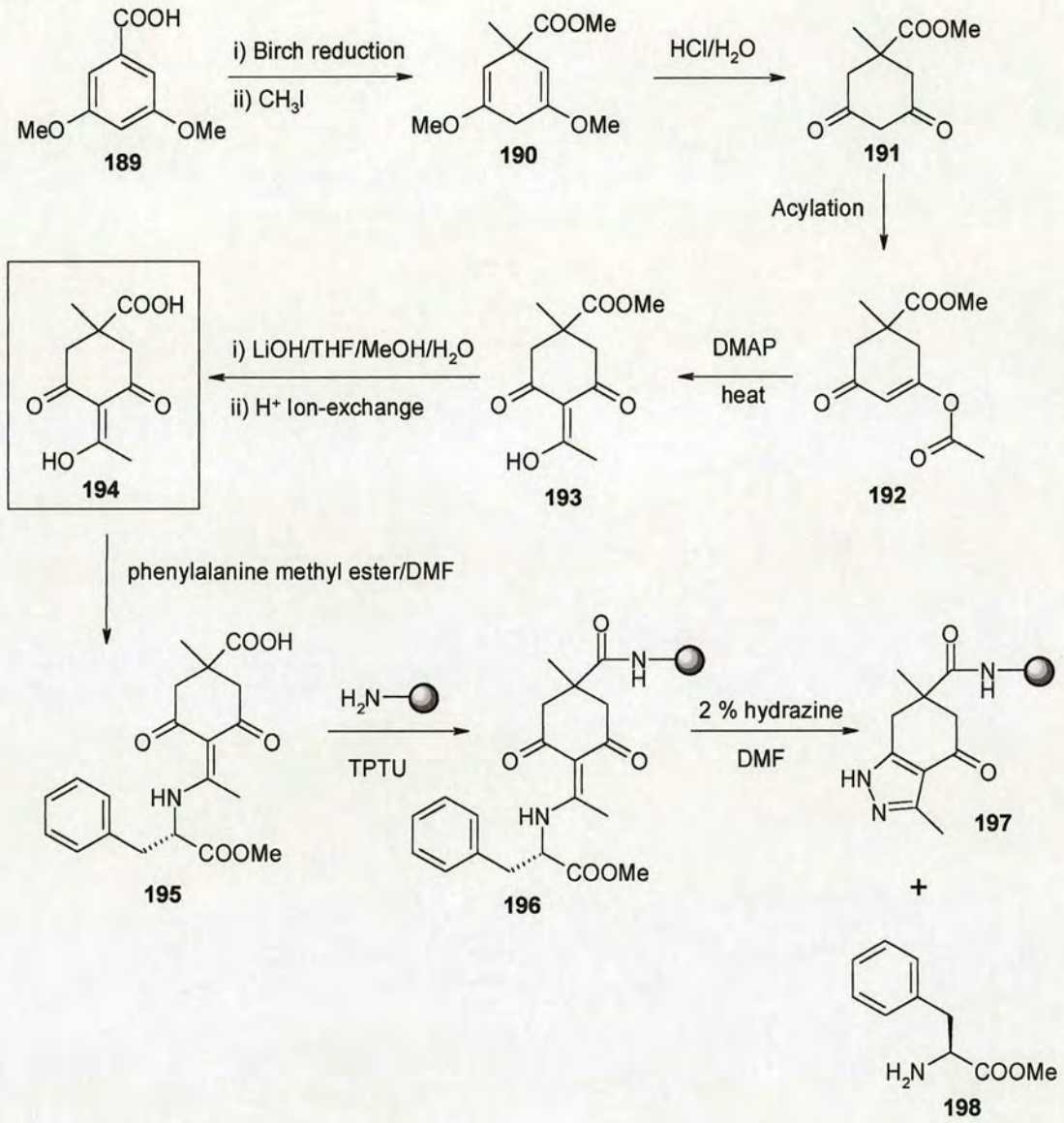

The Bannwarth method of attachment of a cyclohexane-1,3-dione species was particularly relevant to the proposed amide linker, since the cyclohexanedione is functionalised and immobilised via the 5-position, leaving the 1,3-dione system free for coupling to amino acids. However, the Bannwarth strategy involves coupling of the amine (phenylalanine in the example) to the acyl-dimedone linker **194** prior to immobilisation on resin. This was done by formation of the *C*-acyl-dimedone **193** by DMAP catalysed thermal rearrangement of the *O*-acyl species. Earlier work on dimedone reactions (Chapter 2) revealed that this rearrangement is not applicable

when the acylating agent is an amino acid. Additionally, a more general method for generation of resin-bound cyclohexanedione would be required for scavenger applications. Thus, the general principles of the Bannwarth linker strategy required to be adapted by alteration of the coupling events, in order to form an unfunctionalised cyclohexanedione system on resin.

A number of routes, illustrated in Scheme 5.9, were considered for the attachment of diones to resin.

Scheme 5.9

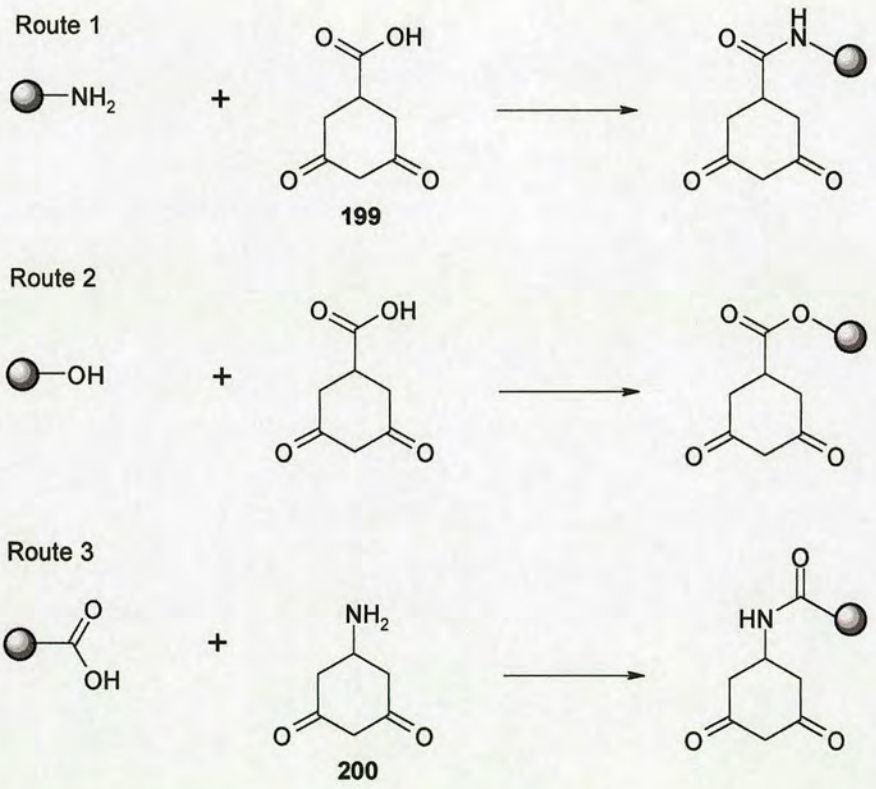

In a very general sense, one might employ a nucleophilic resin with a cyclohexanedione bearing electrophilic functionality (Routes 1 and 2), as in the Bannwarth example. Alternatively an electrophilic resin might be coupled to a cyclohexanedione with nucleophilic functionality (Route 3). This route could be immediately discounted because of the self-condensation problems associated with the unprotected amino functionality and carbonyl functionality of a 5-amino

cyclohexane-1,3-dione **200**. An amide linkage, as seen in Route 1 was deemed more favourable than the corresponding ester linkage (Route 2) for greater stability to a wider variety of reagents. The obvious problem with coupling 5-carboxycyclohexane-1,3-dione **199** to a nucleophilic amino resin is that attack of the carbonyl groups is likely in addition to the required amide formation. Indeed, this outcome was verified experimentally. The 5-carboxycyclohexen-1,3-dione **203** was prepared by Birch reduction of 3,4,5-trimethoxy benzoic acid **201** *via* hydrolysis of the intermediate bis-enol ether **202**, according to the procedure reported by Kuehne *et al.*[8] (Scheme 5.10). Attempted coupling of the acid **203** to aminomethyl polystyrene resin was performed using TPTU/DIPEA. Comparison of the IR of the reacted resin with that of aminomethyl resin starting material and that of acid **203**, indicated that some coupling had occurred as peaks were observed in the carbonyl region. The absence of immobilised free primary amine was confirmed by the Kaiser resin test.[9] However, gel ^{13}C NMR of the reacted resin was incompatible with the desired product. Further investigation of this reaction by coupling the acid **203** to benzylamine in solution, revealed that di-addition of the amine to both the acid and one of the carbonyl groups was occurring to form the enamine **204**. This problem did not occur in the Bannwarth linker synthesis because the cyclohexanedione species was acylated before attachment to the amino resin, which obviously alters the reactivity of the carbonyl system.

Scheme 5.10

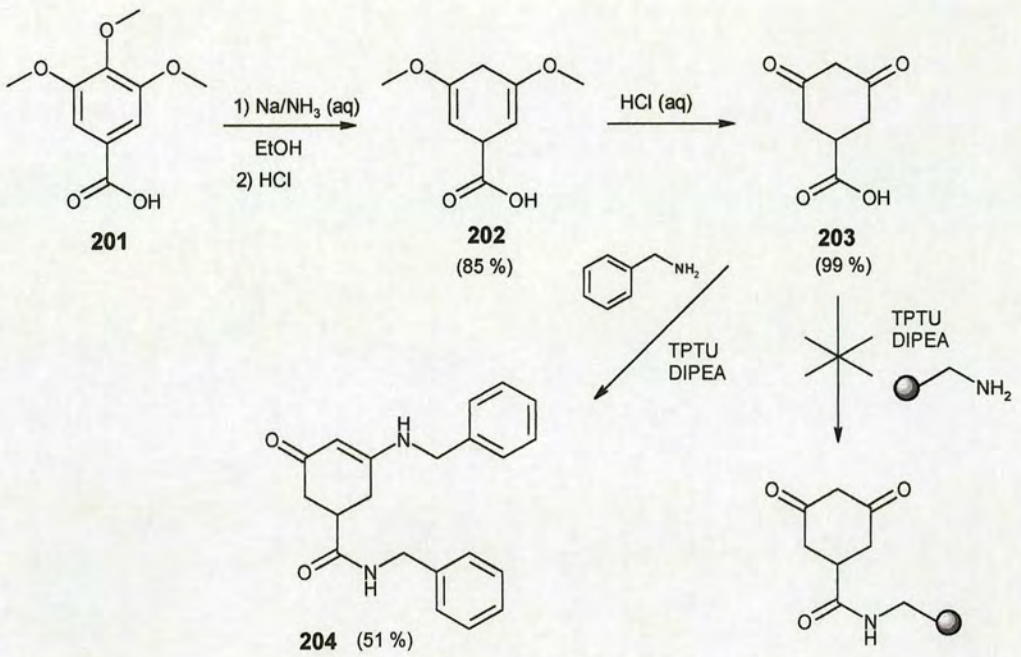

However, returning to the Birch reduction route to cyclohexanediones, it was postulated that the bis-enol ether species **202** could be regarded as a protected dicarbonyl compound, which might be attached to support and then hydrolysed to the diketone **205**, as indicated in Scheme 5.11.

Scheme 5.11

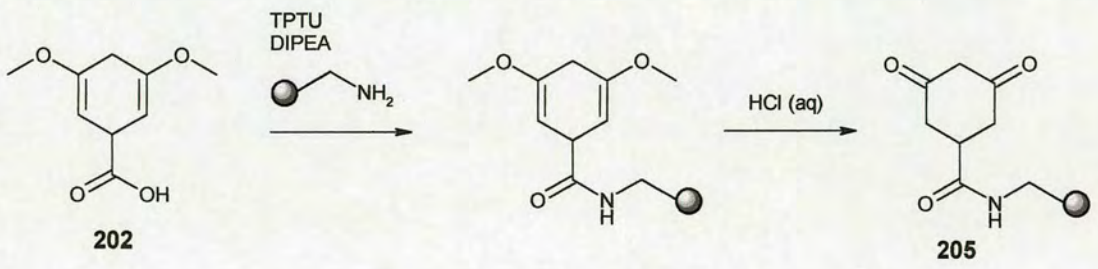

Unfortunately, the test reaction to couple benzylamine to the bis-enol ether **202** under the required conditions, resulted only in recovery of the benzyl amide **206** in 13 % yield (Scheme 5.12). It was thought that this result may be attributed to the presence of 3,5-dimethoxybenzoic acid remaining as an impurity from the partial reduction of

3,4,5-trimethoxybenzoic acid **201** in the Birch reduction step (Scheme 5.10). None of the desired amide was detected.

Scheme 5.12

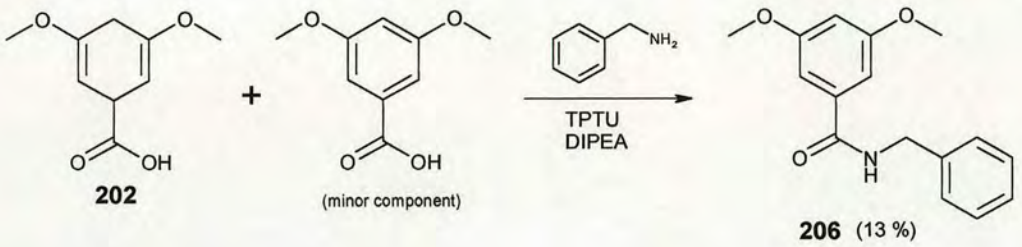

202 (minor component) **206** (13 %)

Returning again to the Bannwarth linker, it was observed that this route used the 5-methylated analogue **190** of the bis-enol ether system. The next step was to try forming the 5-methyl derivative of **202**, for reaction with benzylamine. No detailed experimental details were given for formation of ester **190** in the Bannwarth synthesis, other than reporting that the Birch reduction was followed by quenching with methyl iodide. A search of the literature resulted in several reported methods for generation of the 5-methylated bis-enol ether key intermediate **190**.

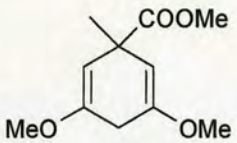

190

The method reported by Liepa *et al.*[10] introduced another important consideration: namely that if successful attachment of the dione linker to support was achieved *via* an amide linkage, then this linkage could interfere in later coupling of electrophilic species (eg activated acids) to the dione, with the possibility of amide *N*-acylation. The aim was therefore to attempt coupling of the bis-enol ether species **207** as the free acid, to *N*-methylbenzylamine, before trying the analogous coupling on solid support.

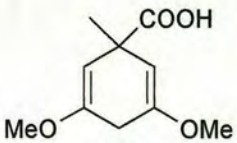

207

The dihydrodimethoxy species **202** was again prepared from 3,4,5-trimethoxy benzoic acid **201**, following the procedure reported by Kuehne *et al.*, using sodium in liquid ammonia with ethanol as the proton source, followed by acidic work-up. Methylation at the 5-position was attempted using potassium amide and methyl iodide, followed by acidification, according to the route reported by Chapman et al.[11] Unexpectedly, this resulted in partial hydrolysis of one of the methoxy groups to the ketone, and formation of the methyl ester to form the mono-ketone **208** (Scheme 5.13).

Scheme 5.13

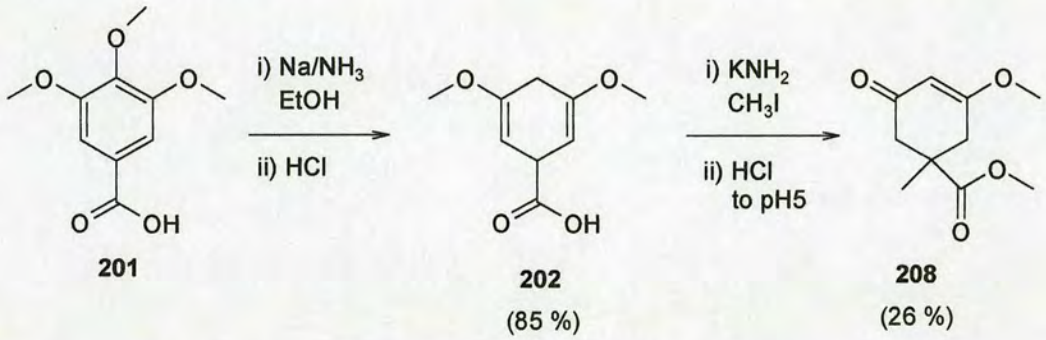

Direct formation of the desired compound **207** by reduction of 3,4,5-trimethoxybenzoic acid using lithium in liquid ammonia with THF, and immediate quench with methyl iodide, followed by acidification, was also attempted with no success (Scheme 5.14). This procedure, reported by Liepa *et al.*,[12] again resulted in the mono-ketone as the free acid **209**. Even when acidification was carried out to a higher pH (4-5), partial hydrolysis always occurred.

Scheme 5.14

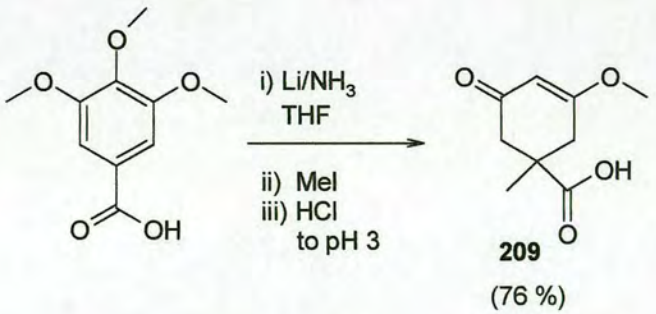

Further investigation of the literature suggested that starting from 3,5-dimethoxybenzoic acid **210** may result in cleaner Birch reduction products.[13] The reduction and methylation were repeated using dimethoxybenzoic acid, but all attempts to quench with methyl iodide resulted in products that were unstable in solution, usually decomposing to the partially hydrolysed mono-ketone species **209**.

However, the ethyl analogue **211** of the elusive bis-enol ether key intermediate **207**, was finally successfully synthesised by simply quenching with ethyl bromide instead of methyl iodide in the Birch reduction of 3,5-dimethoxybenzoic acid **210** (Scheme 5.15). The enol ether **211** was coupled to *N*-methyl benzylamine using TBTU/HOBT, and the amide **212** obtained successfully hydrolysed to the desired diketone system **213**.

Scheme 5.15

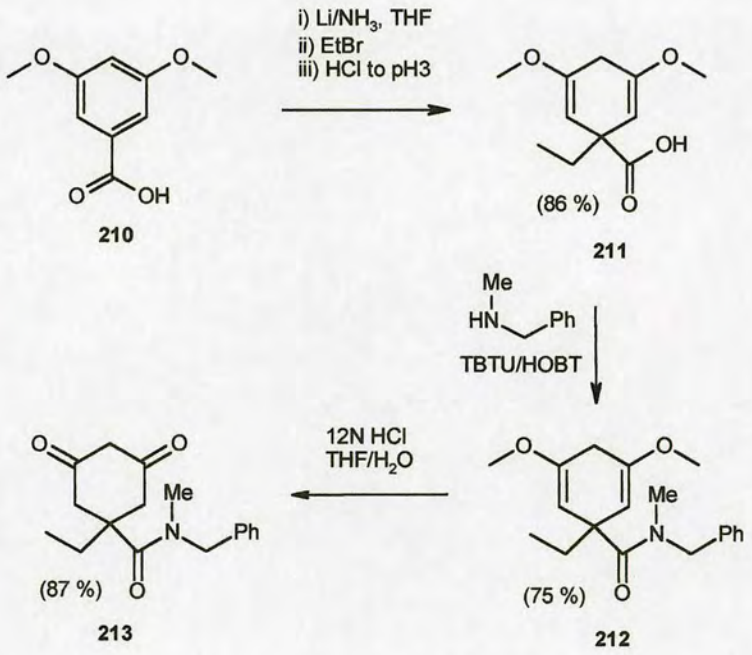

5.4 Oxidative Cleavage

The second requirement in the development the proposed linker for the attachment of peptides and amides in general to solid support, was a means of performing oxidative cleavage of the alkene bond in order to release the amide into solution.

There are several reported cases of the use of periodate and other strong oxidising agents on solid support.[14,15] Sodium periodate has been used in the oxidation of bicyclic pyrrole C=C bonds to form cyclic ketolactams.[16] Initial studies in solution indicated partial periodate cleavage of the double bond of ligand **59** to release the dipeptide **174**, but the yields recovered were very low. Alternative reagents were investigated (Scheme 5.16).

Scheme 5.16

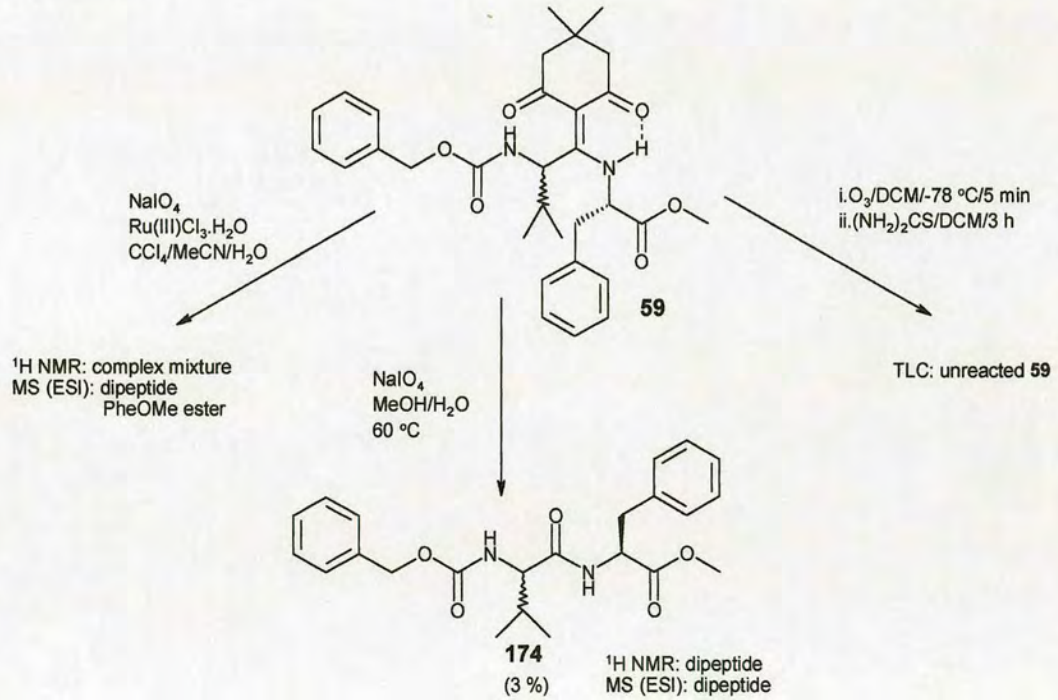

Ozonolysis, also used previously on solid support,[17] did not result in any cleavage of the alkene bond of **59**, and starting material was recovered unchanged.

Oxidative cleavage of hindered alkenes has been successfully achieved by treatment with periodate in the presence of a ruthenium (III) catalyst.[18] MS results indicated minimal cleavage of the dipeptide **174** under these conditions.

Synthesis of a model system for the immobilised cyclohexane-1,3-dione amide linker was proposed in order to establish that selective cleavage of the alkene bond was possible in good yield, and to optimise reagents and conditions. The model was prepared as shown in Scheme 5.17. Propionic acid **214** was first coupled to dimedone using DCC/DMAP, to form the activated alcohol **215**. Treatment with *N*-benzylamine under basic conditions yielded the model system **216**.

Scheme 5.17

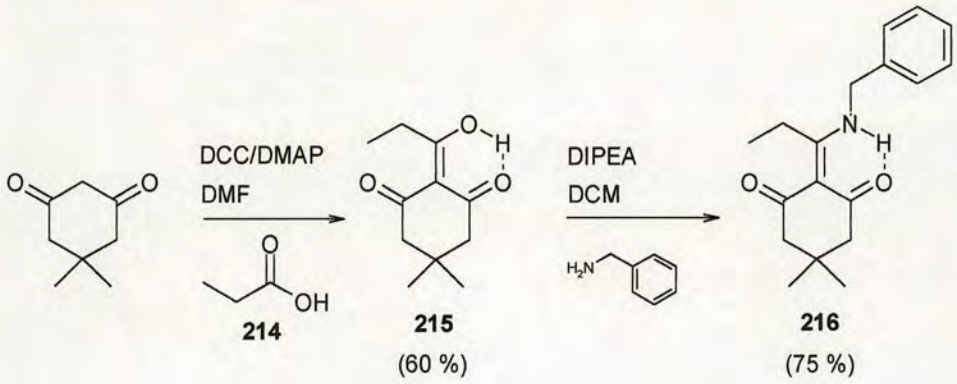

Oxidative cleavage of the alkene of **216** in order to release amide **217** was attempted under several sets of conditions detailed in Scheme 5.18. Treatment of the alkene **216** with sodium periodate afforded a 24 % yield of amide **217**, but the presence of benzylamine (present in the mass spectrum of the crude reaction mixture), indicated that some cleavage of the amide bond of **217** had also occurred. Selenium dioxide catalysed oxidation, using conditions reported by Naota *et al.*[19], resulted in recovery of starting material **216**. Treatment of alkene **216** with chromium oxide, using conditions reported by Kalaus *et al.*[20], was again unsuccessful. The most promising result was obtained by oxidative cleavage of alkene **216** using ammonium molybdate and hydrogen peroxide in acetic acid (conditions published by Witte *et al.*[21]), to

afford the amide **217** in 35 % yield. However evidence of amide bond cleavage was again observed.

Scheme 5.18

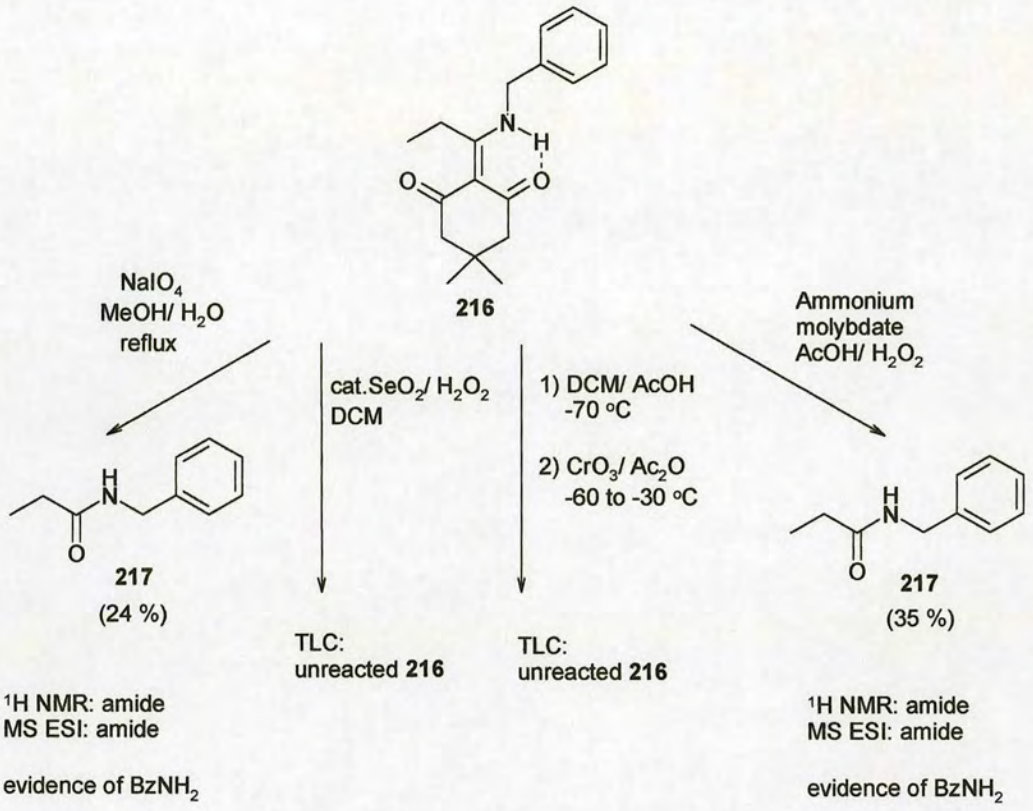

A second model system **218** (Scheme 5.19) was synthesised in a similar manner to **216**, but with *N*-butylamine in place of *N*-benzylamine. Treatment of alkene **218** with molybdate catalysed hydrogen peroxide, resulted in release of amide **219**. There was no evidence of *N*-benzylamine in the mass spectrum of the crude reaction mixture, indicating that the amide bond of **219** was not affected in this case.

Scheme 5.19

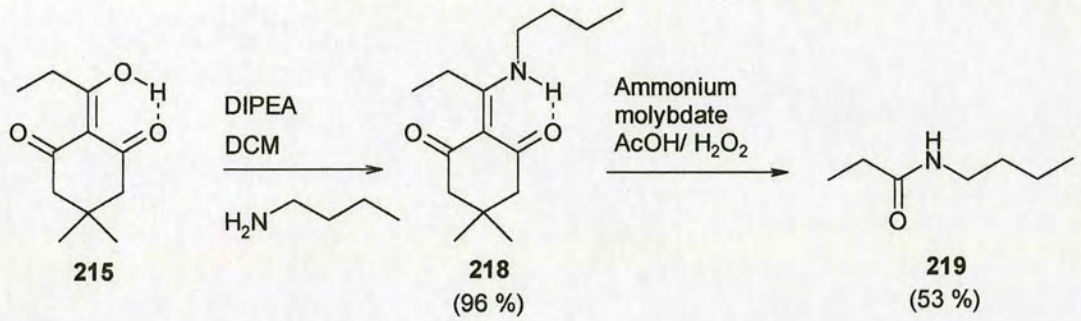

215 **218** (96 %) **219** (53 %)

The molybdate/H_2O_2 cleavage conditions were then tried out on the linker system previously prepared (**213**, Scheme 5.15). Propionic acid was coupled to diketone **213** using DCC/DMAP, to form the activated alcohol **220**, which was then reacted with butylamine to form the cyclohexanedione-supported 'amide' **221** (Scheme 5.20). This promising result verified that the *N*-methyl amide attachment of the cyclohexane to the resin did not interfere with reactions at the dione system. Cleavage of the amide **219** from the dione was again achieved using molybdate catalysed hydrogen peroxide, although some cleavage of the *N*-methyl amide bond, releasing **222**, was also indicated by MS. However, the absence of *N*-methyl benzylamine in the ^{1}H NMR spectrum reassuringly indicated that it was present only in very low yield.

Scheme 5.20

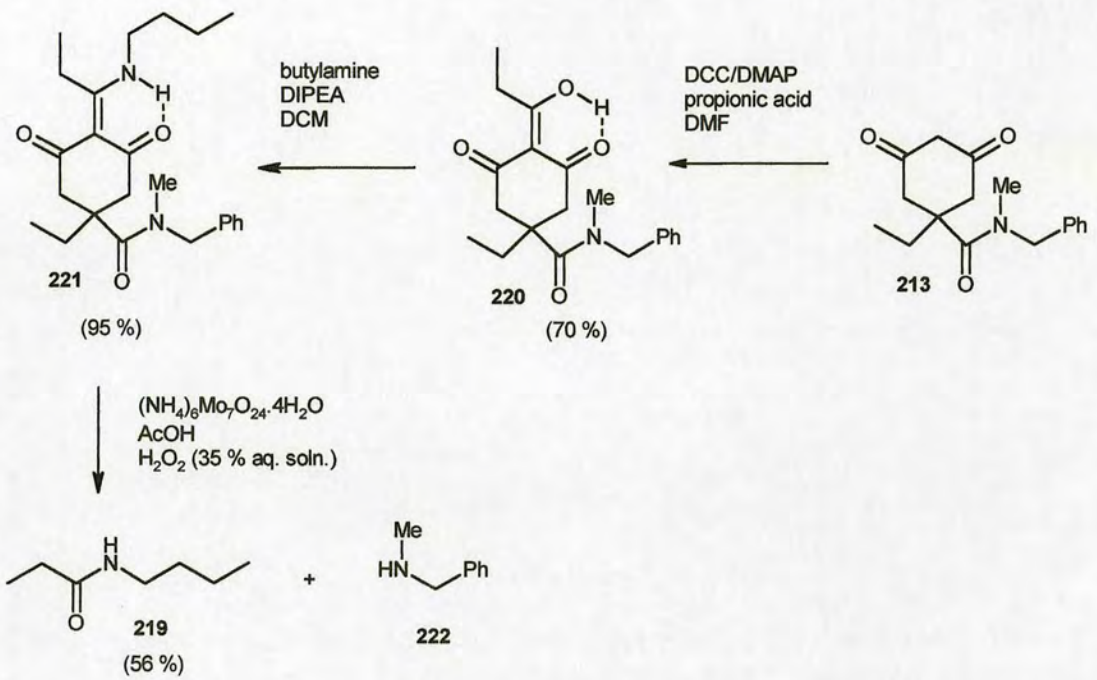

5.5 Summary

Successful solution phase development of a model resin-bound cyclohexane-1,3-dione linker system was achieved. A combined synthesis and coupling of simple amides to the linker system, effectively *via* the amide carbonyl, to form an alkene bond to cyclohexanedione was demonstrated. Finally, oxidative cleavage of the resulting alkene bond to release the amide was illustrated.

5.6 Further Work - Solid Phase Chemistry

Time constraints prevented any further investigation of the transferral of the successfully concluded solution phase model cyclohexanedione linker route, to solid support. However, some suggestions for future adaptation of the solution phase linker route to resin will now be outlined.

5.6.1 Method A

Coupling of the bis-enol ether **211** to solid support, using conditions identical to the solution phase chemistry previously tested, should afford the resin bound diketone **224** (Scheme 5.21). The TBTU/HOBT coupling conditions were previously reported by Berteina et al.[22] for the attachment of carboxylic acids to *N*-methyl polystyrene resin. Coupling of Fmoc-glycine to the resin-bound diketone **224** to form the carbamate species **225** in the final step, is proposed in order to obtain a loading from Fmoc cleavage and analysis.

Scheme 5.21

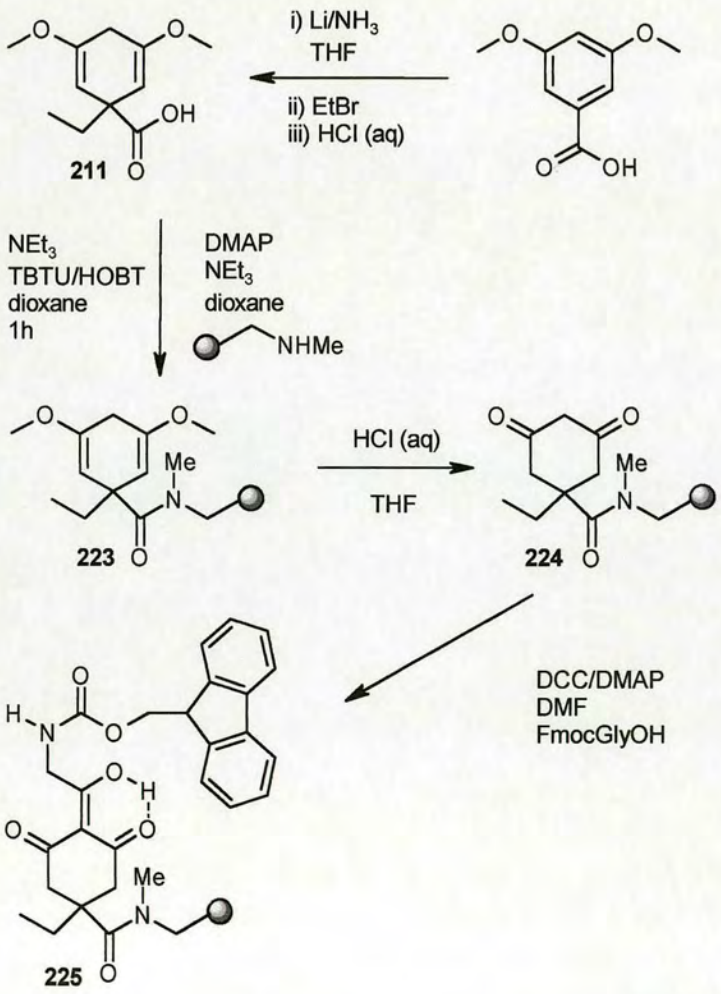

5.6.2 Method B

An alternative method for immobilisation of the cyclohexanedione on solid support would be to exploit the dianion chemistry used previously (Chapter 3) in the preparation of 4-alkyl dimedones. The 4-benzyl dimedone **99** has been prepared in good yield (Scheme 5.22).

Scheme 5.22

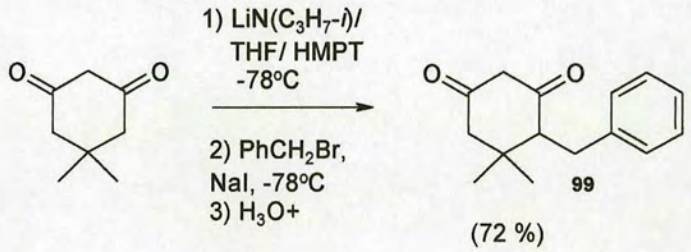

It was envisioned that these conditions might therefore be adapted for coupling dimedone to bromo resin as illustrated in Scheme 5.23.

Scheme 5.23

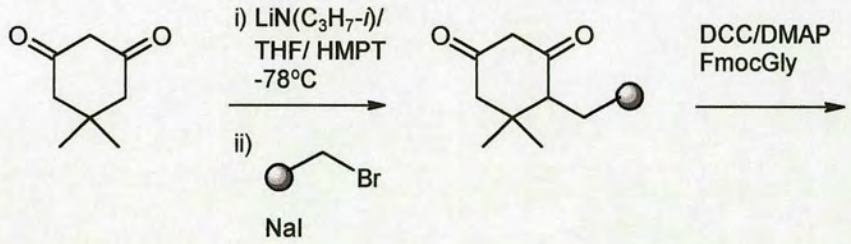

Additional further work should include investigating the scope of employment of resin-bound cyclohexanedione as a scavenger resin.

5.7 References

[1] Merrifield, R. B., *J. Am. Chem. Soc.*, 1963, **85**, 2149-2154.

[2]Jensen, K. J.; Alsina, J.; Songster, M. F.; Vágner, J.; Albericio, F.; Barany, G., *J. Am. Chem. Soc.*,1998, **120**, 5441-5452.

[3] Kunz, H.; Unverzagt, C, *Angew. Chem. Int. Ed. Engl.*, 1984, **23**, 436.

[4] Graf von Roedern, E., *Molecular Diversity*, 1998, **3**, 253-256.

[5] Chhabra S. R.; Khan, A. N.; Bycroft, B. W., *Tet. Lett.*, 1998, **39**, 3585-3588.

[6] Troth, I.; Dekany, G.; Kellam, B., 1998, *Patent Co-operation Treaty Application* PCT AU98/00131.

[7] Bannwarth, W.; Huebscher, J.; Barner, R., *Bioorg. & Med. Chem. Lett.*, 1996, **6**, 1524-1528.

[8] Kuehne, M.E.; Lambert, B.F., *J. Chem. Soc.*, 1959, **81**, 4278-4287.

[9] Kaiser, E., *Anal. Biochem.*, 1970, **34**, 595.

[10] Liepa, A.J.; Wilkie, J.S.; Winzenberg, K.N., *Aust. J. Chem.*, 1989, **42**, 1217-1225.

[11] Chapman, O.L.; Fitton, P., *J. Am. Chem. Soc.*, 1963, **85**, 41-47.

[12] Liepa, A.J.; Wilkie, J.S.; Winzenberg, K.N., *Aust. J. Chem.*, 1989, **42**, 1217-1225.

[13] Birch, A.J.; Slobbe, J., *Tetrahedron Lett.*, 1976, 24, 2079-2082.

[14] Kurth, M.J.; Ahlberg Randall, L.A.; Takenouchi, K., *J. Org. Chem.*, 1996, **61**, 8755-8761.

[15] Bertini, V.; Lucchesini, F.; Pocci, M.; De Munno, A., *Tetrahedron Lett.*, 1998, **39**, 9263.

[16] Gatta, F., *J. Heterocyclic Chem.*, 1989, **26**, 537-539.

[17] Hall, B.J.; Sutherland, J.D., *Tetrahedron Lett.*, 1998, **39**, 6593-6596.

[18] Ott, M.M.; Little, R.D., *J. Org. Chem.*, 1997, **62**, 1610-1616.

[19] Naota, T.; Sasao, S.; Tanaka, K.; Yamamoto, H.;; Murahashi, S., *Tetrahedron Lett.*, 1993, **34**, 30, 4843-4846.

[20] Kalaus, G.; Malkieh, N.; Kajtár-Peredy, M.; Brlik, J.; Szabó, L; Szántay, C., *J. Org. Chem.*, 1988, **53**, 42-45.

[21] Witte, J.; Boekelheide, V., *J. Org. Chem.*, 1972, **37**, 18, 2849-2853.

[22] Berteina, S.; De Mesmaeker, A, *Tetrahedron Lett.*, 1998, **39**, 5759-5762.

6 Experimental

6.1 General Techniques

6.1.1 Instrumentation

^{1}H and ^{13}C NMR spectra were recorded on Brüker AC250, DPX-360 or Varian Gemini-200 instruments. The following abbreviations are used: δ, chemical shift; d, doublet; dd, doublet of doublets; dt, doublet of triplets; dq, doublet of quartets; *J*, coupling constant; m, multiplet; q, quartet; s, singlet; t, triplet. Chemical shifts (δ) are reported in parts per million (ppm) and coupling constants (*J*) in Hz. Residual protic solvent, $CHCl_3$ (δ_H 7.26, s) was used as the internal standard in ^{1}H NMR spectra, and ^{13}C NMR shifts were referenced using $CDCl_3$ (δ_C 77.0, t) with broad band decoupling. Electrospray (ESI) nominal mass spectra were recorded using a Micromass Platform II mass spectrometer (CV=25). Fast Atom Bombardment (FAB) high resolution mass spectra were recorded on a Kratos MS50TC instrument. Infra-red absorption spectroscopy was performed on a Perkin-Elmer FT-IR Paragon 1000 spectrometer, and ν_{max} values are quoted in cm^{-1}. High performance liquid chromatography (HPLC) was carried out using a Waters 486 tunable absorbance detector and Waters 600E controller and pump. A Chiralcel OD-H column with dimensions 25 x 0.46 cm was used. Samples were injected *via* a 20 µl loop and a flow rate of 1 ml/min was employed for elution using an isocratic system of hexane/isopropyl alcohol (95:5). A wavelength of 215 nm was used for sample detection. Melting points were obtained on Gallenkamp melting point apparatus and are uncorrected. Optical rotations were performed on an AA1000 polarimeter from Optical Activity Ltd (measurements made at the sodium D-line). Concentrations are given in g/100ml. Solid phase samples were shaken on a New Brunswick Scientific G76 gyrorotory water bath shaker. Resin samples were spun on a Stuart Scientific Blood Rotator SB1.

6.1.2 Chromatography

Analytical TLC was carried out on Merck aluminium-backed plates coated with silica gel 60 F_{254}, 0.25 mm. Components were visualised using ultra-violet fluorescence (254 nm), and ammonium molybdate or permanganate dips. Flash chromatography was carried out using silica gel 60H (Merck 9385, 0.04-0.063 mm, 230-400 mesh). Alternatively, where stated, a Biotage FLASH 40i system using 40 g (40S) or 90 g (40M) prepacked silica cartridge was employed for chromatographic separation. A Biotage Quad system, capable of separating 4 samples in parallel on 4 prepacked slica cartridges, was used where stated.

6.1.3 Solvents and Reagents

All reagents and solvents were standard laboratory grade and were used as supplied unless otherwise stated. DMF refers to peptide synthesis grade. Wang resin was purchased from Novabiochem.

6.1.4 Solid Phase Protocols

6.1.4.1 Washing protocol: 2 x THF; 2 x DMF; 2 x DMF:MeOH (1:1); 2 x DMF; 2 x THF; 2 x DCM.

6.1.4.2 Protocol for photometric analysis of p-nitrophenol (from Novabiochem, modified by Dr A. Long)

Standard: *p*-nitrophenol (4-6 mg) was dissolved in DMF (2 ml). A standard 20 % solution of piperidine in DMF (2 ml) was added and the resulting solution stirred for 1 h before making up to 25 ml with methanol. An aliquot (250 μl) was removed and diluted to 10 ml with water.

Sample: Resin (4-6 mg) was suspended in DMF (1 ml). The standard 20 % piperidine in DMF solution (1 ml) was added and the resulting solution stirred for 1 h

before making up to 10 ml with methanol. An aliquot (200 µl) was removed and diluted to 5 ml with water.

Blank: DMF (1 ml) and standard 20 % piperidine in DMF solution (1 ml) were stirred for 1 h before making up to 10 ml with methanol. An aliquot (200 µl) was removed and diluted to 5 ml with water.

Measurement: The absorbance of the sample and standard were measured against the blank at 400 nm. The loading was then calculated as follows:

mmol/g = [Abs(sample) x weight of standard x 1000] /
[weight of sample x Abs(standard) x 4 x 139.1]

6.1.4.3 Protocol for photometric analysis of dibenzofulvene piperidine adduct

Two samples of dry resin (4-10 mg) were accurately weighed directly into 10 ml volumetric flasks. The volume was made up with 20 % piperidine in DMF and the flasks sonicated at room temperature for 10 min. The remaining 20 % piperidine in DMF solution was used as a blank, and the absorbance of each sample measured at 301 nm. The loading was calculated using following relationship:

$$mmol/g = (A \times v) / (\varepsilon \times 10^{-3} \times wt)$$

A = absorbance @ 301 nm (λ-max)
v = volume / ml
wt = weight of resin sample / mg
ε = extinction coefficient of *N*-(9-fluorenylmethyl)piperidine[25]
ε 310 nm = 7800 $M^{-1}cm^{-1}$

Cleavage MS samples: Resin (3-5 mg) was suspended in TFA/DCM/H_2O (9:10:1) and spun at room temperature for 1 h. The resin was filtered off, washed with DCM,

and the filtrate concentrated under reduced pressure. Acetonitrile/water (1:1) (1 ml) was added and the solution sonicated for 10 min. An aliquot (100 μl) was removed and made up to 1 ml. The resulting solution was then filtered before analysis.

Gel ^{13}C NMR : Only signals which appear on the peak list are quoted. Some additional signals are present but are barely distinguishable from the baseline noise.

6.2 Experimental Procedures

6.2.1 Results and Discussion I

6.2.1.1 1-(4,4-dimethyl-2,6-dioxocyclohexylidene)-2-benzyloxycarbonyl-aminoethanol (40)

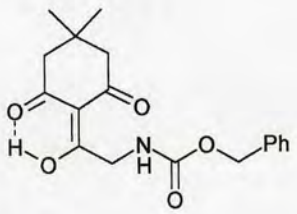

To a stirred solution of *N*-benzyloxycarbonylglycine (1.50 g, 7.17 mmol) in DMF (50 ml), dimedone (1.10 g, 7.89 mmol), DCC (1.48 g, 7.17 mmol) and DMAP (0.88 g, 7.17 mmol) were added and the mixture stirred at room temperature for 40 h. The resulting yellow solution was filtered to remove the white DCU precipitate and concentrated under reduced pressure to an orange residue (4.60 g) which was then dissolved in EtOAc (120 ml) and further DCU precipitate removed by filtration. The EtOAc solution was washed with 1M $KHSO_4$ (40 ml) and the product extracted with $NaHCO_3$ (2 x 200 ml). The aqueous solution was acidified using 2N HCl and extracted with DCM (3 x 100 ml). The solution was concentrated under reduced pressure to afford a yellow oil (1.02 g) which solidified on standing. The residue was recrystallised twice from methanol/water (1:1) and dried in a desiccator overnight to yield a white solid (0.32 g, 13 %): mp 109 °C; R_f=0.41 cyclohexane/EtOAc (1:3); ν_{max}(polyethylene card) 3381br (O-H & N-H), 1716

(urethane C=O), 1661 (α,β-unsaturated ketone), 1567 (amide II); δ_H (200 MHz, $CDCl_3$) 1.08 (6H, s, $C(CH_3)_2$), 2.35 (2H, s, $CH_2C(CH_3)_2$), 2.56 (2H, s, $CH_2C(CH_3)_2$), 4.66 (2H, d, *J* 5.5, CH_2NH), 5.14 (2H, s, OCH_2Ph), 5.43 (1H, br s, N*H*), 7.26-7.36 (5H, m, Ar-*H*), 16.92 (1H, s, O*H*); δ_C (63 MHz, DEPT, $CDCl_3$) 28.0 ($C(CH_3)_2$), 30.9 ($C(CH_3)_2$), 45.2 ($CH_2C(CH_3)_2$), 49.8 ($NHCH_2$), 51.7 ($CH_2C(CH_3)_2$), 66.7 (OCH_2Ph), 111.1 (COC=COH), [127.9 (CH), 128.3 (CH), 5C, *Ar*-H], 136.2 (OCH_2Ph), 156.2 (CONH), 194.9 (COC=CCO), 200.4 (COC=COH); MS ESI (-ve) found m/z 329.9 ($[M-H]^-$, 100 %); HRMS FAB (+ve) found m/z 332.14966 (MH^+), $C_{18}H_{22}NO_5$ requires 332.14980.

6.2.1.2 N-[1-(4,4-dimethyl-2,6-dioxocyclohexylidene)-2-benzyloxy-carbonylaminoethyl]butylamine (41)

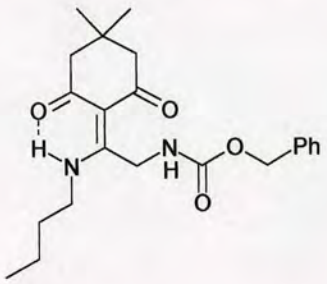

1-(4,4-dimethyl-2,6-dioxocyclohexylidene)-2-benzyloxycarbonylaminoethanol **40** (0.10 g, 0.30 mmol) and *N*-butylamine (30 μl, 0.30 mmol) in DMF (4 ml) were stirred at room temperature for 26 h. The reaction mixture was concentrated under reduced pressure to yield a yellow oil. Flash column chromatography on silica gel using cyclohexane/EtOAc (1:3) as eluent afforded a yellow oil (combined yield 0.19 g, 84 %); R_f=0.58 cyclohexane/EtOAc (1:3); ν_{max}(polyethylene card) 3421 (N-H), 1717 (urethane C=O), 1634 (α,β-unsaturated ketone), 1580 (amide II); δ_H (200 MHz, $CDCl_3$) 0.94 (3H, t, *J* 7.0, CH_2CH_3), 1.01 (6H, s, $C(CH_3)_2$), 1.43 (2H, tq, *J* 7.0, 7.0, CH_2CH_3), 1.57-1.68 (2H, m, $CH_2CH_2CH_3$), 2.33 (2H, s, $CH_2C(CH_3)_2$), 2.38 (2H, s, $CH_2C(CH_3)_2$), 3.78 (2H, dt, *J* 12.5, 7.0, $NHCH_2CH_2$), 4.35 (2H, d, *J* 7.0, $CONHCH_2$), 5.06 (2H, s,OCH_2Ph), 6.37 (1H, t, *J* 7.0, CONH), 7.31 (5H, s, Ar-*H*), 13.44 (1H, br s, $NHCH_2CH_2$); δ_C (63 MHz, DEPT, $CDCl_3$) 13.5 (CH_2CH_3), 19.8

(CH_2CH_3), 28.1 (C(CH_3)$_2$), 30.1 (C(CH_3)$_2$), 31.4 ($CH_2CH_2CH_3$), 38.8 (NHCH_2CH_2), 43.7 (CH_2C(CH_3)$_2$), 52.0 (CH_2C(CH_3)$_2$), 53.0 (CONHCH_2), 66.7 (OCH_2Ph), 106.8 (C=CNH), [127.8 (CH), 128.0 (CH), 128.3 (CH), 5C, *Ar*-H], 136.2 (OCH$_2$*Ph*), 156.2 (O*C*ONH), 169.9 (C=*C*NH), 197.0 (CH_2CO), 199.9 (CH_2CO); MS ESI (+ve) found m/z 386.9 (MH^+, 18 %), 409.1 (MNa^+, 100), 432.1 (22), 450.2 (26); HRMS FAB (+ve) found m/z 387.22828 (MH^+), $C_{22}H_{31}N_2O_4$ requires 387.22838.

6.2.1.3 Attempted preparation of N-benzyloxycarbonyl-L-valine azide (45)

45 **46**

Triethylamine (0.35 ml, 2.5 mmol) and ethyl chloroformate were added to a solution of Cbz-L-valine (0.63 g, 2.5 mmol) in THF (5 ml) at –10 °C. The resulting mixture was stirred for 15 min at –10 °C, before warming to 0 °C and addition of a 2M aqueous solution of sodium azide (2.5 ml, 5.0 mmol). After stirring for 30 min at 0 °C, the reaction was diluted with cold EtOAc (20 ml) and washed with cold brine (3x5 ml). The EtOAc layer was separated, dried ($MgSO_4$) and concentrated under reduced pressure to yield a colourless oil (0.07 g, 10 %): ν_{max}(crude oil) 3319br (N-H), 2966 (acid C=O, from Cbz-L-valine), 2252 (isocyanate –N=C=O), 2140 (azide N_3), 1701 (urethane), 1523 (amide II).

6.2.1.4 3-(N-benzyloxycarbonyl-L-leucinyloxy)-5,5-dimethyl-2-cyclo-hexen-1-one (50)

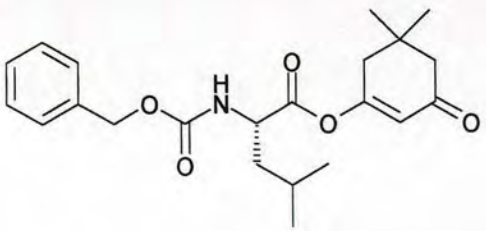

6.2.1.4.1 Method A

To a cold (-10 °C) solution of *N*-benzyloxycarbonyl-L-leucine (0.73 g, 2.74 mmol) in EtOH (5 ml), were added triethylamine (0.38 ml, 2.74 mmol), and ethyl chloroformate (0.26 ml, 2.74 mmol). The mixture was stirred for 15 min at -5 °C, and dimedone (0.38 g, 2.74 mmol) added. After stirring for 1 h 20 min at 0 °C, TLC hexane/EtOAc (1:1) indicated formation of products. The reaction was allowed to warm to room temperature and stirred for 1 h before concentration under reduced pressure to give a colourless oil (1.66 g). Flash column chromatography on silica gel using hexane/EtOAc (4:1→2:1) yielded a colourless oil (0.34 g, 32 %); $[\alpha]_D$ -18.0 (c 2.2, $CHCl_3$); R_f=0.33 cyclohexane/diethyl ether (1:1); ν_{max}(polyethylene card) 3322 (N-H), 1770 (vinyl ester), 1715 (urethane C=O), 1674 (α,β-unsaturated ketone), 1532 (amide II); δ_H (250 MHz, $CDCl_3$) 0.96 (6H, d, *J* 6.0, $CH(CH_3)_2$), 1.06 (6H, s, $C(CH_3)_2$), 1.58-1.76 (3H, m, $CH_2CH(CH_3)_2$), 2.25 (2H, s, $CH_2C(CH_3)_2$), 2.38 (2H, s, $CH_2C(CH_3)_2$), 4.42-4.46 (1H, m, CHNH), 5.11 (2H, s, CH_2Ph), 5.21 (1H, d, *J* 8.0, NH), 5.90 (1H, s, COCH=CO), 7.33 (5H, s, Ar-H); δ_C (63 MHz, DEPT, $CDCl_3$) 21.5 ($CH(C^AH_3C^BH_3)$), 22.7 ($CH(C^AH_3C^BH_3)$), 24.7 ($CH(CH_3)_2$), 27.9 ($C(C^AH_3C^BH_3)$), 28.0 ($C(C^AH_3C^BH_3)$), 33.0 ($C(CH_3)_2$), 40.9 ($CH_2CH(CH_3)_2$), 41.7 ($CH_2C(CH_3)_2$), 50.6 ($CH_2C(CH_3)_2$), 52.6 (NHCH), 67.1 (OCH_2Ph), 116.1 ($COCH=COCH_2$), [127.9 (CH), 128.2 (CH), 128.4 (CH), 5C, *Ar*-H], 135.9 (OCH_2Ph), 155.8 (OCONH), 167.8 (COOC=CH), 170.0 (NHCHCO), 199.2 (COCH=COCO); MS ESI (+ve) found m/z 410.2 (MNa^+, 100 %), 426.0 (MK^+, 17), 433.3 (17), 451.2 (48); HRMS FAB (+ve) found m/z 388.21214 (MH^+), $C_{22}H_{30}NO_5$ requires 388.21240.

The by-product ***carbonic acid 5,5-dimethyl-3-oxo-cyclohex-1-enyl ester ethyl ester (51)*** was also isolated.

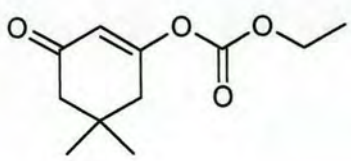

Colourless oil: R_f=0.47 Hexane/EtOAc (2:1); δ_H (200 MHz, $CDCl_3$) 1.11 (6H, s, $C(CH_3)_2$), 1.37 (3H, t, *J* 7.0, CH_2CH_3), 2.28 (2H, s, $CH_2C(CH_3)_2$), 2.45 (2H, s, $CH_2C(CH_3)_2$), 4.29 (2H, q, *J* 7.0, CH_2CH_3), 6.04 (1H, s, COCH=CO).

6.2.1.4.2 Method B

N-benzyloxycarbonyl-L-leucinylfluoride (54)

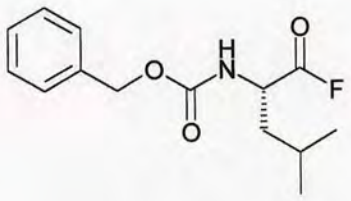

To a stirred solution of *N*-benzyloxycarbonyl-L-leucine (0.50 g, 1.87 mmol) and pyridine (0.15 ml, 1.88 mmol) in anhydrous DCM (5 ml) kept under a N_2 atmosphere was added cyanuric fluoride (0.51 ml, 5.64 mmol) at -15 to -10 °C. A white precipitate formed. After stirring for 1 h at -5 °C, IR of the crude reaction mixture indicated formation of the acyl fluoride. After 2 h crushed ice was added along with DCM (10 ml). The organic layer was separated and the aqueous layer extracted with DCM (5 ml). The combined DCM layers were washed with ice-cold water (10 ml), dried ($MgSO_4$) and concentrated under reduced pressure to afford a colourless oil (0.36 g, 73 %) which was used in subsequent reactions without further purification: ν_{max}(polyethylene card) 3317 (N-H), 1843 (acid fluoride); δ_H (200 MHz, $CDCl_3$) 0.97 (6H, d, *J* 6.0, $CH(CH_3)_2$), 1.62-1.78 (3H, m, $CH(CH_3)_2$ & $CH_2CH(CH_3)_2$), 4.54-4.61 (1H, m, NHC*H*), 5.02 (1H, m, N*H*), 5.14 (2H, s, CH_2Ph), 7.36 (5H, s, Ar-*H*).

N-Benzyloxycarbonyl-L-leucinylfluoride **54** (0.36 g, 1.36 mmol) in DCM (15 ml) was stirred at room temperature with dimedone (0.19 g, 1.36 mmol) and DIPEA (0.47 ml, 2.72 mmol). The solution changed colour from pale yellow to blue/purple. After 20 min IR (crude mixture; polyethylene disc) indicated disappearance of the acyl fluoride. The solution was washed with 2N HCl (2 x 5 ml), saturated $NaHCO_3$ solution (2 x 5 ml), water (2 x 5 ml), dried ($MgSO_4$) and concentrated under reduced

pressure to yield a blue/purple oil (0.42 g). Flash column chromatography on silica gel using cyclohexane/diethyl ether (1:1) as eluent afforded a colourless oil (0.16 g, 29 %). Analysis identical to **50** obtained by 6.2.1.4.1 Method A.

6.2.1.5 3-(N-benzyloxycarbonyl-L-phenylalaninyloxy)-5,5-dimethyl-2-cyclohexen-1-one (52)

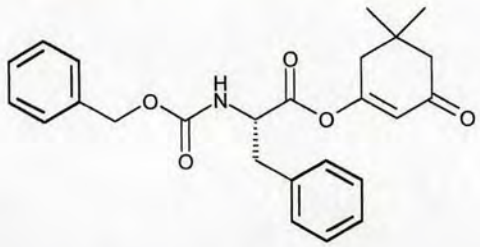

The general procedure outlined above (6.2.1.4, Method A) was followed using Cbz-L-phenylalanine (0.10 g, 0.37 mmol) and methyl chloroformate (45 µl, 0.37 mmol). Flash column chromatography on silica gel using Pet.Ether/EtOAc (4:3) as eluent gave a colourless oil (0.12 g, 77 %): $[\alpha]_D$ –10.3 (c 1.2, $CHCl_3$); R_f=0.66 hexane/EtOAc (1:1); ν_{max}(crude oil) 3319br (N-H), 1761 (vinyl ester), 1720 (urethane C=O), 1669 (α,β-unsaturated ketone), 1528 (amide II); δ_H (250 MHz, $CDCl_3$) 1.04 (3H, d, *J* 7.0, C(C^A*H*$_3C^B$H$_3$)), 1.12 (3H, d, *J* 7.0, C(C^AH$_3C^B$*H*$_3$)), 2.19-2.25 (1H, m, C*H*$(CH_3)_2$), 2.24 (2H, s, CH_2C$(CH_3)_2$), 2.29 (2H, s, CH_2C$(CH_3)_2$), 3.08-3.19 (2H, m, CHCH_2Ph), 4.60-4.82 (1H, m, NHC*H*), 5.10 (2H, s, OCH_2Ph), 5.45 (1H, d, *J* 8.0, N*H*), 5.81 (1H, s, COC*H*=CO), 7.12-7.38 (10H, m, Ar-*H*); δ_C (63 MHz, DEPT, $CDCl_3$) 27.9 (C(C^AH$_3C^B$H$_3$)), 28.0 (C(C^AH$_3C^B$H$_3$)), 33.0 (*C*$(CH_3)_2$), 37.9 (CH*C*H_2Ph), 41.6 (*C*H_2C$(CH_3)_2$), 50.6 (*C*H_2C$(CH_3)_2$), 54.9 (NH*C*H), 67.2 (O*C*H_2Ph), 116.6 (CO*C*H=CO), [128.0 (CH), 128.5 (CH), 128.8 (CH), 129.1 (CH), 10C, *Ar*-H], 134.8 (OCH$_2$*Ph*), 135.6 (CHCH$_2$*Ph*), 155.5 (*C*ONH), 167.6 (COO*C*=CH), 168.6 (NHCH*C*O), 199.2 (*C*OCH=COCO); MS ESI (+ve) found m/z 444.3 (MNa^+, 100 %); HRMS FAB (+ve) found m/z 422.19795 (MH^+), $C_{25}H_{28}NO_5$ requires 422.19675.

The by-product ***carbonic acid 5,5-dimethyl-3-oxo-cyclohex-1-enyl ester methyl ester (53)*** was also isolated.

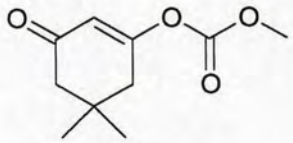

Colourless oil: R_f=0.42 Hexane/EtOAc (3:2); δ_H (200 MHz, $CDCl_3$) 1.10 (6H, s, $C(CH_3)_2$), 2.27 (2H, s, $CH_2C(CH_3)_2$), 2.44 (2H, s, $CH_2C(CH_3)_2$), 3.83 (3H, s, OCH_3), 6.03 (1H, s, COC*H*=CO).

6.2.1.6 carbonic acid 5,5-dimethyl-3-oxo-cyclohex-1-enyl ester isobutyl ester (128)

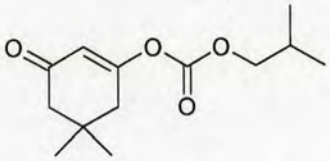

128 was formed as a by-product in the general procedure outlined above (6.2.1.4, Method A) as a colourless oil: R_f=0.39 Pet.Ether/EtOAc (4:1); ν_{max}(crude oil) 1769, 1705 (anhydride), 1673 (α,β-unsaturated ketone); δ_H (250 MHz, $CDCl_3$) 0.97 (6H, d, *J* 7.0, $CH(CH_3)_2$), 1.10 (6H, s, $C(CH_3)_2$), 1.43-2.08 (1H, m, $CH(CH_3)_2$), 2.26 (2H, s, $CH_2C(CH_3)_2$), 2.44 (2H, s, $CH_2C(CH_3)_2$), 3.99 (2H, d, *J* 7.0, $CH_2CH(CH_3)_2$), 6.02 (1H, s, COC*H*=CO); δ_C (63 MHz, DEPT, $CDCl_3$) 19.2 ($CH(CH_3)_2$), 28.1 ($CH(CH_3)_2$), 28.5 ($C(CH_3)_2$), 33.5 ($C(CH_3)_2$), 42.1 ($CH_2C(CH_3)_2$), 51.0 ($CH_2C(CH_3)_2$), 75.6 ($OCH_2CH(CH_3)_2$), 115.7 (COCH=CO), 151.6 (OCOO), 168.3 (COOC=CH), 200.3 (COCH=COCO); HRMS FAB (+ve) found m/z 241.14392 (MH^+), $C_{13}H_{21}O_4$ requires 241.14398.

6.2.1.7 N-benzyloxycarbonyl-L-valinylfluoride (57)

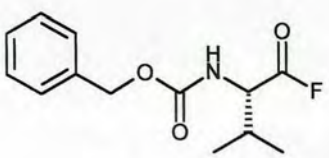

To a stirred solution of *N*-benzyloxycarbonyl-L-valine (0.50 g, 2.00 mmol) and pyridine (0.16 ml, 2.00 mmol) in anhydrous DCM (5 ml) kept under a N_2 atmosphere was added cyanuric fluoride (0.90 ml, 10.00 mmol) at -15 to -10 °C. A white precipitate formed. The reaction was followed by TLC $CHCl_3$/MeOH/AcOH (9:1:0.1) on a small amount of reaction mixture quenched in MeOH. After 1h 40 min, crushed ice was added along with DCM (10 ml). The organic layer was separated and the aqueous layer extracted with DCM (5 ml). The combined DCM layers were washed with ice-cold water (10 ml), dried ($MgSO_4$) and concentrated under reduced pressure to afford a colourless oil (0.60 g, 119 %) which was used in subsequent reactions without further purification: R_f=0.78 $CHCl_3$/MeOH/AcOH (9:1:0.1); ν_{max}(polyethylene card) 3320 (N-H), 1843 (acid fluoride), 1738 (urethane C=O), 1538 (amide II); δ_H (200 MHz, $CDCl_3$) 1.01 (3H, d, *J* 7.0, CH($C^AH_3C^BH_3$)), 1.05 (3H, d, *J* 7.0, CH($C^AH_3C^BH_3$)), 2.26 (1H, m, C*H*(CH_3)$_2$), 4.49 (1H, m, NHC*H*), 5.14 (3H, m, OCH_2Ph & N*H* (masked)), 7.37 (5H, s, Ar-*H*); MS ESI (+ve) found m/z 233.8 ($C_6H_5CH_2CONHCH(CH(CH_3)_2)CO$-, 41 %), 251.8 (*N*-Cbz-Val, 58), 268.9 (*N*-Cbz-ValNH_4^+, 64), 273.8 (*N*-Cbz-ValNa^+, 33), 289.9 (*N*-Cbz-ValK^+, 22), 341.9 (100), 502.1 (*N*-Cbz-Val dimer, 53), 507.1 (M^+ dimer, 55).

6.2.1.8 3-(N-benzyloxycarbonyl-L-valinyloxy)-5,5-dimethyl-2-cyclohexen-1-one (42)

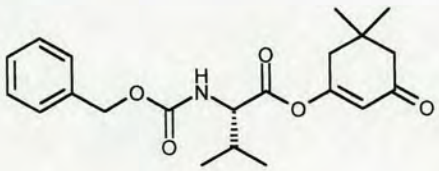

To a stirred room temperature solution of *N*-benzyloxycarbonyl-L-valinylfluoride **57** (0.48 g, 1.89 mmol) in DCM (20 ml) was added dimedone (0.27 g, 1.89 mmol) and DIPEA (0.66 ml, 3.78 mmol). On addition of DIPEA there was an immediate colour change from colourless to green/brown then blue/purple. IR (crude solution; polyethylene disc) indicated disappearance of the acyl fluoride peak @ 1842 cm^{-1}. After stirring for 1/2 h the solution was washed with 1N HCl (2 x 5 ml), saturated

$NaHCO_3$ solution (2 x 5 ml), water (2 x 5 ml), dried ($MgSO_4$) and concentrated under reduced pressure to a blue/purple oil (0.62 g). Flash column chromatography on silica gel using $CHCl_3$/MeOH (9:1) as eluent afforded a pale yellow oil (0.58 g, 82 %); $[\alpha]_D$ -15.6 (c 1.4, $CHCl_3$); R_f=0.75 $CHCl_3$/MeOH (9:1); ν_{max}(NaCl) 3326br (N-H), 1769 (vinyl ester), 1715 (urethane C=O), 1668 (α,β-unsaturated ketone), 1532 (amide II); δ_H (250 MHz, $CDCl_3$) 0.95 (3H, d, *J* 7.0, CH($C^AH_3C^BH_3$)), 1.02 (3H, d, *J* 7.0, CH($C^AH_3C^BH_3$)), 1.10 (6H, s, $C(CH_3)_2$), 2.20-2.27 (1H, m, $CH(CH_3)_2$), 2.27 (2H, s, $CH_2C(CH_3)_2$), 2.39 (2H, s, $CH_2C(CH_3)_2$), 4.39 (1H, dd, *J* 9.0, 5.0, NHC*H*), 5.12 (2H, s, OCH_2Ph), 5.19 (1H, d, *J* 9.0, N*H*), 5.89 (1H, s, COC*H*=CO), 7.35 (5H, s, Ar-*H*); δ_C (63 MHz, DEPT, $CDCl_3$) 17.5 (CH($C^AH_3C^BH_3$)), 18.9 (CH($C^AH_3C^BH_3$)), 27.9 (C($C^AH_3C^BH_3$)), 28.0 (C($C^AH_3C^BH_3$)), 30.9 ($CH(CH_3)_2$), 33.1 ($C(CH_3)_2$), 41.8 ($CH_2C(CH_3)_2$), 50.7 ($CH_2C(CH_3)_2$), 59.1 (NHCH), 67.2 (OCH_2Ph), 116.8 (COCH=CO), [128.0 (CH), 128.2 (CH), 128.5 (CH), 5C, *Ar*-H], 135.9 (OCH_2Ph), 156.1 (CONH), 167.7 (COOC=CH), 169.1 (NHCHCO), 199.0 (COCH=COCO); MS ESI (+ve) found m/z 396.0 (MNa^+, 100 %), 437.1 (22); HRMS FAB (+ve) found m/z 374.19741 (MH^+), $C_{21}H_{28}NO_5$ requires 374.19675.

6.2.1.9 Attempted rearrangement of 3-(N-benzyloxycarbonyl-L-valinyloxy)-5,5-dimethyl-2-cyclohexen-1-one (42)

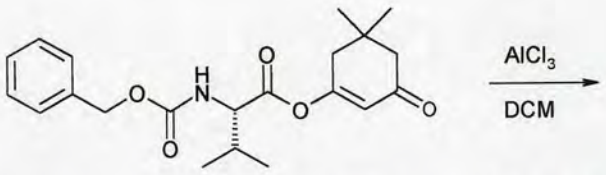

42 (0.23 g, 0.62 mmol) was stirred in anhydrous DCM (2 ml). Anhydrous aluminium chloride (0.17 g, 1.26 mmol) was added and the reaction stirred at –5 °C for 2 h, before pouring into a mixture of ice water (1 ml) and 2 M HCl (1 ml). The organic phase was separated and the aqueous phase extracted with $CHCl_3$ (2 x 2 ml). The combined organic extracts were washed with H_2O (2 ml), dried ($MgSO_4$) and concentrated under reduced pressure. The resulting residue was dissolved in the minimum quantity of ether and treated with 2 M NaOH (3 ml). The solution was acidified with 2M HCl to pH1 and extracted with ether (3 x 2 ml). The combined

ether extracts were dried ($MgSO_4$) and concentrated under reduced pressure to give a colourless oil (0.13 g, 58 %): δ_H (250 MHz, $CDCl_3$) as **42**. Heating the reaction to 45 °C for 2.5 h after addition of the aluminium chloride, with identical work-up again resulted in recovery of starting material **42**.

6.2.1.10 1-(4,4-dimethyl-2,6-dioxocyclohexylidene)-2-benzyloxycarbonyl-amino-3-methylbutanol (58)

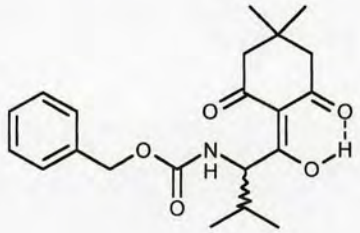

The enol ester **42** (0.56 g, 1.50 mmol) was dissolved in MeCN (8 ml) containing triethylamine (0.84 ml, 6.00 ml) and acetone cyanohydrin (14 µl, 0.15 mmol). After 2.5 h, TLC hexane/EtOAc (1:1) indicated remaining enol ester **42**. The solution was stirred at room temperature overnight then partitioned between hexane (8 ml) and cold 1N HCl (8 ml). The hexane phase was washed with water (2 ml), dried ($MgSO_4$) and concentrated under reduced pressure to yield an off-white solid (0.26 g, 66 %): mp 72 °C; $[\alpha]_D$ +12.4 (c 2.1, $CHCl_3$); R_f=0.41 hexane/EtOAc (1:1); ν_{max} (KBr) 3424 (O-H & N-H), 1722 (urethane C=O), 1667 (α,β-unsaturated ketone), 1513 (amide II); δ_H (200 MHz, $CDCl_3$) 0.75 (3H, d, *J* 7.0, CH($C^AH_3C^BH_3$)), 0.86-1.27 (9H, m, CH($C^AH_3C^BH_3$) & $C(CH_3)_2$), 2.07-2.13 (1H, m, $CH(CH_3)_2$), 2.28-2.35 (2H, m, $CH_2C(CH_3)_2$), 2.54 (2H, s, $CH_2C(CH_3)_2$), 5.08 (2H, s, CH_2Ph), 5.49 (1H, d, *J* 9.5, NH), 5.60 (1H, dd, *J* 9.5, 3.0, $CHCH(CH_3)_2$), 7.34 (5H, s, Ar-H), 17.54 (1H, s, OH); δ_C (63 MHz, DEPT, $CDCl_3$) 15.6 (CH($C^AH_3C^BH_3$)), 20.3 (CH($C^AH_3C^BH_3$)), 27.7 ($C(C^AH_3C^BH_3)$), 28.3 ($C(C^AH_3C^BH_3)$), 30.6 ($CH(CH_3)_2$), 45.9 ($CH_2C(CH_3)_2$), 52.2 ($CH_2C(CH_3)_2$), 60.9 ($CHCH(CH_3)_2$), 66.8 (CH_2Ph), 110.8 (C=COH), [128.0 (CH), 128.4 (CH), 5C, *Ar*-H], 136.3 (OCH_2Ph), 156.2 (OCONH), [194.4 (C), 196.7 (C), 203.5 (C), COC=C(OH)CO]; MS ESI (+ve) found m/z 373.9 (MH^+, 90 %),

396.0 (MNa^+, 100); HRMS FAB (+ve) found m/z 374.19769 (MH^+), $C_{21}H_{28}NO_5$ requires 374.19675.

6.2.1.11 N-[1-(4,4-dimethyl-2,6-dioxocyclohexylidene)-2-benzyloxy-carbonylamino-3-methylbutyl]phenylalanine methyl ester (59)

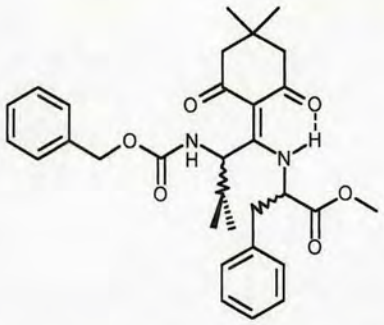

(diastereomers in ratio 60:40, **X**:**Y**)

1-(4,4-dimethyl-2,6-dioxocyclohexylidene)-2-benzyloxycarbonylamino-3-methyl butanol **58** (0.11 g, 0.29 mmol) was dissolved in DMF (1 ml). L-phenylalanine methyl ester HCl salt (0.06 g, 0.29 mmol) was added followed by DIPEA (0.05 ml, 0.29 mmol) and the mixture stirred at room temperature overnight after which time TLC hexane/EtOAc (1:1) indicated remaining **58**. The reaction was heated at 50 °C for 7 h before removal of the solvent under reduced pressure to yield a yellow oil (0.19 g). Flash column chromatography using hexane/EtOAc (1:1) as eluent afforded a colourless oil (0.05 g, 34 %); $[\alpha]_D$ -30.5 (c 2.5, $CHCl_3$); R_f=0.64 hexane/EtOAc (1:1); ν_{max}(polyethylene card) 3352 (N-H), 1748 (ester), 1713 (urethane C=O), 1634 (α,β-unsaturated ketone), 1565 (amide II); δ_H (360 MHz, COSY, $CDCl_3$) 0.33 (3H, d, *J* 7.0, $CH(C^AH_3C^BH_3)$, **Y**), 0.76 (3H, d, *J* 7.0, $CH(C^AH_3C^BH_3)$, **X**), 0.92 (3H, d, *J* 6.5, $CH(C^AH_3C^BH_3)$, **Y**), 1.01 (3H, d, *J* 6.5, $CH(C^AH_3C^BH_3)$, **X**), 1.04-1.07 (12H, m, $C(CH_3)_2$, **X** & **Y**), 2.02-2.11 (1H, m, $CH(CH_3)_2$, **Y**), 2.19-2.26 (1H, m, $CH(CH_3)_2$, **X**), 2.30-2.52 (8H, m, $CH_2C(CH_3)_2CH_2$, **X** & **Y**), 3.17 (1H, dd, *J* 14.0, 9.0, $CHCH_AH_BPh$, **Y**), 3.29 (2H, d, *J* 7.0, $CHCH_2Ph$, **X**), 3.40 (1H, dd, *J* 14.0, 4.5, $CHCH_AH_BPh$, **Y**), 3.69 (3H, s, OCH_3, **Y**), 3.72 (3H, s, OCH_3, **X**), 4.30 (1H, dd, *J* 10.5, 10.5, $CHCH(CH_3)_2$, **Y**), 4.48 (1H, dd, *J* 10.5, 10.5,

C*H*CH(CH$_3$)$_2$, **X**), 5.05-5.19 (5H, m, OC*H*$_2$Ph, **X** & **Y**, C*H*CH$_2$Ph, **Y**), 5.37 (1H, dt, *J* 8.0, 7.0, C*H*CH$_2$Ph, **X**), 7.22-7.39 (20H, m, Ar-*H*, **X** & **Y**), 7.69 (1H, d, *J* 12.5, CON*H*, **Y**), 7.72 (1H, d, *J* 10.5, CON*H*, **X**), 14.61 (1H, d, *J* 8.0, COCHN*H*, **Y**), 14.71 (1H, d, *J* 8.0, COCHN*H*, **X**); δ_C (63 MHz, DEPT, $CDCl_3$) 19.2 (CH(*C*^{A}H$_3$C^{B}H$_3$), **Y**), 19.3 (2C, CH(C^{A}H$_3$*C*^{B}H$_3$), **X** & **Y**), 19.9 (CH(*C*^{A}H$_3$C^{B}H$_3$), **X**), 27.4 (C(*C*^{A}H$_3$C^{B}H$_3$), **Y**), 27.5 (C(*C*^{A}H$_3$C^{B}H$_3$), **X**), 28.5 (C(C^{A}H$_3$*C*^{B}H$_3$), **X**), 28.6 (C(C^{A}H$_3$*C*^{B}H$_3$), **Y**), 29.1 (*C*H(CH$_3$)$_2$, **Y**), 29.4 (*C*H(CH$_3$)$_2$, **X**), 29.8 (2C, *C*(CH$_3$)$_2$, **X** & **Y**), 39.3 (CH*C*H$_2$Ph, **Y**), 39.8 (CH*C*H$_2$Ph, **X**), 52.0 (*C*H$_2$C(CH$_3$)$_2$, **X**), 52.1 (*C*H$_2$C(CH$_3$)$_2$, **Y**), 52.4 (O*C*H$_3$, **X**), 52.7 (O*C*H$_3$, **Y**), 53.4 (2C, *C*H$_2$C(CH$_3$)$_2$, **X** & **Y**), 55.8 (*C*HCH(CH$_3$)$_2$, **Y**), 56.1 (*C*HCH(CH$_3$)$_2$, **X**), 59.1 (*C*HCH$_2$Ph, **X**), 59.7 (*C*HCH$_2$Ph, **Y**), 66.5 (O*C*H$_2$Ph, **Y**), 66.6 (O*C*H$_2$Ph, **X**), 107.0 (CO*C*=CNH, **X**), 107.2 (CO*C*=CNH, **Y**), [127.2 (CH), 127.3 (CH), 127.6 (CH), 127.7 (CH), 127.9 (CH), 128.0 (CH), 128.2 (CH), 128.3 (CH), 128.4 (CH), 128.6 (CH), 129.2 (CH), 129.3 (CH), 20C, *Ar*-H, **X** & **Y**), 134.5 (CHCH$_2$*Ph*, **X**), 135.2 (CHCH$_2$*Ph*, **Y**), 136.4 (OCH$_2$*Ph*, **X**), 136.5 (OCH$_2$*Ph*, **Y**), 156.4 (2C, O*C*ONH, **X** & **Y**), 169.8 (COC=*C*NH, **Y**), 169.9 (COC=*C*NH, **X**), 173.0 (*C*OOCH$_3$, **X**), 173.6 (*C*OOCH$_3$, **Y**), 197.2 (2C, *C*OC=CNH, **X** & **Y**), 200.3 (2C, *C*OC=CNH, **X** & **Y**); MS ESI (+ve) found m/z 535.2 (MH$^+$, 29 %), 557.1 (MNa$^+$, 100); HRMS FAB (+ve) found m/z 535.28083 (MH$^+$), $C_{31}H_{39}N_2O_6$ requires 535.28081.

6.2.1.12 (N-benzyloxycarbonyl-L-valinyl)-L-phenylalanine methyl ester (60)

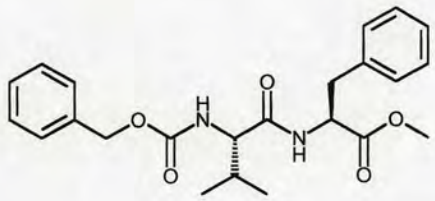

3-(*N*-benzyloxycarbonyl-L-valinyloxy)-5,5-dimethyl-2-cyclohexen-1-one **42** (0.12 g, 0.33 mmol) was dissolved in DMF (2 ml). L-phenylalanine methyl ester. HCl salt (0.07 g, 0.33 mmol) was added along with DIPEA (0.12 ml, 0.66 mmol) and the reaction stirred at room temperature overnight. TLC DCM/MeOH (9:1) indicated **42** remaining so the reaction was heated at 60 °C for 6 h. The solution was then

concentrated under reduced pressure to yield a pale yellow oil (0.25 g). Flash column chromatography on silica gel using $CHCl_3$/diethyl ether (1:2) as eluent afforded a white solid (0.10 g, 70 %): mp 131 °C; $[\alpha]_D$ +40.2 (c 1.8, $CHCl_3$); R_f=0.50 $CHCl_3$/diethyl ether (1:2); ν_{max}(polyethylene card) 3301br (N-H), 1738 (ester) 1693 (urethane C=O), 1651 (amide I) 1538 (amide II); δ_H (250 MHz, $CDCl_3$) 0.86 (3H, d, *J* 7.0, CH($C^AH_3C^BH_3$)), 0.92 (3H, d, *J* 7.0, CH($C^AH_3C^BH_3$)), 1.98-2.11 (1H, m, $CH(CH_3)_2$), 3.07-3.10 (2H, m, $CHCH_2Ph$), 3.69 (3H, s, OCH_3), 4.03 (1H, dd, *J* 9.0, 6.0, $CHCH(CH_3)_2$), 4.87 (1H, dt, *J* 8.0, 6.0, $CHCH_2Ph$), 5.04 (1H, d, *J* 12.0, OCH_AH_BPh), 5.12 (1H, d, *J* 12.0, OCH_AH_BPh), 5.40 (1H, d, *J* 9.0, OCONH), 6.45 (1H, d, *J* 8.0, CONH), 7.05-7.33 (10H, m, Ar-H); δ_C (63 MHz, DEPT, $CDCl_3$) 17.5 ($CH(C^AH_3C^BH_3)$), 19.0 ($CH(C^AH_3C^BH_3)$), 31.0 ($CH(C^AH_3C^BH_3)$), 37.8 ($CHCH_2Ph$), 52.2 (OCH_3), 52.9 ($CHCH_2Ph$), 60.0 ($CHCH(CH_3)_2$), 66.9 (OCH_2Ph), [127.0 (CH), 127.9 (CH), 128.0 (CH), 128.4 (CH), 128.5 (CH), 129.1 (CH), 10C, *Ar*-H], 135.4 ($CHCH_2Ph$), 136.1 (OCH_2Ph), 156.1 (OCONH), [170.7 (C), 171.5 (C), CHCONH & COO]; MS ESI (+ve) found m/z 435.1 (MNa^+, 100 %), 458.2 (16); HRMS FAB (+ve) found m/z 413.20883 (MH^+), $C_{23}H_{29}N_2O_5$ requires 413.20765.

6.2.2 Results and Discussion I - Solid Phase Synthesis

6.2.2.1 p-nitrophenol carbonate Wang resin (65)

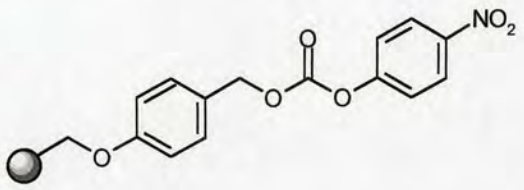

Novabiochem Wang resin (100-200 mesh, loading 0.76 mmol/g) was washed according to protocol and dried under vacuum overnight.

Dry resin (1.00 g, 0.76 mmol) was swollen in anhydrous DCM (5 ml) under argon. An anhydrous solution of *p*-nitrophenol chloroformate (0.46 g, 2.28 mmol) in DCM (10 ml) was added followed by pyridine (0.18 ml, 2.28 mmol). The reaction was shaken overnight at room temperature. The resin was then filtered, washed

according to protocol and dried under vacuum overnight to yield yellow resin (*p*-nitrophenol loading 0.68 mmol/g, 100 %); $\nu_{max}(CH_2Cl_2)$ 1765 (carbonate), 1526,1348 (NO_2); δ_C (63 MHz, Gel, CD_2Cl_2) 70.1 (*C*H_2OAr), 71.0 (O*C*H_2Ar), 115.0 (2C, *o*-OCH_2*Ar*-H), 122.0 (2C, *o*-OCO*Ar*-H), 125.4 (2C, *o*-NO_2*Ar*-H).

6.2.2.2 L-valine fluorenyl methyl ester. p-toluene sulfonic acid salt (66)

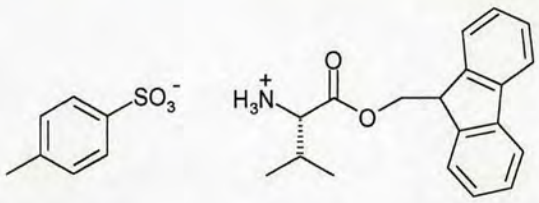

Boc-L-Val (2.50 g, 11.5 mmol), 9-fluorenemethanol (4.52 g, 23.0 mmol) and DMAP (12.0 mg, cat.) in distilled DCM (40 ml) were cooled in an ice bath under argon for 10 min. DIC (2.90 g, 23.0 mmol) was added dropwise and the reaction stirred overnight. A white precipitate formed. The precipitate was filtered off and washed with DCM. The combined DCM layers were washed with water (2 x 50 ml), saturated $NaHCO_3$ (2 x 50 ml) then citric acid (10 %, 2 x 50 ml) alternately, followed by water (2 x 50 ml) then saturated brine (2 x 50 ml) alternately. The organic layers were dried (Na_2SO_4) and concentrated under reduced pressure to a colourless oil which later solidified to an off-white solid (5.60 g). The residue was dissolved in TFA (25 ml) causing effervescence and a green solution resulted. After 15 min *p*-toluene sulfonic acid (3.07 g, 16.15 mmol) was added and a pink colour observed. The TFA was removed under reduced pressure and the resultant yellow oil triturated with diethyl ether to afford a white substance which, after drying in a desiccator over P_2O_5, yielded a white powder (3.23 g, 60 %): mp 157 °C; R_f=0.57 DCM/MeOH (9:1); ν_{max}(KBr) 2965br (-NH_3, & Ar-H & -CH_2, -CH_3), 1751 (ester), 1618, 1534, 1498 (Ar-H); δ_H (200 MHz, CD_3OD) 0.71 (3H, d, *J* 7.0, CH($C^AH_3C^BH_3$)), 0.81 (3H, d, *J* 7.0, CH($C^AH_3C^BH_3$)), 1.94-2.03 (1H, m, C*H*(CH_3)$_2$), 2.42 (3H, s, ArCH_3), 3.79 (1H, d, *J* 4.0, C*H*CH(CH_3)$_2$), 4.32 (1H, dd, *J* 4.5, 4.5, OCH_2CH), 4.75 (1H, dd, *J* 11.0, 4.5, OCH_AH_BCH), 4.99 (1H, OCH_AH_BCH (masked by HDO)), 7.26-7.90 (12H,

m, Ar-*H*); δ_C (63 MHz, DEPT, CD_3OD) 15.8 (CH($C^AH_3C^BH_3$)), 16.1 (CH($C^AH_3C^BH_3$), 19.4 (Ar-CH_3), 28.8 ($CH(CH_3)_2$), 46.1 (OCH_2CHAr), 57.2 (NH*C*H), 66.0 (OCH_2CHAr), 119.1 (2C, (CH), *Ar*-H), 123.8 ((CH), *Ar*-H), 123.9 ((CH), *Ar*-H), 125.0 (2C, (CH), *o*-CH_3*Ar*-H), 126.4 (2C, (CH), *Ar*-H), 127.0 ((CH), *Ar*-H), 127.1 ((CH), *Ar*-H), 127.9 (2C, (CH), *o*-SO_3^-*Ar*-H), 139.8 ((C), *Ar*-CH_3), 140.8 ((C), *Ar*-Ar), 141.0 ((C), Ar-*Ar*), 141.5 ((C), *Ar*SO_3^-), 142.7 ((C), *Ar*-$CHCH_2$), 142.9 ((C), *Ar*-$CHCH_2$), 168.2 ((C), *C*OO); HRMS FAB (+ve) found m/z 468.18403 (MH^+), $C_{26}H_{30}NO_5S$ requires 468.18447.

6.2.2.3 fluorenyl methyl ester-protected L-valine-N-carboxy Wang resin (67)

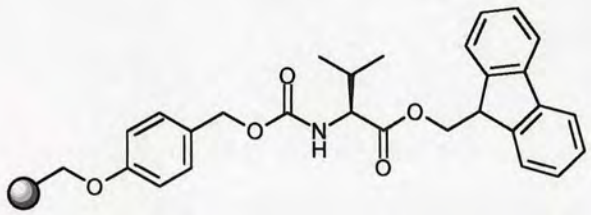

p-Nitrophenol carbonate Wang resin **65** (0.60 g, loading 0.68 mmol/g, 0.41 mmol) was swollen in DMF (10 ml) containing DMAP (0.18 g, 1.43 mmol) and L-valine fluorenyl methyl ester. *p*-toluene sulfonic acid salt **66** (0.57 g, 1.23 mmol). The reaction was spun at room temperature overnight. The resin was then filtered, washed according to protocol and dried under vacuum overnight. The resin changed colour from yellow to white (Fm loading 0.27 mmol/g, 44 %); $\nu_{max}(CH_2Cl_2)$ 1713br (ester & urethane C=O); δ_C (63 MHz, Gel, CD_2Cl_2) 17.4 (CH($C^AH_3C^BH_3$)), 19.1 (CH($C^AH_3C^BH_3$)), 31.2 ($CH(CH_3)_2$), 47.0 (OCH_2CH), 59.3 (NH*C*H), 66.9 (2C, OCH_2Ar & OCH_2CH), 70.1 (CH_2OAr), 114.8 (2C, *o*-OCH_2*Ar*-H), 120.2 (2C, OFm*Ar*-H); Cleavage MS ESI (+ve) found m/z 117.4 (Val, 18 %), 295.8 (MH^+, 100), 336.9 (14); $C_{19}H_{21}NO_2$ requires 295.4; Cleavage LCMS R_t=19.4 min, 118.4 ($ValH^+$, 20 %), 296.5 (MH^+, 100).

6.2.2.4 L-valine N-carboxy Wang resin (68)

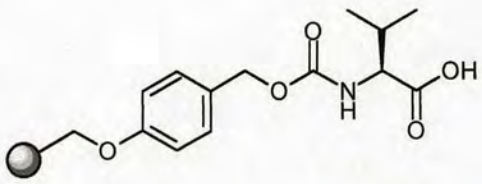

Fluorenyl methyl ester-protected L-valine-*N*-carboxy Wang resin **67** (loading 0.27 mmol/g) was swollen in 20 % piperidine/DMF (10 ml) and the reaction spun at room temperature for 2 h. The resin was then filtered, washed according to protocol and dried under vacuum overnight: $\nu_{max}(CH_2Cl_2)$ 1713 (urethane C=O & carboxylic acid C=O); δ_C (63 MHz, Gel, CD_2Cl_2) 17.7 ($CH(C^AH_3C^BH_3)$), 19.5 ($CH(C^AH_3C^BH_3)$), 31.4 ($CH(CH_3)_2$), 60.8 (NHCH), 66.4 (OCH_2Ar), 70.0 (CH_2OAr), 114.7 (2C, *o*-OCH_2Ar-H), 156.8 (CONH), 158.9 (CH_2OAr), 177.0 (COOH); Cleavage MS ESI (+ve) found m/z 71.4 (18 %), 85.4 (100), 117.4 (M^+, 45), 158.6 (20), $C_5H_{10}NO_2$ requires 117.2.

δ_C (63 MHz, Gel, CD_2Cl_2); 3 unassigned peaks δ_C 22.8, 34.2, 44.4

6.2.2.5 L-valinylfluoride-N-carboxy Wang resin (69)

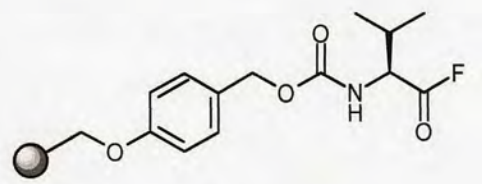

L-valine-*N*-carboxy Wang resin **68** (0.34 g, loading 0.27 mmol/g, 0.09 mmol) was swollen in DCM (3 ml) containing pyridine (7.5 µl, 0.09 mmol). Cyanuric fluoride (8.3 µl, 0.09 mmol) in DCM (2 ml) was added dropwise and the reaction mixture shaken at room temperature for 1 h 40 min. A white precipitate formed. The resin was filtered and washed with 3 x DMF/water (1:1) to remove the cyanuric acid precipitate. The resin was then washed according to protocol and dried under

vacuum overnight: $\nu_{max}(CH_2Cl_2)$ 1844 (acid fluoride), 1723 (urethane C=O); δ_C (63 MHz, Gel, CD_2Cl_2) 17.6 ($CH(C^AH_3C^BH_3)$), 18.8 ($CH(C^AH_3C^BH_3)$), 30.3 ($CH(CH_3)_2$), 59.0 (NHCH), 67.4 (OCH_2Ar), 70.1 (CH_2OAr), 114.9 (2C, *o*-OCH_2Ar-H); δ_F (250 MHz, Gel, CD_2Cl_2) 28.1; Cleavage MS ESI (+ve) found m/z 72.2 (18 %), 91.1 (13), 118.1 ($ValH^+$, 13), 120.1 (MH^+, 62), 130.2 ($(C(OH)N)_3$, 22), 180.1 (100), $C_5H_{10}FNO$ requires 119.1.

6.2.2.6 L-valine-(5,5-dimethyL-3-oxo)cyclohex-1-enylester-N-carboxy Wang resin (70)

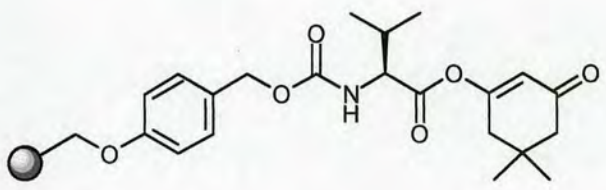

L-valinylfluoride-*N*-carboxy Wang resin **69** (0.14 g, assume max. loading 0.27 mmol/g, 0.04 mmol) was swollen in DCM (2 ml) containing dimedone (0.02 g, 0. 12 mmol) and DIPEA (0.02 g, 0.12 mmol) and the reaction mixture spun at room temperature. A blue/purple colour was observed after 30 min. After 7 h the resin was filtered and washed according to protocol, then dried under vacuum overnight: $\nu_{max}(CH_2Cl_2)$ 1763 (vinyl ester), 1718 (urethane C=O), 1671 (α,β-unsaturated ketone); δ_C (63 MHz, Gel, CD_2Cl_2) 17.6 ($CH(C^AH_3C^BH_3)$), 19.0 ($CH(C^AH_3C^BH_3)$), 28.0 ($C(CH_3)_2$), 31.0 ($CH(CH_3)_2$), 33.1 ($C(CH_3)_2$), 42.0 ($CH_2C(CH_3)_2$), 50.8 ($CH_2C(CH_3)_2$), 59.5 (NHCH), 67.0 (OCH_2Ar), 70.1 (CH_2OAr), 114.8 (2C, *o*-OCH_2Ar-H), 116.9 (COCH=CO), 156.4 (CONH), 159.1 (CH_2OAr), 168.0 (COOC=CH), 169.4 (NHCHCO), 198.9 (COCH=COCO); Cleavage MS ESI (+ve) found m/z 181.6 (16 %), 239.8 (MH^+, 100), $C_{13}H_{21}NO_3$ requires 239.3; Cleavage LCMS R_t=2.39 min, 240.6 (MH^+).

6.2.2.7 (5,5-dimethyl-3-hydroxy)cyclohex-2-ene-1-one:tert-butylammonium fluoride salt (72)

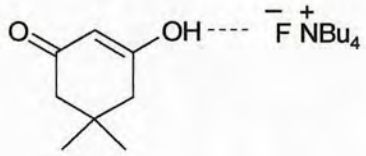

Dimedone (0.25 g, 1.78 mmol) was dissolved in DMF and *tert*-butyl ammonium fluoride (0.56 g, 1.78 mmol) added. Molecular sieves (3 Å) were added and the solution decanted and concentrated under reduced pressure to yield an orange solid (0.71 g, 99 %): δ_H (200 MHz, $CDCl_3$) 0.99 (12H, t, *J* 7.0, 4xCH_2CH_3), 1.03 (6H, s, $C(CH_3)_2$), 1.41 (8H, tq, *J* 7.0, 4xCH_2CH_3), 1.63 (8H, tt, *J* 7.0, 4x$CH_2CH_2CH_3$), 2.16 (4H, s, $CH_2C(CH_3)_2CH_2$), 3.19-3.27 (8H, m, 4x$CH_2CH_2CH_2CH_3$), 5.22 (1H, br s, C*H*=COH); δ_C (63 MHz, DEPT, $CDCl_3$) 13.4 ($CH_2CH_2CH_3$), 19.5 ($CH_2CH_2CH_3$), 23.7 ($CH_2CH_2CH_3$), 28.6 ($C(CH_3)_2$), 32.2 ($C(CH_3)_2$), 48.3 ($CH_2C(CH_3)_2$), 58.4 ($FNCH_2$), 101.2 (COCH=COH), 162.4 (COCH=COH), 192.1 (COCH=COH).

6.2.3 Results and Discussion I - Additional Ligands

6.2.3.1 N-(5,5-dimethyl-2-cyclohex-1-on-3-yl)-L-valine methyl ester (77)[1]

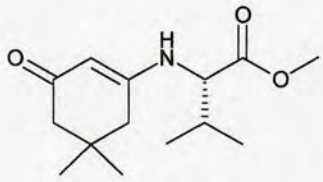

To a solution of dimedone (1.00 g, 7.13 mmol) in $CHCl_3$ (20 ml) was added L-valine methyl ester HCl salt (1.20 g, 7.13 mmol) and the suspension neutralised by the addition of triethylamine (1.00 ml, 7.13 mmol). The resulting solution was stirred at room temperature overnight. The solution was then concentrated under reduced pressure to a yellow residue, which was triturated with hot ether, filtered and washed with ether to yield a white solid (1.66 g). The solid was dissolved in $CHCl_3$, washed with 2N HCl and dried ($MgSO_4$) before concentration under reduced pressure to a white solid (1.02 g, 57 %): mp 123 °C; $[\alpha]_D$ –61.8 (c 1.0, $CHCl_3$); R_f=0.44

DCM/MeOH (9:1); ν_{max}(nujol) 3268 (N-H), 1756 (ester), 1735 (α,β-unsaturated ketone), 1604 (enamine C=C), 1574, 1537 (amide II); δ_H (200 MHz, $CDCl_3$) 0.92 (3H, d, *J* 7.0, CH($C^AH_3C^BH_3$)), 0.94 (3H, d, *J* 7.0, CH($C^AH_3C^BH_3$)), 1.06 (6H, s, C(CH_3)$_2$), 1.82-1.95 (1H, m, C*H*(CH_3)$_2$), 2.17 (2H, s, CH_2C(CH_3)$_2$), 2.23 (2H, s, CH_2C(CH_3)$_2$), 3.91 (1H, dd, *J* 8.0, 5.0, NHC*H*), 4.88 (1H, d, *J* 8.0, N*H*), 5.06 (1H, s, COC*H*=CO); δ_C (63 MHz, DEPT, $CDCl_3$) 18.9 (CH($C^AH_3C^BH_3$)), 19.0 (CH($C^AH_3C^BH_3$)), 28.5 (C($C^AH_3C^BH_3$)), 28.7 (C($C^AH_3C^BH_3$)), 31.4 (*C*H(CH_3)$_2$), 33.2 (*C*(CH_3)$_2$), 44.0 (*C*H_2C(CH_3)$_2$), 50.7 (*C*H_2C(CH_3)$_2$), 52.7 (O*C*H_3), 60.8 (NH*C*H), 97.0 (CO*C*H=CNH), 162.3 (COCH=*C*NH), 172.4 (*C*OOCH$_3$), 197.6 (*C*OCH=CNH); MS ESI (+ve) found m/z 253.9 (MH^+, 100 %), 276.1 (MNa^+, 16) 317.0 (64); HRMS FAB (+ve) found m/z 254.17486 (MH^+), $C_{14}H_{24}NO_3$ requires 254.17562.

6.2.3.2 N-benzyloxycarbonyl-L-valine methyl ester (79)

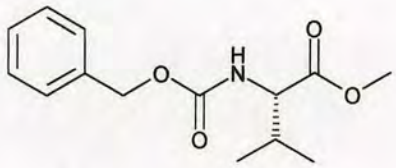

The HCl salt of L-valine methyl ester (1.00 g, 5.97 mmol) was dissolved in DCM (10 ml) and DIPEA (1.04 ml, 5.97 mmol) added. *N*-(benzyloxycarbonyloxy)-succinimide (1.49 g, 5.97 mmol) was added and the reaction stirred overnight at room temperature. The reaction mixture was then washed with water, dried over $MgSO_4$ and concentrated under reduced pressure to a colourless liquid (1.45 g). Flash column chromatography on silica gel using DCM/MeOH (9.5:0.5) as eluent yielded a white solid (1.40g, 88 %): mp 63 °C, Lit.[2] 57-58 °C; $[\alpha]_D$ -10.5 (c 1.0, $CHCl_3$), Lit.[3] –21.3 (c 1.0, MeOH); R_f=0.66 DCM/MeOH (9.5:0.5); ν_{max}(nujol) 3351br (N-H), 1749 (ester), 1694 (urethane C=O), 1538 (amide II); δ_H (250 MHz, $CDCl_3$) 0.89 (3H, d, *J* 7.0, CH($C^AH_3C^BH_3$)), 0.96 (3H, d, *J* 7.0, CH($C^AH_3C^BH_3$)), 2.11-2.20 (1H, m, C*H*(CH_3)$_2$), 3.73 (3H, s, O*C*H_3), 4.30 (1H, dd, *J* 9.0, 5.0, NHC*H*), 5.11 (2H, s, O*C*H_2Ph), 5.26 (1H, d, *J* 9.0, N*H*); δ_C (63 MHz, DEPT, $CDCl_3$) 17.3 (CH($C^AH_3C^BH_3$)), 18.7 (CH($C^AH_3C^BH_3$)), 31.0 (*C*H(CH_3)$_2$), 51.9 (O*C*H_3), 58.8

(NHCH), 66.8 (OCH_2Ph), [127.9 (CH), 128.3 (CH), 5C, *Ar*-H], 136.1 ($OCH_2\textit{Ph}$), 156.0 (*C*ONH), 172.3 ($\textit{C}OOCH_3$); HRMS FAB (+ve) found m/z 266.13928 (MH^+), $C_{14}H_{20}NO_4$ requires 266.13923.

6.2.4 Results and Discussion II

6.2.4.1 3-(N-benzyloxycarbonyl-D-valinyloxy)-5,5-dimethyl-2-cyclohexen-1-one (80)

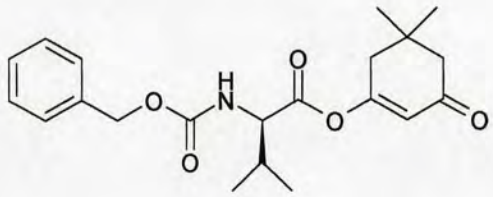

The general procedure outlined above (6.2.1.4, Method B) was followed using Cbz-D-valine (0.20 g, 0.80 mmol) to yield a blue/pink oil. Flash column chromatography on silica gel using Pet.Ether/EtOAc (4:3) as eluent gave a colourless oil (0.19 g, 64 %): $[\alpha]_D$ +20.5 (c 0.5, $CHCl_3$); R_f=0.54 Pet.Ether/EtOAc (4:3); ν_{max}(crude oil) 3326br (N-H), 1767 (vinyl ester), 1720 (urethane C=O), 1672 (α,β-unsaturated ketone), 1527 (amide II); δ_H (250 MHz, $CDCl_3$) 0.94 (3H, d, *J* 7.0, $CH(C^AH_3C^BH_3)$), 1.02 (3H, d, *J* 7.0, $CH(C^AH_3C^BH_3)$), 1.09 (6H, s, $C(CH_3)_2$), 2.19-2.25 (1H, m, $CH(CH_3)_2$), 2.25 (2H, s, $CH_2C(CH_3)_2$), 2.38 (2H, s, $CH_2C(CH_3)_2$), 4.38 (1H, dd, *J* 9.0, 5.0, NHCH), 5.11 (2H, s, OCH_2Ph), 5.29 (1H, d, *J* 9.0, NH), 5.89 (1H, s, COCH=CO), 7.34 (5H, s, Ar-H); δ_C (63 MHz, DEPT, $CDCl_3$) 18.0 ($CH(C^AH_3C^BH_3)$), 19.4 ($CH(C^AH_3C^BH_3)$), 28.5 ($C(C^AH_3C^BH_3)$), 28.6 ($C(C^AH_3C^BH_3)$), 31.4 ($CH(CH_3)_2$), 33.6 ($C(CH_3)_2$), 42.4 ($CH_2C(CH_3)_2$), 51.2 ($CH_2C(CH_3)_2$), 59.7 (NHCH), 67.7 (OCH_2Ph), 117.3 (COCH=CO), [128.6 (CH), 128.8 (CH), 129.0 (CH), 5C, *Ar*-H], 136.4 ($OCH_2\textit{Ph}$), 156.7 (*C*ONH), 168.2 (COO*C*=CH), 169.6 (NHCHCO), 199.7 (*C*OCH=COCO); HRMS FAB (+ve) found m/z 374.19672 (MH^+), $C_{21}H_{28}NO_5$ requires 374.19675.

6.2.4.2 3-(N-tertbutyloxycarbonyl-L-valinyloxy)-5,5-dimethyl-2-cyclohexen-1-one (81)

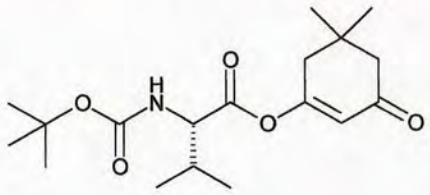

To a cold (-10 °C) solution of *tert*-butyloxycarbonyl-L-valine (5.0 g, 23.0 mmol) in THF (50 ml), were added triethylamine (3.21 ml, 23.0 mmol), and methyl chloroformate (1.96 ml, 25.0 mmol). A white precipitate formed and further THF (30 ml) was added. The mixture was stirred for 5 min at -5 °C, and dimedone (3.22 g, 23.0 mmol) added. The reaction was allowed to warm to room temperature and stirring continued overnight. The reaction mixture was diluted with EtOAc (100 ml), washed with brine (3 x 50 ml), dried over $MgSO_4$ and concentrated under reduced pressure to a colourless oil (4.48 g). Flash column chromatography on silica gel using hexane/EtOAc (3:2) yielded a colourless oil (0.29 g, 37 %): $[\alpha]_D$ –12.0 (c 1.0, $CHCl_3$); R_f=0.49 hexane/EtOAc (3:2); ν_{max}(crude oil) 3329br (N-H), 1767 (vinyl ester), 1712 (urethane C=O), 1674 (α,β-unsaturated ketone), 1514 (amide II); δ_H (250 MHz, $CDCl_3$) 0.92 (3H, d, *J* 7.0, $CH(C^AH_3C^BH_3)$), 0.99 (3H, d, *J* 7.0, $CH(C^AH_3C^BH_3)$), 1.07 (6H, s, $C(CH_3)_2$), 1.41 (9H, s, $C(CH_3)_3$), 2.16-2.21 (1H, m, $CH(CH_3)_2$), 2.24 (2H, s, $CH_2C(CH_3)_2$), 2.38 (2H, s, $CH_2C(CH_3)_2$), 4.26 (1H, dd, *J* 9.0, 5.0, NHC*H*), 4.99 (1H, d, *J* 9.0, N*H*), 5.87 (1H, s, COC*H*=CO); δ_C (63 MHz, DEPT, $CDCl_3$) 17.5 ($CH(C^AH_3C^BH_3)$), 18.9 ($CH(C^AH_3C^BH_3)$), 28.0 ($C(CH_3)_2$), 28.1 ($C(CH_3)_3$), 30.8 ($CH(CH_3)_2$), 33.0 ($C(CH_3)_2$), 41.8 ($CH_2C(CH_3)_2$), 50.6 ($CH_2C(CH_3)_2$), 58.7 (NHCH), 80.1 ($C(CH_3)_3$), 116.6 (COCH=CO), 155.5 (CONH), 167.8 (COOC=CH), 169.3 (NHCHCO), 199.1 (COCH=COCO); MS ESI (+ve) found m/z 141.0 (dimedone, 72 %), 362.0 (MNa^+, 100); HRMS FAB (+ve) found m/z 340.21247 (MH^+), $C_{18}H_{30}NO_5$ requires 340.21240.

6.2.5 4-Alkyl Dimedone Derivatives

6.2.5.1 4,5,5-trimethyl-cyclohexane-1,3-dione (85)

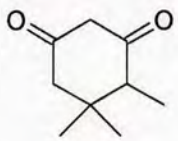

N-Butyllithium (1.6 M solution in hexane, 9.8 ml, 15.7 mmol) was added dropwise to a solution of dry diisopropylamine (2.2 ml, 15.7 mmol) in anhydrous THF (12.5 ml) with stirring at 0 °C. After 30 min, the mixture was cooled to –78 °C and a solution of dimedone (1.0 g, 7.1 mmol) and hexamethylphosphoric triamide (4.0 ml, 24.2 mmol) in anhydrous THF (8 ml) was added over 5 min. After stirring for 1 h at -78 °C, methyl iodide (0.5 ml, 7.8 mmol) was added and the mixture allowed to reach room temperature overnight. The reaction was quenched with water (5 ml), diluted with ether (50 ml), washed with 2N HCl (3 x 50 ml), then water (50 ml). The combined aqueous phased were extracted with ether (2 x 50 ml) and the total organic phase washed with brine (50 ml), dried ($MgSO_4$) and concentrated under reduced pressure to an orange solid (1.2 g). Flash column chromatography using Pet.Ether/EtOAc (1:1) yielded an off-white solid (0.6 g, 55 %): mp 113 °C, Lit.[4] 100-102 °C; $[\alpha]_D$ 0 (c 1.0, $CHCl_3$) racemate; R_f=0.27 Pet.Ether/EtOAc (1:1); ν_{max}(nujol) 1737 (ketone), 1708 (α-branched ketone); δ_H (250 MHz, $CDCl_3$) 0.75 (3H, s, $C(C^AH_3C^BH_3)$), 1.12 (3H, s, $C(C^AH_3C^BH_3)$), 1.13 (3H, d, *J* 7.0, $CHCH_3$), 2.50 (1H, dd, *J* 15.0, 2.0, $COCH^AH^BC(CH_3)_2$), 2.58 (1H, q, *J* 7.0, $CHCH_3$), 2.62 (1H, d, *J* 15.0, $COCH^AH^BC(CH_3)_2$), 3.31 (1H, dd, *J* 17.0, 2.0, $COCH^ACH^BCO$), 3.41 (1H, d, *J* 17.0, $COCH^ACH^BCO$); δ_C (63 MHz, DEPT, $CDCl_3$) 8.7 ($C(C^AH_3C^BH_3)$), 21.3 ($C(C^AH_3C^BH_3)$), 28.5 ($CHCH_3$), 33.7 ($C(CH_3)_2$), 54.0 ($CHCH_3$), 55.2 ($COCH_2C(CH_3)_2$), 57.4 ($COCH_2CO$), 203.4 (*C*O), 205.2 (*C*O); MS ESI (+ve) found m/z 154.7 (MH^+, 100 %), 309.0 (dimer, 57); HRMS FAB (+ve) found m/z 155.10715 (MH^+), $C_9H_{15}O_2$ requires 155.10720.

6.2.5.2 3-(N-tertbutyloxycarbonyl-L-valinyloxy)-5,5-dimethyl-6-methyl-2-cyclohexen-1-one (87)

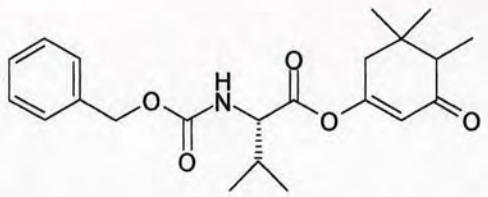

diastereomeric mixture (**X** & **Y**)

The general procedure outlined above (6.2.1.4, Method B) was followed using Cbz-L-valine (0.20 g, 0.80 mmol) and **85** (0.09 g, 0.57 mmol), to yield a blue/pink oil. Flash column chromatography on silica gel using DCM/MeOH (9.5:0.5) as eluent gave a colourless oil (0.17 g, 78 %): chiral HPLC, single peak 4.6 min; $[\alpha]_D$ –11.8 (c 1.3, $CHCl_3$); R_f=0.83 DCM/MeOH (9:1); ν_{max}(crude oil) 3329br (N-H), 1767 (vinyl ester), 1712 (urethane C=O), 1674 (α,β-unsaturated ketone), 1514 (amide II); δ_H (250 MHz, $CDCl_3$) 0.92 (3H, d, *J* 7.0, CH($C^AH_3C^BH_3$)), 0.93-1.11 (15H, m, CH(CH_3)$_2$, C(CH_3)$_2$CH(CH_3)), 2.19-2.58 (4H, m, C*H*(CH_3)$_2$, CH_2C(CH_3)$_2$C*H*(CH_3)), 4.38 (1H, dd, *J* 9.0, 5.0, NHC*H*), 5.11 (2H, s, OCH_2Ph), 5.25 (1H, d, *J* 9.0, N*H*), 5.85 (1H, s, COC*H*=CO), 7.35 (5H, s, Ar-*H*); δ_C (63 MHz, DEPT, $CDCl_3$) 9.3 (COCHCH_3, **X**), 9.4 (COCHCH_3, **Y**), 17.4 (CH($C^AH_3C^BH_3$), **X** & **Y**), 18.9 (CH($C^AH_3C^BH_3$), **X** & **Y**), 22.0 (C($C^AH_3C^BH_3$), **X**), 22.1 (C($C^AH_3C^BH_3$), **Y**), 28.4 (C($C^AH_3C^BH_3$), **X** & **Y**), 31.0 (*C*H(CH_3)$_2$, **X** & **Y**), 35.8 (*C*(CH_3)$_2$, **X**), 35.9 (*C*(CH_3)$_2$, **Y**), 41.8 (*C*H_2C(CH_3)$_2$, **X**), 41.9 (*C*H_2C(CH_3)$_2$, **Y**), 51.3 (COCHCH$_3$, **X** & **Y**), 59.0 (NHCH, **X** & **Y**), 67.1 (OCH_2Ph, **X** & **Y**), 116.3 (COCH=CO, **X** & **Y**), [128.0 (CH), 128.2 (CH), 128.5 (CH), 10C, *Ar*-H, **X** & **Y**], 135.9 (OCH_2*Ph*, **X** & **Y**), 156.1 (*C*ONH, **X** & **Y**), 166.2 (COO*C*=CH, **X** & **Y**), 169.1 (NHCH*C*O, **X** & **Y**), 201.7 (*C*OCH=COCO, **X** & **Y**); MS ESI (+ve) found m/z 387.9 (MH^+, 20 %), 404.9 (MNH_4^+, 51), 410.04 (MNa^+, 100); HRMS FAB (+ve) found m/z 388.21228 (MH^+), $C_{22}H_{29}NO_5$ requires 388.21240.

6.2.5.3 4-allyl-5,5-dimethyl-cyclohexane-1,3-dione (88)

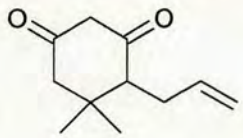

N-Butyllithium (1.6 M solution in hexane, 9.8 ml, 15.7 mmol) was added dropwise to a solution of dry diisopropylamine (2.2 ml, 15.7 mmol) in anhydrous THF (12.5 ml) with stirring at 0 °C. After 30 min, the mixture was cooled to –78 °C and a solution of dimedone (1.0 g, 7.1 mmol) and hexamethylphosphoric triamide (4.0 ml, 24.2 mmol) in anhydrous THF (8 ml) was added over 5 min. After stirring for 1 h at -78 °C, a suspension of allyl bromide (0.7 ml, 7.8 mmol) and sodium iodide (1.2 g, 7.8 mmol) in anhydrous THF (2 ml) was added and the mixture allowed to reach room temperature overnight. The reaction was quenched with water (5 ml), diluted with ether (50 ml), washed with 2N HCl (3 x 50 ml), then water (50 ml). The combined aqueous phased were extracted with ether (2 x 50 ml) and the total organic phase washed with brine (50 ml), dried ($MgSO_4$) and concentrated under reduced pressure to an orange solid (1.2 g). Flash column chromatography using Pet.Ether/EtOAc (2:1) yielded a colourless oil (0.52 g, 41 %): R_f=0.16 Pet.Ether/EtOAc (2:1); ν_{max}(crude oil) 1739 (ketone), 1709 (α-branched ketone); δ_H (250 MHz, $CDCl_3$) 0.83 (3H, s, $C(C^AH_3C^BH_3)$), 1.11 (3H, s, $C(C^AH_3C^BH_3)$), 2.24-2.35 (1H, m, $CHCH^AH^BCH{=}CH_2$), 2.43-2.55 (4H, m, $CHCH_2CH{=}CH_2$, $COCH_2C(CH_3)_2$, $CHCH^AH^BCH{=}CH_2$), 3.32 (1H, dd, *J* 16.5, 1.5, $COCH^AH^BCO$), 3.41 (1H, d, *J* 16.5, $COCH^AH^BCO$), 4.98-5.12 (2H, m, $CHCH_2CH{=}CH_2$), 5.74-5.90 (1H, m, $CHCH_2CH{=}CH_2$); δ_C (63 MHz, DEPT, $CDCl_3$) 22.8 ($C(C^AH_3C^BH_3)$), 28.7 ($C(C^AH_3C^BH_3)$), 28.8 ($CHCH_2CH{=}CH_2$), 33.6 ($C(CH_3)_2$), 54.4 ($COCH_2C(CH_3)_2$), 57.9 ($COCH_2CO$), 60.0 ($CHCH_2CH{=}CH_2$), 116.3 ($CHCH_2CH{=}CH_2$), 136.3 ($CHCH_2CH{=}CH_2$), 203.0 (*C*O), 203.9 (*C*O); HRMS FAB (+ve) found m/z 181.12279 (MH^+), $C_{11}H_{17}O_2$ requires 181.12285.

6.2.5.4 (2,2-Dimethyl-4,6-dioxo-cyclohexyl)-acetic acid methyl ester (89)

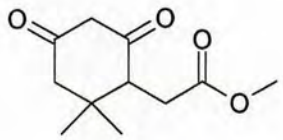

The procedure outlined above (6.2.4.5) was followed using methyl bromoacetate (0.74 ml, 7.84 mmol) to yield a brown liquid (0.95 g). Flash column chromatography on silica gel using Pet.Ether/EtOAc (1:1) as eluent yielded a yellow oil (0.32 g, 21 %): R_f=0.16 Pet.Ether/EtOAc (1:1); ν_{max}(crude oil); δ_H (250 MHz, $CDCl_3$); δ_C (63 MHz, DEPT, $CDCl_3$) 21.5 ($C(C^AH_3C^BH_3)$), 28.3 ($C(C^AH_3C^BH_3)$), 28.4 ($CH_2C(O)OCH_3$), 33.4 ($C(CH_3)_2$), 51.9 ($CHCH_2C(O)OCH_3$), 55.6 (OCH_3), 56.0 ($CH_2C(CH_3)_2$), 58.1 ($COCH_2CO$), 173.1 ($C(O)OCH_3$), 202.5 ($COCH_2CO$), 202.7 ($COCH_2CO$); MS ESI (+ve) found m/z 212.6 (MH^+, 100 %), 234.7 (MNa^+, 57); HRMS FAB (+ve) found m/z 213.11243 (MH^+), $C_{11}H_{17}O_4$ requires 213.11268.

6.2.5.5 4,7,7-Trimethyl-3-oxo-2-oxa-bicyclo[2.2.1]heptane-1-carboxylic acid 4,5,5-trimethyl-3-oxo-cyclohex-1-enyl ester (91)

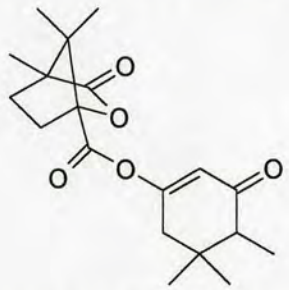

85 (0.17 g, 1.07 mmol) was dissolved in anhydrous DCM (4 ml). Pyridine (0.13 ml, 1.60 mmol) was added, followed by (-)-camphanic acid chloride (0.26 g, 1.18 mmol) and the solution stirred at room temperature for 1h. DCM (6 ml) was added and the reaction mixture washed with saturated $NaHCO_3$ solution, dried ($MgSO_4$) and concentrated under reduced pressure to yield an orange oil (0.36 g). Flash column chromatography on silica gel using Pet.Ether/EtOAc (2:1) as eluent afforded a pale yellow solid **91a** (43 mg, 12 %): chiral HPLC, single peak 4.5 min; mp 103 °C; $[\alpha]_D$ –15.4 (c 1.1, $CHCl_3$); R_f=0.37 Pet.Ether/EtOAc (2:1); ν_{max}(nujol) 3020-2877 (C-H),

1790br (ester C=O), 1677 (C=O); δ_H (250 MHz, $CDCl_3$) 0.95 (3H, s, $CH_2C(C^AH_3C^BH_3)$), 1.00 (3H, s, $CH_2C(CH_3)C(CH_3)_2$), 1.06 (3H, s, $CH_2C(C^AH_3C^BH_3)$), 1.06 (3H, d, *J* 7.0, $CHCH_3$), 1.10 (3H, s, $CH_2C(CH_3)C(C^AH_3C^BH_3)$), 1.11 (3H, s, $CH_2C(CH_3)C(C^AH_3C^BH_3)$), 1.65-1.76 (1H, m, $CH^AH^BCH_2$), 1.89-2.14 (2H, m, $CH^AH^BCH_2$ & $CH_2CH^AH^B$), 2.23 (1H, q, *J* 7.0, $CHCH_3$), 2.30-2.55 (3H, m, $CH_2CH^AH^B$ & $CH_2C(CH_3)_2$), 5.88 (1H, s, OC=C*H*); δ_C (63 MHz, DEPT, $CDCl_3$) 9.3 ($CH_2C(CH_3)C(C^AH_3C^BH_3)$), 9.5 ($CH_2C(CH_3)C(C^AH_3C^BH_3)$), 16.6 ($CH_2C(CH_3)C(CH_3)_2$), 22.0 ($CH_2C(C^AH_3C^BH_3)$), 28.4 ($CH_2C(C^AH_3C^BH_3)$), 28.7 ($CH_2CH_2$), 30.5 ($CH_2CH_2$), 35.9 ($CH_2C(CH_3)_2$), 41.9 ($CH_2C(CH_3)_2$), 51.2 ($CHCH_3$), 54.6 ($CH_2C(CH_3)C(CH_3)_2$), 54.7 ($CH_2C(CH_3)C(CH_3)_2$), 90.3 ($CH_2CC(O)O$), 116.6 (OC=CH), 164.5 ($OC(O)C(CH_3)$), 165.7 (OC=CH), 177.3 (C(O)OC=CH), 201.4 (OC=CHC(O)); MS ESI (+ve) found m/z 335.0 (MH^+, 100 %); HRMS FAB (+ve) found m/z 335.18551 (MH^+), $C_{19}H_{27}O_5$ requires 335.18585.

A second fraction was isolated from the column as a pale yellow solid (79 mg, 22 %), corresponding to a mixture of the two diastereomers **91** by TLC R_f=0.35, 0.37 Pet.Ether/EtOAc (2:1).

6.2.5.6 Cleavage of camphanic ester (91)

91 (0.20 g, 0.60 mmol) was dissolved in 0.5 M NaOMe solution in MeOH (1.2 ml, 0.6 mmol) and the solution stirred at room temperature for 5 min. The reaction mixture was diluted with DCM (4 ml) and acidified to pH1 using 2M HCl. The organic layer was separated, dried ($MgSO_4$), and concentrated under reduced pressure to an off-white solid (0.20 g). Flash column chromatography on silica gel using DCM/MeOH (9.5:0.5) as eluent afforded a white solid (0.08 g, 87 %); R_f=0.42 DCM/MeOH (9.5:0.5); analysis identical to **85**, 6.2.4.3.

6.2.5.7 5,5-Dimethyl-3-(1,3,3-trimethyl-bicyclo[2.2.1]hept-2-yloxy)-cyclohex-2-enone (94)

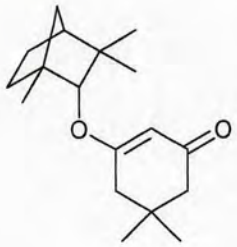

Dimedone (1.00 g, 7.03 mmol) was dissolved in DCM (10 ml) with TsOH (1.35 g, 7.84 mmol) and fenchol (1.21 g, 7.84 mmol). The solution was stirred at room temperature overnight, before concentration under reduced pressure to give a yellow oil (4.06 g). Flash column chromatography on the Biotage system (40M column) using hexane/EtOAc (4:1) as eluent afforded a colourless oil (0.27 g, 14 %): $[\alpha]_D$ +154.3 (c 1.0, $CHCl_3$); R_f=0.22 hexane/EtOAc (4:1); ν_{max}(crude oil) 2960-2872br (C-H), 1639 (ketone C=O), 1601 (α,β-unsaturated ketone); δ_H (250 MHz, $CDCl_3$) 0.78 (3H, s, C(C*H*$_3$)CH_2CH_2), 1.01 (3H, s, C(O)HC($C^AH_3C^BH_3$)), 1.04 (6H, s, $CH_2C(CH_3)_2$), 1.11 (3H, s, C(O)HC($C^AH_3C^BH_3$)), 0.98-1.86 (7H, m, $C(CH_3)CH_2CH_2CHCH_2$), 2.17 (2H, s, $CH_2C(CH_3)_2CH_2$), 2.27 (2H, d, *J* 4.5, $CH_2C(CH_3)CH_2$), 3.77 (1H, d, *J* 1.5, C(O)*H*), 5.34 (1H, d, *J* 0.5, OC=C*H*); δ_C (63 MHz, DEPT, $CDCl_3$) 19.4 (C(O)HC($C^AH_3C^BH_3$)), 19.5 (C(O)HC($C^AH_3C^BH_3$)), 25.4 ($C(CH_3)CH_2CH_2$), 26.3 ($C(CH_3)CH_2CH_2$), 27.6 ($CH_2C(C^AH_3C^BH_3)$), 28.5 ($CH_2C(C^AH_3C^BH_3)$), 30.0 ($C(CH_3)CH_2CH_2$), 32.2 ($CH_2C(CH_3)_2$), 39.7 ($C(CH_3)CH_2CH_2$), 41.1 ($CH_2C(CH_3)CH_2$), 43.1 ($C(CH_3)CH_2CHC(CH_3)_2$), 48.8 ($C(CH_3)CH_2CHC(CH_3)_2$), 49.0 ($C(O)HC(CH_3)_2$), 50.5 ($CH_2C(CH_3)_2CH_2$), 89.8 (*C*(O)H), 102.0 (OC=*C*H), 177.2 (*O*C=CH), 199.6 (*C*=O); MS ESI (+ve) found m/z 277.1 (MH^+, 14 %), 300.1 (MNa^+, 100); HRMS FAB (+ve) found m/z 277.21709 (MH^+), $C_{18}H_{29}O_2$ requires 277.21676.

6.2.5.8 6-Benzyl-5,5-dimethyl-3-(1,3,3-trimethyl-bicyclo[2.2.1]hept-2-yloxy)-cyclohex-2-enone (95)

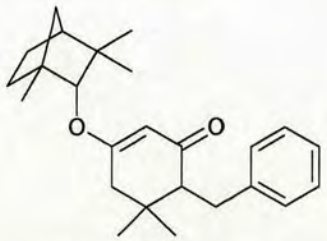

(diastereomers **X**;**Y**)

N-Butyllithium (1.6 M solution in hexane, 0.90 ml, 1.43 mmol) was added dropwise to a solution of dry diisopropylamine (0.20 ml, 1.43 mmol) in anhydrous THF (1 ml) with stirring at 0 °C. After 30 min, the mixture was cooled to –78 °C and a solution of **94** (0.18 g, 0.65 mmol) in anhydrous THF (0.5 ml) was added over 5 min. After stirring for 1 h at -78 °C, benzyl bromide (0.09 ml, 0.72 mmol) was added and the mixture allowed to reach room temperature overnight. The reaction was quenched with water (1 ml), diluted with ether (5 ml) and washed with 2N HCl (3 x 5 ml). The combined aqueous phased were extracted with ether (2 x 5 ml) and the total organic phase washed with brine (10 ml), dried ($MgSO_4$) and concentrated under reduced pressure to a yellow liquid (0.31 g). Flash column chromatography on the Biotage system (20M column) using DCM as eluent yielded a colourless oil (0.05 g, 22 %): chiral HPLC, 2 peaks, 4.4 min (48.0 Area %), 5.8 min (50.1 Area %); $[\alpha]_D$ +64.9 (c 1.0, $CHCl_3$); R_f=0.58 DCM; ν_{max}(crude oil) 3084-2872 (C-H), 1653 (ketone C=O), 1609 (α,β-unsaturated ketone); δ_H (250 MHz, $CDCl_3$) 0.78 (3H, s, $C(CH_3)CH_2CH_2$, **X**), 0.83 (3H, s, $C(CH_3)CH_2CH_2$, **Y**), 1.01-1.15 (24H, m, $C(O)HC(CH_3)_2$, $CH_2C(CH_3)_2$, **X** & **Y**), 1.18-1.82 (14H, m, $C(CH_3)CH_2CH_2CHCH_2$, **X** & **Y**), 2.32-2.39 (6H, m, $CH_2C(CH_3)CHCH_2Ph$, **X** & **Y**), 2.65-2.75 (2H, m, CH^AH^BPh, **X** & **Y**), 2.98-3.12 (2H, m, CH^AH^BPh, **X** & **Y**), 3.78 (2H, d, *J* 6.5, C(O)*H*, **X** & **Y**), 5.32 (2H, s, OC=C*H*, **X** & **Y**), 7.12-7.28 (10H, m, Ar-*H*, **X** & **Y**); δ_C (63 MHz, DEPT, $CDCl_3$) 19.4 ($C(O)HC(C^AH_3C^BH_3)$, **X** & **Y**), 19.6 ($C(O)HC(C^AH_3C^BH_3)$, **X** & **Y**), 22.9 ($CH_2C(C^AH_3C^BH_3)$, **X**), 23.3 ($CH_2C(C^AH_3C^BH_3)$, **Y**), 25.5 ($C(CH_3)CH_2CH_2$, **X** & **Y**), 26.2 ($C(CH_3)CH_2CH_2$, **X** & **Y**), 28.8 ($CH_2C(C^AH_3C^BH_3)$, **X**), 28.9

($CH_2C(C^AH_3C^BH_3)$, **Y**), 30.0 ($C(CH_3)CH_2CH_2$, **X** & **Y**), 31.4 (CH_2Ph, **X**), 31.7 (CH_2Ph, **Y**), 35.6 ($CH_2C(CH_3)_2$, **X** & **Y**), 39.7 ($C(CH_3)CH_2CH_2$, **X**), 39.8 ($C(CH_3)CH_2CH_2$, **Y**), 41.2 ($C(CH_3)CH_2CH_2CHCH_2$, **X** & **Y**), 42.8 ($CH_2C(CH_3)_2$, **X**), 43.2 ($CH_2C(CH_3)_2$, **Y**), 48.8 ($CHC(CH_3)_2CO$, **X** & **Y**), 49.0 ($C(O)HC(CH_3)_2$, **X** & **Y**), 59.0 ($CHCH_2Ph$, **X** & **Y**), 89.5 (*C*(O)H, **X**), 89.7 (*C*(O)H, **Y**), 101.6 (OC=*C*H, **X**), 101.7 (OC=*C*H, **Y**), [125.5 (CH), 128.0 (CH), 128.8 (CH), 128.9 (CH), *Ar*-H], 141.7 (CH_2Ph, **X**), 141.9 (CH_2Ph, **Y**), 174.9 (O*C*=CH, **X** & **Y**), 200.2 (*C*=O, **X** & **Y**); MS ESI (+ve) found m/z 367.3 (MH^+, 47 %), 389.3 (MNa^+, 100); HRMS FAB (+ve) found m/z 367.26396 (MH^+), $C_{25}H_{35}O_2$ requires 367.26371.

6.2.5.9 5,5-Dimethyl-3-(1,7,7-trimethyl-bicyclo[2.2.1]hept-2-yloxy)-cyclohex-2-enone (97)

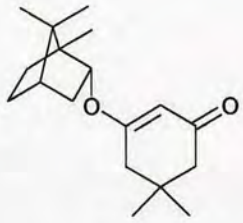

Dimedone (1.0 g, 7.13 mmol) was suspended in DCM (10 ml) with TsOH (1.2 g, 7.80 mmol) and borneol (1.21 g, 7.85 mmol). The resulting mixture was stirred at room temperature overnight. The solution was then washed with saturated $NaHCO_3$ solution (5 ml), dried ($MgSO_4$) and concentrated under reduced pressure to a pale yellow oil. Flash column chromatography on silica gel using hexane/EtOAc (1:1) as eluent afforded a colourless oil (1.49 g, 76 %): $[\alpha]_D$ –234.3 (c 0.9, $CHCl_3$); R_f=0.52 hexane/EtOAc (1:1); ν_{max}(crude oil) 2952-2875br (C-H), 1639 (ketone C=O), 1602 (α,β-unsaturated ketone); δ_H (250 MHz, $CDCl_3$) 0.81 (6H, s, $C(CH_3)C(CH_3)_2$), 0.82 (3H, s, $C(CH_3)C(CH_3)_2$), 0.83 (3H, s, $CH_2C(C^AH_3C^BH_3)$), 0.87-0.96 (1H, m, $CHCH^AH^BCH^{A'}H^{B'}$), 1.04 (3H, s, $CH_2C(C^AH_3C^BH_3)$), 1.13-1.29 (2H, m, $CHCH^AH^BCH^{A'}H^{B'}$), 1.56-2.02 (4H, m, $CH_2CHCH^AH^B$), 2.17-2.29 (4H, m, $CH_2C(CH_3)_2CH_2$), 3.94-4.00 (1H, m, C*H*O), 5.20 (1H, s, OC=C*H*); δ_C (63 MHz, DEPT, $CDCl_3$) 13.4 ($C(CH_3)C(CH_3)_2$), 18.6 ($C(CH_3)C(C^AH_3C^BH_3)$), 19.4 ($C(CH_3)C(C^AH_3C^BH_3)$), 26.6 ($CHCH_2CH_2$), 27.6 ($CHCH_2CH_2$), 27.9

($CH_2C(C^AH_3C^BH_3)$), 28.3 ($CH_2C(C^AH_3C^BH_3)$), 32.3 ($CH_2C(CH_3)_2$), 36.5 ($CH(O)CH_2$), 42.8 ($CH_2C(CH_3)_2CH_2$), 44.7 ($CHCH_2CH_2$), 47.5 ($C(CH_3)C(CH_3)_2$), 49.0 ($C(CH_3)C(CH_3)_2$), 50.5 ($CH_2C(CH_3)_2CH_2$), 83.9 (*C*HO), 102.3 (OC=*C*H), 176.2 (O*C*=CH), 199.7 (*C*=O); MS ESI (+ve) found m/z 276.9 (MH^+, 100 %); HRMS FAB (+ve) found m/z 277.21650 (MH^+), $C_{18}H_{29}O_2$ requires 277.21676.

6.2.5.10 6-Benzyl-5,5-dimethyl-3-(1,7,7-trimethyl-bicyclo[2.2.1]hept-2-yloxy)-cyclohex-2-enone (98)

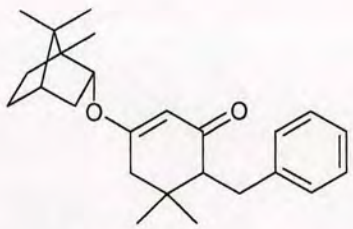

(diastereomers **X**:**Y**)

N-Butyllithium (1.6 M solution in hexane, 6.88 ml, 11 mmol) was added dropwise to a solution of dry diisopropylamine (1.54 ml, 11 mmol) in anhydrous THF (9 ml) with stirring at 0 °C. After 30 min, the mixture was cooled to –78 °C and a solution of **97** (1.38 g, 5 mmol) and hexamethylphosphoric triamide (2.81 ml, 17 mmol) in anhydrous THF (5.5 ml) was added over 5 min. After stirring for 1 h at -78 °C, a suspension of benzyl bromide (0.65 ml, 5.5 mmol) and sodium iodide (0.82 g, 5.5 mmol) in anhydrous THF (2 ml) was added and the mixture allowed to reach room temperature overnight. The reaction was quenched with water (5 ml), diluted with ether (50 ml) and washed with 2N HCl (3 x 50 ml). The combined aqueous phased were extracted with ether (2 x 50 ml) and the total organic phase washed with brine (50 ml), dried ($MgSO_4$) and concentrated under reduced pressure to an orange oil (2.72 g). Flash column chromatography on the Biotage system (40M column) using hexane/EtOAc (4:1) yielded a colourless oil (0.27 g, 15 %): chiral HPLC, 2 peaks, 5.1 min (45.4 Area %), 6.6 min (51.8 Area %); $[\alpha]_D$ –69.5 (c 1.5, $CHCl_3$); R_f=0.61 hexane/EtOAc (4:1); ν_{max}(crude oil) 3084-2873br (C-H), 1654 (ketone C=O), 1614 (α,β-unsaturated ketone); δ_H (250 MHz, $CDCl_3$) 0.85-0.89 (18H, m,

$C(CH_3)C(CH_3)_2$, **X** & **Y**), 0.85-1.35 (6H, m, $CHCH^AH^BCH_2$, **X** & **Y**), 1.02 (3H, s, $CH_2C(C^AH_3C^BH_3)$, **X**), 1.03 (3H, s, $CH_2C(C^AH_3C^BH_3)$, **Y**), 1.10 (3H, s, $CH_2C(C^AH_3C^BH_3)$, **X**), 1.12 (3H, s, $CH_2C(C^AH_3C^BH_3)$, **Y**), 1.68-1.76 (4H, m, $CHCH^AH^BCH_2$ & $CH(O)CH^AH^B$, **X** & **Y**), 1.96-2.06 (2H, m, $CH(O)CH^AH^B$, **X** & **Y**), 2.24-2.39 (8H, m, $CHCH_2CH_2$ & $CH_2C(CH_3)_2CHCH_2Ph$, **X** & **Y**), 2.67-2.76 (2H, m, CH^AH^BPh, **X** & **Y**), 2.98-3.12 (2H, m, CH^AH^BPh, **X** & **Y**), 4.16-4.21 (2H, m, CHO, **X** & **Y**), 5.17 (1H, s, OC=CH, **X**), 5.19 (1H, s, OC=CH, **Y**); δ_C (63 MHz, DEPT, $CDCl_3$) 13.5 ($C(CH_3)C(CH_3)_2$, **X** & **Y**), 18.6 ($C(CH_3)C(C^AH_3C^BH_3)$, **X** & **Y**), 19.5 ($C(CH_3)C(C^AH_3C^BH_3)$, **X** & **Y**), 23.2 ($CH_2C(C^AH_3C^BH_3)$, **X**), 23.5 ($CH_2C(C^AH_3C^BH_3)$, **Y**), 26.6 ($CHCH_2CH_2$, **X** & **Y**), 27.7 ($CHCH_2CH_2$, **X** & **Y**), 28.9 ($CH_2C(C^AH_3C^BH_3)$, **X**), 29.6 ($CH_2C(C^AH_3C^BH_3)$, **Y**), 31.6 (CH_2Ph, **X**), 31.7 (CH_2Ph, **Y**), 35.7 ($CH(O)CH_2$, **X** & **Y**), 36.5 ($CH_2C(CH_3)_2$, **X**), 36.6 ($CH_2C(CH_3)_2$, **Y**), 42.6 ($CH_2C(CH_3)_2$, **X**), 42.8 ($CH_2C(CH_3)_2$, **Y**), 44.7 ($CHCH_2CH_2$, **X** & **Y**), 47.5 ($C(CH_3)C(CH_3)_2$, **X** & **Y**), 49.0 ($C(CH_3)C(CH_3)_2$, **X** & **Y**), 58.9 ($CHCH_2Ph$, **X**), 59.0 ($CHCH_2Ph$, **Y**), 83.6 (CHO, **X**), 83.8 (CHO, **Y**), 101.8 (OC=CH, **X**), 101.9 (OC=CH, **Y**), [125.5 (CH), 125.6 (CH), 128.1 (CH), 128.8 (CH), *Ar*-H, **X** & **Y**], 141.7 (CH_2Ph, **X**), 141.8 (CH_2Ph, **Y**), 173.8 (OC=CH, **X**), 173.9 (OC=CH, **Y**), 200.7 (C=O, **X**), 200.8 (C=O, **Y**); MS ESI (+ve) found m/z 389.3 (MNa^+, 100 %); HRMS FAB (+ve) found m/z 367.26360 (MH^+), $C_{25}H_{35}O_2$ requires 367.26371.

Attempts to separate the diastereomeric mixture by TLC using numerous different solvent systems were unsuccessful.

6.2.5.11 Cleavage of borneol from (98)

98 (0.25 g, 0.68 mmol) was dissolved in THF (5 ml) containing 12N HCl (1.67 ml, 20 mmol). The solution was stirred at room temperature overnight. The mixture was diluted with DCM (20 ml), washed with saturated $NaHCO_3$ solution (10 ml), dried ($MgSO_4$) and concentrated under reduced pressure to a colourless oil. Flash column chromatography on silica gel using hexane/EtOAc (3:1) as eluent afforded a colourless oil **99** (0.13 g, 82 %): chiral HPLC, single peak 6.4 min; R_f=0.35 hexane/EtOAc (1:1); analysis identical to **99**, 6.2.5.12.

6.2.5.12 4-benzyl-5,5-dimethyl-cyclohexane-1,3-dione (99)

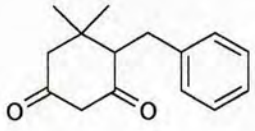

N-Butyllithium (1.6 M solution in hexane, 39.2 ml, 62.8 mmol) was added dropwise to a solution of dry diisopropylamine (8.8 ml, 62.8 mmol) in anhydrous THF (40 ml) with stirring at 0 °C. After 30 min, the mixture was cooled to –78 °C and a solution of dimedone (4.0 g, 28.5 mmol) and hexamethylphosphoric triamide (16.0 ml, 97.0 mmol) in anhydrous THF (20 ml) was added over 5 min. After stirring for 1 h at -78 °C, a suspension of benzyl bromide (3.7 ml, 31.4 mmol) and sodium iodide (4.7 g, 31.4 mmol) in anhydrous THF (5 ml) was added and the mixture allowed to reach room temperature overnight. The reaction was quenched with water (15 ml), diluted with ether (150 ml) and washed with 2N HCl (3 x 150 ml). The combined aqueous phased were extracted with ether (2 x 150 ml) and the total organic phase washed with brine (150 ml), dried ($MgSO_4$) and concentrated under reduced pressure to an orange liquid (27.12 g). Flash column chromatography on the Biotage Quad system (40M column, several loadings) using hexane/EtOAc (2.5:1) yielded a yellow oil (2.08 g, 32 %): R_f=0.35 hexane/EtOAc (1:1); ν_{max}(crude oil) 1640 (ketone), 1612 (ketone); δ_H (250 MHz, $CDCl_3$) 0.85 (3H, s, $C(C^AH_3C^BH_3)$), 1.25 (3H, s, $C(C^AH_3C^BH_3)$), 2.53 (1H, dd, *J* 15.0, 2.0, $COCH^AH^BC(CH_3)_2$), 2.65 (1H, d, *J* 15.0, $COCH^AH^BC(CH_3)_2$), 2.78 (1H, dd, *J* 14.5, 1.5, CH^AH^BPh), 2.80 (1H, dd, *J* 10.0, 1.5, $COCHCH_2Ph$), 3.13 (1H, dd, *J* 14.5, 10.0, CH^AH^BPh), 3.31 (1H, dd, *J* 16.0, 2.0, $COCH^ACH^BCO$), 3.41 (1H, d, *J* 16.0, $COCH^ACH^BCO$), 7.17-7.30 (5H, m, Ar-*H*); δ_C (63 MHz, DEPT, $CDCl_3$) 22.2 ($C(CH_3)_2$), 29.0 ($C(C^AH_3C^BH_3)$), 29.7 (CH_2Ph), 34.1 ($C(CH_3)_2$), 55.2 ($COCH_2C(CH_3)_2$), 58.6 ($COCH_2CO$), 62.3 ($CHCH_2Ph$), [126.1 (CH), 128.3 (CH), 128.8 (CH), 5C, *Ar*-H], 140.5 (CH_2Ph), 202.8 (*C*O), 203.0 (*C*O); MS ESI (+ve) found m/z 230.7 (MH^+, 70 %), 247.8 (MNH_4^+, 21), 252.8 (MNa^+, 100), 293.8 (59); HRMS FAB (+ve) found m/z 231.13862 (MH^+), $C_{15}H_{19}O_2$ requires 231.13851.

6.2.5.13 1-benzyl-2-(hydroxy-quinolin-4-yl-methyl)-5-vinyl-1-azonia-bicyclo[2.2.2]octane; fluoride (104)

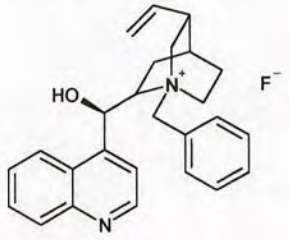

Amberlite IRA 410 (OH) ion exchange resin (10 ml) was loaded onto a glass column using H_2O. The resin was washed through with H_2O, then MeOH. 1M aqueous HF (100 ml) was passed through the column, followed by several column volumes of MeOH. Finally benzyl cinchonidinium bromide (0.95 g, 2.04 mmol) in MeOH (2 ml) was passed through the column followed by several more column volumes of MeOH. The combined MeOH washings were concentrated under reduced pressure to yield an off-white solid, which was dried in a vacuum desiccator over P_2O_5, affording a white solid (0.67 g, 81 %): mp 165 °C; $[\alpha]_D$ –155.9 (c 1.0, $CHCl_3$); δ_H (250 MHz, $CDCl_3$) and δ_C (63 MHz, DEPT, $CDCl_3$) , signals identical to 1-benzyl-2-(hydroxy-quinolin-4-yl-methyl)-5-vinyl-1-azonia-bicyclo[2.2.2]octane; bromide (**103**) starting material; δ_F ($CDCl_3$) -126.6 (4-fluorophenol), -125.4 (fluoride **104**).

6.2.5.14 4-cyclohexylmethyl-5,5-dimethyl-cyclohexane-1,3-dione (105)

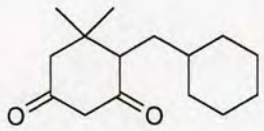

The general procedure outlined above (6.2.5.12) was followed using methylcyclohexyl bromide (4.38 ml, 31.38 mmol) to yield a dark orange liquid (11.86 g). Flash column chromatography on the Biotage Quad system (40M column, several loadings) using hexane/EtOAc (3.5:1) yielded a white solid (3.46 g, 51 %): mp 122 °C; R_f=0.50 hexane/EtOAc (1:1); ν_{max}(nujol) 1616 (ketone); δ_H (250 MHz, $CDCl_3$) 0.84 (3H, s, $C(C^AH_3C^BH_3)$), 1.07 (3H, s, $C(C^AH_3C^BH_3)$), 0.89-1.34 (7H, m,

$COCHCH^{A}H^{B}CH(CH_2)_5$, $COCHCH_2CHCH_2(CH_2)_3CH_2$), 1.68-1.86 (6H, m, $COCHCH^{A}H^{B}CH(CH_2)_5$, $COCHCH_2CH(CH_2)_5$, $COCHCH_2CHCH_2(CH_2)_3CH_2$), 2.49 (1H, dd, *J* 10.5, 2.0 $CHCH_2CH(CH_2)_5$), 2.55 (2H, s, $COCH_2C(CH_3)_2$), 3.39 (2H, s, $COCH_2CO$); δ_C (63 MHz, DEPT, $CDCl_3$) 23.7 ($C(C^{A}H_3C^{B}H_3)$), [26.5 (CH_2), 26.7 (CH_2), 26.9 (CH_2), 3C, $COCHCH_2CHCH_2(CH_2)_3CH_2$)] 29.2 ($C(C^{A}H_3C^{B}H_3)$), [32.4 ($CH_2$), 32.8 ($CH_2$), 2C, $COCHCH_2CHCH_2(CH_2)_3CH_2$)], 34.0 ($C(CH_3)_2$), 34.8 ($CH_2CH(CH_2)_5$), 36.7 ($CH_2CH(CH_2)_5$), 54.3 ($COCH_2C(CH_3)_2$), 57.7 ($COCHCH_2CH(CH_2)_5$), 58.0 ($COCH_2CO$), 203.9 (*C*O), 205.5 (*C*O); HRMS FAB (+ve) found m/z 237.18539 (MH^+), $C_{15}H_{25}O_2$ requires 237.18546.

6.2.5.15 Attempted preparation of 6-cyclohexylmethyl-3-hydroxy-5,5-dimethyl-cyclohex-2-enone benzyl cinchonidinium fluoride salt (106)

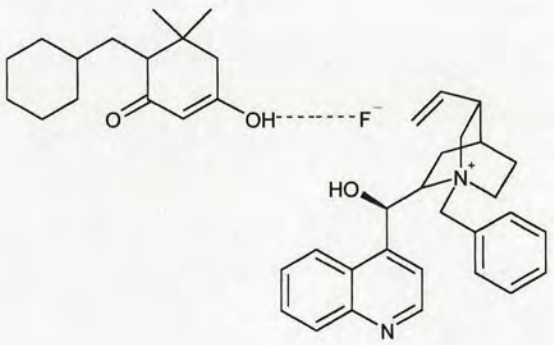

105 (0.23 g, 1 mmol) was dissolved in THF (2 ml) and **104** (0.20 g, 0.5 mmol) added. The reaction mixture was heated until all of the suspended solid had dissolved. On cooling to room temperature a white solid precipitated out and was filtered off and dried in a vacuum desiccator to yield an off-white powder (0.07 g): δ_H (250 MHz, $CDCl_3$) and δ_C (63 MHz, DEPT, $CDCl_3$) indicated a 1:1 mixture of **104** and **105** starting materials.

6.2.5.16 Attempted cleavage of Boc group of (81)

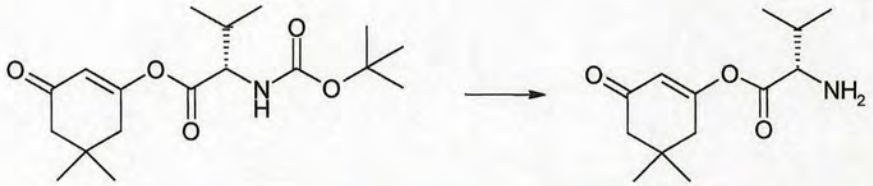

6.2.5.16.1 Method A

81 (0.76 g, 2.43 mmol) was dissolved in DCM (5 ml) and TFA (0.22 ml, 2.92 mmol) added. The solution was stirred at room temperature for 1.5 h, after which time TLC DCM/MeOH (9:1) indicated disappearance of **81**. The solution was concentrated under reduced pressure to a pale yellow liquid (0.87 g). Flash column chromatography on silica gel using DCM/MeOH (9.5:0.5) as eluent afforded a yellow solid (0.17 g, 49 %): δ_H (250 MHz, $CDCl_3$) analysis indicated recovery of dimedone starting material.

6.2.5.16.2 Method B

81 (0.13 g, 0.38 mmol) was dissolved in 10 % H_2SO_4 in EtOAc. TLC DCM/MeOH (9:1) indicated immediate disappearance of **81**. The solution was diluted with further EtOAc, washed (H_2O), dried ($MgSO_4$), and evaporated to a white solid (32 mg, 61 %): δ_H (250 MHz, $CDCl_3$) analysis indicated recovery of dimedone starting material.

6.2.5.17 3-(N-fluorenylmethoxycarbonyl-L-valinyloxy)-5,5-dimethyl-2-cyclohexen-1-one (108)

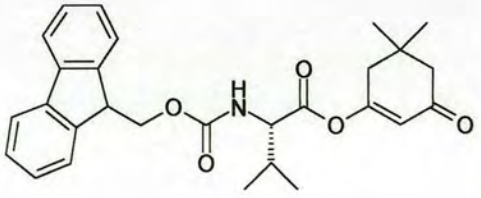

The general procedure outlined above (6.2.1.4, Method B) was followed using Fmoc-L-valine (0.25 g, 0.74 mmol) to yield a pale yellow oil. Flash column chromatography on silica gel using Pet.Ether/EtOAc (1:1) as eluent gave a pale yellow oil (41 mg, 12 %): R_f=0.76 Pet.Ether/EtOAc (1:1); ν_{max}(crude oil) 3325br (N-H), 1762 (vinyl ester), 1718 (urethane C=O), 1673 (α,β-unsaturated ketone), 1525 (amide II); δ_H (250 MHz, $CDCl_3$) 0.93-1.04 (6H, m, $CH(CH_3)_2$), 1.10 (6H, s, $C(CH_3)_2$), 2.13-2.37 (1H, m, $CH(CH_3)_2$), 2.27 (2H, s, $CH_2C(CH_3)_2$), 2.41 (2H, s, $CH_2C(CH_3)_2$), 4.23 (1H, t, *J* 7.0, $CHCH_2O$), 4.34 (1H, dd, *J* 9.0, 4.5, NHCH), 4.40 (1H, dd, *J* 12.0, 6.5, $CHCH_AH_BO$), 4.42 (1H, dd, *J* 12.0, 6.5, $CHCH_AH_BO$), 5.26 (1H, t, *J* 9.0, NH), 5.92 (1H, s, COCH=CO), 7.25-7.42 (4H, m, Ar-H), 7.59 (2H, d, *J* 7.0, Ar-H), 7.76 (2H, d, *J* 7.5, Ar-H); δ_C (63 MHz, DEPT, $CDCl_3$) 17.3 ($CH(C^AH_3C^BH_3)$), 18.9 ($CH(C^AH_3C^BH_3)$), 28.0 ($C(C^AH_3C^BH_3)$), 28.1 ($C(C^AH_3C^BH_3)$), 30.9 ($CH(CH_3)_2$), 33.1 ($C(CH_3)_2$), 41.9 ($CH_2C(CH_3)_2$), 47.1 (OCH_2CH), 50.6 ($CH_2C(CH_3)_2$), 58.7 (NHCH), 67.0 (OCH_2CH), 116.8 (COCH=CO), [119.9, (CH), 124.9 (CH), 127.0 (CH), 127.6 (CH), 8C, OFmAr-H], 141.2 (2C, Ar-Ar), 143.6 (2C, Ar-$CHCH_2$), 156.2 (CONH), 167.6 (COOC=CH), 168.9 (NHCHCO), 199.2 (COCH=COCO); MS ESI (+ve) found m/z 484.3 (MNa^+, 100 %); HRMS FAB (+ve) found m/z 462.22833 (MH^+), $C_{28}H_{32}NO_5$ requires 462.22805.

6.2.5.18 N-benzoyl-L-valine (110)

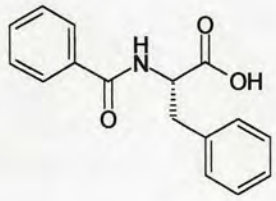

To a stirred solution of L-phenylalanine (1.82 g, 11 mmol) in anhydrous DCM (20 ml) was added chlorotrimethylsilane (1.4 ml, 11 mmol). The mixture was refluxed for 2 h before cooling to –15 °C. Benzoyl chloride (1.2 ml, 10 mmol) was added dropwise, followed by triethylamine (3.1 ml, 22 mmol) with the temperature kept

below 5 °C. The solution was stirred at –10 °C for 1.5 h, then stirring continued for a further 0.5 h at 0 °C. 0.5N HCl (2 x 10 ml) was added and the phases separated. The combined aqueous phase was washed with DCM (2 x 10 ml), dried ($MgSO_4$) and concentrated under reduced pressure to a yellow solid (3.07 g) which was triturated with ether yielding a pale yellow solid (1.72 g, 64 %): mp 179 °C, Lit.[5] 184-185 °C; $[\alpha]_D$ –8.2 (c 1.0, MeOH), Lit.[6] –3.6 (c 0.7, MeOH); R_f=0.19 DCM/MeOH (9:1); ν_{max}(nujol) 3324br (O-H), 1718 (acid C=O), 1613 (amide C=O), 1536 (amide II); δ_H (250 MHz, DMSO) 3.05-3.25 (2H, m, C*H*$_2$Ph), 4.59-4.68 (1H, m, NHC*H*), 7.14-7.35 (5H, m, Ar-*H*), 7.41-7.55 (3H, m, Ar-*H*), 7.78-7.83 (2H, m, Ar-*H*), 8.74 (1H, d, *J* 8.0, N*H*); δ_C (63 MHz, DEPT, DMSO) 36.4 (*C*H$_2$Ph), 54.4 (NH*C*H), [126.5 (CH), 127.5 (CH), 128.3 (CH), 128.4 (CH), 129.2 (CH), 131.5 (CH), 10C, *Ar*-H], 134.1 (CH$_2$*Ph*), 138.4 (CO*Ph*), 166.6 (*C*ONH), 173.4 (*C*OOH); MS ESI (-ve) found m/z 267.8 ([M-H]$^-$, 100 %); HRMS FAB (+ve) found m/z 270.11304 (MH^+), $C_{16}H_{16}NO_3$ requires 270.11302.

6.2.5.19 N-methoxycarbonyl-L-valine (115)

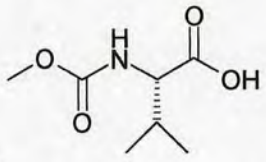

To a stirred solution of L-valine (1.29 g, 11 mmol) in anhydrous DCM (20 ml) was added chlorotrimethylsilane (1.4 ml, 11 mmol). The mixture was refluxed for 2 h before cooling to –20 °C. Methyl chloroformate (0.77 ml, 10 mmol) was added dropwise, followed by triethylamine (3.1 ml, 22 mmol) with the temperature kept below –20 °C. The solution was stirred for 2 h at –20 to –40 °C, then stirring continued for a further 1 h at 0 °C. 0.5 N HCl (2 x 10 ml) was added and the phases separated. The combined aqueous phase was washed with DCM (2 x 10 ml), dried ($MgSO_4$) and concentrated under reduced pressure to a pale yellow oil which solidified on cooling. The oil was triturated with ether to yield a white solid (1.79 g, 93 %): 110 °C, Lit.[7] 109-110 °C; $[\alpha]_D$ –6.6 (c 1.1, MeOH), Lit.[8] –8.4 (c 1.2, MeOH); ν_{max}(nujol) 3397br (O-H), 1749 (acid C=O), 1733 (urethane C=O), 1666 (C=O),

1552 (amide II); δ_H (250 MHz, DMSO) 0.86 (3H, d, *J* 6.5, CH($C^A H_3 C^B H_3$)), 0.88 (3H, d, *J* 6.5, CH($C^A H_3 C^B H_3$)), 1.96-2.07 (1H, m, C*H*(CH_3)$_2$), 3.53 (3H, s, OCH_3), 3.83 (1H, dd, *J* 8.5, 6.0, NHC*H*), 7.33 (1H, d, *J* 8.5, N*H*); δ_C (63 MHz, DEPT, DMSO) 18.1 (CH($C^A H_3 C^B H_3$)), 19.3 (CH($C^A H_3 C^B H_3$)), 29.7 (*C*H(CH_3)$_2$), 51.6 (O*C*H_3), 59.7 (NH*C*H), 157.2 (*C*ONH), 173.5 (*C*OOH); MS ESI (-ve) found m/z 173.5 ([M-H]$^-$, 100 %); HRMS FAB (+ve) found m/z 176.09215 (MH^+), $C_7H_{14}NO_4$ requires 176.09228.

6.2.5.20 3-(N-methoxycarbonyl-L-valinyloxy)-5,5-dimethyl-2-cyclohexen-1-one (116)

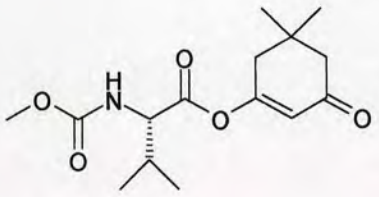

The general procedure outlined above (6.2.1.4, Method B) was followed using **115** (0.15 g, 0.86 mmol) to yield a blue/pink oil. Flash column chromatography on silica gel using Pet.Ether/EtOAc (4:3) as eluent to give a colourless oil (0.12 g, 46 %): $[\alpha]_D$ –2.4 (c 1.6, $CHCl_3$); R_f=0.59 Pet.Ether/EtOAc (4:3); ν_{max}(crude oil) 3325br (N-H), 1767 (vinyl ester), 1717 (urethane C=O), 1674 (α,β-unsaturated ketone), 1534 (amide II); δ_H (250 MHz, $CDCl_3$) 0.90 (3H, d, *J* 7.0, CH($C^A H_3 C^B H_3$)), 1.07 (3H, d, *J* 7.0, CH($C^A H_3 C^B H_3$)), 1.54 (6H, s, C(CH_3)$_2$), 2.18-2.25 (1H, m, C*H*(CH_3)$_2$), 2.28 (2H, s, CH_2C(CH_3)$_2$), 2.41 (2H, s, CH_2C(CH_3)$_2$), 3.71 (3H, s, OCH_3), 4.38 (1H, dd, *J* 9.0, 5.0, NHC*H*), 5.12 (1H, d, *J* 9.0, N*H*), 5.90 (1H, s, COC*H*=CO); δ_C (63 MHz, DEPT, $CDCl_3$) 17.8 (CH($C^A H_3 C^B H_3$)), 19.5 (CH($C^A H_3 C^B H_3$)), 28.6 (C($C^A H_3 C^B H_3$)), 28.7 (C($C^A H_3 C^B H_3$)), 31.4 (*C*H(CH_3)$_2$), 33.7 (*C*(CH_3)$_2$), 42.5 (*C*H_2C(CH_3)$_2$), 51.1 (*C*H_2C(CH_3)$_2$), 53.0 (O*C*H_3), 59.3 (NH*C*H), 117.3 (CO*C*H=CO), 157.6 (*C*ONH), 168.5 (COO*C*=CH), 169.8 (NHCH*C*O), 200.1 (*C*OCH=COCO); HRMS FAB (+ve) found m/z 298.16539 (MH^+), $C_{15}H_{24}NO_5$ requires 298.16545.

6.2.5.21 Attempted preparation of N-cyclohexylaminocarbonyl-L-valine (hydantoin product isolated)

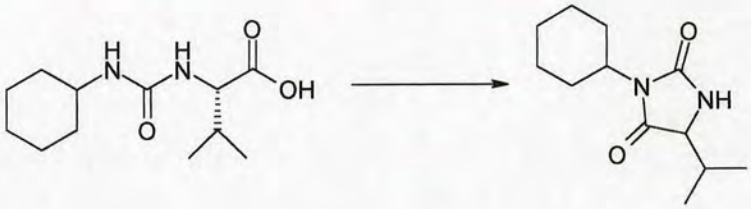

To a solution of cyclohexylamine (0.24 ml, 2.13 mmol) in DCM (5 ml) and MeCN (5 ml) were added DSC (0.55 g, 2.13 mmol) and DMAP (0.13 g, 1.07 mmol). The mixture was stirred at room temperature overnight resulting in a cloudy white solution. L-valine (0.25 g, 2.13 mmol) was added followed by triethylamine (0.15 ml, 1.07 mmol) and the reaction again stirred overnight. The mixture was concentrated under reduced pressure to a white residue which was dissolved in saturated $NaHCO_3$ solution (20 ml). The reaction mixture was acidified to pH1 with 2M HCl and extracted with EtOAc (2 x 20 ml). The combined extracts were washed with 2M HCl (5 ml), dried ($MgSO_4$) and concentrated under reduced pressure to a white solid (0.32 g):MS ESI (+ve) found m/z 225.0 (hydantoin, 100 %), 248.0 (hydantoinNa^+, 42).

6.2.5.22 Attempted preparation of N-butylaminocarbonyl-L-valine

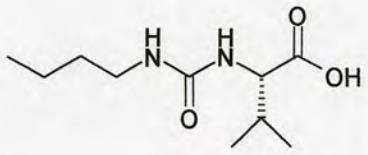

The general procedure outlined above (6.2.5.21) was followed using *N*-butylamine (0.21 ml, 2.13 mmol) to yield a white solid (0.18 g): analysis indicated recovery of L-valine starting material.

6.2.5.23 N-cyclohexyloxycarbonyl-L-valine (123)

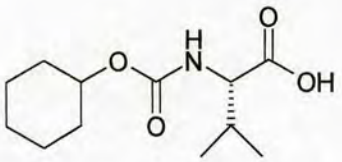

To a solution of cyclohexanol (0.23 ml, 2.13 mmol) in DCM (5 ml) and MeCN (5 ml) were added DSC (0.55 g, 2.13 mmol) and DMAP (0.13 g, 1.07 mmol). The mixture was stirred at room temperature overnight resulting in a cloudy white solution. L-valine (0.25 g, 2.13 mmol) was added followed by triethylamine (0.15 ml, 1.07 mmol) and the reaction again stirred overnight. The mixture was concentrated under reduced pressure to a white residue which was dissolved in saturated $NaHCO_3$ solution (20 ml). The reaction mixture was acidified to pH1 with 2M HCl and extracted with EtOAc (2 x 20 ml). The combined extracts were washed with 2M HCl (5 ml), dried ($MgSO_4$) and concentrated under reduced pressure to yield a colourless oil (0.47 g). Flash column chromatography on the Biotage system (column 40S) using DCM/MeOH (9.5:0.5) as eluent afforded a colourless oil (0.21 g, 40 %): $[\alpha]_D$ –1.4 (c 1.2, $CHCl_3$); R_f=0.40 DCM/MeOH (9.5:0.5); ν_{max}(crude oil) 3468br (O-H), 1779 (acid C=O), 1706 (urethane C=O); δ_H (200 MHz, $CDCl_3$) 0.92 (3H, d, *J* 7.0, CH($C^AH_3C^BH_3$)), 0.99 (3H, d, *J* 7.0, CH($C^AH_3C^BH_3$)), 1.26-1.56 (6H, m, $OCHCH_2(CH_2)_3CH_2$), 1.71-1.88 (4H, m, $OCHCH_2(CH_2)_3CH_2$), 2.20-2.24 (1H, m, $CH(CH_3)_2$), 4.20 (1H, dd, *J* 8.5, 4.0, NHC*H*), 4.55-4.70 (1H, m, C*H*OCO), 5.48 (1H, d, *J* 8.5, N*H*), 8.31 (1H, br s, COO*H*); δ_C (63 MHz, DEPT, $CDCl_3$) 17.9 ($CH(CH_3C^BH_3)$), 19.8 ($CH(C^AH_3CH_3)$), [24.3, (CH_2), 25.9, (CH_2), 3C, $OCHCH_2(CH_2)_3CH_2$)], 32.0 ($CH(CH_3)_2$), [32.4, (CH_2), 2C, $OCHCH_2(CH_2)_3CH_2$)], 60.5 (NHCH), 73.3 (CHOCO), 157.3 (CONH), 176.7 (COOH); MS ESI (+ve) found m/z 244.0 (MH^+, 45 %), 265.9 (MNa^+, 100); HRMS FAB (+ve) found m/z 244.15473 (MH^+), $C_{12}H_{22}NO_4$ requires 244.15488.

6.2.5.24 N-(2-methyl-allyloxycarbonyl)-L-valine (124)

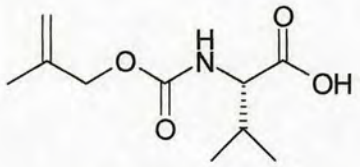

The general procedure outlined above (6.2.5.23) was followed using 2-methyl-prop-2-enol (0.18 ml, 2.13 mmol) to yield a colourless oil (0.23 g, 51 %): $[\alpha]_D$ –3.1 (c 1.3, $CHCl_3$); R_f=0.41 DCM/MeOH (9:1); ν_{max}(crude oil) 3328br (O-H), 1716br (acid C=O & urethane C=O), 1530 (amide II); δ_H (200 MHz, $CDCl_3$) 0.92 (3H, d, *J* 7.0, $CH(C^AH_3C^BH_3)$), 0.98 (3H, d, *J* 7.0, $CH(C^AH_3C^BH_3)$), 1.75 (3H, s, $CH_2{=}CCH_3$), 2.20-2.25 (1H, m, $CH(CH_3)_2$), 4.13 (1H, dd, *J* 8.0, 4.0, NHCH), 4.42 (1H, d, *J* 13.5, CH^AH^BOCO), 4.52 (1H, d, *J* 13.5, CH^AH^BOCO), 4.93 (2H, d, *J* 24.0, $CH_2{=}CCH_3$), 5.80 (1H, d, *J* 8.0, NH), 8.13 (1H, br s, COOH); δ_C (63 MHz, DEPT, $CDCl_3$) 18.0 ($CH(CH_3)_2$), 19.8 ($CH_2{=}CCH_3$), 31.9 ($CH(CH_3)_2$), 61.2 (NHCH), 68.2 (CH_2OCO), 112.3 ($CH_2{=}CCH_3$), 141.3 ($CH_2{=}CCH_3$), 157.0 (CONH), 177.5 (COOH); MS ESI (+ve) found m/z 215.7 (MH^+, 35 %), 232.9 (MNH_4^+, 23), 237.8 (MNa^+, 100); HRMS FAB (+ve) found m/z 216.12313 (MH^+), $C_{10}H_{18}NO_4$ requires 216.12358.

6.2.5.25 carbonic acid 5,5-dimethyl-3-oxo-cyclohex-1-enyl ester isobutyl ester (128)

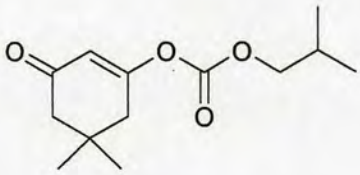

128 was isolated as a by-product of 6.2.1.4, Method A, using isobutyl chloroformate; R_f=0.39 Pet.Ether/EtOAc (4:1); ν_{max}(crude oil) 1769, 1705 (anhydride), 1673 (α,β-unsaturated ketone); δ_H (250 MHz, $CDCl_3$) 0.97 (6H, d, *J* 7.0, $CH(CH_3)_2$), 1.10 (6H, s, $C(CH_3)_2$), 1.43-2.08 (1H, m, $CH(CH_3)_2$), 2.26 (2H, s, $CH_2C(CH_3)_2$), 2.44 (2H, s, $CH_2C(CH_3)_2$), 3.99 (2H, d, *J* 7.0, $CH_2CH(CH_3)_2$), 6.02 (1H, s, COCH=CO); δ_C (63

MHz, DEPT, $CDCl_3$) 19.2 ($CH(CH_3)_2$), 28.1 ($CH(CH_3)_2$), 28.5 ($C(CH_3)_2$), 33.5 ($C(CH_3)_2$), 42.1 ($CH_2C(CH_3)_2$), 51.0 ($CH_2C(CH_3)_2$), 75.6 ($OCH_2CH(CH_3)_2$), 115.7 (COCH=CO), 151.6 (OCOO), 168.3 (COOC=CH), 200.3 (COCH=COCO); HRMS FAB (+ve) found m/z 241.14392 (MH^+), $C_{13}H_{21}O_4$ requires 241.14398.

6.2.5.26 5,5-dimethyl-4-(3-phenyl-allyl)-cyclohexane-1,3-dione (129)

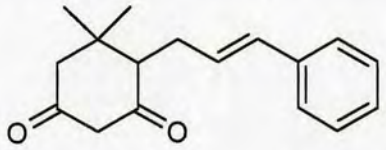

The general procedure outlined above (6.2.5.12) was followed using cinnamyl bromide (6.18 g, 31.38 mmol) to yield a dark orange liquid (29.07 g). Flash column chromatography on the Biotage Quad system (40M column, several loadings) using hexane/EtOAc (2.5:1) yielded a yellow oil (2.05 g, 28 %): R_f=0.31 hexane/EtOAc (1:1); ν_{max}(crude oil) 1705 (α-branched ketone); δ_H (250 MHz, $CDCl_3$) 0.84 (3H, s, $C(C^AH_3C^BH_3)$), 1.16 (3H, s, $C(C^AH_3C^BH_3)$), 2.15-2.74 (5H, m, $COCH_2C(CH_3)_2$, $CHCH_2CH$=CHPh, $CHCH_2CH$=CHPh), 3.33 (1H, d, *J* 16.5, $COCH^AH^BCO$), 3.44 (1H, d, *J* 16.5, $COCH^AH^BCO$), 6.15-6.29 (1H, m, $CHCH_2CH$=CHPh), 6.45 (1H, d, *J* 16.0, $CHCH_2CH$=CHPh) 7.16-7.34 (5H, m, Ar-*H*); MS ESI (+ve) 257.0 (MH^+, 22 %), 278.9 (MNa^+, 100), 319.9 (19); HRMS FAB (+ve) found m/z 257.15414 (MH^+), $C_{17}H_{21}O_2$ requires 257.15416.

6.2.5.27 3-(N-benzyloxycarbonyl-L-valinyloxy)-6,6-dimethyl-2-cyclohexen-1-one (131)

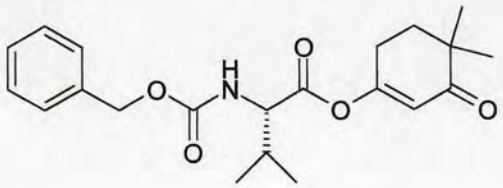

The general procedure outlined above (6.2.1.4, Method B) was followed using 4,4-dimethylcyclohexane-1,3-dione (0.12 g, 0.82 mmol) to yield a colourless oil (0.14 g, 45 %): R_f=0.52 Pet.Ether/EtOAc (4:3); $[\alpha]_D$ –5.7 (c 1.4, $CHCl_3$); ν_{max}(crude oil)

3330br (N-H), 1766 (vinyl ester), 1719 (urethane C=O), 1673 (α,β-unsaturated ketone), 1525 (amide II); δ_H (250 MHz, $CDCl_3$) 0.96 (3H, d, *J* 7.0, CH($C^AH_3C^BH_3$)), 1.03 (3H, d, *J* 7.0, CH($C^AH_3C^BH_3$)), 1.13 (6H, s, $C(CH_3)_2$), 1.86 (2H, t, *J* 6.0, $CH_2C(CH_3)_2$), 2.19-2.28 (1H, m, $CH(CH_3)_2$), 2.54 (2H, t, *J* 6.0, $CH_2CH_2C(CH_3)_2$), 4.39 (1H, dd, *J* 9.0, 5.0, NHC*H*), 5.12 (2H, s, OCH_2Ph), 5.22 (1H, d, *J* 9.0, N*H*), 5.79 (1H, s, COC*H*=CO), 7.36 (5H, s, Ar-*H*); δ_C (63 MHz, DEPT, $CDCl_3$) 18.0 (CH($C^AH_3C^BH_3$)), 19.4 (CH($C^AH_3C^BH_3$)), 24.4 ($C(CH_3)_2$), 26.1 ($CH_2C(CH_3)_2$), 31.5 ($CH(CH_3)_2$), 35.2 ($CH_2CH_2C(CH_3)_2$), 41.1 ($C(CH_3)_2$), 59.6 (NHCH), 67.7 (OCH_2Ph), 116.7 (COCH=CO), [128.6 (CH), 128.8 (CH), 129.0 (CH), 5C, *Ar*-H], 136.4 (OCH_2Ph), 156.6 (CONH), 167.8 (COOC=CH), 169.6 (NHCHCO), 204.3 (COCH=COCO); MS ESI (+ve) 396.3 (MNa^+, 100 %), 459.5 (23); HRMS FAB (+ve) found m/z 374.19673 (MH^+), $C_{21}H_{28}NO_5$ requires 374.19675.

6.2.6 Results and Discussion III - Library Rehearsal

For experimental conditions refer to **Library Synthesis 6.2.7**.

Table 6.1

No.	Structure	^{1}H & ^{13}C NMR
134	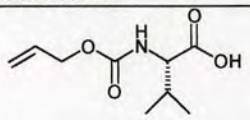	δ_H (360 MHz, $CDCl_3$) 0.92 (3H, d, *J* 7.0, CH($C^AH_3C^BH_3$)), 0.99 (3H, d, *J* 7.0, CH($C^AH_3C^BH_3$)), 2.19-2.29 (1H, m, $CH(CH_3)_2$), 4.21 (1H, dd, *J* 9.0, 4.0, NHC*H*), 4.56 (1H, dd, *J* 5.5, 4.5, CH^AH^BOCO), 4.58 (1H, dd, *J* 5.5, 4.5, CH^AH^BOCO), 5.17-5.36 (2H, m, CH_2=CH), 5.65 (1H, d, *J* 9.0, N*H*), 5.85-6.01 (1H, m, CH_2=C*H*), 8.68 (1H, br s, COO*H*); δ_C (63 MHz, DEPT, $CDCl_3$) 17.9 (CH($C^AH_3C^BH_3$)), 19.8 (CH($C^AH_3C^BH_3$)), 31.8 ($CH(CH_3)_2$), 60.6 (NHCH), 65.8 (CH_2OCO), 117.7 (CH_2=CH), 133.5 (CH_2=CH), 157.3 (CONH), 176.7 (COOH). DMAP present

123	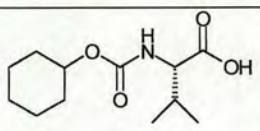	δ_H (360 MHz, $CDCl_3$) 0.92 (3H, d, *J* 7.0, CH($C^AH_3C^BH_3$)), 0.99 (3H, d, *J* 7.0, CH($C^AH_3C^BH_3$)), 1.26-1.56 (6H, m, $OCHCH_2(CH_2)_3CH_2$), 1.71-1.88 (4H, m, $OCHCH_2(CH_2)_3CH_2$), 2.20-2.24 (1H, m, $CH(CH_3)_2$), 4.20 (1H, dd, *J* 8.5, 4.0, NHC*H*), 4.55-4.70 (1H, m, C*H*OCO), 5.48 (1H, d, *J* 8.5, N*H*), 8.31 (1H, br s, COO*H*); δ_C (63 MHz, DEPT, $CDCl_3$) 17.9 (CH($C^AH_3C^BH_3$)), 19.8 (CH($C^AH_3C^BH_3$)), [24.3, (CH_2), 25.9, (CH_2), 3C, $OCHCH_2(CH_2)_3CH_2$)], 32.0 ($CH(CH_3)_2$), [32.4, (CH_2), 2C, $OCHCH_2(CH_2)_3CH_2$)], 60.5 (NHCH), 73.3 (CHOCO), 157.3 (CONH), 176.7 (COOH). DMAP present
145	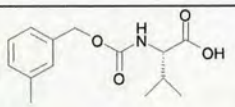	δ_H (360 MHz, $CDCl_3$) 0.92 (3H, d, *J* 7.0, CH($C^AH_3C^BH_3$)), 1.00 (3H, d, *J* 7.0, CH($C^AH_3C^BH_3$)), 2.11-2.30 (1H, m, $CH(CH_3)_2$), 3.19 (3H, s, CH_3Ph), 4.15-4.30 (1H, m, NHC*H*), 5.08 (2H, s, CH_2OCO), 5.65 (1H, d, *J* 7.0, N*H*), 7.11-7.34 (4H, m, Ar-*H*), 7.61 (1H, br s, COO*H*); δ_C (63 MHz, DEPT, $CDCl_3$) 17.9 (CH($C^AH_3C^BH_3$)), 19.7 (CH($C^AH_3C^BH_3$)), 21.8 ($PhCH_3$), 31.8 ($CH(CH_3)_2$), 60.5 (NHCH), 67.1 (CH_2OCO), [125.4 (CH), 128.8 (CH), 129.1 (CH), 4C, *Ar*-H], 136.9 (OCH_2Ph), 138.5 (CH_3Ph), 157.5 (CONH), 176.0 (COOH). DMAP present
124	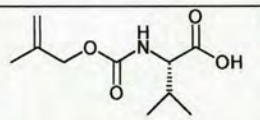	δ_H (360 MHz, $CDCl_3$) 0.92 (3H, d, *J* 7.0, CH($C^AH_3C^BH_3$)), 0.98 (3H, d, *J* 7.0, CH($C^AH_3C^BH_3$)), 1.75 (3H, s, $CH_2=CCH_3$), 2.20-2.25 (1H, m, $CH(CH_3)_2$), 4.13 (1H, dd, *J* 8.0, 4.0, NHC*H*), 4.42 (1H, d, *J* 13.5, CH^{A}H^{B}OCO), 4.52 (1H, d, *J* 13.5, CH^{A}H^{B}OCO), 4.93 (2H, d, *J* 24.0, $CH_2=CCH_3$), 5.80 (1H, d, *J* 8.0, N*H*), 8.13 (1H, br s, COO*H*); δ_C (63 MHz, DEPT, $CDCl_3$) 18.0 ($CH(CH_3)_2$), 19.8 ($CH_2=CCH_3$), 31.9 ($CH(CH_3)_2$), 61.2 (NHCH), 68.2 (CH_2OCO), 112.3 ($CH_2=CCH_3$), 141.3 ($CH_2=CCH_3$), 157.0 (CONH), 177.5 (COOH). DMAP present

156	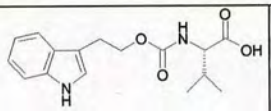	δ_H (360 MHz, $CDCl_3$) 0.89 (3H, d, *J* 7.0, CH($C^AH_3C^BH_3$)), 0.97 (3H, d, *J* 7.0, CH($C^AH_3C^BH_3$)), 2.14-2.26 (1H, m, C*H*(CH_3)$_2$), 3.07 (2H, t, *J* 6.5,CH_2CH_2O), 4.14-4.24 (1H, m, NHC*H*), 4.31-4.42 (2H, m, CH_2CH_2O), 5.42 (1H, d, *J* 8.5, N*H*), 7.03 (1H, s, NHC*H*=C), 7.06-7.19 (2H, m, Ar-*H*), 7.33 (1H, d, *J* 8.0, Ar-*H*), 7.59 (1H, d, *J*, 7.0, Ar-*H*), 8.27 (1H, br s, COO*H*); δ_C (63 MHz, DEPT, $CDCl_3$) 17.3 (CH($C^AH_3C^BH_3$)), 19.1 (CH($C^AH_3C^BH_3$)), 29.6 (CH_2CH_2O), 30.9 (*C*H(CH_3)$_2$), 59.5 (NH*C*H), 65.0 (CH_2CH_2O), 111.1 (NHCH=C), 111.1 (NHCH=*C*), [118.5 (CH), 119.2 (CH), 121.8 (CH), 122.2 (CH), 4C, *Ar*-H], 127.3 (*Ar*-C), 136.0 (*Ar*-C), 156.7 (*C*ONH), 176.0 (*C*OOH).
162	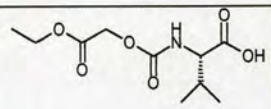	δ_H (360 MHz, $CDCl_3$) 0.98 (3H, d, *J* 7.0, CH($C^AH_3C^BH_3$)), 1.05 (3H, d, *J* 7.0, CH($C^AH_3C^BH_3$)), 1.32 (3H, t, *J* 7.0, OCH_2CH_3), 2.21-2.28 (1H, m, C*H*(CH_3)$_2$), 4.15-4.17 (1H, m, NHC*H*), 4.26 (2H, q, *J* 7.0, OCH_2CH_3), 4.60 (1H, d, *J* 16.0, C(O)CH^AH^BO), 4.67 (1H, d, *J* 16.0, C(O)CH^AH^BO), 5.61 (1H, d, *J* 8.5, N*H*); δ_C (63 MHz, DEPT, $CDCl_3$) 14.5 (OCH_2CH_3), 17.7 (CH($C^AH_3C^BH_3$)), 19.4 (CH($C^AH_3C^BH_3$)), 31.5 (*C*H(CH_3)$_2$), 60.5 (NH*C*H), 61.9 OCH_2CH_3), 77.6 (C(O)CH_2O), 156.0 (*C*ONH), 169.1 (*C*(O)CH_2O), 176.0 (*C*OOH).

151	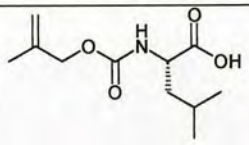	δ_H (360 MHz, $CDCl_3$) 0.95 (3H, d, *J* 7.0, $CH(C^AH_3C^BH_3)$), 0.97 (3H, d, *J* 7.0, $CH(C^AH_3C^BH_3)$), 1.50-1.65 (1H, m, $CH(CH_3)_2$), 1.65-1.81 (2H, m, $CH_2CH(CH_3)_2$), 1.75 (3H, s, $CH_2=CCH_3$), 4.30-4.42 (1H, m, NHC*H*), 4.48 (2H, s, CH_2OCO), 4.93 (2H, d, *J* 23.0, $CH_2=CCH_3$), 5.61 (1H, d, *J* 8.0, N*H*), 8.30 (1H, br s, COO*H*); δ_C (63 MHz, DEPT, $CDCl_3$) 19.8 ($CH_2=CCH_3$), 22.4 ($CH(CH_3C^BH_3)$), 23.6 ($CH(C^AH_3CH_3)$), 25.3 ($CH(CH_3)_2$), 43.1 ($CH_2CH(CH_3)_2$), 54.2 (NH*C*H), 68.2 (CH_2OCO), 112.3 ($CH_2=CCH_3$), 141.2 ($CH_2=CCH_3$), 157.3 (*C*ONH), 178.1 (*C*OOH). DMAP present
152	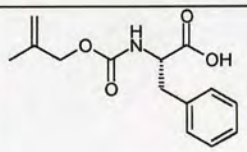	δ_H (250 MHz, $CDCl_3$) 1.74 (3H, s, $CH_2=CCH_3$), 3.12 (1H, dd, *J* 14.0, 6.0, CH^AH^BPh), 3.26 (1H, dd, *J* 14.0, 5.0, CH^AH^BPh), 4.37 (1H, d, *J* 13.5, CH^AH^BOCO), 4.45-4.61 (1H, m, NHC*H*), 4.52 (1H, d, *J* 13.5, CH^AH^BOCO), 4.92 (2H, d, *J* 15.0, $CH_2=CCH_3$), 5.58 (1H, d, *J* 7.5, N*H*), 7.70 (1H, br s, COO*H*); δ_C (63 MHz, DEPT, $CDCl_3$) 19.8 ($CH_2=CCH_3$), 38.6 (CH_2Ph), 56.2 (NH*C*H), 68.3 (CH_2OCO), 112.4 ($CH_2=CCH_3$), [126.9 (CH), 128.7 (CH), 130.1 (CH), 5C, *Ar*-H], 137.6 (CH_2Ph), 141.1 ($CH_2=CCH_3$), 157.4 (*C*ONH), 175.9 (*C*OOH). DMAP present
153	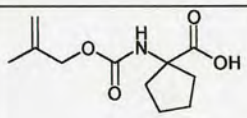	δ_H (360 MHz, $CDCl_3$) 1.76 (3H, s, $CH_2=CCH_3$), 1.77-1.85 (4H, m, $CCH_2(CH_2)_2CH_2$), 2.08-2.37 (4H, m, $CCH_2(CH_2)_2CH_2$), 4.48 (2H, s, CH_2OCO), 4.96 (2H, d, *J* 23.0, $CH_2=CCH_3$), 5.88 (1H, s, N*H*); δ_C (63 MHz, DEPT, $CDCl_3$) 19.8 ($CH_2=CCH_3$), [26.0 (CH_2), 30.1 (CH_2), 38.0 (CH_2), 4C, ($C(CH_2)_4$)], 68.0 ($C(CH_2)_4$), 69.1 (CH_2OCO), 113.3 ($CH_2=CCH_3$), 141.3 ($CH_2=CCH_3$), 159.0 (*C*ONH), 178.2 (*C*OOH). DMAP present

154	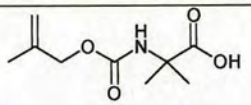	δ_H (360 MHz, $CDCl_3$) 1.59 (6H, s, $C(CH_3)_2$), 1.73 (3H, s, $CH_2=CCH_3$), 4.43 (2H, s, CH_2OCO), 4.89 (2H, d, *J* 23.0, $CH_2=CCH_3$), 5.56 (1H, s, NH); δ_C (63 MHz, DEPT, $CDCl_3$) 19.3 ($CH_2=CCH_3$), 24.7 ($C(CH_3)_2$), 57.5 ($C(CH_3)_2$), 68.7 (CH_2OCO), 112.8 ($CH_2=CCH_3$), 141.7 ($CH_2=CCH_3$), 159.0 (CONH), 181.0 (COOH). DMAP present
155	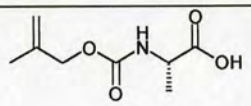	δ_H (360 MHz, $CDCl_3$) 1.47 (3H, d, *J* 7.0, $CHCH_3$), 1.75 (3H, s, $CH_2=CCH_3$), 4.24 (1H, dq, *J* 7.0, 7.0, NHCH), 4.48 (2H, s, CH_2OCO), 4.93 (2H, d, *J* 23.0, $CH_2=CCH_3$), 5.86 (1H, d, *J* 7.0, NH), 8.71 (1H, br s, COOH); δ_C (63 MHz, DEPT, $CDCl_3$) 19.8 ($CH_2=CCH_3$), 40.2 ($CHCH_3$), 51.4 (NHCH), 68.1 (CH_2OCO), 112.3 ($CH_2=CCH_3$), 141.3 ($CH_2=CCH_3$), 157.2 (CONH), 178.2 (COOH). DMAP present

6.2.7 Results and Discussion III - Library Synthesis

6.2.7.1 Synthesis step 1

Table 6.2 Reagents

Reagent	**Molarity (M)**	**No. Moles Dispensed (mmol)**	**Volume Dispensed (ml)**	**Solvent**
DSC	0.63	0.44	0.70	MeCN
DMAP	0.27	0.20		
Alcohol	2.00	0.40	0.20	MeCN
NEt_3	0.44	0.40	0.90	0.5M $NaHCO_3$
Acid	0.44	0.40		

Alcohols	**Acids**
allyl alcohol	L-valine
cyclohexanol	L-leucine
3-methyl benzylalcohol	L-phenylalanine
2-methyl prop-2-enol	1-amino-1-cyclopentane carboxylic acid
tryptophol	2-amino isobutyric acid
ethyl glycolate	L-alanine

6.2.7.1.1 Experimental conditions step 1

1. A solution was prepared with concentration 0.63 M DSC and 0.27 M DMAP and distributed into reaction vessels on the Bodhan Neptune™-MB Automated Workstation.
2. The Neptune was used to prepare 2.00 M solutions of each of the 6 alcohols in reaction vessels.
3. The DSC/DMAP solution (0.70 ml) was dispensed to 36 tubes in each of four MiniBlocks using the Neptune.
4. Each alcohol solution (0.20 ml) was dispensed to a horizontal line of 6 tubes in each of the four MiniBlocks using the Neptune.
5. The four MiniBlocks were shaken on the MiniBlock™ High Capacity Shaking and Washing Station for 4 h.
6. The Neptune was used to prepare six amino acid solutions of concentration 0.40 M amino acid and 0.40 M NEt_3 in reaction vessels.
7. Each amino acid/NEt_3 solution (0.90 ml) was dispensed to a vertical line of 6 tubes in each of the four MiniBlocks using the Neptune.
8. The Miniblocks were shaken on the Shaking Station overnight.
9. The four MiniBlocks were drained into four 96 well plates and the MeCN/$NaHCO_3$ solutions concentrated under reduced pressure using the Christ ALPHA-2-4 Freeze Dryer, BETA-RVC Ceramic Vacuum Measurement system (4 h, 25 °C, 100; 6 h, 25 °C, 10).
10. The samples in each 96 well plate were manually redissolved in MeCN/H_2O (1:1) immediately prior to running on the ZMD 4000.

11. Each plate was transferred in turn to the ZMD 4000 (7 min run, gradient H_2O/MeCN (95:5)→(5:95), CV=25) for mass-directed purification of the samples.
12. The fractions collected from the ZMD 4000 fraction collector were transferred from test tubes to labelled 20 ml reaction vials (compatible with the Christ fittings) and the H_2O/MeCN solutions concentrated under reduced pressure using the Christ.
13. Samples from two of the blocks were then redissolved in DCM using the Neptune and manually transferred (in order to limit loss of sample) to a set of tared test tubes in a 48 position block (compatible with the Christ fittings) The samples were again concentrated under reduced pressure using the Christ, and the tubes reweighed in order to establish an average yield for the 36 samples per block prepared in step 1.

The highest yield obtained from the sample sets studied was 73 %, corresponding to 0.22 mmol of this particular sample. Reagents for step 2 were therefore added on a 0.22 mmol scale.

6.2.7.2 Synthesis step 2

Dimedone analogues

5,5-dimethyl-cyclohexane-1,3-dione

4-allyl-5,5-dimethyl-cyclohexane-1,3-dione

4-benzyl-5,5-dimethyl-cyclohexane-1,3-dione

4-cyclohexylmethyl-5,5-dimethyl-cyclohexane-1,3-dione

6.2.7.2.1 Experimental conditions step 2

1. The Neptune was used to prepare four 2.2 M solutions of NEt_3, ethyl chloroformate, 4-allyldimedone and 4-benzyldimedone respectively, in DCM.
2. The Neptune was used to prepare a solution of concentration 2.2 M dimedone and 2.2 M NEt_3 (addition of NEt_3 was required to get dimedone into solution) in DCM.
3. The Neptune was used to prepare a solution of concentration 2.2 M 4-cyclohexyldimedone and 2.2 M NEt_3 in DCM.
4. The 36 samples from each block were redissolved in DCM (0.5 ml) and manually transferred to one of four MiniBlocks.
5. The four MiniBlocks were placed on the MiniBlock Shaking and Washing Station and cooled to –10 °C using the Julabo FP40. The blocks were shaken at setting 540.
6. The triethylamine (0.10 ml) and ethyl chloroformate (0.10 ml) solutions were dispensed in turn to 36 tubes in each of four MiniBlocks using the Neptune.
7. The Julabo FP40 was reset to 0 °C and shaking continued for 2 h.
8. The dimedone solution (0.1 ml) was dispensed to 36 tubes of one MiniBlock. Similarly, the three 4-alkyldimedone solutions were dispensed to the other three MiniBlocks respectively. The reactions were allowed to warm to room temperature with shaking overnight.
9. The four MiniBlocks were drained into four 96 well plates and the DCM solutions concentrated under reduced pressure using the Christ.
10. The samples in each 96 well plate were manually redissolved in MeCN/H_2O (1:1) immediately prior to running on the ZMD 4000.
11. Each plate was transferred in turn to the ZMD 4000 (7 min run, gradient H_2O/MeCN (95:5)→(5:95), CV=25) for mass-directed purification of the samples.
12. The fractions collected from the ZMD 4000 fraction collector were transferred from test tubes to labelled 20 ml reaction vials (compatible with the Christ fittings) and the H_2O/MeCN solutions concentrated under reduced pressure using the Christ.

13. All 82 samples successfully collected from the ZMD 4000 were then manually redissolved in DCM and transferred to a set of tared test tubes for weighing (as in step 1, 13), before final transferral to a 96 well plate.

6.2.8 Results and Discussion IV

6.2.8.1 3,5-dimethoxy-1,4-dihydrobenzoic acid (202)

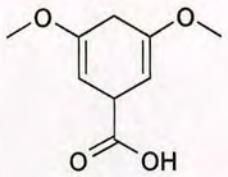

To a solution 3,4,5-trimethoxybenzoic acid (5.0 g, 24.0 mmol) in ethanol (35 ml) and liquid ammonia (230 ml) at –78 °C, was added sodium (2.9 g, 126 mmol) in small pieces. When the blue colouration had disappeared ammonium chloride (11.6 g, 216 mmol) was added. The ammonia was allowed to evaporate overnight. The resulting residue was dissolved in ice-water (300 ml). Alternate additions of 2N HCl followed by immediate extraction with DCM were carried out until the solution reached pH1. The combined DCM extracts were washed with H_2O x 2, dried ($MgSO_4$) and concentrated under reduced pressure to a white solid (3.73 g, 85 %): mp 117 °C, Lit.[9] 118 °C; R_f=0.71 DCM/MeOH (9:1); ν_{max}(nujol) 2727br (OH), 1720 (acid C=O), 1592br (vinyl ether, C=C); δ_H (200 MHz, $CDCl_3$) 2.79 (2H, dt, *J* 7.0, 1.0, CH_2COCH_3), 3.60 (6H, s, 2xOCH_3), 3.97 (1H, tt, *J* 7.0, 3.5, C*H*COOH), 4.76 (2H, dt, *J* 3.5, 1.0, 2xC*H*=$COCH_3$); δ_C (63 MHz, $CDCl_3$) 36.8 (*C*HCOOH), 40.4 (CH_2COCH_3), 51.8 (OCH_3), 86.4 (*C*H=$COCH_3$), 154.7 (CH=*C*OCH_3), 176.0 (*C*OOH); HRMS FAB (+ve) found m/z 185.08138 (MH^+), $C_9H_{13}O_4$ requires 185.08133.

6.2.8.2 5-carboxy-cyclohexane-1,3-dione (203)

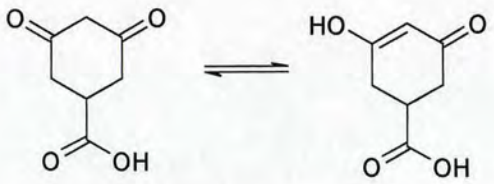

The bis enol ether **202** (0.21 g, 1.12 mmol) was suspended in 2.4 % HCl solution (2 ml) and heated in a water bath at 60 °C for 15 min. The resulting clear solution was concentrated under reduced pressure and the residue obtained was triturated with a small amount of ether and filtered to give a pale yellow solid (0.18 g, 99 %): mp 191 °C, Lit.[10] 182 °C; ν_{max}(nujol) 1721 (acid C=O), 1685 (ketone); δ_H (200 MHz, DMSO); 2.42 (4H, d, *J* 7.0, 2xCH_2CHCO$_2$H), 2.88-3.03 (1H, m, C*H*CO$_2$H), 5.21 (1H, s, COC*H*=COH); δ_C (63 MHz, DMSO) 34.6 (*C*H$_2$CHCO$_2$H), 37.9 (*C*HCO$_2$H), 104.0 (COCH=COH), 174.8 (CO), 186.6 (*C*O$_2$H); MS ESI (+ve) found m/z 82.8 (100 %), 156.8 (MH^+, 88), 197.8 (52), 313.1 (dimer, 24); HRMS FAB (+ve) found m/z 157.04942 (MH^+), $C_7H_9O_4$ requires 157.05008.

6.2.8.3 3-benzylamino-5-oxo-cyclohex-3-enecarboxylic acid benzylamide (204)

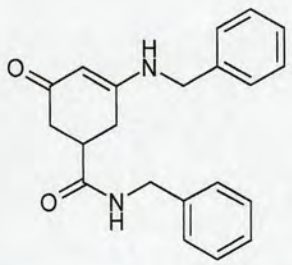

To a stirred solution of 5-carboxy-cyclohexane-1,3-dione **203** (50 mg, 0.32 mmol), TBTU (103 mg, 0.32 mmol) and DIPEA (56 µl, 0.32 mmol) in DMF (1 ml) was added benzylamine (35 µl, 0.32 mmol) and the reaction stirred at room temperature for 48 h. The reaction mixture was diluted with ether resulting in a brown suspension. EtOAc and H_2O were added, and the organic layer (containing precipitate) separated and concentrated under reduced pressure. The resulting yellow

residue was triturated with EtOAc, filtered and washed with ether to yield a pale yellow solid. ^{1}H NMR and MS results were unclear so the solid was re-suspended in EtOAc, washed with 2N HCl, filtered and washed with ether to give a white solid (55 mg, 51 %): mp 218 °C; ν_{max}(crude oil) 3275 (N-H), 1651 (α,β-unsaturated ketone), 1604 (enamine C=C), 1549 (amide II); δ_H (200 MHz, DMSO) 2.66 (2H, d, *J* 6.0, C*H*$_2$CHCONH), 2.82 (2H, d, *J* 6.0, C*H*$_2$CHCONH), 3.05-3.10 (1H, m, CH$_2$C*H*CO), 4.25 (2H, s, C*H*$_2$Ph), 4.53 (2H, d, *J* 4.5, C*H*$_2$Ph), 5.74 (1H, s, C*H*=CNH), 7.24-7.34 (10H, m, Ar-*H*); MS ESI (+ve) found m/z 335.1 (MH^+, 100 %); HRMS FAB (+ve) found m/z 335.17523 (MH^+), $C_{21}H_{23}N_2O_2$ requires 335.17595.

6.2.8.4 N-benzyl-3,5-dimethoxy-benzamide (206)

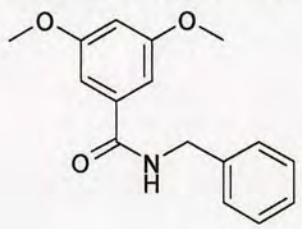

To a stirred solution of bis enol ether **202** (non-recrystallised sample) (0.11 g, 0.61 mmol) in DMF (2 ml) were added DIPEA (0.10 ml, 0.61 mmol), TBTU (0.20 g, 0.61 mmol) and benzylamine (0.07 ml, 0.61 mmol). The solution turned orange in colour on addition of TBTU, then went pale yellow. Stirring was continued overnight at room temperature. The resulting solution was diluted with ether, washed with H_2O x 2, and the ether layer dried ($MgSO_4$) and concentrated under reduced pressure to a yellow oil (0.06 g), a complex mixture by TLC. Flash column chromatography yielded off-white crystals (0.02 g, 13 %): mp 108 °C; R_f=0.37 hexane/EtOAc (1:1); ν_{max}(nujol) 3283 (N-H), 1631 (aryl ether C=C), 1601 (Ar-H), 1533 (amide II); δ_H (200 MHz, $CDCl_3$) 3.80 (6H, s, 2xOC*H*$_3$), 4.62 (2H, d, *J* 6.0, C*H*$_2$Ph), 6.41 (1H, br s, N*H*), 6.57 (1H, t, *J* 2.5, COCH$_3$C*H*COCH$_3$), 6.91 (2H, d, *J* 2.5, 2xC*H*COCH$_3$), 7.28-7.36 (5H, m, Ar-*H*); MS ESI (+ve) found m/z 334.8 (100 %).

A second fraction was also isolated from the column as an off-white residue (2 mg); R_f=0.21 hexane/EtOAc (1:1); δ_H (200 MHz, $CDCl_3$) 3.82 (3H, s, OCH_3), 3.83 (6H, s, 2x OCH_3), 4.59 (2H, d, *J* 6.0, CH_2Ph), 6.97 (2H, s, 2x$CHCOCH_3$), 7.22-7.36 (5H, m, Ar-*H*); MS ESI (+ve) found m/z 301.8 (MH^+, 21 %), 323.7 (MNa^+, 24), 336.9 (23), 365.0 (100). The analysis corresponds to *N*-benzyl-3,4,5-trimethoxy-benzamide (**226**), formed from **201** starting material.

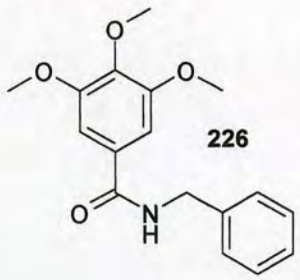

226

6.2.8.5 3-methoxy-1-methyl-5-oxo-cyclohex-3-enecarboxylic acid methyl ester (208)

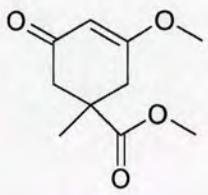

3,5-Dimethoxy-1,4-dihydrobenzoic acid **202** (1.0 g, 5.4 mmol) was added to a stirred solution of potassium amide (13 mmol, prepared *in situ* from potassium (0.5 g) in liquid ammonia (20 ml)). Methyl iodide (1.1 ml, 17 mmol) was added and the solution stirred for 30 mins. Ammonium chloride (1.65 g, 30.8 mmol) was added and the ammonia allowed to evaporate overnight. The resulting orange residue was dissolved in ice/water (20 ml) and acidified to pH5 at 0 °C. The solution was extracted with DCM (2 x 30 ml), then gradually further acidified by addition of small portions of 2M HCl, followed immediately by extraction with DCM. Acidification progressed from pH5 to pH1, when extraction ceased. The combined DCM extracts were dried ($MgSO_4$) and concentrated under reduced pressure to give an orange residue (0.88 g). Flash column chromatography on silica gel using DCM/MeOH (9.5:0.5) as eluent afforded a white solid (0.28 g, 26 %): mp 136 °C; R_f=0.11

DCM/MeOH (9.5:0.5); ν_{max}(nujol) 1720 (C=O), 1691 (C=O), 1596 (C=C); δ_H (250 MHz, $CDCl_3$) 1.38 (3H, s, C(CH_3)), 2.27-2.45 (2H, m, $CH_2C(CH_3)$), 2.81-2.97 (2H, m, $CH_2C(CH_3)$), 3.70 (3H, s, OCH_3), 3.82 (3H, s, OCH_3), 5.40 (1H, s, $COCH{=}COCH_3$); MS ESI (+ve) found m/z 198.6 (MH^+, 77 %), 220.7 (MNa^+, 100).

6.2.8.6 3-methoxy-1-methyl-5-oxo-cyclohex-3-enecarboxylic acid (209)

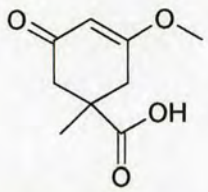

To a stirred solution of 3,4,5-trimethoxybenzoic acid (5.0 g, 24 mmol) in anhydrous THF (50 ml) and ammonia (75 ml) at –78 °C, was added lithium metal (0.42 g, 60 mmol) in small pieces, until a blue colour persisted. MeI (3.7 ml, 60 mmol) was added and the solution stirred for 1 h at –78 °C. The ammonia was allowed to evaporate overnight and the resulting solution concentrated under reduced pressure to a brown/orange residue. H_2O (25 ml) and $CHCl_3$ (50 ml) were added to the residue. The stirred mixture was cooled to 0 °C and the aqueous layer acidified to pH3 by dropwise addition of 12M HCl. The aqueous layer was separated and extracted with $CHCl_3$ (50 ml, then 12 ml). The combined organic layers were dried ($MgSO_4$) and concentrated under reduced pressure to form an orange solid (4.70 g). The solid was triturated with hexane/EtOAc (1:3) and the resulting white precipitate removed. The filtrate was concentrated under reduced pressure to yield a white solid (3.30 g, 76 %): ν_{max}(nujol) 2604br (OH), 1702 (acid C=O), 1685 (C=O), 1598 (C=C); δ_H (250 MHz, $CDCl_3$) 1.37 (3H, s, C(CH_3)), 2.26-2.44 (2H, m, $CH_2C(CH_3)$), 2.79-2.96 (2H, m, $CH_2C(CH_3)$), 3.70 (3H, s, OCH_3), 5.40 (1H, s, $COCH{=}COCH_3$); MS ESI (+ve) found m/z 184.6 (MH^+, 100 %), 206.6 (MNa^+, 83).

6.2.8.7 1-ethyl-3,5-dimethoxy-cyclohexa-2,5-dienecarboxylic acid (211)

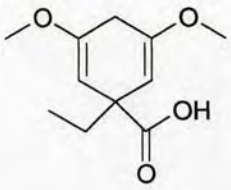

To a stirred solution of 3,5-dimethoxybenzoic acid (4.0 g, 22 mmol) in anhydrous THF (40 ml) and ammonia (60 ml) at –78 °C, was added lithium metal (0.4 g, 58 mmol) in small pieces, until a blue colour persisted. Bromoethane (4.1 ml, 55 mmol) was added in one portion (solution turned yellow, then colourless) and the solution stirred for 1 h at –78 °C. The ammonia was allowed to evaporate overnight and the remaining THF solution concentrated under reduced pressure to yield a pale orange residue. The residue was dissolved in ice/water (100 ml) and $CHCl_3$ (200 ml) added. The solution was acidified to pH1 using 2M HCl. The $CHCl_3$ layer was separated and the aqueous layer extracted with $CHCl_3$ (3 x 100 ml). The combined organic extracts were dried ($MgSO_4$) and concentrated under educed pressure to afford a pale orange solid which was recrystallised from DCM/Pet.Ether (1:1) to yield white crystals (4.33 g, 86 %): mp 134 °C, Lit.[11] 141-144 °C; R_f=0.36 Hexane/EtOAc (19:1); ν_{max}(nujol) 2634br (OH), 1698 (C=O), 1686 (C=O), 1657 (vinyl ether C=C); δ_H (200 MHz, $CDCl_3$) 0.80 (3H, t, *J* 7.5, CH_2CH_3), 1.73 (2H, q, *J* 7.5, CH_2CH_3), 2.75 (2H, s, CH_2COCH_3), 3.59 (6H, s, 2 x OCH_3), 4.64 (2H, s, 2 x CH=$COCH_3$); δ_C (63 MHz, DEPT, $CDCl_3$) 8.5 (CH_2CH_3), 31.0 (CH_2CH_3), 33.6 (CH_2COCH_3), 50.2 ($C(CO_2H)CH_2CH_3$), 54.3 (2 x OCH_3), 94.2 (2 x CH=$COCH_3$), 153.2 (2 x CH=$COCH_3$), 182.6 (CO_2H); MS ESI (-ve) found m/z 210.8 ($[M-H]^-$, 100 %); HRMS FAB (+ve) found m/z 213.11264 (MH^+), $C_{11}H_{17}O_4$ requires 213.11268.

6.2.8.8 1-ethyl-3,5-dimethoxy-cyclohexa-2,5-dienecarboxylic acid benzyl-methyl-amide (212)

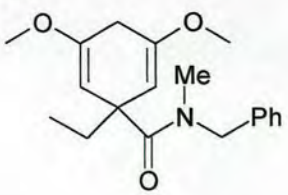

To a stirred solution of **211** (1.50 g, 7.08 mmol in 1,4-dioxane (40 ml) was added triethylamine (1.10 ml, 7.78 mmol), TBTU (2.50 g, 7.78 mmol) and HOBt (0.48 g, 3.54 mmol), followed by *N*-methylbenzylamine (1.00 ml, 7.78 mmol). The solution was stirred at room temperature overnight. The resulting orange mixture was diluted with ether (40 ml), washed with H_2O (30 ml), dried ($MgSO_4$) and concentrated under reduced pressure to yield a yellow oil (4.29 g). Flash column chromatography on silica gel using hexane:EtOAc (1:1) as eluent afforded a colourless oil (1.66 g, 75 %): R_f=0.58 hexane/EtOAc (1:1); ν_{max}(crude oil) 2826-3086br (Ar & OH), 1738 (C=O), 1689 (vinyl ether C=C), 1633 (amide C=O); δ_H (200 MHz, $CDCl_3$) 0.71 (3H, t, *J* 7.5, CH_2CH_3), 1.86 (2H, q, *J* 7.5, CH_2CH_3), 2.60 (1H, d, *J* 21.0, $CH^AH^BCOCH_3$), 2.81 (1H, d, *J* 21.0, $CH^AH^BCOCH_3$), 2.88 (3H, s, NCH_3), 3.22-3.52 (6H, br s, 2 x $COCH_3$), 4.47 (2H, s, CH_2Ph), 4.58 (2H, s, 2 x $CH=COCH_3$), 7.10-7.34 (5H, m, Ar-*H*); δ_C (63 MHz, DEPT, $CDCl_3$) 8.2 (CH_2CH_3), 31.1 (CH_2CH_3), 33.3 (CH_2COCH_3), 35.8 (NCH_3), 50.2 (CCH_2CH_3), 52.8 (CH_2Ph), 54.1 (2 x OCH_3), 95.5 (2 x $CH=COCH_3$), [126.7 (CH), 127.1 (CH), 128.0 (CH), 128.3 (CH), 5C, *Ar*-H], 138.0 (CH_2Ph), 152.7 (2 x $CH=COCH_3$), 175.3 (CONH); HRMS FAB (+ve) found m/z 316.19135 (MH^+), $C_{19}H_{26}NO_3$ requires 316.19127.

6.2.8.9 1-ethyl-3,5-dioxo-cyclohexanecarboxylic acid benzyl-methyl-amide (213)

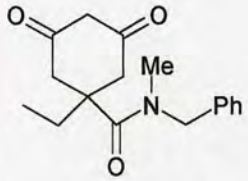

To a stirred solution of **212** (0.76 g, 2.43 mmol) in THF (70 ml) was added H_2O (10 ml), followed by 12 M HCl (2 ml). The solution was stirred overnight at room temperature before concentration under reduced pressure to yield a pale yellow residue (0.96 g). Flash column chromatography on silica gel using hexane/EtOAc (1:5) as eluent afforded a sticky white solid (0.61 g, 87 %): R_f=0.28 DCM/MeOH (9:1); ν_{max}(nujol) 1636 (C=O), 1611 (amide C=O); δ_H (200 MHz, MeOD) 1.01 (3H, t, *J* 7.5, CH_2CH_3), 1.99 (2H, q, *J* 7.5, CH_2CH_3), 2.56 (2H, d, *J* 16.5,

$CH^AH^BCOCH_2COCH^AH^B$), 3.11 (3H, s, NCH_3), 3.12 (2H, d, *J* 16.5, $CH^AH^BCOCH_2COCH^AH^B$), 4.69 (2H, s, CH_2Ph), 7.26-7.44 (5H, m, Ar-*H*); δ_C (63 MHz, DEPT, MeOD) 7.1 (CH_2CH_3), 29.1 (CH_2CH_3), 34.7 (NCH_3), 41.5 (2C, $CH_2COCH_2COCH_2$), 49.5 (CCH_2CH_3), 52.4 (CH_2Ph), 59.6 ($COCH_2CO$), [126.6 (CH), 126.7 (CH), 127.7 (CH), 5C, *Ar*-H], 136.4 (CH_2Ph), 172.9 (CONH), 203.1 (CO); MS ESI (+ve) found m/z 287.8 (MH^+, 78 %), 304.8 (MNH_4^+, 21), 309.8 (MNa^+, 100); HRMS FAB (+ve) found m/z 288.15994 (MH^+), $C_{17}H_{22}NO_3$ requires 288.15997.

6.2.8.10 Oxidative cleavage of N-[1-(4,4-dimethyl-2,6-dioxocyclo hexylidene)-2-benzyloxycarbonylamino-3-methylbutyl] phenylalanine methyl ester (59)

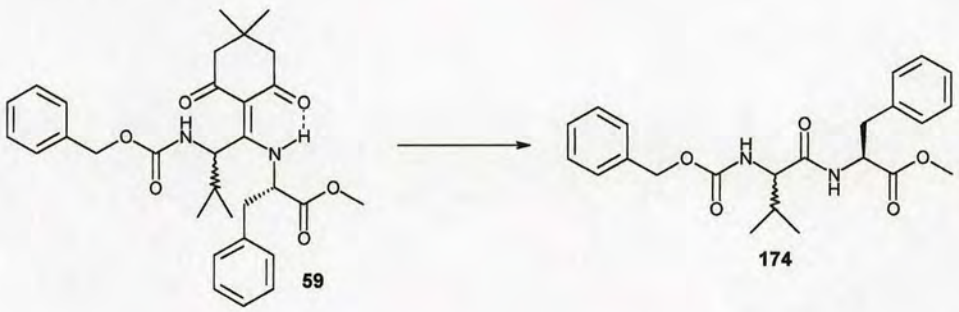

6.2.8.10.1 Periodate

59 (0.22 g, 0.42 mmol) was dissolved in methanol (4 ml). A solution of $NaIO_4$ (0.89 g, 4.17 mmol) in H_2O (2 ml) was added and the reaction refluxed at 60 °C for 4 h. H_2O (12 ml) was added and the aqueous solution extracted with DCM (3 x 4 ml), dried ($MgSO_4$) and concentrated under reduced pressure to yield a yellow oil (0.20 g). The oil was triturated with hexane/EtOAc (1:1) and the resulting white solid filtered off and dried in a desiccator over P_2O_5, to afford a white powder (5 mg, 3 %): δ_H (250 MHz, $CDCl_3$); complex mixture; MS ESI (+ve) found m/z 435.1 (MNa^+, 100 %), 451.0 (MK^+, 64).

6.2.8.10.2 Ozonolysis

59 (0.15 g, 0.28 mmol) was dissolved in anhydrous DCM (15 ml). The solution was cooled with stirring to –70 °C and subjected to a stream of ozone for 5 min. The reaction was then treated with a solution of thiourea (32 mg, 0.42 mmol) in MeOH (5 ml) and the resulting mixture stirred at –60 °C for 1.5 h, before warming to room temperature. TLC $CHCl_3$/ether (1:1) of the crude reaction mixture indicated that no reaction had taken place.

6.2.8.10.3 Ruthenium (III) catalyst

CCl_4 (2 ml), MeCN (2 ml) and H_2O (3 ml) were added to **59** (0.15 g, 0.28 mmol). $NaIO_4$ (0.25 g, 1.15 mmol) was added to the stirred reaction. To the resulting black biphasic solution, $RuCl_3.H_2O$ (4 mg) was added and the mixture stirred at room temperature overnight. The reaction was diluted with DCM (10 ml) and the 2 phases separated. The aqueous layer was washed with DCM (3 x 5 ml) and the combined organic extracts dried ($MgSO_4$) and concentrated under reduced pressure to give a dark brown oil. The oil was diluted with ether (20 ml), filtered through Celite and concentrated under reduced pressure to afford an orange oil (0.14 g). Flash column chromatography on silica gel using $CHCl_3$/ether (1:1) as eluent yielded a yellow oil (16 mg, 14 %):δ_H (200 MHz, $CDCl_3$) complex mixture; MS ESI (+ve) found m/z 435.2 (MNa^+, 100 %), (179.6, PheOMe ester, 61).

6.2.8.11 2-(1-hydroxy-propylidene)-5,5-dimethyl-cyclohexane-1,3-dione (215)

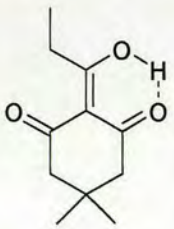

To a stirred solution of propionic acid **214** (1.0 ml, 13 mmol) in DMF (130 ml) was added DCC (2 68 g, 13 mmol) and DMAP (1.59 g, 13 mmol), followed by dimedone

(2.01 g, 14 mmol) and the solution stirred at room temperature overnight. The resulting white DCU precipitate was removed by filtration and the filtrate concentrated under reduced pressure. The residue obtained was diluted with EtOAc (200 ml) and further DCU filtered off. The filtrate was washed with 1M $KHSO_4$ (50 ml) and extracted with saturated $NaHCO_3$ solution (2 x 150 ml). The aqueous layer was acidified with 2M HCl to pH1 and the resulting milky solution extracted with DCM (2 x 150 ml). The combined DCM extracts were concentrated under reduced pressure to yield a pale yellow residue (1.92 g). Flash column chromatography on silica gel using hexane/EtOAc (1:3) as eluent afforded a bright yellow liquid (1.53 g, 60 %): R_f=0.62 hexane/EtOAc (1:3); ν_{max}(nujol) 1671 (α,β-unsaturated ketone), 1559 (C=C); δ_H (250 MHz, $CDCl_3$) 0.94 (6H, s, $C(CH_3)_2$), 0.98 (3H, t, *J* 7.0, CH_2CH_3), 2.22 (2H, s, $CH_2C(CH_3)_2$), 2.41 (2H, s, $CH_2C(CH_3)_2$), 2.90 (2H, q, *J* 7.0, CH_2CH_3), 17.52 (1H, s, O*H*); δ_C (63 MHz, DEPT, $CDCl_3$) 7.9 (CH_2CH_3), 27.8 ($CH(CH_3)_2$), 30.3 ($CH(CH_3)_2$), 33.7 (CH_2CH_3), 46.2 ($CH_2C(CH_3)_2$), 52.2 ($CH_2C(CH_3)_2$), 111.4 (COC=COH), 194.6 (COC=COH), 196.7 (COC=COH), 206.0 (COC=COH); MS ESI (-ve) found m/z 195.0 ($[M-H]^-$, 100 %); HRMS FAB (+ve) found m/z 197.11780 (MH^+), $C_{11}H_{17}O_3$ requires 197.11777.

6.2.8.12 2-(1-benzylamino-propylidene)-5,5-dimethyl-cyclohexane-1,3-dione (216)

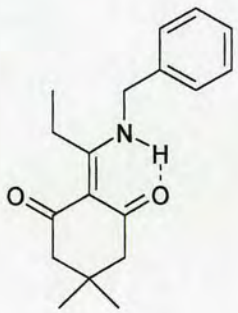

215 (1.51 g, 7.70 mmol) was dissolved in DCM (5 ml) and DIPEA (1.34 ml, 7.70 mmol) added followed by benzylamine (0.84 ml, 7.70 mmol). The reaction was stirred at room temperature overnight. The resulting orange solution was washed with 2M HCl (5 ml), brine (5 ml) dried ($MgSO_4$) and concentrated under reduced

pressure to afford pale yellow crystals (1.64 g, 75 %): mp 72 °C; R_f=0.54 hexane/EtOAc (1:3); ν_{max}(nujol) 1632 (α,β-unsaturated ketone), 1560 (C=C); δ_H (250 MHz, $CDCl_3$) 1.02 (6H, s, $C(CH_3)_2$), 1.19 (3H, t, *J* 7.5, CH_2CH_3), 2.36 (4H, s, $CH_2C(CH_3)_2CH_2$), 3.06 (2H, q, *J* 7.5, CH_2CH_3), 4.61 (2H, d *J* 5.5, CH_2Ph), 7.24-7.40 (5H, m, Ar-*H*), 13.77 (1H, br s, N*H*); δ_C (63 MHz, DEPT, $CDCl_3$) 11.6 (CH_2CH_3), 23.1 (CH_2CH_3), 28.1 ($C(CH_3)_2$), 29.8 ($C(CH_3)_2$), 46.4 (CH_2Ph), 52.4 ($CH_2C(CH_3)_2$), 53.3 ($CH_2C(CH_3)_2$), 106.8 (COC=COH), [127.0 (CH), 127.9 (CH), 128.9 (CH), 5C, *Ar*-H], 135.7 (CH_2Ph), 177.9 (COC=COH), 196.2 (COC=COH), 199.8 (COC=COH); MS ESI (+ve) found m/z 286.3 (MH^+, 100 %), 349.4 (72), 396.5 (53); HRMS FAB (+ve) found m/z 286.18111(MH^+), $C_{18}H_{24}NO_2$ requires 286.18070.

6.2.8.13 Oxidation of 2-(1-benzylamino-propylidene)-5,5-dimethyl-cyclohexane-1,3-dione (216)

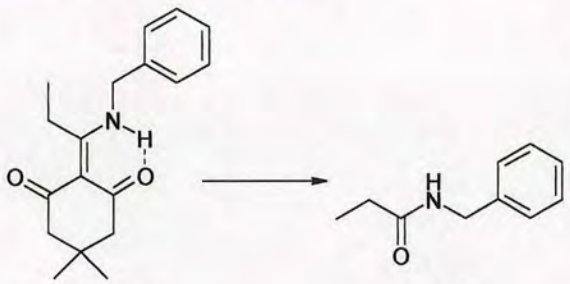

216 **217**

6.2.8.13.1 Periodate

216 (0.10 g, 0.36 mmol) was dissolved in MeOH (2 ml). A solution of $NaIO_4$ (0.31 g, 1.43 mmol) in H_2O (2 ml) was added and the solution heated under reflux overnight. The resulting brown/red solution was diluted with water (6 ml) and extracted with DCM (3 x 2ml). The combined organic extracts were dried ($MgSO_4$) and concentrated under reduced pressure to yield a dark brown/red residue. Crude mixture MS ESI (+ve) found m/z 107.5 (benzylamine, 54 %), 163.5 (MH^+, 100), (185.5, MNa^+, 80). Flash column chromatography using hexane/EtOAc (1:3) as eluent afforded a yellow oil (14 mg, 24 %): R_f=0.40 hexane/EtOAc (1:3); δ_H (250 MHz, $CDCl_3$) 1.17 (3H, t, *J* 7.5, CH_2CH_3), 2.24 (2H, q, *J* 7.5, CH_2CH_3), 4.43 (2H, d,

J 5.5, C*H*$_2$Ph), 5.74 (1H, br s, N*H*), 7.23-7.37 (5H, m, Ar-*H*); MS ESI (+ve) found m/z 163.5 (**217** MH^+, 82 %), (185.5, MNa^+, 100).

6.2.8.13.2 Selenium dioxide catalyst

To a stirred soution of **216** (0.15 g, 0.53 mmol) and SeO_2 (6 mg, 0.05 mmol) in DCM (3 ml) was added a 53 % wt H_2O_2 aqueous solution (0.10 ml, 1.16 mmol) dropwise over 2 min. After stirring for 2 h, the mixture was slowly poured into saturated Na_2SO_3 solution (5 ml). The resulting solution was extracted with DCM (3 x 5 ml) and the combined organic layers dried (Na_2SO_4) and concentrated under reduced pressure to form pale yellow crystals (0.14 g): R_f=0.54 hexane/EtOAc (1:3); MS ESI (+ve) found m/z 285.7 (**216**, 100 %).

6.2.8.13.3 Chromium oxide

A solution of **216** (0.15 g, 0.53 mmol) in DCM (15 ml) and AcOH (7.5 ml) was cooled to –70 °C and CrO_3 (0.16 g, 1.58 mmol) added in small portions. The solution turned dark green in colour. The reaction mixture was stirred at –40 °C for 2 h, then poured into a mixture of 33 % NH_3 solution (10 ml) and ice (60 ml). The organic layer was separated and the inorganic layer extracted with DCM (60 ml). The combined DCM extracts were dried ($MgSO_4$) and concentrated under reduced pressure to form pale yellow crystals (0.10 g): R_f=0.54 hexane/EtOAc (1:3); MS ESI (+ve) found m/z 285.7 (**216**, 100 %).

6.2.8.13.4 Ammonium molybdated catalysed hydrogen peroxide

To a suspension of **216** (0.15 g, 0.53 mmol) and ammonium molybdate (0.02 g, 0.01 mmol) in acetic acid (3 ml), H_2O_2:35 % wt solution in H_2O (0.38 ml, 4.31 mmol) was added dropwise with stirring. The reaction mixture was stirred at 35 °C for 7.5 h. Crude mixture MS ESI (+ve) found m/z 107.5 (benzylamine, 57 %), 163.5 (MH^+, 100), (185.5, MNa^+, 30). The resulting solution was diluted with water and extracted with $CHCl_3$. The combined extractions were washed with saturated

$NaHCO_3$ solution, dried ($MgSO_4$) and concentrated under reduced pressure to yield a colourless oil (0.03 g, 35 %): R_f=0.40 hexane/EtOAc (1:3); δ_H (250 MHz, $CDCl_3$) 1.17 (3H, t, *J* 7.5, CH_2CH_3), 2.24 (2H, q, *J* 7.5, CH_2CH_3), 4.43 (2H, d, *J* 5.5, CH_2Ph), 5.74 (1H, br s, N*H*), 7.23-7.37 (5H, m, Ar-*H*); MS ESI (+ve) found m/z 163.6 (**217** MH^+, 100 %), (185.6, MNa^+, 80).

6.2.8.14 2-(1-butylamino-propylidene)-5,5-dimethyl-cyclohexane-1,3-dione (218)

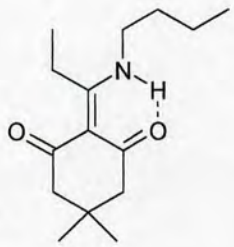

The procedure outlined above (6.2.8.11) was followed using **215** (0.85 g, 4.34 mmol) and *N*-butylamine (0.43 ml, 4.34 mmol) to afford a yellow liquid (1.05 g, 96 %): R_f=0.49 hexane/EtOAc (1:3); ν_{max}(crude oil) 1639 (α,β-unsaturated ketone), 1575 (C=C); δ_H (250 MHz, $CDCl_3$) 0.92 (3H, t, *J* 7.0, $CH_2CH_2CH_3$), 0.98 (6H, s, $C(CH_3)_2$), 1.15 (3H, t, *J* 7.5, CCH_2CH_3), 1.34-1.49 (2H, m, $CH_2CH_2CH_3$), 1.57-1.68 (2H, m, $CH_2CH_2CH_3$), 2.31 (4H, s, $CH_2C(CH_3)_2CH_2$), 2.98 (2H, q, *J* 7.5, CCH_2CH_3), 3.38 (2H, dt, *J* 7.0, 5.5, $NHCH_2$), 13.39 (1H, br s, N*H*); δ_C (63 MHz, DEPT, $CDCl_3$) 11.5 (CCH_2CH_3), 13.5 ($CH_2CH_2CH_3$), 19.9 ($CH_2CH_2CH_3$), 23.0 ($CH_2CH_2CH_3$), 28.0 ($C(CH_3)_2$), 29.8 ($C(CH_3)_2$), 31.1 ($NHCH_2$), 42.2 (CCH_2CH_3), 52.8 ($CH_2C(CH_3)_2CH_2$), 106.4 (COC=CNH), 177.7 (COC=CNH), 196.0 (COC=CNH), 198.6 (COC=CNH); MS ESI (+ve) found m/z 252.0 (MH^+, 100 %), 274.0 (MNa^+, 19), 315.0 (39); HRMS FAB (+ve) found m/z 252.19672 (MH^+), $C_{15}H_{26}NO_2$ requires 252.19635.

6.2.8.15 N-Butyl-propionamide (219)

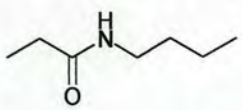

To a suspension of **218** (0.20 g, 0.80 mmol) and ammonium molybdate (0.03 g, 0.02 mmol) in acetic acid (3.5 ml), H_2O_2:35 % wt solution in H_2O (0.57 ml, 6.54 mmol) was added dropwise with stirring. The reaction mixture was stirred at 35 °C for 16.5 h. The resulting solution was diluted with water and extracted with $CHCl_3$. The combined extractions were washed with saturated $NaHCO_3$ solution, dried ($MgSO_4$) and concentrated under reduced pressure to yield a colourless oil (54 mg, 53 %): R_f=0.25 DCM/MeOH (9:1); δ_H (250 MHz, $CDCl_3$) 0.89 (3H, t, *J* 7.0, $CH_2CH_2CH_3$), 1.12 (3H, t, *J* 7.5, $COCH_2CH_3$), 1.22-1.53 (4H, m, $CH_2CH_2CH_3$), 2.17 (2H, q, *J* 7.5, $COCH_2CH_3$), 3.21 (2H, q, *J* 7.0, $NHCH_2$); MS ESI (+ve) found m/z 130.0 (MH^+, 25 %), 153.0 (MNa^+, 100); HRMS FAB (+ve) found m/z 130.12273 (MH^+), $C_7H_{16}NO$ requires 130.12319.

6.2.8.16 1-ethyl-4-(1-hydroxy-propylidene)-3,5-dioxo-cyclohexane carboxylic acid benzyl-methyl-amide (220)

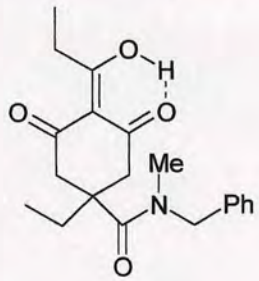

213 (0.37 g, 1.30 mmol) was dissolved in DMF (25 ml) with stirring. DCC (0.30 g, 1.43 mmol), DMAP (0.18 g, 1.43 mmol) and propionic acid (0.11 ml, 1.43 mmol) were added and the resulting solution stirred at room temperature for 2 days. The resulting white DCU precipitate was removed and the filtrate concentrated under reduced pressure to a yellow residue. The residue was diluted with EtOAc (40 ml) and further DCU filtered off. The EtOAc filtrate was washed with 2M HCl, dried ($MgSO_4$) and concentrated under reduced pressure to give a yellow liquid (0.52 g). Flash column chromatography on silica gel using hexane/EtOAc (1:3) as eluent yielded off-white needles (0.31 g, 70 %): mp 89 °C; R_f=0.43 Hexane/EtOAc (1:3); ν_{max}(nujol) 3321br (O-H), 1670 (α,β-unsaturated ketone), 1613 (amide C=O), 1556 (C=C); δ_H (200 MHz, $CDCl_3$) 0.92 (3H, t, *J* 7.5, CCH_2CH_3), 1.10 (3H, t, *J* 7.5,

C=C(OH)CH_2CH_3), 1.73 (1H, dq, *J* 15.0, 7.5, CC$H^AH^BCH_3$), 1.89 (1H, dq, *J* 15.0, 7.5, CC$H^AH^BCH_3$), 2.52 (1H, d, *J* 16.5, CH^AH^BCOC(=C(OH)CH_2CH_3)COCH^AH^B), 2.54 (1H, d, *J* 16.5, CH^AH^BCOC(=C(OH)CH_2CH_3)COCH^AH^B), 2.99 (3H, s, NCH_3), 3.04 (2H, d, *J* 7.5, C=C(OH)CH_2CH_3), 2.98-3.09 (1H, m (masked), CH^AH^BCOC(=C(OH)CH_2CH_3)COCH^AH^B), 3.33 (1H, dd, *J* 17.0, 3.0, CH^AH^BCOC(=C(OH)CH_2CH_3)COCH^AH^B), 4.50 (1H, d, *J* 15.0, CH^AH^BPh), 4.60 (1H, d, *J* 15.0, CH^AH^BPh), 7.09-7.32 (5H, m, Ar-*H*), 18.26 (1H, s, O*H*); δ_C (63 MHz, DEPT, $CDCl_3$) 8.1 (CCH_2CH_3), 8.5 (C=C(OH)CH_2CH_3), 30.1 (CCH_2CH_3), 33.7 (C=C(OH)CH_2CH_3), 35.7 (NCH_3), 43.4 (CH_2CO), 47.7 (CCH_2CH_3), 48.1 (CH_2CO), 53.5 (CH_2Ph), 111.6 (C=C(OH)CH_2CH_3), [127.4 (CH), 127.5 (CH), 128.5 (CH), 5C, *Ar*-H], 136.6 (CH_2Ph), 172.0 (CONH), 192.5 (C=C(OH)CH_2CH_3), 197.5 (CO), 205.6 (CO); MS ESI (+ve) found m/z 343.9 (MH^+, 34 %), 366.0 (MNa^+, 100), 407.0 (32); HRMS FAB (+ve) found m/z 344.18621 (MH^+), $C_{20}H_{26}NO_4$ requires 344.18618.

6.2.8.17 4-(1-Butylamino-propylidene)-1-ethyl-3,5-dioxo-cyclohexane carboxylic acid benzyl-methyl-amide (221)

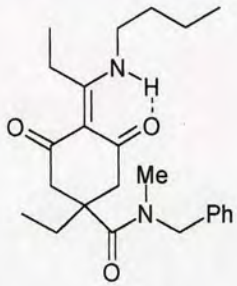

220 (0.24 g, 0.70 mmol) was dissolved in DCM (1 ml) and DIPEA (0.13 ml, 0.77 mmol) added followed by *N*-butylamine (0.08 ml, 0.77 mmol). The reaction was stirred at room temperature overnight. The resulting solution was diluted with DCM (10 ml) and washed with 2M HCl (2 x 5 ml). The combined organic extracts were dried ($MgSO_4$) and concentrated under reduced pressure to afford a colourless oil (0.27 g, 95 %): R_f=0.30 Hexane/EtOAc (1:3); ν_{max}(nujol) 3458br (O-H &N-H), 1634br (ketone & amide C=O), 1574br (C=C); δ_H (200 MHz, $CDCl_3$) 0.90 (3H, t, *J* 7.0, $CH_2CH_2CH_3$), 0.95 (3H, t, *J* 7.5, CCH_2CH_3), 1.16 (3H, t, *J* 7.5, C=CCH_2CH_3),

1.39-1.51 (2H, m, $CH_2CH_2CH_3$), 1.60-1.69 (2H, m, $CH_2CH_2CH_3$), 1.76 (2H, q, *J* 7.5, CCH_2CH_3), 2.52 (2H, d, *J* 16.0, CH_2CO), 2.98 (3H, s, NCH_3), 2.99 (2H, q, *J* 7.5, $C{=}CCH_2CH_3$), 3.12 (2H, d, *J* 16.0, CH_2CO), 3.36-3.44 (2H, m, CH_2NH), 4.56 (2H, s, CH_2Ph), 7.12-7.28 (5H, m, Ar-*H*), 13.33 (1H, s, N*H*); δ_C (63 MHz, DEPT, $CDCl_3$) 8.6 ($CH_2CH_2CH_3$), 11.4 (CCH_2CH_3), 13.5 ($C{=}CCH_2CH_3$), 19.9 ($CH_2CH_2CH_3$), 23.1 $CH_2CH_2CH_3$), 29.7 (CCH_2CH_3), 31.1 ($C{=}CCH_2CH_3$), 35.6 (NCH_3), 42.4 (CH_2NH), 46.6 (CCH_2CH_3), 48.4 (CH_2CO), 53.1 (CH_2Ph), 106.2 ($C{=}CCH_2CH_3$), [127.1 (CH), 127.6 (CH), 128.4 (CH), 5C, *Ar*-H], 137.0 (CH_2Ph), 173.0 (CONH), 177.7 ($C{=}CCH_2CH_3$), 195.9 (CO); MS ESI (+ve) found m/z 399.1 (MH^+, 68 %), 421.1 (MNa^+, 100), 462.1 (26); HRMS FAB (+ve) found m/z 399.26480 (MH^+), $C_{24}H_{35}N_2O_3$ requires 399.26477.

6.2.8.18 Oxidation of 4-(1-butylamino-propylidene)-1-ethyl-3,5-dioxo-cyclohexanecarboxylic acid benzyl-methyl-amide (221 → 219)

The general procedure outlined above (6.2.8.14) was followed using **221** (0.14 g, 0.37 mmol) to yield a pale yellow oil (27 mg, 56 %): δ_H (250 MHz, $CDCl_3$) as 4/48/1; MS ESI (+ve) found m/z 129.5 (**219** MH^+, 87 %), 152.5 (MNa^+, 100).

6.3 References

[1] Halpern, B.; James, L.B., *Aust. J. Chem.*, 1964, **17**, 1282-1287.

[2] Plass, M.; Kolbe, A., *J. Mol. Struct.*, 1994, **322**, 241-246.

[3] Knoelker, H-J.; Braxmeier, T., *Synlett.*, 1997, **8**, 925-8.

[4] Berry, N.M.; Darey, M.C.P.; Harwood, L.M., *Synth. Comm.*, 1986, 476-480.

[5] Jursic, B.S.; Neumann, D, *Synth. Comm.*, 2001, **31**, 555 – 564.

[6] Yamashita, M.; Naoi, M.; Imoto, H.; Oshikawa, T., *Bull. Chem. Soc. Jpn.*, 1989, **62**, 942-944.

[7] Chen, F.M.F.; Benoiton, N.L, *Can. J. Chem.*, 1987, **65**, 1228-1229;

[8] Irie, H.; Nakanishi, H.; Fujii, N.; Mizuno, Y.; Fushimi, T., *Chem. Lett*, 1980, 705-708;

[9] Kuehne, M.E.; Lambert, B.F., *J. Chem. Soc.*, 1959, **81**, 4278-4287.

[10] Kuehne, M.E.; Lambert, B.F., *J. Chem. Soc.*, 1959, **81**, 4278-4287.

[11] Liepa, A.J.; Wilkie, J.S.; Winzenberg, K.N., *Aust. J. Chem.*, 1989, **42**, 1217-1225.